



THE UNIVERSITY *of* EDINBURGH

Edinburgh Research Explorer

Period estimation and rhythm detection in timeseries data using BioDare2, the free, online, community resource

Citation for published version:

Zieliski, T, Hay, J & Millar, AJ 2021, Period estimation and rhythm detection in timeseries data using BioDare2, the free, online, community resource. in *Plant Circadian Networks: Methods and Protocols*. vol. 2398, Methods in molecular biology (Clifton, N.J.), Springer, pp. 15-32. https://doi.org/10.1007/978-1-0716-1912-4_2

Digital Object Identifier (DOI):

[10.1007/978-1-0716-1912-4_2](https://doi.org/10.1007/978-1-0716-1912-4_2)

Link:

[Link to publication record in Edinburgh Research Explorer](#)

Document Version:

Publisher's PDF, also known as Version of record

Published In:

Plant Circadian Networks

General rights

Copyright for the publications made accessible via the Edinburgh Research Explorer is retained by the author(s) and / or other copyright owners and it is a condition of accessing these publications that users recognise and abide by the legal requirements associated with these rights.

Take down policy

The University of Edinburgh has made every reasonable effort to ensure that Edinburgh Research Explorer content complies with UK legislation. If you believe that the public display of this file breaches copyright please contact openaccess@ed.ac.uk providing details, and we will remove access to the work immediately and investigate your claim.



Methods in
Molecular Biology 2398

Springer Protocols

Dorothee Staiger
Seth Davis
Amanda Melaragno Davis *Editors*

Plant Circadian Networks

Methods and Protocols

Second Edition

 Humana Press

METHODS IN MOLECULAR BIOLOGY

Series Editor

John M. Walker

**School of Life and Medical Sciences,
University of Hertfordshire
Hatfield, Hertfordshire, UK**

For further volumes:

<http://www.springer.com/series/7651>

For over 35 years, biological scientists have come to rely on the research protocols and methodologies in the critically acclaimed *Methods in Molecular Biology* series. The series was the first to introduce the step-by-step protocols approach that has become the standard in all biomedical protocol publishing. Each protocol is provided in readily-reproducible step-by-step fashion, opening with an introductory overview, a list of the materials and reagents needed to complete the experiment, and followed by a detailed procedure that is supported with a helpful notes section offering tips and tricks of the trade as well as troubleshooting advice. These hallmark features were introduced by series editor Dr. John Walker and constitute the key ingredient in each and every volume of the *Methods in Molecular Biology* series. Tested and trusted, comprehensive and reliable, all protocols from the series are indexed in PubMed.

Plant Circadian Networks

Methods and Protocols

Second Edition

Edited by

Dorothee Staiger

Department of Biology, University of Bielefeld, Bielefeld, Nordrhein-Westfalen, Germany

Seth Davis

Department of Biology, University of York, Heslington, UK

Amanda Melaragno Davis

Department of Biology, University of York, Heslington, UK

Editors

Dorothee Staiger
Department of Biology
University of Bielefeld
Bielefeld, Nordrhein-Westfalen,
Germany

Seth Davis
Department of Biology
University of York
Heslington, UK

Amanda Melaragno Davis
Department of Biology
University of York
Heslington, UK

ISSN 1064-3745

Methods in Molecular Biology

ISBN 978-1-0716-1911-7

<https://doi.org/10.1007/978-1-0716-1912-4>

ISSN 1940-6029 (electronic)

ISBN 978-1-0716-1912-4 (eBook)

© The Editor(s) (if applicable) and The Author(s), under exclusive license to Springer Science+Business Media, LLC, part of Springer Nature 2022, Corrected Publication 2022

Chapter 2 is licensed under the terms of the Creative Commons Attribution 4.0 International License (<http://creativecommons.org/licenses/by/4.0/>). For further details see license information in the chapter.

This work is subject to copyright. All rights are reserved by the Publisher, whether the whole or part of the material is concerned, specifically the rights of translation, reprinting, reuse of illustrations, recitation, broadcasting, reproduction on microfilms or in any other physical way, and transmission or information storage and retrieval, electronic adaptation, computer software, or by similar or dissimilar methodology now known or hereafter developed.

The use of general descriptive names, registered names, trademarks, service marks, etc. in this publication does not imply, even in the absence of a specific statement, that such names are exempt from the relevant protective laws and regulations and therefore free for general use.

The publisher, the authors, and the editors are safe to assume that the advice and information in this book are believed to be true and accurate at the date of publication. Neither the publisher nor the authors or the editors give a warranty, expressed or implied, with respect to the material contained herein or for any errors or omissions that may have been made. The publisher remains neutral with regard to jurisdictional claims in published maps and institutional affiliations.

This Humana imprint is published by the registered company Springer Science+Business Media, LLC part of Springer Nature.

The registered company address is: 1 New York Plaza, New York, NY 10004, U.S.A.

Preface

The second edition of *Plant Circadian Networks* comprises a collection of state-of-the-art protocols to monitor circadian rhythmicity in plants. Like most organisms, plants utilize an endogenous timekeeper, the biological or “circadian” clock (from Latin *circa diem*, about a day), to organize their life throughout the day in synchrony with environmental cycles of light and dark and associated temperature cycles. This circadian clock generates an internal time structure, causing major processes in the cell to occur at regular 24-h intervals.

In 2017, the Nobel Prize in Physiology or Medicine was awarded to Jeff Hall, Michael Rosbash, and Mike Young for their discoveries of the molecular mechanism constituting the circadian timekeeper. This also acknowledges the importance circadian timekeeping has for human well-being and plant fitness. In fact, basic principles of circadian rhythmicity were first described several centuries ago. Today, the plant community is well aware that almost all aspects of a plant’s life are influenced by the circadian clock. Thus, an awareness for endogenous rhythms is imperative in designing experimental setups in plant research.

This volume comprises a collection of protocols to assay circadian rhythmicity and clock regulation in plants, both at the physiological and molecular level. A chapter on curve fitting rhythms initiates the methods. Bioinformatics are essential to process high-throughput data and extract parameters of circadian rhythms. We thus include a chapter on the updated version of BioDare. Additionally there is a chapter on mathematical projections of data in chronobiological terms and another on modeling clock parameters in Matlab. There are several chapters detailing the measurement of circadian-regulated parameters including chlorophyll fluorescence, hypocotyl elongation, or imaging of luciferase reporters in transiently transfected *Arabidopsis* seedlings and soybean hairy roots. Fructan measurements are described. Furthermore, determination of QTLs based on luciferase reporters is described.

At the molecular level, alternative pre-mRNA splicing has lately emerged as a key mechanism mediating adjustment of the core oscillator to temperature changes. This has provoked interest in analyzing alternative splicing events genome-wide. In particular, analyzing splicing around the clock requires numerous time points and large data sets. One chapter provides a computational tool for wet lab biologists to analyze such data with little bioinformatics knowledge. Another chapter describes 3’ tag sequencing. Furthermore, nuclei isolation and chromatin immunoprecipitation to identify targets of clock proteins are described. Two chapters provide methods to identify protein-protein interaction of clock proteins. While many protocols deal with the reference plant *Arabidopsis thaliana*, we include two chapters that deal with specific aspects of clock control in the perennial plant *Populus*.

We would like to thank all our colleagues contributing to this second edition of the *Plant Circadian Networks*.

Bielefeld, Nordrhein-Westfalen, Germany
Heslington, UK
Heslington, UK

Dorothee Staiger
Amanda M. Davis
Seth J. Davis

Contents

<i>Preface</i>	<i>v</i>
<i>Contributors</i>	<i>ix</i>
1 Circadian Rhythm: Phase Response Curve and Light Entrainment	1
<i>Xiaodong Xu, Li Yuan, and Qiguang Xie</i>	
2 Period Estimation and Rhythm Detection in Timeseries Data Using BioDare2, the Free, Online, Community Resource	15
<i>Tomasz Zieliński, Johnny Hay, and Andrew J. Millar</i>	
3 Detection and Analysis of Circadian Rhythms Via Prompt Chlorophyll Fluorescence	33
<i>Yuri Dakhiya and Rachel Green</i>	
4 High Spatial Resolution Luciferase Imaging of the <i>Arabidopsis thaliana</i> Circadian Clock	47
<i>Mark Greenwood, Anthony J. W. Hall, and James C. W. Locke</i>	
5 <i>Agrobacterium</i> -Mediated Seedling Transformation to Measure Circadian Rhythms in <i>Arabidopsis</i>	57
<i>Michael K. Y. Ting, Reimo Zoschke, and Michael J. Haydon</i>	
6 Measurement of Luciferase Rhythms in Soybean Hairy Roots	65
<i>Qiguang Xie, Yu Wang, Li Yuan, and Xiaodong Xu</i>	
7 ODE (Ordinary Differential Equation) Models for Plant Circadian Networks: What the Models Are and How They Should Be Used	75
<i>Jonathan W. Pitchford and Paula Avello</i>	
8 How to Detect QTLs in the Plant Circadian Clock	89
<i>Muhammad Usman Anwer and Marcel Quint</i>	
9 Measuring Hypocotyl Length in <i>Arabidopsis</i>	99
<i>James Ronald and Seth Jon Davis</i>	
10 High-Throughput Extraction and Enzymatic Determination of Sugars and Fructans in Fructan-Accumulating Plants	107
<i>Kallyne A. Barros, Masami Inaba, Auxiliadora Oliveira Martins, and Ronan Sulpice</i>	
11 Simple Nuclei Preparation and Co-immunoprecipitation Procedures for Studying Protein Abundance and Interactions in Plant Circadian Time Courses	121
<i>Akane Kubota, Young Hun Song, and Takato Imaizumi</i>	
12 Chromatin Immunoprecipitation Protocol for Circadian Clock Proteins	135
<i>Sally Adams and Isabelle A. Carré</i>	
13 A High-Throughput 3'-Tag RNA Sequencing for Large-Scale Time-Series Transcriptome Studies	151
<i>Xiaoyu Weng and Thomas E. Juenger</i>	

14 Experimental Design for Time-Series RNA-Seq Analysis of Gene Expression and Alternative Splicing 173
Nikoleta A. Tzioutziou, Allan B. James, Wenbin Guo, Cristiane P. G. Calixto, Runxuan Zhang, Hugh G. Nimmo, and John W. S. Brown

15 Using Tandem Affinity Purification to Identify Circadian Clock Protein Complexes from *Arabidopsis* 189
Maria L. Sorkin and Dmitri A. Nusinow

16 Firefly Luciferase Complementation-Based Analysis of Dynamic Protein-Protein Interactions Under Diurnal and Circadian Conditions in *Arabidopsis* 205
Qiguang Xie, Qiao Wang, and Xiaodong Xu

17 Monitoring Seasonal Bud Set, Bud Burst, and Cold Hardiness in *Populus* 215
Mikael Johansson, Naoki Takata, Cristian Ibañez, and Maria E. Eriksson

18 The Perennial Clock Is an Essential Timer for Seasonal Growth Events and Cold Hardiness 227
Mikael Johansson, Cristian Ibañez, Naoki Takata, and Maria E. Eriksson

Correction to: Period Estimation and Rhythm Detection in Timeseries Data Using BioDare2, the Free, Online, Community Resource C1

Index 243

Contributors

- SALLY ADAMS • *School of Life Sciences, University of Warwick, Coventry, UK*
- MUHAMMAD USMAN ANWER • *Institute of Agricultural and Nutritional Sciences, Martin Luther University Halle-Wittenberg, Halle (Saale), Germany*
- PAULA AVELLO • *Department of Mathematics, University of York, York, UK; Faculty of Biological Sciences, School of Biology, University of Leeds, Leeds, UK*
- KALLYNE A. BARROS • *NUI Galway, Plant Systems Biology Laboratory, Ryan Institute, School of Natural Sciences, Galway, Ireland*
- JOHN W. S. BROWN • *Division of Plant Sciences, University of Dundee at the James Hutton Institute, Dundee, UK; Cell and Molecular Sciences, The James Hutton Institute, Dundee, UK*
- CRISTIANE P. G. CALIXTO • *Division of Plant Sciences, University of Dundee at the James Hutton Institute, Dundee, UK*
- ISABELLE A. CARRÉ • *School of Life Sciences, University of Warwick, Coventry, UK*
- YURI DAKHIYA • *Department of Plant and Environmental Sciences, The Silberman Institute for Life Sciences, The Hebrew University, Jerusalem, Israel*
- SETH JON DAVIS • *Department of Biology, University of York, York, UK; Key Laboratory of Plant Stress Biology, School of Life Sciences, Henan University, Kaifeng, China*
- MARIA E. ERIKSSON • *Department of Plant Physiology, Umeå Plant Science Centre, Umeå University, Umeå, Sweden*
- RACHEL GREEN • *Department of Plant and Environmental Sciences, The Silberman Institute for Life Sciences, The Hebrew University, Jerusalem, Israel*
- MARK GREENWOOD • *Sainsbury Laboratory, University of Cambridge, Cambridge, UK; Department of Biochemistry, University of Cambridge, Cambridge, UK*
- WENBIN GUO • *Division of Plant Sciences, University of Dundee at the James Hutton Institute, Dundee, UK*
- ANTHONY J. W. HALL • *Earlham Institute, Norwich, UK*
- JOHNNY HAY • *EPCC, University of Edinburgh, Edinburgh, UK*
- MICHAEL J. HAYDON • *School of BioSciences, University of Melbourne, Parkville, VIC, Australia*
- CRISTIAN IBÁÑEZ • *Biology Department, La Serena University, La Serena, Chile*
- TAKATO IMAIZUMI • *Department of Biology, University of Washington, Seattle, WA, USA*
- MASAMI INABA • *NUI Galway, Plant Systems Biology Laboratory, Ryan Institute, School of Natural Sciences, Galway, Ireland*
- ALLAN B. JAMES • *Institute of Molecular, Cell, and Systems Biology, College of Medical, Veterinary and Life Sciences, University of Glasgow, Glasgow, UK*
- MIKAEL JOHANSSON • *RNA Biology and Molecular Physiology, Faculty of Biology, Bielefeld University, Bielefeld, Germany*
- THOMAS E. JUENGER • *Department of Integrative Biology, University of Texas at Austin, Austin, TX, USA*
- AKANE KUBOTA • *Division of Biological Science, Nara Institute of Science and Technology, Nara, Japan*
- JAMES C. W. LOCKE • *Sainsbury Laboratory, University of Cambridge, Cambridge, UK*

- AUXILIADORA OLIVEIRA MARTINS • *NUI Galway, Plant Systems Biology Laboratory, Ryan Institute, School of Natural Sciences, Galway, Ireland; Departamento de Biologia Vegetal, Universidade Federal de Viçosa, Viçosa, Minas Gerais, Brazil*
- ANDREW J. MILLAR • *SynthSys and School of Biological Sciences, C. H. Waddington Building, University of Edinburgh, Edinburgh, UK*
- HUGH G. NIMMO • *Institute of Molecular, Cell, and Systems Biology, College of Medical, Veterinary and Life Sciences, University of Glasgow, Glasgow, UK*
- DMITRI A. NUSINOW • *Donald Danforth Plant Science Center, St. Louis, MO, USA*
- JONATHAN W. PITCHFORD • *Department of Biology, University of York, York, UK; Department of Mathematics, University of York, York, UK*
- MARCEL QUINT • *Institute of Agricultural and Nutritional Sciences, Martin Luther University Halle-Wittenberg, Halle (Saale), Germany*
- JAMES RONALD • *Department of Biology, University of York, York, UK*
- YOUNG HUN SONG • *Department of Agricultural Biotechnology, Seoul National University, Seoul, Korea*
- MARIA L. SORKIN • *Donald Danforth Plant Science Center, St. Louis, MO, USA; Division of Biology and Biomedical Sciences, Washington University in St. Louis, St. Louis, MO, USA*
- RONAN SULPICE • *NUI Galway, Plant Systems Biology Laboratory, Ryan Institute, School of Natural Sciences, Galway, Ireland*
- NAOKI TAKATA • *Forest Bio-Research Center, Forestry and Forest Products Research Institute, Hitachi, Japan*
- MICHAEL K. Y. TING • *School of BioSciences, University of Melbourne, Parkville, VIC, Australia; Max Planck Institute of Molecular Plant Physiology, Potsdam-Golm, Germany; Institute of Biochemistry and Biology, University of Potsdam, Potsdam-Golm, Germany*
- NIKOLETA A. TZIOUTZIOU • *Division of Plant Sciences, University of Dundee at the James Hutton Institute, Dundee, UK*
- QIAO WANG • *Institute of Plant Stress Biology, State Key Laboratory of Cotton Biology, School of Life Sciences, Henan University, Kaifeng, China*
- YU WANG • *College of Biological Sciences, Hebei Normal University, Shijiazhuang, Hebei, China*
- XIAOYU WENG • *Department of Integrative Biology, University of Texas at Austin, Austin, TX, USA*
- QIGUANG XIE • *State Key Laboratory of Crop Stress Adaptation and Improvement, School of Life Sciences, Henan University, Kaifeng, China; Institute of Plant Stress Biology, State Key Laboratory of Cotton Biology, School of Life Sciences, Henan University, Kaifeng, China; College of Biological Sciences, Hebei Normal University, Shijiazhuang, Hebei, China*
- XIAODONG XU • *State Key Laboratory of Crop Stress Adaptation and Improvement, School of Life Sciences, Henan University, Kaifeng, China; Institute of Plant Stress Biology, State Key Laboratory of Cotton Biology, School of Life Sciences, Henan University, Kaifeng, China; College of Biological Sciences, Hebei Normal University, Shijiazhuang, Hebei, China*
- LI YUAN • *State Key Laboratory of Crop Stress Adaptation and Improvement, School of Life Sciences, Henan University, Kaifeng, China*

- RUNXUAN ZHANG • *Information and Computational Sciences, The James Hutton Institute, Dundee, UK*
- TOMASZ ZIELIŃSKI • *SynthSys and School of Biological Sciences, C. H. Waddington Building, University of Edinburgh, Edinburgh, UK*
- REIMO ZOSCHKE • *Max Planck Institute of Molecular Plant Physiology, Potsdam-Golm, Germany*



Chapter 1

Circadian Rhythm: Phase Response Curve and Light Entrainment

Xiaodong Xu, Li Yuan, and Qiguang Xie

Abstract

The circadian clock responds to light signals and therefore participates in the plant's daily response to light. The phase response curve (PRC) is typically used in the study of chronobiology to detect the effect of various environmental cues on a given circadian rhythm. In this chapter we describe protocols on measuring the setting of the light pulses at different times of a day, the measurement of circadian rhythm, and the calculation of phase shift in response to light pulses. The *promoter:luciferase* reporter was used to provide fine rhythmic traces and the subsequent circadian parameters of mathematical analysis. A classical PRC assay to light pulses is the key experimental basis for determining the signal components of resetting the circadian clock.

Key words Phase response curve, Circadian clock, Circadian rhythms, Light, Entrainment, Zeitgeber, Phase shift, Free-running period, Photoentrainment

1 Introduction

Circadian clock is endogenous time-keeping system in most if not all organisms. The 24-hour rhythm that is driven by circadian clock synchronizes biological processes to the solar day by cyclic external cues [1–4]. Light is the most important input signaling to the circadian clock, and responses to light in time are critical for plant success [5]. The period length and phase timing of the circadian rhythm are consistent with that of the light-dark (LD) cycles due to the entrainment to a LD *zeitgeber*. Many components possess light-sensing properties and functions in LD cycles, such as light receptors, which can enable the circadian oscillators to regulate the light sensitivity of clock resetting [6–10]. Furthermore, the oscillation of light intensity and the variation of light regimes (i.e., spectral quality) of a day in nature are also critical aspects of circadian photoentrainment. The modulation of free-running period (FRP), for example, or acceleration or deceleration, depends to a

large extent on light intensity, which is a continuous action on the clock (also termed “parametric entrainment”) [8, 11], while the clock in multicellular organisms can also respond to transit stimuli, such as light pulses, with rapidly shifted phase of circadian rhythm. According to the “nonparametric entrainment,” or discrete model, the resetting results in keeping the rhythmicity in phase with functional oscillators which has been moved to a different isochron by a light stimulus in a limit cycle [12–15]. The map of phase-dependent resetting is called the phase response curve (PRC) that can be acted upon in interpreting the responses of circadian clocks to various zeitgebers [7, 9, 16–21].

In this chapter, we introduce our circadian entrainment techniques and subsequent protocols to demonstrate the representative “Type 0” PRC that plotted as strong phase shift against the circadian time of onset of the pulse [14]. Transgenic *Arabidopsis* materials carrying the reporter gene *CCA1:luciferase* (*CCA1:LUC*) are used for rhythm detection. Under the free-running darkness conditions, seedlings were exposed to light pulses at 3-h intervals scanning a 24-h circadian cycle to test the sensitivity of circadian clock to light intensity and spectrum (Fig. 1). In this study, we presented the typical PRCs for plants exposed to light stimulus. The maximum phase shifts of circadian rhythm can be induced by light pulses with higher intensity and a long duration time (up to 3-h). The reaction time of the circadian clock to different light regimes

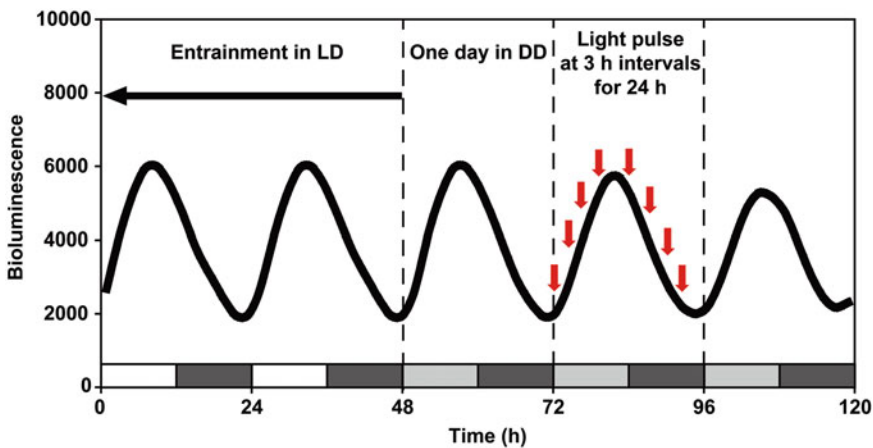


Fig. 1 Schematic representation of light/dark setting in the experiment. Transgenic *CCA1:LUC* seedlings were entrained since germination in 12-h light:12-h dark for 7 days before released to constant darkness conditions for light PRC treatment and circadian rhythms of luciferase measurement. The experimental materials in microplates were divided into nine groups (one group for “no pulse” treatment control), and after a full day in continuous darkness (e.g., CT 0–24), another eight groups were used for light treatment (red arrows). Light pulses were given at 3-h intervals scanning a 24-h circadian cycle (e.g., CT 24–48). Only one of the total eight groups of seedlings was illuminated with light pulses (3-h pulse of $60 \mu\text{mol m}^{-2} \text{s}^{-1}$ red light, or 30-min pulse of $100 \mu\text{mol m}^{-2} \text{s}^{-1}$ white light) at each indicated circadian time (red arrow) and then transferred back to constant dark for luciferase measurement over the ensuing 5 days. CT0 indicates the beginning of a subjective day (light gray bar), and CT12 is the beginning of a subjective night (dark gray bar)

also differs. This method can be widely used to analyze the light sensitivity of circadian rhythm and to identify the components in the light entrainment of biological clock.

2 Materials

Prepare all solutions and reagents using deionized water and analytical grade reagents. Prepare and store all reagents at room temperature (unless indicated otherwise).

1. Murashige and Skoog basal salts mixture (M524, PhytoTechnology Laboratories).
2. D-Luciferin (Potassium Salt, Gold Biotechnology).
3. Absolute alcohol.
4. Sucrose.
5. Agar, solidifying agent for plant tissue culture (A0930, USBiological).
6. Micropore tape (3 M Micropore Tape).
7. 96-well white microtiter plates (ProxiPlate-96, White Opaque 96-shallow well Microplate, PerkinElmer).
8. Sealing films for microtiter or microplates.
9. LED color light chamber (cool white, red, far red, and blue LEDs included) specifically designed for plant growth light quality studies (LED-30HL1, Percival Scientific).
10. Microplate reader with the integration of a photomultiplier tube (PMT) for high sensitivity in luminescence measurement (Packard TopCount™ NXT luminometer).
11. Deep cooled scientific camera with low-noise performance allowing significantly longer exposure time (Andor's DU934P-BV Deep-Cooled CCD).
12. Growth chamber with precise control over cool-white fluorescent lighting at $120 \mu\text{mol m}^{-2} \text{s}^{-1}$ at constant 22°C within the chamber (CU-36L5, Percival Scientific).
13. Sterile hood (laminar flow hood).
14. Data analysis computer and software (Biological Rhythms Analysis Software System, BRASS).

3 Methods

3.1 Preparing *Arabidopsis* Seedlings Culture Medium

1. Weigh 4.33 g dried Murashige and Skoog (MS) salts, 20 g sucrose, and place into a 1 L beaker.
2. Add ~1 L deionized water (~5% less than final volume), adjust to pH 5.7 with KOH, and then adjust to final volume of 1 L.

3. Add to 1 L glass media vial with 8 g agar, or split in two bottles, wrap the top of the bottle with aluminum foil or with screw cap loosened, and place the glass media vial into an autoclave (*see Note 1*).
4. Autoclave the medium with liquid cycle for 30–40 min, allow it to cool down enough (to about 85 °C) to allow extraction of bottle from the autoclave.
5. Shake the bottle gently to allow the agar in the bottle to mix well, pour about 25–30 mL of the warm agar medium (about 60 °C) into petri dishes (90 mm in diameter), which gives 35–40 petri dishes per 1 L medium (*see Note 2*).
6. Leave the hood on while cooling the petri dishes if using a flow hood, or leave the medium in a place of low microbiological contamination (*see Note 3*).

3.2 Growth of Plant Seedlings in Sterile Conditions

Complete the following operation in a sterile flow hood.

1. Place certain amount of seeds (~300 seeds for each treatment) in Eppendorf tube, rinse with 1 mL 70% ethanol for 30 s, and pour off the supernatant carefully (*see Note 4*).
2. Add 1 mL sterile water to suspend the seeds, wait for the seeds to sink to the bottom of the tube, and carefully remove the wash solution using a 1 mL pipettor tip. Repeat this step three times (*see Note 5*).
3. Add 1 mL 20% commercial bleach (containing ~5% sodium hypochlorite) to the seeds, let the seeds immersed in the bleach for 5 min, and gently invert the tubes to mix the liquid.
4. Repeat **step 2** and rinse three times with sterile distilled water.
5. Suspend sterile seeds in 100 µL sterile distilled water, plate individual seeds onto the culture medium (*see Note 6*).
6. Seal the plate with adhesive paper tape, wrap half a dozen plates in aluminum foil or bags/boxes to avoid light, and stratify for 3 days in the dark at 4 °C (*see Note 7*).
7. Transfer plates to the growth chamber in the early morning (ZT0), keeping the plates horizontally and seeds facing upwards (*see Subheading 3.3* for light/temperature setting).
8. Wait for the seeds to germinate for about 3 days.

3.3 Environmental Conditions in Experimental Setting and Light Entrainment

The circadian rhythm-related experiments need to be conducted under highly controlled ambient conditions. Terrestrial plant growth chamber with light and temperature independently programmable is required.

1. Measure light intensities of the environmental chamber using photometer (*see Note 8*).

2. Adjust the cool-white fluorescent lighting of broad spectrum to $120 \mu\text{mol m}^{-2} \text{s}^{-1}$ for *Arabidopsis* seedlings which is grown in sterile conditions.
3. Set light cycles of 12-h light followed by 12-h darkness, with lights being switched on at 8:00 a.m. (Zeitgeber time 0) and lights off at 8:00 p.m. (Zeitgeber time 12) (*see Note 9*).
4. Program the chamber for constant temperature of 22°C .

3.4 Preparing Luciferin for Bioluminescent Assays

1. Thaw D-Luciferin Firefly potassium salt at room temperature and dissolve in sterile water to prepare a $40\times$ Luciferin stock solution (100 mM) (*see Note 10*).
2. Gently mix the solution by inversion until D-luciferin is completely dissolved, and avoid light during stock solution preparation.
3. Use immediately or store aliquots at -20°C for about 2 years.
4. Dilute with sterile water containing 0.05% Triton X-100 for the assay procedure (*see Note 11*).

3.5 Using Real-Time Reporter for Circadian Dynamics

1. Gently remove individual 7-day-old transgenic seedlings carrying *CCA1:LUC* (*see* Subheadings 3.2 and 3.3 for seedlings growth and light entrainment information) from petri dishes into one well of a 96-well culture microplates (*see Notes 12 and 13*).
2. Add $30 \mu\text{L}$ of 2.5 mM luciferin to the well of microtiter plates containing $200 \mu\text{L}$ of culture medium.
3. Seal the microplate with clear sealing film.
4. Gently leave two tiny holes on the sealing film of each well using a sterile syringe needle (*see Note 14*).
5. Return the 96-well microplates with seedlings to growth chamber to complete entrainment of the last day at 22°C of 12-h light/12-h dark cycle, and then transfer the microplates to constant darkness (DD) at ZT0 on the next day (*see Note 15*).

3.6 Applying Light Pulses at all Possible Phases Across the Circadian Cycle

1. After 1 day in constant dark (DD), the seedlings in 96-well microplates were exposed to 30-min white light ($100 \mu\text{mol m}^{-2} \text{s}^{-1}$) or 3-h red light ($60 \mu\text{mol m}^{-2} \text{s}^{-1}$) treatment (Fig. 2) starting at ZT0 (*see Note 16*).
2. Return the seedlings to continuous darkness (DD) and start the luciferase measurement (*see Note 17*).
3. Repeat **steps 1 and 2** with other separate experimental materials at 3-h intervals to complete the subsequent seven groups of light treatments (i.e., ZT3, ZT6, ZT9, ZT12, ZT15, ZT18, and ZT21) scanning one complete circadian cycle (24 h). A

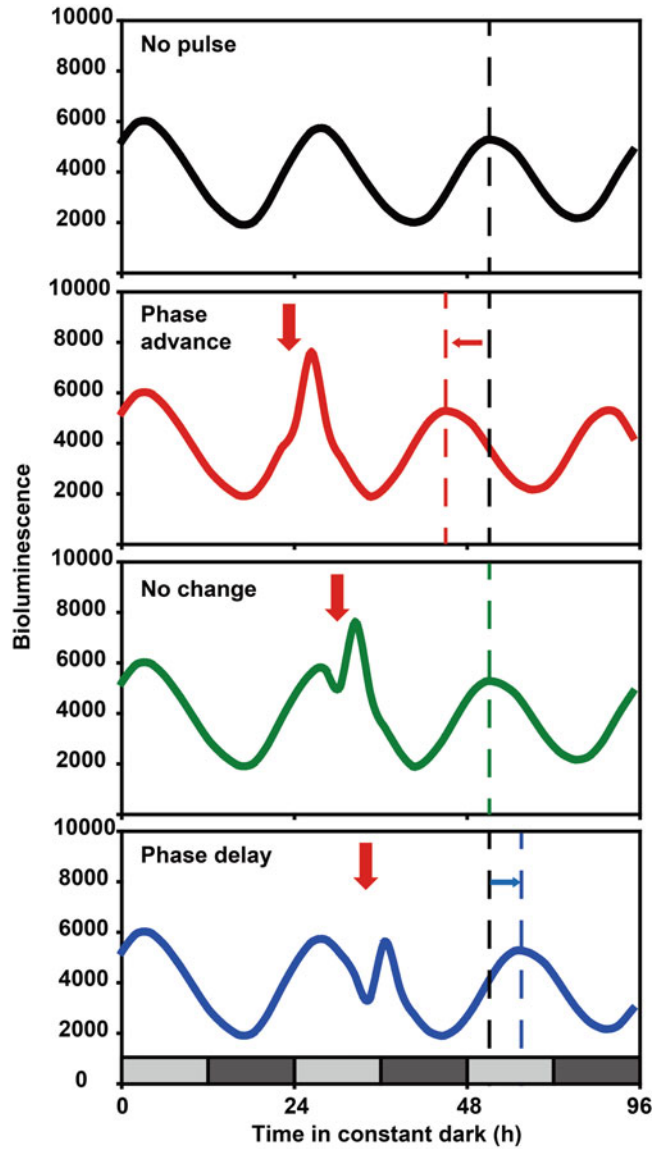


Fig. 2 Phase-dependent responses of circadian clock to *zeitgeber*. The figure displays the analysis of the relationship between the phase shifts of *promoter: LUC* activity rhythm in free-running conditions and circadian time of the perturbing stimulus (abscissa). Advance phase shifts occur when the light pulses are given lately in the subjective night and around dawn (e.g., ZT 0, red traces), while delay phase shifts occur when the light pulses are given early in the subjective night or around dusk (e.g., ZT 12, blue traces). Light pulses presented in certain time of the subjective day have little or no effect on the reset of rhythmicity on subsequent days. Light and dark gray shading represents subjective day and night, respectively

total of eight independent groups of materials were processed with light treatment to monitor the response of the biological clock to the external light stimuli (zeitgeber) at different time within one light/dark cycle.

4. Monitor the *CCA1:LUC* bioluminescence count of the above eight groups of light treatment plus “no pulse” control over the ensuing 4 days. In our laboratory, the long-term measurement of bioluminescence from the *LUC* reporter was performed by either automated photomultiplier apparatus or photon-counting camera. The former apparatus recorded the *CCA1:LUC* luminescence from one seedling per well every 80 min for 10 s. The photon-counting camera captured the images of 96-well microplates (i.e., 96 individual seedlings per plate) every 3 h for 200 s (*see Note 18*).

3.7 Determining Free-Running Period (Tau) and Circadian Time Phase

1. Collect raw data of at least 24 individual seedlings for each analysis.
2. Download the “Biological Rhythms Analysis Software System (BRASS 2.1.4)” from www.amillar.org. This software integrates the fast Fourier transform-nonlinear least squares (FFT-NLLS) analysis for circadian rhythms.
3. Analyze the defined rhythmic traces of the period in the range of between 20 and 30 h and the RAE (relative amplitude error) value less than 0.7 (*see Note 19*).
4. Obtain the typical circadian parameters (including sidereal phase, period length, amplitude, and relative amplitude error) using data analysis software.
5. Calculate circadian time phase (CT phase) values by dividing sidereal phase (peak phase) values by the individual’s period length of free-running rhythm and then multiplying the value by 24 h(circadian) (*see Note 20*). The mathematical formula is as follows:

$$[\text{CT phase} = (\text{sidereal phase}/\text{period}) \times 24]$$

3.8 Determining Phase Response Characteristics and Plotting the Phase Response Curve

1. Calculate the CT phase changes relative to the seedlings not exposed to external light pulse, and obtain the phase shift values of each pulse at different times during the 24-h. Positive values and negative values represented phase advances and delays, respectively (*see Note 21*).
2. Plot the phase advance or delay values at each circadian time to show clock responses to light signals at each. The produced phase response curve provides critical dynamic information on the state of clock at each zeitgeber time and circadian time during the day (*see Note 22*).

4 Notes

1. Our laboratory currently employs the following reagents and formulation with final concentration of 1 L culture medium: 1xMS basal salt mixture, 2% sucrose, 0.8% agar. The purpose of the medium is to obtain the 7–10 days old seedlings. However, there are certain variations on the theme, and other recipes in other references can also be used. Half strength MS basal media can also be used to generate the seedlings. In *Arabidopsis*, sucrose produced by plants through photosynthesis can regulate the expression of the biological clock gene, so in the process of seedling entrainment, sucrose is added to maintain the oscillation of biological rhythms. The carbon source concentration in the medium influenced the development and circadian rhythms of *Arabidopsis* seedlings; therefore, a suitable sucrose of 1–3% is utilized for circadian assay.
2. When shaking high-temperature media, be careful with liquid bumps, be sure to wear insulated gloves, and keep exposed skin away from the bottle.
3. Leave the lid slightly open in the flow hood for about 1 h till the plates cool down and solidify. You can also leave the petri dishes in a sterile hood to harden and incubate overnight, the next day wrapped up in refrigerated or immediately use.
4. Ethanol is used to sterilize the surface of the seed coat, but prolonged ethanol immersion will inhibit the germination of seeds. Therefore, ethanol immersion time is best not to exceed 1 min.
5. Full and effective rinsing is necessary and can be slightly vortexed to wash the seeds. For the removal of the washing fluid, keep the tube vertically stand for a while, or centrifuge the seeds to concentrate on the bottom of the tube.
6. Alternatively, the tubes with sterilized seeds can be placed directly into the darkness at 4 °C for stratification and be plated to the culture medium later. To equidistantly sow seeds and control the spacing density of planting, it is suggested to place a printed grid as plotting guide underneath the petri dishes.
7. For better control of humidity and breathability inside the petri dishes, it is recommended to use surgical paper tape with microspores, which adheres well and removes easier with little adhesive residue.
8. As stated in the introduction, in higher plants, the free-running period of circadian rhythm decreased with increasing light intensity; the brighter the constant light, the faster the clock

runs. To test and compare the responsibilities of circadian oscillators to the light pulses, we should determine the accurate light intensities the seedlings exposed to. The high-quality absorption photometer is needed to provide the flux of photos per unit surface and time, which is suitable for the measurement from wavelength around 240 nm up to 750 nm.

9. In the study of chronobiology, zeitgebers refer to the external or environmental cues that can entrain or synchronize the biological rhythms to daily 24-h cycles, lunar cycles, and annual cycles. *Zeitgeber* time (ZT) is a notation based on the experimental time in entrained circadian cycle. Under a standard earth's light-dark cycles, the time of lights on usually defines ZT 0 for diurnal organisms.
10. Solubility of D-luciferin Potassium Salt is 10 mg in 0.25 mL water. Luciferin is a light sensitive, and the stock tube should be wrapped with tinfoil paper during the stock solution preparation.
11. For LUC imaging with CCD camera, adult plants grown in petri dishes were sprayed with 2.5 mM luciferin and 0.05% Triton X-100 the day before start of imaging. The 200 μ L medium in each well of the microplate is the same as the one mentioned in Subheading 3.1.
12. In this experiment, the *Arabidopsis* core oscillator *CCA1* (*Circadian Clock Associated 1*) promoter is sufficient to mediate transcriptional regulation by the circadian clock. The promoter of other rhythm reporter genes, such as *LATE ELONGATED HYPOCOTYL (LHY)*, *TIMING OF CAB EXPRESSION 1 (TOC1)*, and *CHLOROPHYLL A/B-BINDING PROTEIN2 (LHCB)* and *COLD CIRCADIAN RHYTHM AND RNA BINDING 2 (CCR2)*, which are subject to the biological clock and light regulation is also used to create the construct. The modified luciferase gene, *LUC+*, was widely used for promoter: *LUC* construct, and this commercially available clone (Promega, Madison, WI) yielded at least tenfold higher signals than wild-type *LUC* in transgenic plant lines. In this study, stably introduce the *CCA1:LUC* construct into *Arabidopsis* ecotype Columbia-0 by *A. tumefaciens* strain GV3101-mediated transformation.
13. This step is prone to damage to the seedlings; thus it is necessary to prepare more materials, and the use of long-handled tweezers, 12 in. straight and curved tip, is recommended.
14. This step is critical because maintaining breathability facilitates the growth of seedlings during subsequent measurements.

15. Strictly speaking, circadian rhythm is distinguished from some daily rhythms that are simply a response to 24-h environmental changes. The experimental design of measuring the endogenous rhythm is to detect whether the material still show rhythmicity under constant light and temperature conditions.
16. According to “nonparametric or phasic” entrainment theory, light-entrained circadian pacemaker is in equilibrium with the 12-h light: 12-h dark cycles consisting of repetitive environmental signals as the *zeitgeber*. In this experiment, the *zeitgeber* is “mimicked” in the laboratory by brief light treatment. In addition, the strength (intensity and/or duration) of the zeitgeber stimulus affects the PRC waveform significantly. In this study, light pulses were given at 3-h intervals scanning a 24-h circadian cycle. White light or red light was used as two kinds of light signals, respectively. The increased light dose and prolonged pulse can elicit larger phase advances/delays and shifts the circadian time of the singularity point.
17. The endogenous circadian rhythms are usually determined under constant temperature and continuous light or darkness. Therefore, for light PRC experiment, the conditions for determining the endogenous *CCA1:LUC* rhythm are set to constant temperature and constant darkness.
18. For photomultiplier tube-based equipment, the measurement time depends on the strength of the promoter activity. For high-sensitivity single-photon counting cameras, the software usually allow phosphorescence delay of chlorophyll; therefore, the camera software in my lab was set for 30-min delay in counting. Based on our self-assembled imaging equipment, high-throughput analysis of 12 plates can be acquired simultaneously at a time.
19. The RAE value is used to evaluate the strength of the rhythmicity; $RAE = 0$ is an ideal cosine wave, and $RAE = 1$ is the limit of statistical significance for a given rhythmic amplitude (i.e., arrhythmicity).
20. In nature, light, the *zeitgeber*, affects the period and phase of the pacemaker. The phase in a circadian cycle (24 h) is a notation which represented an estimation of the organism’s subjective time (e.g., CT 0 indicates the beginning of a subjective day, and CT 12 is the beginning of a subjective night).
21. Light signaling functions as *zeitgeber* in the dawn and dusk transitions in nature LD cycle; thus light pulses processing in the experiment at different phases can mimic circadian entrainment. The assay of phase-dependent resetting of pacemaker is

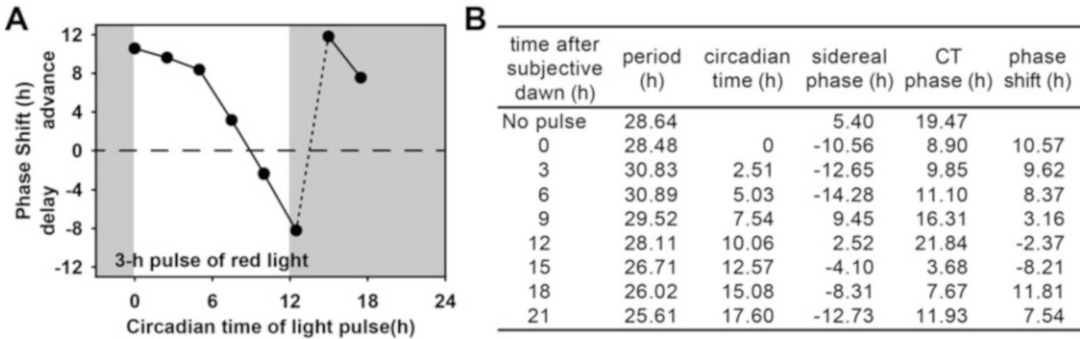


Fig. 3 Analysis of circadian parameters using the Biological Rhythms Analysis Software System. Furthermore, the circadian time of red light stimulus treatment (left panel) and phase point of the free-running rhythm need to be normalized to 24 h; then the phase shifts were calculated as the difference in phase between the pre- and post-stimulus of light (table in the right panel). BRASS, 2.1.4; www.amillar.org

used simply and effectively to interpret the limit-cycle equilibrium, in which each light pulse falls at on the phase of a given rhythm and further causes a phase shift. The elicited phase shifts compensate the difference between the free-running period and the period of the photo-entrained cycle.

- The light PRCs of different species have some common characteristics; for example, advance phase shifts occur when the light pulses are given lately in the subjective night and around dawn, while delay phase shifts occur when the light pulses are given early in the subjective night or around dusk. In this study, the strong circadian phase advances were observed in response to either white or red light pulses in the early subjective morning and late subjective night, and strong phase delays were observed in the subjective evening using this method (Fig. 2). The circadian times (CT time) of maximal phase shifts to white light signals were 0 (+4.5-h advances, in subjective dawn) or 18 (−8-h delays, in the late subjective night) (Fig. 3). The CT time of maximal phase shifts to red light signals were 15.1 (+18.8-h advances, in the late subjective night) or 12.6 (−8.2-h delays, in the subjective evening) (Fig. 4). In addition, the curves of light PRC also show the typical “breakpoint,” which appears between the maximum delay at approximately CT12–18 h and the maximum advance at approximately CT 12–24 h. The points that appear in the middle of the subjective day and appear to be little phase shift in the PRC are called the singularity. The mechanism for the skip phenomenon of delay to advance via the singularity point is less clear. It seems that the sensitivity of pacemaker to the perturbing stimulus is significantly decreased.

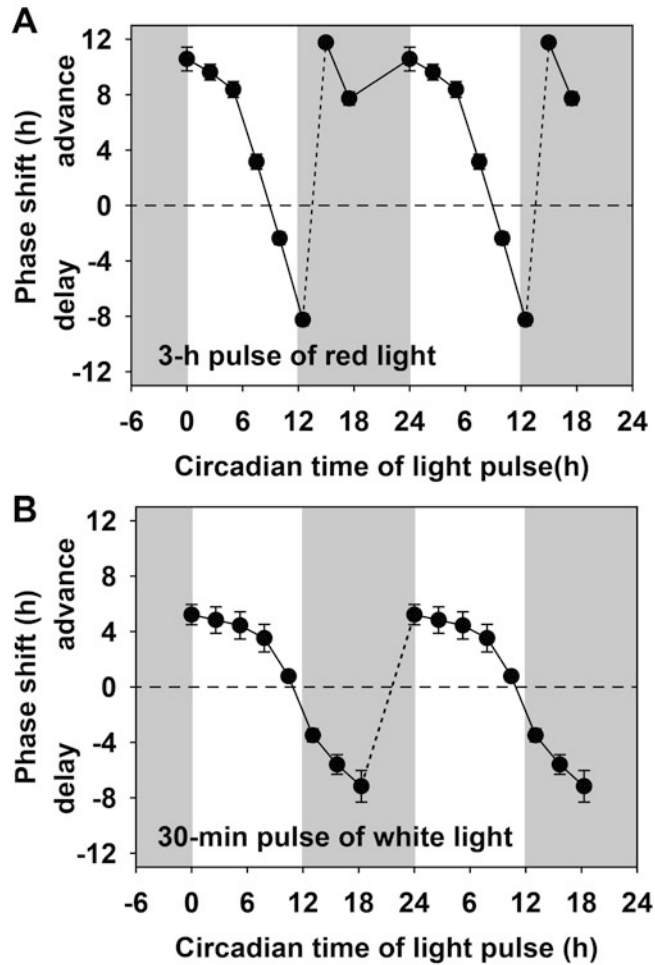


Fig. 4 Phase response curves (PRCs) of *CCA1:LUC* circadian expression to light pulses. PRCs are constructed by plotting the amount of phase shift versus the circadian timing of the onset of red or white light stimulus. Data represents mean \pm pooled s.e.m.; at least 24 individual seedlings were used for each analysis. Shading indicates subjective night, and lack of shading indicates subjective day. PRC waveforms are double plotted to emphasize the pacemaker sensitivity to light pulses

Acknowledgments

This work was supported by grants from the National Natural Science Foundation of China to X.X. (U1904202) and Q.X. (31670285).

References

1. Greenham K, McClung CR (2015) Integrating circadian dynamics with physiological processes in plants. *Nat Rev Genet* 16:598–610
2. Millar AJ (2016) The intracellular dynamics of circadian clocks reach for the light of ecology and evolution. *Annu Rev Plant Biol* 67:595–618
3. Johnson CH, J.A. E., and Foster, R. (2003) Entrainment of circadian programs. *Chronobiol Int* 20:741–774
4. Aschoff J (1960) Exogenous and endogenous components in circadian rhythms. *Cold Spring Harb Symp Quant Biol* 25:11–28
5. Pittendrigh CS, Minis DH (1964) The entrainment of circadian oscillations by light and their role as photoperiodic clocks. *Am Nat* 98:261–322
6. Devlin PF, Kay SA (2000) Cryptochromes are required for phytochrome signaling to the circadian clock but not for rhythmicity. *Plant Cell* 12:2499–2510
7. Covington MF, Panda S, Liu XL, Strayer CA, Wagner DR, Kay SA (2001) ELF3 modulates resetting of the circadian clock in *Arabidopsis*. *Plant Cell* 13:1305–1316
8. Somers DE, Devlin P, Kay SA (1998) Phytochromes and cryptochromes in the entrainment of the *Arabidopsis* circadian clock. *Science* 282:1488–1490
9. Feher B, Kozma-Bognar L, Kevei E, Hajdu A, Binkert M, Davis SJ, Schafer E, Ulm R, Nagy F (2011) Functional interaction of the circadian clock and UV RESISTANCE LOCUS 8-controlled UV-B signaling pathways in *Arabidopsis thaliana*. *Plant J* 67:37–48
10. Devlin PF, Kay SA (2001) Circadian photoperception. *Annu Rev Physiol* 63:677–694
11. Aschoff J (1999) Masking and parametric effects of high-frequency light-dark cycles. *Jpn J Physiol* 49:11–18
12. Crosthwaite SK, Loros JJ, Dunlap JC (1995) Light-induced resetting of a circadian clock is mediated by a rapid increase in *frequency* transcript. *Cell* 81:1003–1012
13. Johnson CH (1990). An atlas of phase response curves for circadian and circatidal rhythms, (Nashville: Department of Biology, Vanderbilt University)
14. Johnson CH (1999) Forty years of PRCs-- what have we learned? *Chronobiol Int* 16:711–743
15. Pittendrigh CS (1960) Circadian rhythms and the circadian organization of living systems. *Cold Spring Harb Symp Quant Biol* 25:159–184
16. Xu X, Xie Q, McClung CR (2010) Robust circadian rhythms of gene expression in *Brassica rapa* tissue culture. *Plant Physiol* 153:841–850
17. Salomé PA, McClung CR (2005) *PSEUDO-RESPONSE REGULATOR 7* and *9* are partially redundant genes essential for the temperature responsiveness of the *Arabidopsis* circadian clock. *Plant Cell* 17:791–803
18. Salomé PA, McClung CR (2005) What makes the *Arabidopsis* clock tick on time?: A review on entrainment. *Plant Cell Environ* 28:21–38
19. Haydon MJ, Mielczarek O, Robertson FC, Hubbard KE, Webb AA (2013) Photosynthetic entrainment of the *Arabidopsis thaliana* circadian clock. *Nature* 502:689–692
20. Gutiérrez RA, Stokes TL, Thum K, Xu X, Obertello M, Katari MS, Tanurdzic M, Dean A, Nero DC, McClung CR et al (2008) Systems approach identifies an organic nitrogen-responsive gene network that is regulated by the master clock control gene *CCA1*. *Proc Natl Acad Sci U S A* 105:4939–4944
21. Michael TP, Salomé PA, McClung CR (2003) Two *Arabidopsis* circadian oscillators can be distinguished by differential temperature sensitivity. *Proc Natl Acad Sci U S A* 100:6878–6883



Chapter 2

Period Estimation and Rhythm Detection in Timeseries Data Using BioDare2, the Free, Online, Community Resource

Tomasz Zieliński , Johnny Hay , and Andrew J. Millar 

Abstract

One of the key objectives of data analysis in circadian research is to quantify the rhythmic properties of the experimental data. BioDare2 is a free, online service which provides fast timeseries analysis, attractive visualizations, and data sharing. This chapter outlines the description of an experiment for BioDare2 and how to upload and analyze the numerical timeseries data.

Keywords Circadian rhythms, Biological clocks, Research data management, Period analysis, Rhythmicity, Data repository, Data sharing, Metadata

1 Introduction

Circadian research touches many fields from agriculture to biomedicine. Circadian timeseries over several days are costly to obtain, and mathematical analysis is required to measure the timing features in the data. Analysis of and access to timeseries data are therefore critical, across the diverse, rhythm research community. However, we still encounter barriers in making data fair and open, because high-quality data deposition takes time and substantial effort. Linking the process of data sharing to routine data analysis can compensate users for the time spent on data deposition and thus promote data sharing. This is the main principle behind BioDare2 (<https://biodare2.ed.ac.uk>).

BioDare2 provides fast timing analysis, summary statistics, and attractive data visualizations in a modern web interface, all to ensure the best user experience. Access to BioDare2 is provided on condition that data will be made public. Thus, public data sharing is a “side effect” of using our analysis tools and is not

The original version of this chapter was revised. The correction to this chapter is available at https://doi.org/10.1007/978-1-0716-1912-4_19

Dorothee Staiger et al. (eds.), *Plant Circadian Networks: Methods and Protocols*, Methods in Molecular Biology, vol. 2398, https://doi.org/10.1007/978-1-0716-1912-4_2, © The Author(s) 2022, Corrected Publication 2022

perceived as an additional burden. On the contrary, BioDare2 increases research productivity as its analysis methods are faster and easier to use than any alternative. This approach has successfully attracted data from worldwide users, gaining over 400,000 data timeseries in the 2 years since inception, with continuing fast growth.

Here, we describe how BioDare2 can be used to visualize and pre-process data, perform rhythm detection, and estimate period, phase, and amplitude values of individual timeseries.

2 Materials

1. Access to a modern web browser with JavaScript enabled; we use Google Chrome (there are currently no known issues of compatibility with any other up to date browsers).
2. An account in BioDare2 (new accounts can be registered at the BioDare2 website: <https://biodare2.ed.ac.uk>).
3. Numerical, timeseries data file: typically an Excel file in a tabular form, with one column containing time values followed by one or more columns of measured data values (*see Note 1*).

3 Methods

The basic entity in BioDare2 is an experiment. Although a timeseries is the basic data unit to be processed and analyzed, many timeseries are typically collected in parallel in contemporary circadian research. The behavior of the circadian system is greatly influenced by the environmental conditions under which the data were generated, which typically vary between experiments. Thus, it is important to store not only the timeseries data in BioDare2 but also the context of the measurement, the experimental details.

The procedure for processing data with BioDare2 is a multi-stage operation as follows:

1. Creating and describing the new experiment in BioDare2.
2. Importing and labeling numerical timeseries data.
3. Visualizing the timeseries.
4. Analyzing timeseries data to estimate period, phase, and amplitude values or test for rhythmicity.

Conventions. Text in bold and in quotation marks, e.g., “**New experiment**,” refers to buttons, links, and menu options found on BioDare2 screens, which trigger specific actions. Text in *italics* refers to the visual elements on the screen, for example, dialog titles or labels for input fields.

Disclaimer. The layout of the screens or action labels may have changed since the publication of this book, as new functionalities

are continually added to BioDare2. However, the features described below are “core” functions of BioDare2; the typical processing steps and their mechanics will not change even if the user interface is modified in the future.

3.1 Creation of a New Experiment in BioDare2

1. In your web browser, navigate to the BioDare2 home page (<https://biodare2.ed.ac.uk>) and login.
2. Click “**New experiment**” in the top menu (Fig. 1a), which will load the page shown in Fig. 1.
3. Complete the form provided to describe the details of the experiment, by filling in the free text fields, selecting from the options list, or using the autocompletion fields (Fig. 1b). At the minimum, the following items should be provided:
 - (a) Descriptive name of the experiment which helps to distinguish this data set from others.
 - (b) Purpose/hypothesis which summarizes the main aims of the experiment.
 - (c) Description which outlines the specifics of the experiment, for example, environmental conditions and biological materials.
 - (d) Species.
 - (e) Data category that distinguishes between experimental data types, usually on the basis of the assay method.

The form is divided into sections, and each section has an “**Accept**” button that stores its state (Fig. 1c). The fields contain hints on how to complete them (Fig. 1d), and uncompleted fields are marked in red (Fig. 1e).

At the bottom of the form, the “**Create**” button will create a new record in BioDare2 with the information provided.

4. After the creation form is submitted, the experiment dashboard screen is presented, which is the launch pad of most of the activities undertaken in BioDare2.

3.2 Import of Numerical Data

1. Start adding the numerical data by clicking the “**Import data**” button.
2. Select the appropriate file format from the list and drag the data file into the upload area on the screen or click inside to open the file selection dialog. Press “**Upload selected.**”
3. The next step of the description process will expand in the form (here we limit the procedure only to the Excel table format, *see Note 1*).
4. Define the layout of the data; for example, if timeseries data points are in rows or if they are already labeled in the file.
5. In the next step (Fig. 2), define time column properties by clicking on the cell containing the time of the first

BioDare2 Home Experiments **New Experiment** Docs Account

BioDare2

Create experiment

General description

Name

Testing clock robustness at low light

Purpose/Hypothesis

Describe the main aim of the experiment. What you tried to achieve, test, verify, on what kind of samples.

Sensible description with more than few words is required

Description

Describe how the experiment was conducted, what environmental conditions, sampling procedure.
For example: seedlings were exposed to short day light regime (LD 6:18) at two temperatures 15 and 25. Samples were harvested every 4 hours for 3 days and the genes levels measured with RT PCR

Accept Cancel

Biological details

Species

Arabidopsis thaliana

Data category

Expression reporter (e.g. Luc/GFP-imaging)

Accept Cancel

Fig. 1 Screenshot of the *Create Experiment* screen. (a) Menu item that opens the form. (b) Input form elements. (c) Accept button to store the section entries. (d) Input fields contain hints about the desired content. (e) Erroneous fields are marked in red and accompanied by an error description

measurement and then selecting the time unit. It is also possible to define the time offset which should be applied during import (*see Note 2*).

6. Labeling the data is the most laborious step in BioDare2, so two options are available to streamline the process:
 - (a) Importing existing labels from the file.

BioDare2 Home Experiments New Experiment Docs Account Logout

1 Data layout

3 Define time column A

Excel Table: **wt_prr_simpl.xlsx**

Time series in columns

Times in column **A**; First time point: **1 h** [A:2]

Time unit *
time in hours

Time offset

Click on the first timepoint in the time column and then select a time unit. C

	A	B	C	D	E	F	G
1	id	WT LHY	WT LHY	WT LHY	WT LHY	WT LHY	WT LHY
2	1	1.64313382080089	1.11345929902012	1.28561275895891	1.27698935054428	1.4262914687803	1.55071017754356
3	3	1.42137705335791	0.89829628953527	0.997016615012846	0.990512990122226	1.1734569390445	1.29636080762641
4	5	1.18967969746675	0.673627639069439	0.747867039661575	0.728405300857896	0.95805749434675	1.06821965667871
5	7	0.978052361261426	0.483385535671379	0.580621838577903	0.54443121749148	0.826573973250255	0.90211344492190

Even if only the top part of the data table is presented all times from the selected column will be imported

Back Next

4 Select labels row

Fig. 2 Screenshot of the *Timeseries import* screen. (a) A current step of the import process. (b) The first time point selected by clicking. (c) Each step contains hints how it can be completed. (d) Column headings can be selected to label their content

Very often, the data table already contains the labels. The labels might have been provided during the quantification step of the image processing, written by a PCR machine, or the user may simply find it easier to label the data in Excel rather than using the web UI. In that case, the row containing labels must be clicked, and the labels will be read during import.

- (b) Selecting columns for labeling.

Click on a column header (cells containing letters at the top of the table) to select one column or click and drag to select a column range. The “*Label column(s)*” popup

will appear which allows the user to enter the label text. Clicking “**Assign**” or pressing “Enter” assigns the label to the selected columns and then automatically moves focus to the next column on the right, so that the proceeding block of data can be described.

Data content is presented in pages; in order to describe all the data, the next page must be loaded using the “>” of the pagination widget on top. The number of columns loaded can be set with the “*Columns per page*” drop-down.

7. Optionally select which labels signify “*Background noise*”; columns with these labels will be used for data pre-processing (*see Note 3*).
8. Once the time column has been defined and the data columns are labeled, press “**Import timeseries**” to initiate conversion of the selected data from the file into a timeseries. After the timeseries is successfully imported, the “*Show timeseries*” screen is displayed, which presents the data visualization dashboard.

3.3 Visualizing Timeseries

The timeseries can be visualized on traditional line plots via the “**Show data**” button (Fig. 3b).

Options available for customizing the timeseries visualizations are (Fig. 3a):

1. Scaling data using the “*from*” and “*to*” fields (leaving at the default of 0 simply scales the timeseries according to their minimum and maximum data values, respectively).
2. Detrending and normalizing data by one of the available methods (*see Note 4*).
3. Organizing data on the plots by applying sorting (*see Note 5*), trace alignments, and pagination.

The individual traces plotted within each chart can be hidden or revealed by clicking on the data labels beneath the x -axis on each chart.

Alternatively, data can be visualized in a heatmap by pressing the “**Heatmap**” button (Fig. 3c). This visualization is especially useful when analyzing large data sets. The heatmap screen offers similar customization options as for the line plots. Hovering over a heatmap cell shows the value for the corresponding data point, while hovering over the widgets on the left of the graph displays the data label.

The version of the processed data used for plotting (e.g., cubic detrended timeseries normalized to the maximum) can be downloaded in the numerical CSV format. Two download buttons are available: “**current view**,” which retrieves the currently viewed data

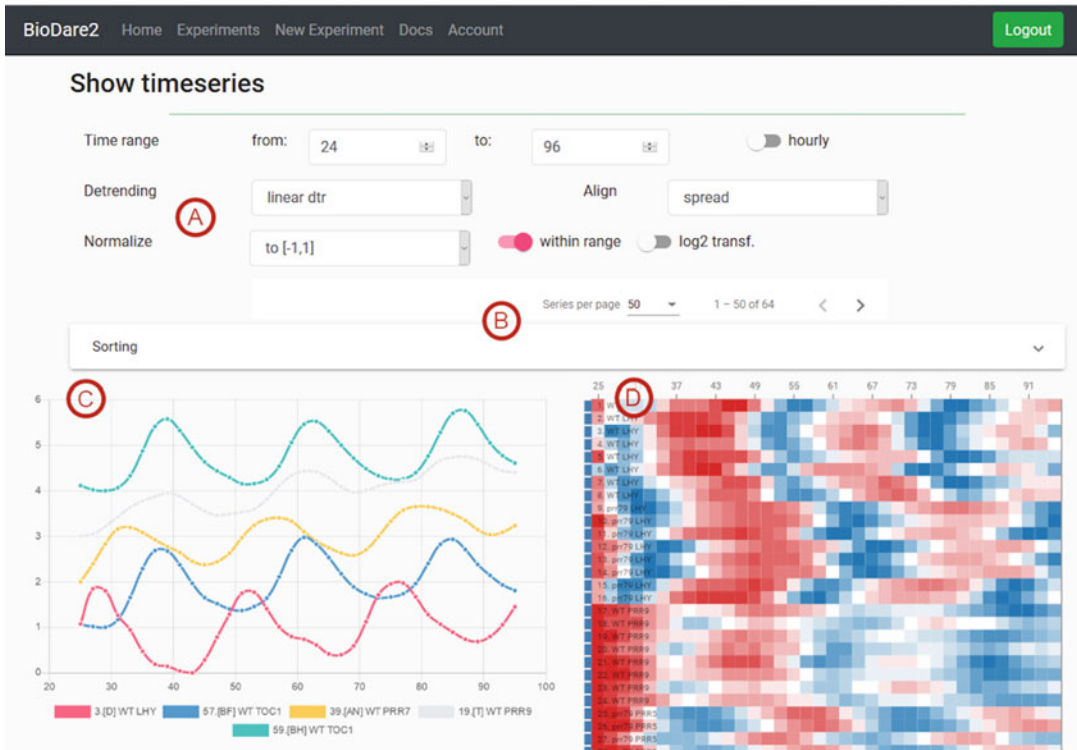


Fig. 3 Data visualization. (a) Pre-processing options for timeseries plotting. (b) Pagination and sorting panel. (c) Line plot of a data set. (d) Heatmap chart of the same data set

subset, and “full,” which retrieves the entire data set. This output can be useful for plotting and analysis with other software.

3.4 Period Estimation

A rhythmic signal can be characterized by its period, amplitude, and phase (*see Note 6*), and BioDare2 provides six methods for estimating period values: FFT-NLLS [1], mFourFit [2], MESA [3], Enright Periodogram [4], Lomb-Scargle periodogram [5], and Spectrum resampling [6].

3.4.1 Starting a New Analysis

1. Click on “**Period analysis**” to open the “*Start period analysis*” screen, which contains a form for setting analysis parameters and plots of the input data to be analyzed.
2. Define the “*Data window*” by specifying the two time points between which the timeseries data will be analyzed. The default values of 0 “from” and 0 “to” indicate the first and last time points in the data, respectively, so the entire timeseries is analyzed.
3. In “*Input data,*” select the detrending method that should be applied prior to analysis. The plots are automatically refreshed to show the detrended data. The default detrending method is linear, but more vigorous detrending methods such as cubic or

baseline can be used. The more severe detrending should be used if individual oscillations are not clearly visible on the plots due to the presence of a trend (i.e., the trend level is larger than the oscillation amplitude). You can read more about the impact of trends on the period analysis in our Zieliński et al.'s (2014) paper [7].

4. Populate the “*from*” and “*to*” fields for “*Expected periods*,” which define the range of periods that are considered to be circadian. This range affects the behavior of certain analytical methods as described in **Note 7**. The default values are from 18 to 34 h, respectively, and should be changed only if input data suggest periods outside this range.
5. Select an option from the “*Analysis Method*” drop-down list. The strengths and limitations of each method are described in our paper [7]. We recommend using two distinct methods FFT-NLLS and MESA, as these methods are based on completely different principles which permit the cross-validation. FFT-NLLS is a well-established and commonly used analysis method in the field of circadian studies, while MESA proved to be the most accurate in our method evaluations.
6. Press “**Analyse**,” which will initiate the analysis with the specified parameters, and advance to the “*Period analyses*” screen which contains details of all analysis jobs and their results.
7. The newly submitted analysis (“*job*”) is displayed at the top of the screen, and its status is continually auto refreshed until all calculations are completed (a typical analysis takes few seconds). Once completed, the status of the job is updated to *FINISHED*, and the results are available for examination.

3.4.2 Examining Results of Period Estimates

Each analysis has its own pane, which contains a summary of its parameters at the top, followed by action buttons and sections with result graphs and the numerical output values (Fig. 4). The results pane of the most recent analysis is expanded by default, while other analysis panes can be accessed by clicking their associated headers.

1. Period estimates are illustrated on a box-and-whisker plot (*see Note 8*, Fig. 4a) which shows period distributions in each group of replicates (grouping is based on the label values). The groups can be sorted in the original input order by selecting “**None**,” ordered alphabetically by data “**Labels**” or by the “**Period**” median value (Fig. 3b). Sorting by median is probably the most useful during interpretation of the results.

The individual groups can be hidden by clicking on their labels in the legend below the graph (Fig. 4c). The plot can be downloaded by pressing the button featuring the downward-pointing arrow icon (Fig. 4d), and it is saved in .svg format,

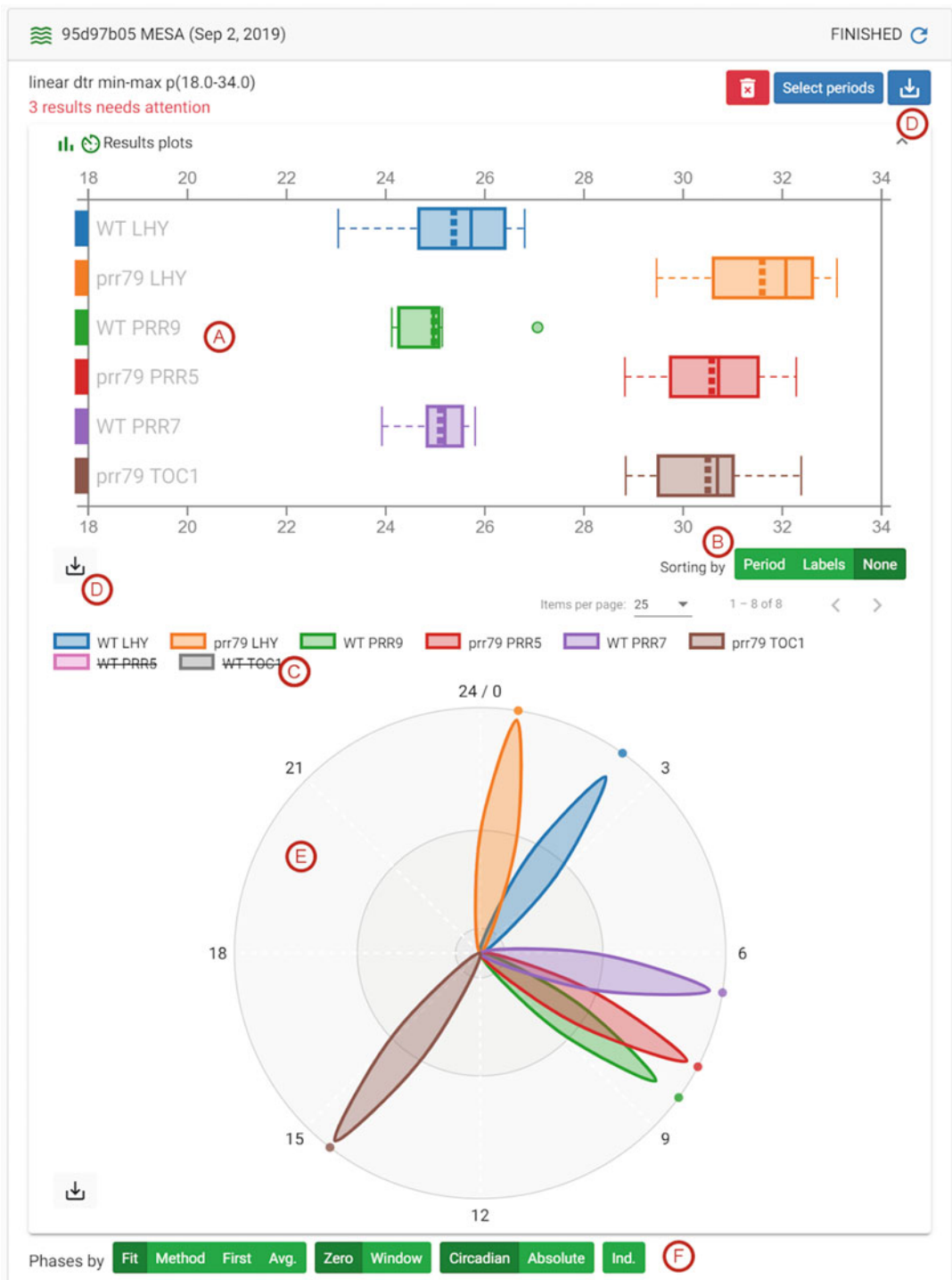


Fig. 4 Screenshot of the job pane presenting period analysis results. (a) Period values represented on a box plot. (b) Switches for ordering the plot content. (c) Clicking on a data label can hide the corresponding timeseries from the graph. (d) Download buttons for downloading numerical data or plots in SVG format. (e) Polar plot with phase values. (f) Switches that control methods for calculating phase/amplitude and their units

enabling further editing in vector graphics software such as the free Inkscape application.

2. Phase estimates are illustrated on a polar plot (Fig. 4e) showing a representation of a 24-h clock face, with hands pointing to the average phase value for each data group (with values grouped by label). Individual phase values can be drawn by pressing the “**Ind.**” button. The values can be reported relative to time point 0 by pressing “**Zero**” or relative to the start of the analysis window by pressing “**Window**” (Fig. 4f). The phases can be represented in “Circadian” units (in the range 0–24, **Note 9**) or “**Absolute**,” in which case the clock face runs from 0 to the maximum phase value in the data set (*see Note 10*). There are four ways of calculating phases: “**Fit**,” “**Method**,” “**First**,” and “**Avg.**,” which are described in detail in **Note 11** and in the BioDare2 documentation (Fig. 3f). We recommend that users calculate phase using the “*by fit*” method and report it in circadian time units (CT; 24th’s of the period). As with the period plot, there is a button to download the graph in .svg format (Fig. 4d).
3. The average values for the period, phase, and amplitude parameters of each data group are available after clicking on “**Summary statistics**” (Fig. 4g), which opens a table with the mean and standard deviation values for each parameter. Calculation of amplitude values is based on the same methods as for phase (*see Note 12*). Changing the switches next to the phase plot (e.g., selecting absolute unit, or methods for phase) also updates the values for phase and amplitude in the summary table. The number reported (“*N*”) is the number of individual timeseries included in the statistics, which may be less than the number submitted for analysis.
4. “**Individual results**” opens a table with estimates for period, phase, and amplitude estimates for each data trace. Again, the method and units for phase and amplitude calculations are set using the switches next to the polar plot. There is also an *ERR* column with an analysis error as determined by each method (for FFT-NLLS, it is relative amplitude error, RAE) and *GOF* column containing goodness of fit values as described in **Note 13**. Clicking on the “**fit**” cell value in the final column opens a popup displaying a plot of the original timeseries along with the fitted line generated by the analysis method, which is a practical method of verifying the soundness of the fit-based methods of analysis (*see Note 14*).
5. All the numerical values (for individuals and data groups) can be downloaded in tabular csv format using the download button (arrow down) at the top of the analysis pane (Fig. 4d).

6. The “**Select periods**” button at the top of the analysis pane navigates to a new screen, “*Select periods from job.*” On this screen, all the individual results are presented with radio button switches labeled “*ignored,*” allowing certain results to be excluded from the summary statistics. We would recommend using this screen to remove outliers from the results. This screen is also used to deal with multiple periodic components identified by the FFT-NLLS method; *see Note 15* for details.

3.5 Rhythm Detection

In short timeseries (e.g., 48 h), there may be only one full period within the data, so any estimate of the period value makes little sense. Typical examples are -omics data which are sparsely sampled (e.g., every 4 h) over a relatively short duration (e.g., 1 or 2 days). For these types of data, rhythmicity tests were developed. At present, BioDare2 provides an implementation of the classic JTK_Cycle test [8] and its more robust version: the empirical JTK_Cycle method [9].

3.5.1 Starting a New Rhythmicity Test

1. Click on “**Rhythmicity**” to open the “*Start rhythmicity test*” screen which contains a form for setting analysis parameters and plots of the input data being analyzed.
2. Define the “*Data window,*” i.e., the start and end time between which the timeseries will be analyzed. A value of 0 in “*from*” or “*to*” denotes from the beginning and to the end of the data, respectively.
3. In “*Input data,*” linear detrending can be performed prior to the analysis. By default, no detrending is used which is a typical approach for rhythmicity tests of -omics data.
4. The “*test method*” currently offers the classic JTK and empirical JTK (*BD2 eJTK*) methods, but the ARSER [10] implementation is underdevelopment.
5. “*Analysis Presets*” is used to define the standard curves to which the data are compared in the rhythmicity test. The default “*eJTK Classic*” pre-set analysis tests against a set of asymmetric cosine waveforms with a 24 h period, as in the original eJTK publication [9], and is recommended for typical -omics experiments. “*BD2 Classic*” is a pre-set analysis that can be used for testing against a wider period range or longer timeseries, but it has a higher rate of false negatives for typical 24-h rhythmic data.
6. Press “**Test Rhythmicity**” to start a new analysis, and the screen will update to display “*Rhythmicity tests.*”
7. The newly submitted analysis (“*job*”) is displayed at the top of the screen, and its status is automatically refreshed until all calculations are completed. Rhythmicity tests are generally slower than period estimates and can take up to 10 min.

Once completed, the job status is updated to *SUCCESS*, and the results are available for examination.

3.5.2 Examining Rhythmicity Test Results

Each analysis has its own pane, which contains a summary of its parameters at the top, followed by action buttons and the sections with the analysis results. The pane for the most recent analysis is expanded by default, while other analysis panes can be accessed by clicking the associated headers.

There is a “*P-value threshold*” parameter switch for specifying the threshold value above which the timeseries data should be rejected as arrhythmic.

At the bottom of the test pane, there is a table with individual results for each data trace. The “*Rhythmic*” column is populated with true or false values according to the test result *p*-value and the set threshold. “*emp-p*” (or “*p*”) contains the empirical *p*-value as determined by the eJTK method (or *p* for classic JTK); “*Tau*” contains the Kendall τ rank correlation coefficient. False discovery rate can be controlled with Benjamini-Hochberg correction of *p*-values. “*Show pattern*” generates a description of the standard curve that best matches the data trace, such as its period or peak time (see **Note 16**). The results can be sorted by data labels, *p*-values, or pattern properties. The numerical values can be downloaded in a csv format using the download button (the downward-pointing arrow symbol).

4 Notes

1. Timeseries data can be stored in an Excel, CSV, or TSV file in the following form: one of the columns holds the measurement time for each data point, while the other columns contain recordings of measured values at each time. The time column can represent either the actual time from the experiment start or a serial number (such as an image number) which will be converted to the time during import, depending on the value of the parameter: “*Images interval*.”

Alternatively, data can be recorded in rows rather than columns following similar principles.

Details and Constraints

- (a) Only the first data sheet is read from an uploaded Excel file.
- (b) The time column should be located before (to the left of) the first data column, although it does not have to be the first column in the sheet.
- (c) There may be missing data points in timeseries; they should be represented as blank cells in the sheet.

- (d) For time in hours, the time is represented as a fraction of an hour, so 1.25 means 1 h and 15 min.
- (e) Where time values are provided as a series of image numbers, they must be integers starting from 1 (first picture taken), and they must be taken at equal intervals as indicated by the “*Images interval*” property.

BioDare2 can also read raw data files produced by the Packard (now PerkinElmer) TopCount reader for multi-well plates. The TopCount can write data in multiple ways, so please see the current documentation of BioDare2 for details.

2. In BioDare2, time 0 should coincide with the beginning of the experimental conditions/ZT/subjective dusk/dawn. For that reason, when raw data are uploaded, then the time offset parameter can be used to adjust the time values accordingly. So, for example, if the data were recorded from 12:00 o'clock and the first point in the raw data file is recorded as time 0, but subjective dawn was at 9:00, then first data point should be corrected to have a time of 3 h. To do so, a time offset of +3 h must be specified when the raw data are uploaded.
3. One way of accounting for technical noise in the data (e.g., caused by detector dark current, light leakage, etc.) is by placing black tokens within the imaging field. The recorded values for those tokens should in principle represent a constant level of 0, so the actual measured values can be used for correction of the background noise. The timeseries described as “*Background noise*” are treated as the background levels. All “*Background noise*” columns are averaged, and the averaged background timeseries is then subtracted from all the other timeseries during the raw data import.
4. The options for detrending are the following:
 - Linear detrending** is the least intrusive detrending method; it simply applies a linear regression model to the data and subtracts the optimum fitted, straight line from the data points.
 - Cubic detrending** fits a polynomial model of degree 3 to the data and subtracts the resulting curve from the data. It may introduce artifacts for short data series or even remove the oscillations for very short data (e.g., timeseries with only one full oscillation).
 - Baseline detrending** is based on kernel smoothing. Kernel smoothing can be explained as a more sophisticated form of moving average. Once the smoothed version of the data (the trend) is found, it is subtracted from the original. This detrending works well, with the exception that the detrended data points towards the beginning and end of

the timeseries—usually the first and last half cycle of data—must be discarded.

Amp&baseline detrending removes the trend not only in the baseline but also in the amplitude. It first finds the baseline trend using the kernel smoothing procedure above and then uses it as the reference to establish the amplitude change in the data. The change in amplitude is then smoothed, giving the amplitude trend, which is used to scale the original data. The beginning and end of the data suffer from strong artifacts, but it is the only available method that can remove amplitude dampening.

The options for normalization are the following:

To $[-1,1]$ rescales the timeseries values to produce a mean value of 0 and oscillations in the range $[-1,1]$. Rescaling is achieved by subtracting first the mean value for each data point and then dividing by either peak or trough height whichever is larger.

Fold change normalizes the data set by dividing each data point by the minimum value; if the minimum value is less than or equal to 0, an empty timeseries is produced.

Z-Score calculates the number of standard deviations by which the point is above or below the mean value.

To extreme normalizes the timeseries data to 1 by dividing each data point by either the peak value or the absolute value of the trough (i.e., the positive distance between the trough and 0), whichever is greater.

5. In addition to standard sorting by label or ID, once data has been analyzed, data traces can be sorted according to the results of a period analysis or rhythmicity test, for example, by the estimated period values or significance of the rhythms.
6. The concept of phase and amplitude is consistently defined and “mathematically sound” only for cosine-like functions, $y = A \cdot \cos(x-f)$, where f is the phase parameter and A is the signal amplitude. For other waveforms, phase is linked to the peak time; amplitude is computed as half the distance between the peaks and the troughs.
7. The period range defines which period values should be considered (e.g., as circadian) by the analysis methods. Firstly, some of the methods (e.g., MESA, or periodograms) scan and discretize period values within the period range (in BioDare2 with a step of 0.1 h), calculating some statistic and then selecting a period value with the best statistic. Period range therefore determines which period values will be tested during analysis. Secondly, methods such as FFT-NLLS can find multiple period components that together describe the data.

Only those periods within the defined period range will be reported and included in summary statistics. Periods outside this range may be detected but are ignored unless user selects them (*see Note 14*).

8. A box-and-whisker plot is a standard way of showing multiple values from biological replicates. Assuming that period values are sorted, the box encompasses the interquartile range of the values from the 25% smallest value to the 75% largest (in other words, half of the data points centered around the median). The median is the middle dotted line in the box, and the mean is drawn as a solid line (they coincide if the distribution of values is symmetrical). The whiskers are at the lowest value still within 1.5 IQR (interquartile range) of the lower quartile and the highest point still within 1.5 IQR of the upper quartile. The circled points outside the box represent outliers, which in general should be removed before looking at *Summary statistics*.
9. Circadian units are scaled to 24 h using the estimated free-running period. Imagine two traces: one with a period of 24 h and peaking time at 6 h and another one with period 32 h and peaking time 8 h. In absolute units, it looks as if the phase of the second clock was delayed by 2 h (to 8 instead of 6), while in reality only its clock runs slower. The peak time is still at 1/4 of the whole cycle (8/32), which is why circadian units are better for looking at phases since they can accommodate different speeds of the underlying clocks.
10. Phases in BioDare2 are always reported in the range from 0 to period: phase $\in [0, \text{period}]$ so values should roughly coincide with the time of the peak (for circadian units phase $\in [0, 24)$). This differs from some mathematical approaches in which phase is defined from $-\text{period}/2, \text{period}/2$, but our approach is more natural in chronobiology and easier to interpret. For example, if a data timeseries peaks at 18, 42, 66, and 90 h, then the phase would be 18 h (not -6 h).
11. As only the analysis methods based on cosine fitting define the method of calculating phase, BioDare2 provides a set of options that can be used to obtain phase estimates from all period analysis methods.

In the phase “*by fit*” method, after obtaining the period value, one cosine function having that period is fitted to the data. The fitting procedure finds phase and amplitude parameters of the cosine that follows the data the most closely and reports those values as phase and amplitude. Such a phase value is well defined, but it may not coincide with the peaks in the data if the signals are not symmetrical.

As the name suggests, phase “*by first peak*” reports the time of the first peak (potentially back-calculated to 0 using the estimated period if the timeseries data do not start at 0). However, the peak is found in the fit that has been generated by the analysis method rather than a peak in the original data. Phase “*by average peak*” finds one peak per period in the generated fit and uses their times to calculate circular averages (modulo period and wrapping around zero).

Phase “*method*”-specific reports the phase using the original approach of the analysis algorithm. For FFT NNLS, it is the phase of the main circadian component found by the method. If FFT-NLLS finds only one component, the value should be the same as phase by fit; otherwise they may be slightly different. MESA does not define phase, so phase by fit is reported here instead.

12. Amplitude depends on the estimation method selected for the phase. Phase “*by fit*” reports the amplitude of the fitted cosine. Phase “*by first peak*” amplitude is calculated using the first trough and peak (of the method fit). Phase “*by average peak*” amplitude is calculated using trough and peak values in each periodic cycle.
13. Goodness of fit (GOF) is defined as the ratio of two errors: the method fit error, i.e., the error between the original timeseries and the curve predicted by the user-selected algorithm, and the “polynomial fit error,” i.e., the error between the original timeseries and a polynomial (cubic) curve fitted to the timeseries. The ratio can vary from 0 (where the model provides a perfect fit) to a large number, indicating that the model is no better than (or is worse than) a cubic fit to the data.
14. MESA is not a fit-based method; it does not fit a curve to the data. It finds a model that generalizes the input data as combinations of preceding and subsequent points. BioDare2 uses this model to simulate a fit; however, it may produce artifacts at the first and last few data points.
15. The analysis pane may contain a message like “5 results needs attention,” which would mean that for five data traces, the method found period values but these were not automatically included in the *Summary statistics*. The “**Select periods**” button allows the inspection of results details and manual corrections. Those time series which yielded a period outside the specified circadian range or have multiple circadian periods will be listed first (in red). In order to reproduce the complex signal shape, FFT-NLLS often finds multiple oscillating components that need to be composed in order to give a good data fit. If more than one of them has a period inside the circadian range, then the user must decide which should be treated as the

“correct” component. It is possible to view the period analysis fit graph which shows the original timeseries, the method fit, and the cosines for each of the proposed periods. That is the easiest way to decide which period value should be selected, since it should be the cosine which most closely follows the input data on the graph.

16. The periodic properties (such as period and peak time) of pattern curves used for testing with JTK methods are often reported as period values of the data. We strongly discourage such an approach. Data sets collected from experiments of shorter durations (i.e., a duration of less than 48 h) cannot give meaningful period estimates, and it would be even more inappropriate for such “period” values to be reported for data collected over only 24 h. Our tests also demonstrated that for typical cases of timeseries with a period in the range of 22–26 h and measured over 48 h, the rhythmicity tests performed better when using the smaller pre-set of cosines with only 24 h than a pre-set spanning 22–26 h. Obviously, JTK always reports only the 24-h period when using the smaller pre-set.

Acknowledgments

Funded by the European Commission through FP7 Integrated Project TiMet (award 245143), by the Wellcome Trust (award 204804/Z/16/Z) and by the Biotechnology and Biological Sciences Research Council (BBSRC) through the Centre for Systems Biology at Edinburgh [BB/D019621] and UK Centre for Mammalian Synthetic Biology [BB/M018040].

References

1. Plautz JD, Straume M, Stanewsky R, Jamison CF, Brandes C, Dowse HB, Hall JC, Kay SA (1997) Quantitative analysis of drosophila period gene transcription in living animals. *J Biol Rhythms* 12:204–217. Erratum in: *J Biol Rhythms* 1999 14:77
2. Edwards KD, Akman OE, Knox K, Lumsden PJ, Thomson AW et al (2010) Quantitative analysis of regulatory flexibility under changing environmental conditions. *Mol Syst Biol* 6:424
3. Burg JP (1972) The relationship between maximum entropy spectra and maximum likelihood spectra. *Geophysics* 37:375–376
4. Enright JT (1965) The search for rhythmicity in biological time-series. *J Theoret Biol* 8:426–268
5. Lomb NR (1976) Least-squares frequency analysis of unequally spaced data. *Astrophys Space Sci* 39:447–462
6. Costa MJ, Finkenstädt B, Roche V, Lévi F, Gould PD et al (2013) Inference on periodicity of circadian time series. *Biostatistics* 14 (4):792–806
7. Zielinski T, Moore AM, Troup E, Halliday KJ, Millar AJ (2014) Strengths and limitations of period estimation methods for circadian data. *PLoS One* 9:e96462. <https://doi.org/10.1371/journal.pone.0096462>
8. Hughes M, Hogenesch J, Kornacker K (2010) JTK CYCLE: an efficient non-parametric algorithm for detecting rhythmic components in genome-scale datasets. *J Biol Rhythm* 25:372–380. <https://doi.org/10.1177/0748730410379711>

9. Hutchison AL, Maienschein-Cline M, Chiang AH et al (2015) Improved statistical methods enable greater sensitivity in rhythm detection for genome-wide data. *PLoS Comput Biol* 11 (3):e1004094. <https://doi.org/10.1371/journal.pcbi.1004094>
10. Yang R, Su Z (2010) Analyzing circadian expression data by harmonic regression based on autoregressive spectral estimation. *Bioinformatics* 26(12):i168–i174. <https://doi.org/10.1093/bioinformatics/btq189>

Open Access This chapter is licensed under the terms of the Creative Commons Attribution 4.0 International License (<http://creativecommons.org/licenses/by/4.0/>), which permits use, sharing, adaptation, distribution and reproduction in any medium or format, as long as you give appropriate credit to the original author(s) and the source, provide a link to the Creative Commons license and indicate if changes were made.

The images or other third party material in this chapter are included in the chapter's Creative Commons license, unless indicated otherwise in a credit line to the material. If material is not included in the chapter's Creative Commons license and your intended use is not permitted by statutory regulation or exceeds the permitted use, you will need to obtain permission directly from the copyright holder.





Detection and Analysis of Circadian Rhythms Via Prompt Chlorophyll Fluorescence

Yuri Dakhiya and Rachel Green

Abstract

Monitoring prompt chlorophyll fluorescence (F) by making consecutive pulse amplitude modulation (PAM) measurements is a noninvasive, nondestructive, potentially high-throughput technique for evaluating circadian rhythms in diverse plant species. The technique is also less labor-intensive than many others currently used and requires no transgenic procedures.

Keywords Chlorophyll fluorescence, Circadian, Photosynthesis

1 Introduction

Despite growing interest in the field of plant chronobiology, many of the methods used for measuring circadian rhythms are either labor-intensive or exclusively suited to a few model plants. This makes it harder for researchers to lay the groundwork for new studies or to explore rhythms in important non-model plant species such as agriculturally relevant plants. The finding that chlorophyll fluorescence is under circadian control has opened up the possibilities of new platforms for analyzing circadian rhythms.

Light energy absorbed by chlorophyll molecules results in singlet-state excited molecules (Chl*) that can return to the ground state by photosynthesis (quantum yield), dissipation as heat (non-photochemical quenching), or re-emission as fluorescence [1]. At room temperature, most chlorophyll fluorescence is from PSII and can be divided into two types: prompt and delayed. Prompt chlorophyll fluorescence [F, within ~ 2 ns; [2]] originates from chlorophyll molecules that have been excited directly by light or fast exciton energy transfer from other chlorophyll molecules. Delayed chlorophyll fluorescence [DF, seconds time scale] is from the regeneration of the excited state of the primary donor of PSII,

P680, under conditions (such as dark) in which forward electron transfer is blocked and electrons flow back from the secondary electron acceptor, quinone Qb, of PSII to the Mn cluster [3]. DF is at least two orders of magnitude less intense than F but, due to its uphill energetics, is emitted for a long time after the disappearance of F. DF was the first fluorescence to be utilized for circadian measurements [4–6]. Recently, several F parameters were also shown to be under circadian control [7, 8].

F can be measured by means of a pulse amplitude modulation (PAM) protocol that involves inducing chlorophyll fluorescence by applying high-intensity light flashes and imaging the plants with a fluorescence camera. Various F parameters may be measured directly or calculated, including quantum yield and non-photochemical quenching [9]. Generally, researchers use PAM to obtain data from a single or a few fluorescence images, to compare treatments or different plant species. However, imaging can also be carried out over longer time periods, and we describe here how F may be used as a robust high-throughput tool to measure circadian rhythms. Our method involves monitoring F parameters at set intervals over the course of several days and using FFT-NLLS analysis of the resulting F data to identify circadian phenotypes, such as period and amplitude in different plant species, accessions, or mutants (Fig. 1).

2 Materials

Measuring circadian-controlled F requires a growth chamber with accurate and precise light and temperature regulation. Our chamber is equipped with an LED light panel with four light arrays—red (615 nm) and blue (450 nm) actinic lights, supersaturating 5700 K white light, and far red light (735 nm). The light array and F-imaging camera are installed within the growth chamber and are connected to an outside computer from which they can be controlled by an operator. Each experiment is automatically run by a script which specifies the actions and timing of the measuring equipment. The system has to be capable of executing the F measurement protocol at set intervals (our script includes measurements in 2-h intervals) for long periods of time. Each measurement is done according to protocols that vary in measurement time and measured F parameters.

Our system (FS-FI-2200 growth chamber, an Open FluorCam and the FluorCam 7 software) was obtained from Photon Systems Instruments (PSI) <http://psi.cz/contacts/>. Similar systems can be purchased from other manufacturers such as Heinz Walz GmbH. We used the quenching with actinic light protocol provided by PSI. Our versions of the PSI protocol and scripts, customized for circadian measurements, are available on our laboratory website.

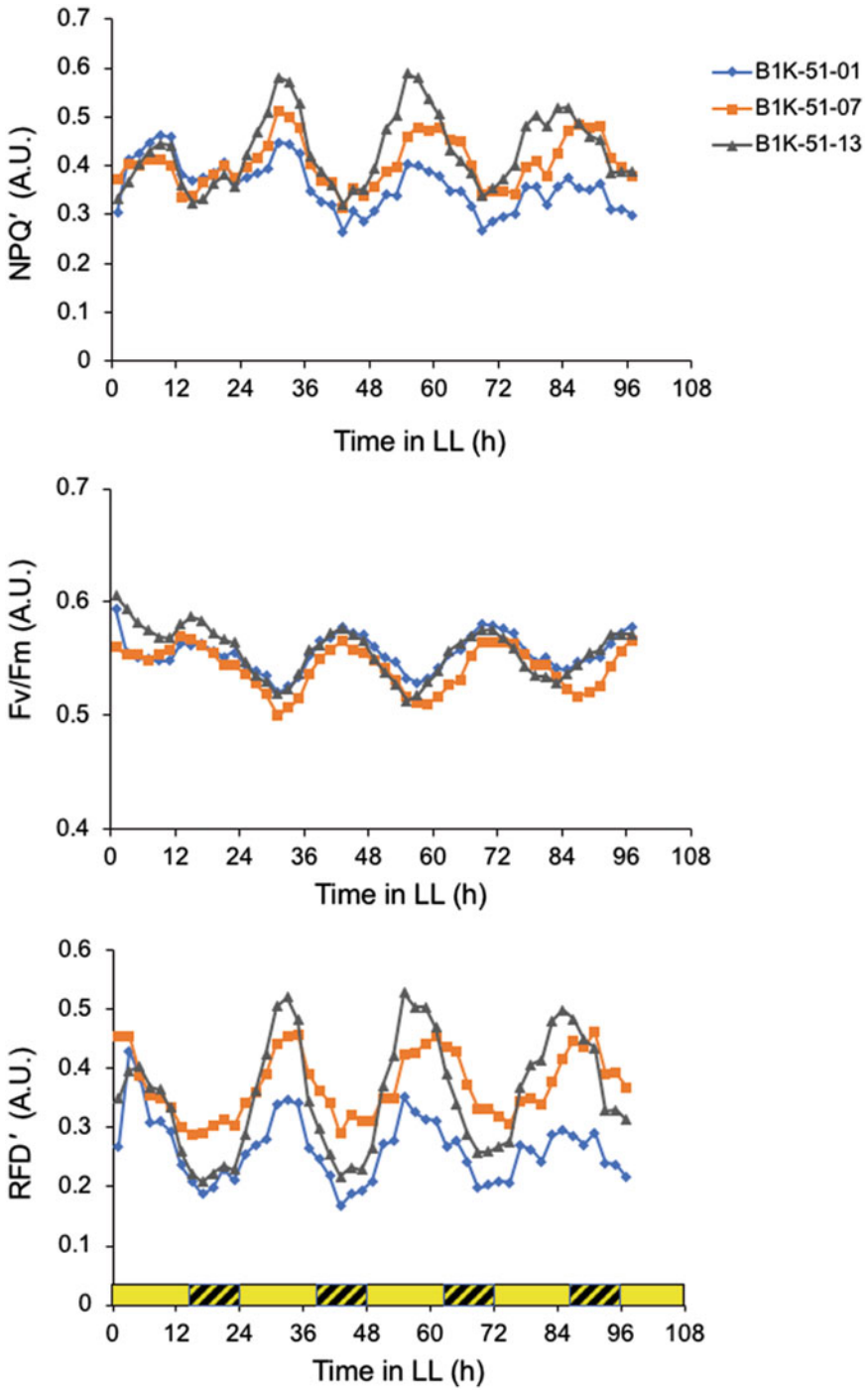


Fig. 1 Daily changes in three fluorescence-related parameters in constant light conditions in wild barley. (a) NPQ', (b) Fv/Fm, and (c) RFD' in wild barley plants collected from three sites (01,07,13) in Mount Meron, Israel. Yellow bars indicated subjective day, and dashed bars indicate subjective night

2.1 System Setup

1. Make sure the light arrays and camera are responsive to the system software.
2. Place a light meter below the camera and measure the capacity of the light array that is needed in order to reach a light intensity of $200 \mu\text{E m}^{-2} \text{s}^{-1}$ (*see Note 1*).
3. Move the light meter sideways and define the area in which the light intensity decreases no more than $50 \mu\text{E m}^{-2} \text{s}^{-1}$. This will be the appropriate field of vision for the camera. Make sure the plants to be measured are placed only in this area.
4. Download the following files from our website <http://www.rachelgreenlab.com/resources.html>: **Quenching F protocol**, **LD acclimation script** and **Circadian LL conditions script** (*see Note 2*).
5. Place the **Quenching F protocol** file in the following directory: C:\Users\Owner\Documents\FluorCam7\protocols. Place the **LD acclimation script** and the **Circadian LL conditions script** in the following directory: C:\Users\Owner\Documents\FluorCam7\scripts.

3 Methods

3.1 Determining Light Intensities for the Experiment

The experimental setup uses different light conditions with varying light qualities and intensities. In the Fluorcam7 program, the light intensities are described in terms of capacity percentage for each light array. Prior to the experiment, you will need to establish how capacity values in the program translate to light-intensity values in $\mu\text{E m}^{-2} \text{s}^{-1}$ for each light array. This part of the guide will teach you how to calibrate the light arrays for your experiments.

1. Setting the **actinic protocol light conditions**: Protocol actinic light drives photosynthesis while the F measurements are being made. In the PSI system actinic blue light is provided by the act2 array. Place a light meter below the camera and determine the capacity of the act2 light array that is needed in order to reach a light intensity appropriate for your plants (*see Note 3*); we recommend $200 \mu\text{E m}^{-2} \text{s}^{-1}$. In the PSI system, the light intensity provided by the light array can be adjusted in the “Live” view folder in the light intensities section (Fig. 2d, e). If you are using another platform, please check the system instructions for actinic light array controls and find the light capacity that provides the plants with $200 \mu\text{E m}^{-2} \text{s}^{-1}$ of light. Note the act2 light array capacity value that corresponds to the appropriate light intensity for your plants for later use.
2. Setting the **normal actinic light conditions**: Normal actinic light is used during the acclimation period and between F measurements. Normal actinic light is comprised of blue and

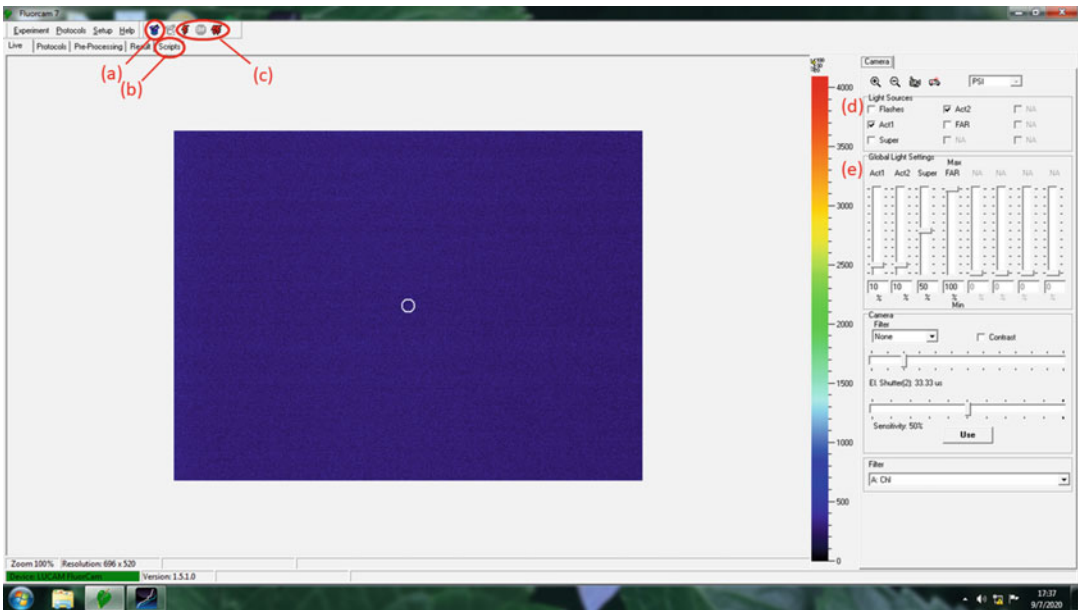


Fig. 2 Experimental setup screen in FluorCam 7. Use this screen to establish the parameters of the experiment. Use the protocol wizard tool (a) to select a measurement protocol. Use the script folder (b) to select and to customize the script for the experiment. Essential operation icons (c) such as single measurement, stop script, and start script experiment are arranged from left to right, respectively. The light source panel (d) allows turning on/off of specific light arrays installed in the experimental system. The light settings panel (e) controls the capacity of lighting provided by each array

red lights provided, in the PSI system, by the act2 and act1 arrays. Place a light meter below the camera and measure the capacity of act2 and act1 light arrays needed in order to reach a light intensity appropriate for your plants (*see Note 3*). For *Arabidopsis* we recommend $200 \mu\text{E m}^{-2} \text{s}^{-1}$ of 50% blue and 50% red light. The light intensity provided by the light array can be adjusted in the “Live” view folder in the light intensities section (Fig. 2d, e). If you are using another platform, please check the system instructions for actinic light array controls and find the light capacity that provides the plants with $200 \mu\text{E m}^{-2} \text{s}^{-1}$ of light. It is important for the normal actinic light conditions to match the actinic protocol light conditions in terms of total light intensity. Note the act2 and act1 light array capacity values that correspond to the appropriate light intensity for your plants.

3. Setting the **saturation light conditions**: Saturating light is the rapid series of high-intensity light flashes that induce F during the measurements. Saturating light is provided by the super array. Place a light meter below the camera and measure the capacity of the super light array necessary for a light intensity that is at least ten times the actinic light intensity in the

experiment (*see Note 3*); we routinely use $2250 \mu\text{E m}^{-2} \text{s}^{-1}$. The light intensity can be changed from in the “Live” view folder in the light intensities section (Fig. 2d, e). If you are using another platform, please check the system instructions for actinic light array controls and find the light capacity that provides the plants with $2250 \mu\text{E m}^{-2} \text{s}^{-1}$ of light. Note the super light array capacity value that corresponds to the appropriate light intensity for your plants.

3.2 Plant Placement and Acclimation

Even if plants were previously entrained in a different growth chamber, we found that allowing the plants to entrain for at least 24 h in the measurement chamber before the start of the measurements significantly reduced the noise in the experiment (*see Note 4*).

1. Place the plants in the effective measurement zone inside the chamber.
2. Plants with high growth rates, such as some cereals, may change their orientation toward the camera during the course of the experiment. We suggest gently pinning the leaves down horizontally.
3. Figure 2 shows the FluorCam screen for establishing the experiment. Open the script folder (Fig. 2b) and load an acclimation script with a day-night cycle in a normal actinic light intensity and no measurements. If you are using a non-PSI platform, program your script according to these parameters. We recommend using the **LD acclimation script** file provided by our lab.
4. In the script, look for the command lines that start with the phrase (define-action), some of these commands turn on/off the different light arrays in your experiment. Make sure that the capacity values for the light arrays match the required light intensity of the **normal actinic light conditions** (*see* Subheading 3.1, step 2) (*see Note 5*). You can also customize the time of lights on and lights off using the (define-action) commands. We recommend to set the times of lights on and lights off to match the conditions the plants grew in previous to the experiment in order to reduce noise during the experiment. Make sure to issue the commands for the two light arrays at least 1 s apart as demonstrated in our provided script (*see Note 11*).
5. In the “Live” view folder, set the act1 and act2 light arrays to the capacity values that correspond to **normal actinic light conditions** (*see* Subheading 3.1, step 2) (Fig. 2d, e), before running the script (*see Note 6*).
6. Run the **LD acclimation script** for at least 1 full day by pressing the start script experiment button (Fig. 2c).

3.3 Determining Measurement Areas

The next step is to make a test image and define the plant leaf areas in the image that the data will be collected from. The areas of interest are saved in a “mask” file.

1. Use the protocol wizard tool (Fig. 2a), select the **Quenching F protocol**, and take a single image of the plants in the chamber by pressing the single measurement button (Fig. 2c).
2. After the image is taken, the program will shift automatically to the pre-processing folder and present the measured image. Use the area selection tool (Fig. 3c) to define areas of interest on the plants (*see Note 7*).
3. Use the sliding scale to determine the appropriate signal intensity for the experiment (Fig. 3b). All measured areas of interest should be visibly green, indicating strong fluorescence detection, while noise, indicated by red pixels, should be minimal. Make sure that a prompt stating the index of the measured area is visible (*see Note 8*).
4. Save the areas of interest placement pattern to create a “mask” file. Click the save icon in the area selection section (Fig. 3d).

3.4 Protocol and Script Selection

In order to carry out automated fluorescence measurements, a script and a protocol are needed (available from our laboratory). Note that our scripts and protocol are already adjusted for many of the following steps:

1. Use the protocol wizard tool (Fig. 2a) and select the **Quenching F protocol** provided by our lab (*see Note 9*).
2. Set the capacity value of the act2 light array (protocol code line 7) to a value corresponding to **actinic protocol light conditions** intensity you determined earlier (*see Subheading 3.1, step 1*). In the protocol, only one of the two actinic light arrays will be used.
3. Set the capacity value of the super light array (protocol code line 8) to the value corresponding to **saturating light conditions** intensity you determined earlier (*see Subheading 3.1, step 3*).
4. Go to the scripts folder (Fig. 2b) and press the load icon. Select the **Circadian LL conditions script** with measurements every 2 h and 15 min of dark adaptation (*see Note 10*).
5. Verify that the light capacity used in the (define-action) commands in the script corresponds to the **normal actinic light conditions** intensities you determined earlier (*see Subheading 3.1, step 2*).
6. In the (define-action) script command lines, make sure to issue commands to turn the lights off 15 min before the

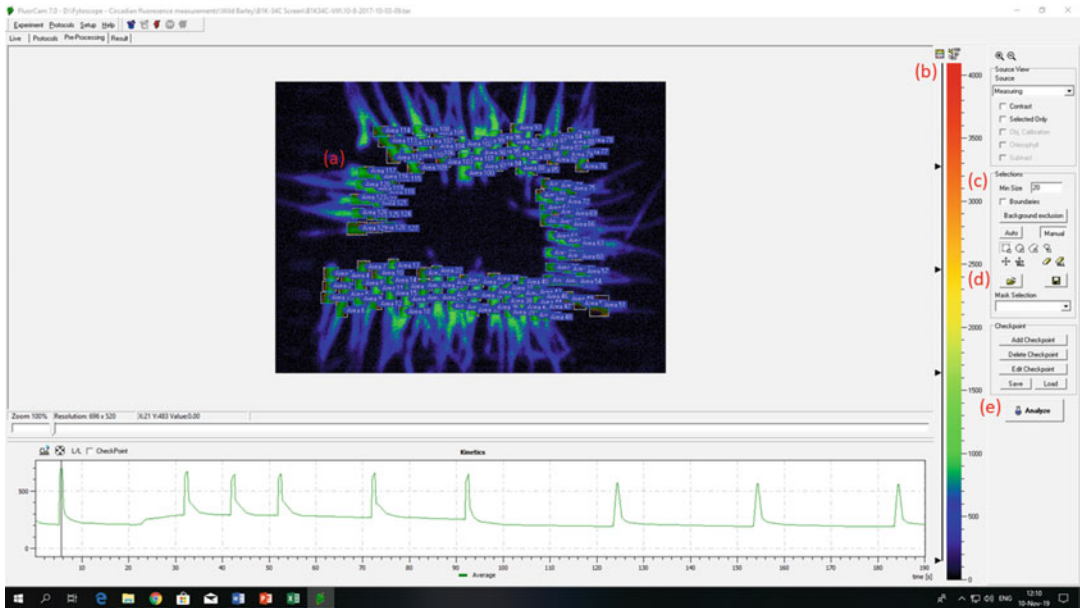


Fig. 3 Pre-processing screen in FluorCam 7. Wild barley leaves are being imaged in this experiment. Three areas of interest have been established on each leaf, (a) and data will be extracted for each of these areas. The signal intensity scale (b) can be adjusted for an optimal signal/noise ratio and should be maintained at a constant level in all measurements throughout the experiment. The area selection screen (c) is used to assign areas of interest. The minimum size parameter can be lowered if the areas of interest are relatively small and are not registered as a proper signal (*see Note 8*). The load/save areas icon (d) can be used to load or save a mask file which is an area of interest placement pattern. The analysis button (e) will extract data from the areas of interest once all other parameters are set

measurement for the purpose of dark adaptation [already present in the provided script] (*see Note 11*).

7. Issue a command in the script to turn the lights on again at the **normal actinic light conditions** intensities you determined earlier (*see Subheading 3.1, step 2*), 5 min after measurement times [this is already present in the provided script but may require adjustment].
8. In between measurements, the light should always be on except during the dark adaptation periods, 15 min before each measurement. Use the **normal actinic light conditions** intensities you determined earlier (*see Subheading 3.1, step 2*) [already present in the provided script but may require adjustment] (*see Note 11*).
9. Make sure that commands to turn the lights off and on for the two actinic light arrays do not have similar timestamps. Issue the commands to the light arrays at least 1 s apart [already present in the provided script] (*see Note 12*).
10. It is recommended to make the script apply the mask automatically rather than applying it manually for each image. In the

code line (shapes – load “c:\fytoscope\maskbar.sel”), change the term “maskbar” to the name of your relevant mask file.

11. Make sure that images are saved in the: C:/fytoscope directory. Make sure the code line (define path “c:\fytoscope\”) is present [already present in the provided script].
12. Press the Start Script Experiment button to start an automated experiment (Fig. 2c).
13. Stop the experiment 4 days after activation (Fig. 2c).

3.5 Data Processing

1. Once the experiment is over, you will have a .tar file for every measurement taken during the course of the experiment.
2. Open each .tar file individually. If the areas of interest are not visible, load the mask file manually (Fig. 2d) (*see Note 13*). Adjust the sliding scale of signal intensity to the optimal spot you determined earlier (Fig. 2b) (*see Subheading 3.2, step 3*). It is important to make sure that the scale is approximately at the same position in every measurement (*see Note 14*).
3. Press analyze and export the numeric values (Fig. 3e). This will extract the mean numeric values for each F parameter in each areas of interest and save it as a .text file (Fig. 4b).
4. Aggregate all .text files into one Excel file. Paste the data from each experiment one after the other in the same folder.
5. Use the Sort option in Excel on the first column containing the F parameter titles. This will rearrange the data to present all values of the same parameter together. The first value is from the first F measurement, the second from the F measurement 2 h later, etc.

3.6 Rhythm Analysis

Various tools exist for the analysis of plant circadian rhythms. BRASS (Biological Rhythms Analysis Software System) is an established and widely used tool but can be challenging to install on new computer systems. BioDare2 is a newer tool for rhythm analysis with distinct advantages; as an online tool, BioDare2 requires no installation, which reduces compatibility issues with your computer platform. Moreover, BioDare2 features a user-friendly interface which makes all analysis options clear and visible. We provide instructions for both the BRASS system and the novel BioDare2.

3.6.1 Rhythm Analysis with BRASS

1. Import the data for the selected markers into the Biological Rhythms Analysis Software System (available from <http://www.amillar.org>) (*see Note 15*).
2. Load your BRASS compatible Excel file and select “derandomize data,” after which you will be prompted to continue to an FFT-NLLS analysis. Through the FFT-NLLS procedure, you

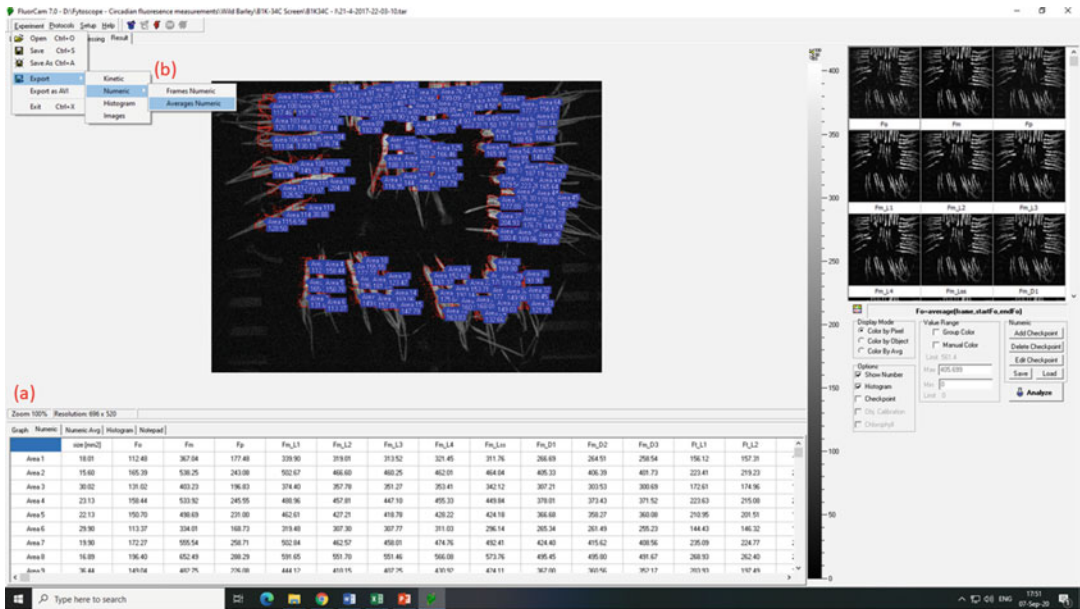


Fig. 4 The results screen in FluorCam 7. A numeric results table (a) specifies the values extracted for each measured parameter. The measured parameters are determined by the selected experiment protocol. Use the export average numeric results command pathway (b) to convert the data to a text file

will obtain the circadian phenotypes (period time, amplitude, and RAE) for the measured plants.

3. We suggest obtaining the circadian phenotypes for several F parameters and then calculating the mean circadian traits for each experimental group.

3.6.2 Rhythm Analysis with BioDare2

1. Enter the BioDare2 website (<https://biodare2.ed.ac.uk/>) and register.
2. Upload your Excel file in the “New experiment” tab (see Note 15).
3. Select “Start period analysis” and choose how to input the data in the “Input Data” option. You can choose to input raw data or use a detrending method which will apply a correction to the data and might help reduce the effect of experimental noise. We suggest using linear detrending. Select an analysis method to obtain circadian phenotypes; we suggest using FFT-NLLS.
4. We suggest obtaining the circadian phenotypes for several F parameters and then to calculate the mean circadian traits for each experimental group.

4 Notes

1. Throughout the entire process, the FluorCam 7 program will refer to light intensity in terms of capacity percentage. You will need to make sure that you know how the capacity percentages translate to light intensity in $\mu\text{E m}^{-2} \text{s}^{-1}$ units for all light arrays.
2. Protocols contain the specifics of the measurement process. We will use the “**Quenching F protocol.**” Scripts specify what action the system should execute and at what time, for example, a script can issue a command to measure at 14:00. The measurement will be done according to the selected protocol. We will use the “**LD acclimation script**” for plant acclimation the chamber and the “**Circadian LL conditions script**” for the actual experiment.
3. The intensity of actinic light necessary for photosynthesis may vary between plant species. For example, in our experiments, $200 \mu\text{E m}^{-2} \text{s}^{-1}$ was sufficient for *Arabidopsis*, but $400 \mu\text{E m}^{-2} \text{s}^{-1}$ was required for tomatoes which have a higher light requirement. Saturating light which is used to induce prompt fluorescence should be in an order of magnitude higher intensity than the actinic light; we recommend working with saturating light with an intensity of at least $2000 \mu\text{E m}^{-2} \text{s}^{-1}$.
4. Plants are very sensitive to light quality, humidity, and temperature. Entraining the plants in the growth chamber used for measurements reduces noise in the data at the beginning of the experiment time frame.
5. (define-action) command lines are the orders that tell the system which actions to execute and at what times. Some actions change the work capacity of the light arrays; these contain the phrase (action-set-light) and refer to a specific light array. Others are responsible for taking measurements according to the selected protocol; these contain the phrase (action-measuring). Note that the **LD acclimation script** does not contain measurement commands since it is used exclusively for plant acclimation to the chamber.
6. It is important to note that the script will not perform actions retroactively. The program will turn lights on/off and measure only at the specified time of day. Before starting a script, manually adjust the light conditions to the appropriate value.
7. Several recent studies have shown tissue-specific circadian rhythmicity, for example, leaves display a higher circadian variability than shoot apical meristem [10]; we therefore suggest creating multiple measurement areas on the same plant to account for possible intra-tissue variance in circadian rhythms

(Fig. 3a). We also use at least four plants for each experimental group.

8. The Quenching F protocol contains an elaborate set of consecutive fluorescence measurements in varying conditions. This protocol will allow you to obtain many fluorescence, photosynthetic, and non-photochemical quenching-related parameters. If you want to read more about the quenching protocol or would like to compare it to a protocol used in a non-PSI system, please consult the FluorCam operational manual V2.0 (page 8) available at the PSI website.
9. Green pixels indicate that a strong fluorescent signal is detected. Red pixels indicate a weak fluorescent signal which is typically accounted to experimental noise. Red plant edges are common and pose no problem, but make sure that the main leaf body is colored in green and the non-biological background does not give off a fluorescent signal (Fig. 3a). If a prompt stating the number of the measured area is not visible next to the area of interest, it means that the area has not been registered by the program. This usually results from insufficient intensity, which is easy adjusted by the sliding scale (Fig. 3b), or due to a relatively small fluorescent region; in this case it is possible to lower the minimum size in the area selection menu (Fig. 3c) to ensure that small fluorescent areas are registered and measured.
10. Decreasing the interval between measurements is not recommended as the light flashes and period of dark adaptation might interfere with the assumption of constant conditions if conducted too often.
11. The dark period before measurement is called dark adaptation. A reliable measurement of several F parameters, especially NPQ, depends on the plant being dark adapted, so that there is no electron flow between PSII and PSI at the beginning of the measurement [11]. In order to maintain a balance between the need for a dark adaptation period and the need for constant condition during the circadian experiment, we suggest working with a dark adaptation duration of 15 min. It may not be full dark adaptation for some plants but is certainly substantial. If you measure negative values of NPQ throughout the experiment, we suggest increasing the length of the dark adaptation but make sure not to compromise the constant conditions assumption.
12. If two actions are scheduled for exactly same time, the program will only perform one of the commands. The commands must be kept at least 1 s apart.

13. This can occur if the proper command for mask loading was not issued in the script at the start of the experiment. The data can still be analyzed, but the mask must be applied manually.
14. The sliding scale (Fig. 3b) will artificially increase or decrease the intensity of detected fluorescent. Try to maintain the scale at the same position. Small deviations will not result in significant change, but large deviations (of around 300 pixels) will introduce noise that will make the circadian rhythms harder to detect.
15. We use NPQ', Fv/Fm, and RFD' as circadian rhythm markers since they show robust, coordinated oscillation and are relevant to other important physiological aspects. NPQ' is the steady-state non-photochemical quenching in light, Fv/Fm is the PSII quantum yield in light-adapted steady state, and RFD' is an empiric parameter used to assess plant vitality based on the fluorescence decline ratio in steady state. Note that the nomenclature for F parameters may vary [7].

Acknowledgments

This research was supported by the Israel Science Foundation (81/7681) and the United States-Israel Binational Science Foundation (2015316).

References

1. Croce R, Van Amerongen H (2014) Natural strategies for photosynthetic light harvesting. *Nat Chem Biol* 10:492–501
2. Kalaji HM, Goltsev V, Bosa K et al (2012) Experimental in vivo measurements of light emission in plants: a perspective dedicated to David Walker. *Photosynth Res* 114:69–96
3. Keren N, Berg A, Van Kan PJ et al (1997) Mechanism of photosystem II photoinactivation and D1 protein degradation at low light: the role of back electron flow. *Proc Natl Acad Sci U S A* 94:1579–1584
4. Gawronski P, Ariyadasa R, Himmelbach A et al (2014) A distorted circadian clock causes early flowering and temperature-dependent variation in spike development in the *eps-3Am* mutant of einkorn wheat. *Genetics* 196:1253–1261
5. Goltsev V, Chernev P, Zaharieva I et al (2005) Kinetics of delayed chlorophyll a fluorescence registered in milliseconds time range. *Photosynth Res* 84:209–215
6. Gould PD, Diaz P, Hogben C et al (2009) Delayed fluorescence as a universal tool for the measurement of circadian rhythms in higher plants. *Plant J* 58:893–901
7. Dakhiya Y, Hussien D, Fridman E et al (2017) Correlations between circadian rhythms and growth in challenging environments. *Plant Physiol* 173:1724–1734
8. Litthauer S, Battle MW, Lawson T et al (2015) Phototropins maintain robust circadian oscillation of PSII operating efficiency under blue light. *Plant J* 83:1034–1045
9. Nedbal L, Soukupova J, Kaftan D et al (2000) Kinetic imaging of chlorophyll fluorescence using modulated light. *Photosynth Res* 66:3–12
10. Takahashi N, Hirata Y, Aihara K et al (2015) A hierarchical multi-oscillator network orchestrates the Arabidopsis circadian system. *Cell* 163:148–159
11. Murchie EH, Lawson T (2013) Chlorophyll fluorescence analysis: a guide to good practice and understanding some new applications. *J Exp Bot* 64:3983–3998



High Spatial Resolution Luciferase Imaging of the *Arabidopsis thaliana* Circadian Clock

Mark Greenwood, Anthony J. W. Hall, and James C. W. Locke

Abstract

The *A. thaliana* circadian clock is an example of a gene network that generates rich temporal and spatial dynamics. Bioluminescent imaging has proven a powerful method to help dissect the genetic mechanisms that generate oscillations of gene expression over the course of the day. However, its use for the study of spatial regulation is often limited by resolution. Here, we describe a modified luciferase imaging method for the study of the *Arabidopsis* circadian clock across the plant at sub-tissue-level resolution.

Keywords Circadian clock, Luciferase, High resolution, Spatial, Imaging, Tissue specific, Coordination

1 Introduction

The circadian clock is an endogenous oscillator that generates rhythms in physiology, from the cellular to the ecosystem scale [1]. Environmental inputs entrain an oscillating network of molecules to the day-night cycle. These oscillations then regulate various aspects of physiology, matching them to the optimum time of day. Recently, a number of studies have demonstrated spatial differences in the regulation of plant clocks. Clocks in different parts of the plant receive different inputs [2, 3], can be wired differently [4–7], and regulate different aspects of physiology [5, 8, 9].

The firefly *LUCIFERASE* (*LUC*) reporter gene is often utilized for the study of circadian gene expression. By fusing the promoter of the gene of interest to the *LUC* protein-coding region, levels of transcription can be monitored non-destructively over several days [10, 11]. Typically, expression of *LUC* is measured across the entire seedling or groups of seedlings, ignoring cell- or tissue-specific differences. The use of fluorescent reporter proteins to examine clock gene expression in individual cells has been used to address

this limitation [12, 13]. This approach has been extended to allow the tracking of clock gene expression across seedlings for several days [14]. However, experiments remain technically challenging and low throughput.

Adaptations to luciferase imaging methods for higher spatial resolution have also had success. Modified split luciferase assays have been successfully applied for the tissue-specific measurement of rhythms [5, 15]. Alternatively, tissue- or sub-tissue-level resolution can be achieved by modifying only the camera optics [2, 3, 16–19]. We recently applied such an assay for measuring rhythms across entire seedlings in vivo [3]. Here, we describe the details.

2 Materials

1. Charge-Coupled Device (CCD) camera (Retiga LUMO; QImaging, Canada; *see Note 1*).
2. Desktop personal computer (PC; *see Note 2*).
3. Growth incubator chamber (MIR-154; Panasonic, Japan).
4. Red and blue 12 V light emitting diodes (LEDs; *see Note 3*).
5. High transmission C-mount lens (Xenon 25 mm f/0.95; Schneider, Germany).
6. 5-mm optical spacer (Cosmicar, Japan; *see Note 4*).
7. Microcontroller development board (Uno; Arduino, USA).
8. Arduino firmware source code for Micro-Manager (available from: micro-manager.org/wiki/Arduino#Firmware).
9. Arduino IDE (V1.8.10; Arduino, USA).
10. Micro-Manager microscopy software (V2.0; Open Imaging).
11. We use *Arabidopsis* lines transformed with constructs containing the promoter region of clock genes fused to the *LUC+* reporter gene (*see Note 5*). Many such lines have already been introduced into a range of different ecotypes and genetic mutants by a range of laboratories. Much of these are available from seed stock centers (e.g., NASC, UK).
12. One-half strength Murashige and Skoog (MS) supplemented agar medium: 2% agar, MS salts, pH adjusted to 5.7, without sucrose.
13. Watchmaker forceps.
14. 5 mM D-Luciferin potassium salt solution in 0.01% Triton-X100 (*see Note 6*).
15. 20 mL amber glass bottle with pump vaporizer (*see Note 7*).
16. 25 mm width black strong adhesive tape.
17. 100 mm × 100 mm laboratory jack.

18. Matte black aluminum foil tape (*see Note 8*).
19. Imaris microscopy image analysis software (BitPlane, Switzerland; *see Note 9*).

3 Methods

3.1 Description of the Imaging Setup

Time-lapse luciferase imaging requires taking images at regular intervals while the environmental conditions are carefully controlled. In this section we describe the hardware and software required for doing so, with the modifications required for increased resolution.

Imaging experiments are performed inside of a growth incubator for the careful control of temperature and light (Fig. 1). The incubator keeps the temperature constant; for our experiments, we set this to be 22 °C. The light is provided by a custom-made LED array retrofitted to the chamber (*see Note 3*). The array consists of red (632 nm) and blue (464 nm) LEDs wired in series to create an interweave of colors. Since each individual red LED produces slightly less energy than the blue, the array is designed to include a slightly larger number of red LEDs, so that the overall output energy of the two colors is equal. The total energy is 40 $\mu\text{mol m}^{-2} \text{s}^{-1}$ measured at the height of the sample (*see Note 10*). The lights connect to the personal computer (PC) via an Arduino development board, which enables control of the lights by digital signals sent from the PC. Finally, we keep the incubator inside of a dark room to decrease the background light levels (*see Note 11*).

We use a CCD camera designed for long exposures (*see Note 1*) with a high-light transmission lens (Xenon f/0.95 25 mm; Schneider, Germany). The CCD camera is also kept inside the incubator, laid horizontally below the LEDs. We modify the optics by including a 5 mm optical spacer between the lens and the camera. Doing so increases the focal length of the optics, which decreases the working distance, meaning the image can be focused closer to the sample. This particular configuration results in a pixel size of approximately 61 μm (*see Note 4*). This spatial resolution represents a compromise—high enough to observe the sub-tissue dynamics but sufficiently low for observation across all organs in the same frame.

Both the camera and LEDs are controlled with the open-source Micro-Manager software run on a desktop PC. Micro-Manager communicates with the LEDs through digital on-off signals sent via the Arduino development board. To do so, the board must be pre-configured with the Micro-Manager firmware (available from: micro-manager.org/wiki/Arduino#Firmware), uploaded from the Arduino IDE software. The camera communicates directly with

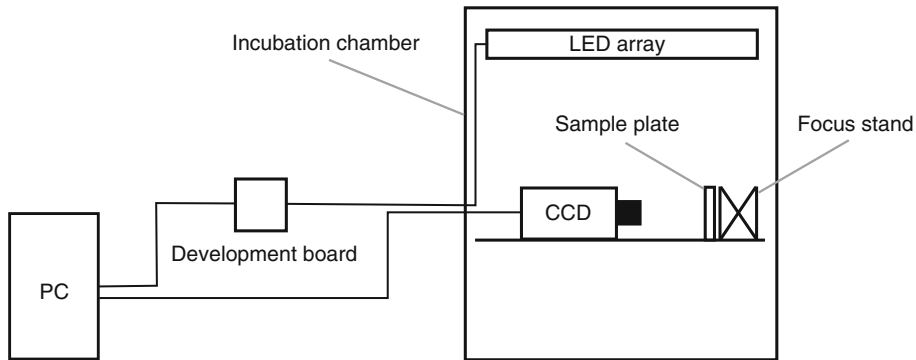


Fig. 1 Experimental setup for high-resolution imaging of luciferase reporter expression in *Arabidopsis*. Imaging is performed inside of a growth incubator chamber with custom-fitted LEDs for the control of the environment. The CCD camera is laid horizontally so that seedlings can be imaged vertically. *PC*, personal computer; *CCD*, charge-coupled device; *LED*, light-emitting diode

Micro-Manager via USB connection. Micro-Manager provides an easy-to-use graphical user interface for the control of the lights and camera together. This is used to efficiently frame the sample and to capture single images. However, time-lapse imaging requires coordination between the lights and camera over multiple days. We therefore utilize the scripting functionality of Micro-Manager for programming time-lapse experiments, as has been done previously [20]. Scripts are written in the Java-like programming language BeanShell and run through the “Script Panel” window within Micro-Manager. A typical program for an experiment under constant light involves: (1) turning the lights on for 65 min, (2) turning the lights off for 5 min to disperse the delayed fluorescence from chloroplasts [21], (3) exposing an image for 20 min while maintaining the lights off, and (4) saving the image to file (*see Note 12*). This cycle is repeated for a minimum of 6 days. Scripts can be easily modified for different exposure times and time intervals or to include light-dark cycles. Example BeanShell scripts for time-lapse imaging are available from [22].

3.2 Setting up a Time-Lapse Experiment

1. Surface sterilize seeds and stratify for 72 h at 4 °C in the dark.
2. Sow 20–30 seeds individually onto half-strength MS, 2% (w/v) agar media. Transfer plates to a plant growth cabinet for 4 days of growth and entrainment under 12-h light–12-h dark cycles. Orientate the plates vertically and keep at the center of a shelf within the cabinet (*see Note 13*), running with $80 \mu\text{mol m}^{-2} \text{s}^{-1}$ cool white light and a constant temperature of 22 °C.
3. During the evening of the fourth day of growth (*see Note 14*), remove the plates from the growth chamber. Select six to eight healthy seedlings and gently transfer by forceps into a 3- by 3-cm area of a fresh 10- by 10-cm media plate (*see Note 15*).

The media should contain half-strength MS 2% agar, as before. This area represents the camera's field of view, and seedlings must fit within this region if they are to be imaged together. The seedlings should be arranged in a row with no horizontal overlap.

4. Spray seedlings with 5 mM luciferin solution in 0.01% Triton-X100 (*see Note 6*). Seedlings must be maintained in sterile conditions throughout. After spraying, return plates to the growth cabinet.
5. At dawn of the fifth day of growth, remove the sample plate from the growth cabinet and affix to a laboratory jack stand. The stand acts as a focus mount, moving the sample back and forth within the imaging chamber (*see Note 16*). Position the stand horizontally on its side and affix the sample plate to the flat surface with adhesive tape, maintaining the sample in a vertical orientation.
6. Transfer the focus stand with the affixed sample to the imaging cabinet (*see Note 17*). The adjustment knob of the stand should be used to focus the sample under the camera. The "Live" function of Micro-Manager can be used to observe the sample during this process.
7. Time-lapse imaging should be commenced by running the appropriate BeanShell script, as described in Subheading 3.1.

3.3 Analysis of Luciferase Images

Two levels of analysis on the luciferase images are possible: organ-level and sub-tissue level. Here, we describe the former. Interpretation of the sub-tissue dynamics can be done simply by observing the videos or by extracting the luminescence from the pixels programmatically. However, the design of such programs will be dependent on the research question. We therefore instead point the reader towards some well-described analyses of circadian sub-tissue-level luciferase data [3, 17, 19].

1. For the organ-level analysis of rhythms, luminescence values must first be extracted from images. Import the .tiff files into Imaris as an image stack to view and extract the luminescence from images. Within the "Surpass" taskbar, apply a colormap, and adjust the range, in order to improve the visual contrast of the luminescence.
2. Create a "Spots" module to manually track the positions of the organs over time. We use a circular region of interest (ROI) of approximately 315 μm diameter to track the center of a single cotyledon, hypocotyl, root, and root tip from each seedling (Fig. 2; *see Note 18*). Click the center of each organ to place the ROI. Repeat sequentially for each image of the stack to create a track of the organ as the seedling grows (*see Note 19*). In addition, take a background ROI close to the seedling

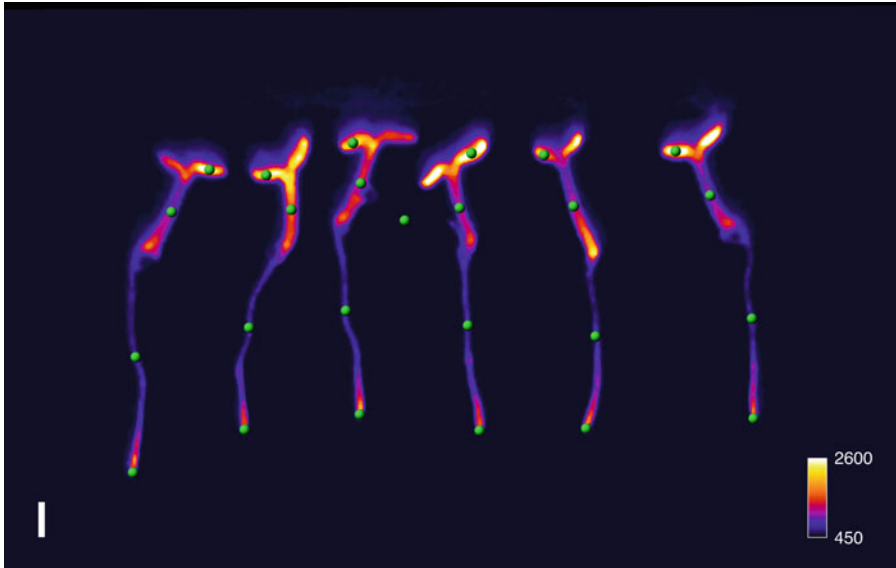


Fig. 2 Organ-level analysis of luciferase reporter expression. Expression of *GIGANTEA::LUC* from within individual *Arabidopsis* seedlings. Circular ROI (green circles) are manually placed within the cotyledon, hypocotyl, root, and root tip to track luciferase reporter expression over time. A background ROI is also included to aid later data analysis. Scale bar shows 1 mm. ROI, region of interest. The image is taken from our previous study [3]

(Fig. 2; see **Note 20**). Finally, check the tracks for completeness and accuracy using the “Edit Tracks” panel and correct as necessary.

3. Prior to export, select the parameter of interest to be exported from the “Statistics” panel. We use the median value of the ROI for our analyses. Statistics for the tracks should then be exported to .csv file, to give the time series. The Imaris workspace file should also be saved to preserve the ROI positions for future reference.
4. The user can analyze the time series contained in the .csv files in their program of choice. We use custom-developed MATLAB scripts for simple peak detection, and Biodare2 for period analysis (biodare2.ed.ac.uk) [23].

4 Notes

1. Other high quantum efficiency, low-noise CCD cameras designed for long exposure times are also suitable.
2. The PC should meet the minimum requirements for the operation of the CCD camera. All power saving settings should be disabled.

3. Care should be taken not to exceed the heat capacity of the incubator used. We do this by using only low-voltage LEDs due to their minimal heat output. For experiments that require higher light, we use an incubator with a higher heating capacity (BDR16; Conviron, UK).
4. The length of the optical spacer can be increased or decreased to alter the working depth. A longer spacer results in a shorter working depth.
5. The *LUC+* (Promega, USA) gene is a modified version of the endogenous firefly *LUC* gene and is several times brighter. We found the increased brightness necessary for reliable high-resolution imaging. Other luciferase versions including *LUC2* and *NanoLUC* (Promega, USA) may achieve similar results but have not been tested in this assay.
6. We typically store aliquots of 50 mM stock solution at -80°C to protect the stability. A working solution is then made by diluting the stock tenfold in 0.001% Triton-X100. The working solution is filter sterilized into amber spray bottles.
7. Spray bottles are sterilized by soaking in 70% ethanol solution overnight.
8. We cover the surface of the laboratory jack with matte black aluminum foil tape to prevent reflection of the luminescence.
9. The “Surpass” task is the relevant optional (and additionally licensed) part of the software. Similar analyses are possible in open-source image analysis software, although it is more laborious (*see* [24]).
10. We designed the LED array to produce the fixed amount of light used for experiments in our lab. However, it may be possible to include a dimmer switch in the design.
11. Luciferase images require a long exposure time and are therefore highly sensitive to background light. We find the use of a dark room important for the quality of the images even when the camera is kept inside of a growth incubator.
12. We recommend saving the images as .tiff files.
13. We calibrate the light levels to be $80\ \mu\text{mol m}^{-2}\ \text{s}^{-1}$ at the center of the shelf, to avoid positional effects on growth.
14. We manipulate the seedlings and apply the luciferin 16 h prior to dawn of the fifth day of growth. Although the choice of time of day is somewhat arbitrary, care should be taken to do it at a consistent time of day, and 12–24 h prior to the dawn of the fifth day.
15. For experiments in which we image multiple genotypes or treatments, we include three to four test seedlings and three to four controls on the same plate. Multi-well dishes can be

used for imaging seedlings under multiple media conditions if required. We use 8-well rectangular tissue culture dishes (NUNC; Thermo-Fisher Scientific, USA).

16. We focus the sample by physically moving the position of the sample, rather than by adjusting the lens iris. This allows us to keep the iris fully open and maximize the light transmission.
17. We find it useful to place a piece of plastic acrylic on the wire shelf of the cabinet to provide a flat surface to focus the sample.
18. We place the “cotyledon” and “hypocotyl” ROI at the middle position of the respective organ, tracking the center as the seedling grows. The “root” ROI is set at approximately the middle position between the hypocotyl junction and the root tip. This ROI is fixed as the root grows. The “root tip” ROI is placed over the lattermost 315 μm of the root, tracking the growth of the root. The positions and number of ROI can easily be changed depending on the experiment.
19. Occasionally the cotyledon and hypocotyl are positioned in such a way that they are not trackable. These organs should be excluded from the analysis.
20. In the subsequent analysis, we subtract the time series of the background ROI from that of the organ ROI. This removes the offset value from the images and mitigates the effect of background noise than can arise from several sources.

Acknowledgments

M.G. and J.L. are funded by the Gatsby Charitable Foundation (grant number GAT3395/GLC). A.H. is funded by the BBSRC (grant number BB/P016774/1).

References

1. Greenwood M, Locke JC (2020) The circadian clock coordinates plant development through specificity at the tissue and cellular level. *Curr Opin Plant Biol* 53:65–72. <https://doi.org/10.1016/j.pbi.2019.09.004>
2. Bordage S, Sullivan S, Laird J et al (2016) Organ specificity in the plant circadian system is explained by different light inputs to the shoot and root clocks. *New Phytol* 212:136–149. <https://doi.org/10.1111/nph.14024>
3. Greenwood M, Domijan M, Gould PD et al (2019) Coordinated circadian timing through the integration of local inputs in *Arabidopsis thaliana*. *PLoS Biol* 17:e3000407. <https://doi.org/10.1371/journal.pbio.3000407>
4. Para A, Farré EM, Imaizumi T et al (2007) PRR3 is a vascular regulator of TOC1 stability in the Arabidopsis circadian clock. *Plant Cell* 19:3462–3473. <https://doi.org/10.1105/tpc.107.054775>
5. Endo M, Shimizu H, Nohales MA et al (2014) Tissue-specific clocks in Arabidopsis show asymmetric coupling. *Nature* 515:419–422. <https://doi.org/10.1038/nature13919>
6. Lee HG, Seo PJ (2018) Dependence and independence of the root clock on the shoot clock in Arabidopsis. *Genes Genomics* 40:1063–1068. <https://doi.org/10.1007/s13258-018-0710-4>
7. Edwards J, Martin AP, Andriunas F et al (2010) GIGANTEA is a component of a

- regulatory pathway determining wall ingrowth deposition in phloem parenchyma transfer cells of *Arabidopsis thaliana*. *Plant J* 63:651–661. <https://doi.org/10.1111/j.1365-313X.2010.04269.x>
8. Shimizu H, Katayama K, Koto T et al (2015) Decentralized circadian clocks process thermal and photoperiodic cues in specific tissues. *Nat Plants* 1:15163. <https://doi.org/10.1038/nplants.2015.163>
 9. Shimizu H, Torii K, Araki T, Endo M (2016) Importance of epidermal clocks for regulation of hypocotyl elongation through PIF4 and IAA29. *Plant Signal Behav* 11:e1143999. <https://doi.org/10.1080/15592324.2016.1143999>
 10. Millar AJ, Short SR, Chua NH, Kay SA (1992) A novel circadian phenotype based on firefly luciferase expression in transgenic plants. *Plant Cell* 4:1075–1087. <https://doi.org/10.1105/tpc.4.9.1075>
 11. McClung CR, Xie Q (2014) Measurement of luciferase rhythms. *Methods Mol Biol* 1158. https://doi.org/10.1007/978-1-4939-0700-7_1
 12. Takahashi N, Hirata Y, Aihara K, Mas P (2015) A hierarchical multi-oscillator network orchestrates the Arabidopsis circadian system. *Cell* 163:148–159. <https://doi.org/10.1016/j.cell.2015.08.062>
 13. Yakir E, Hassidim M, Melamed-Book N et al (2011) Cell autonomous and cell-type specific circadian rhythms in Arabidopsis. *Plant J* 68:520–531. <https://doi.org/10.1111/j.1365-313X.2011.04707.x>
 14. Gould PD, Domijan M, Greenwood M et al (2018) Coordination of robust single cell rhythms in the Arabidopsis circadian clock via spatial waves of gene expression. *Elife* 7:e31700. <https://doi.org/10.7554/eLife.31700>
 15. Román Á, Golz JF, Webb AA et al (2019) Combining GAL4 GFP enhancer trap with split luciferase to measure spatiotemporal promoter activity in *Arabidopsis*. *Plant J: tpj*.14603. <https://doi.org/10.1111/tpj.14603>
 16. Muranaka T, Kubota S, Oyama T (2013) A single-cell bioluminescence imaging system for monitoring cellular gene expression in a plant body. *Plant Cell Physiol* 54:2085–2093. <https://doi.org/10.1093/pcp/pct131>
 17. Wenden B, Toner DLK, Hodge SK et al (2012) Spontaneous spatiotemporal waves of gene expression from biological clocks in the leaf. *Proc Natl Acad Sci U S A* 109:6757–6762. <https://doi.org/10.1073/pnas.1118814109>
 18. Fukuda H, Nakamichi N, Hisatsune M et al (2007) Synchronization of plant circadian oscillators with a phase delay effect of the vein network. *Phys Rev Lett* 99:098102. <https://doi.org/10.1103/PhysRevLett.99.098102>
 19. Fukuda H, Ukai K, Oyama T (2012) Self-arrangement of cellular circadian rhythms through phase-resetting in plant roots. *Phys Rev E* 86:041917. <https://doi.org/10.1103/PhysRevE.86.041917>
 20. Litthauer S, Battle MW, Lawson T, Jones MA (2015) Phototropins maintain robust circadian oscillation of PSII operating efficiency under blue light. *Plant J* 83:1034–1045. <https://doi.org/10.1111/tpj.12947>
 21. Gould PD, Diaz P, Hogben C et al (2009) Delayed fluorescence as a universal tool for the measurement of circadian rhythms in higher plants. *Plant J* 58:893–901. <https://doi.org/10.1111/j.1365-313X.2009.03819.x>
 22. Rees H, Duncan S, Gould P et al (2019) A high-throughput delayed fluorescence method reveals underlying differences in the control of circadian rhythms in *Triticum aestivum* and *Brassica napus*. *Plant Methods* 15:51. <https://doi.org/10.1186/s13007-019-0436-6>
 23. Zielinski T, Moore AM, Troup E et al (2014) Strengths and limitations of period estimation methods for circadian data. *PLoS One* 9:e96462. <https://doi.org/10.1371/journal.pone.0096462>
 24. Tindall AJ (2016) Identification & characterisation of transcription factors affecting the circadian system of *Arabidopsis thaliana*. University of Liverpool, Liverpool



Agrobacterium*-Mediated Seedling Transformation to Measure Circadian Rhythms in *Arabidopsis

Michael K. Y. Ting, Reimo Zoschke, and Michael J. Haydon

Abstract

Circadian clocks are endogenous timing mechanisms that allow an organism to adapt cellular processes in anticipation of predictable changes in the environment. Luciferase reporters are well utilized as an effective, nondestructive method to measure circadian rhythms of promoter activity in *Arabidopsis*. Obtaining stable transgenic reporter lines can be laborious. Here, we report a protocol for *Agrobacterium*-mediated seedling transformation tailored for plant circadian studies. We show that period estimates generated from wild-type and clock-mutant seedlings transformed with circadian luciferase reporters are similar to rhythms obtained from equivalent stable transgenic seedlings. These experiments demonstrate the versatility and robustness of the protocol for testing new constructs or quickly assessing circadian effects in any genotype of interest.

Keywords *Agrobacterium* transformation, Circadian clock, Luciferase, *Arabidopsis*

1 Introduction

Circadian clocks are biological time-keepers that allow organisms to anticipate and adapt to predictable and unpredictable daily and seasonal variation in the rhythmic environment. The circadian network is comprised of three components: inputs, an oscillator, and outputs. In plants, the oscillator is comprised of a complex network of negative and positive feedback loops that occur at the transcriptional, translational, and posttranslational levels [1]. Rhythmic environmental signals (inputs), such as light and temperature, can adjust the phase, pace, or amplitude of the clock, and, in turn, the clock controls a wide range of developmental, metabolic, and physiological responses (outputs) [2].

To study the behavior of the circadian network, rhythms of numerous circadian outputs have been measured. These include leaf movement [3], plant growth [4], chlorophyll fluorescence [5, 6], leaf temperature [7], gene promoter activity [8], and gene expression [9]. Stable transgenic lines of transcriptional luciferase

reporters have been widely adopted to measure circadian rhythms in *Arabidopsis*. The principle advantage of these is the noninvasive quantification with high temporal resolution and the ability to monitor individual oscillator components, rather than outputs. However, generating transgenic lines can be time-consuming, particularly for investigating rhythms in multiple genotypes.

Effective “transient” transformation techniques could accelerate experimental progress. Mesophyll protoplast transformation using luciferase reporters and artificial miRNAs has been used to assess clock function in *Arabidopsis* [10]. However, there is spatial heterogeneity in circadian clocks within and between tissues [11–15]. Furthermore, there appears to be coupling of oscillators between cells, and protoplast density can affect circadian rhythms [13]. Thus, measuring circadian rhythms in intact tissue is strongly preferred.

Several protocols have been developed for *Agrobacterium*-mediated transformation of *Arabidopsis* seedlings [16–18]. These have been developed for protein localization or protein-protein interaction studies and involve steps that are not suitable for circadian experiments. For example, the “FAST” method [16] requires co-cultivation of the *Agrobacteria* for 2 days under constant darkness, which disrupts light entrainment. In addition, previous protocols have been optimized with sucrose in the infiltration solution or in plant growth media, which can affect period, phase, and amplitude of circadian rhythms in *Arabidopsis* [19–21]. The inclusion of sugars also requires that antibiotics and/or vigorous washing steps are required to prevent bacterial proliferation after infiltration.

Here, we describe an adapted *Agrobacterium*-mediated seedling transformation to measure circadian rhythms of transcriptional luciferase reporters in *Arabidopsis* wild-type and mutant seedlings using a sugar-free infiltration media. Using constructs for four commonly used circadian promoters, we show robust circadian rhythms in infiltrated seedlings with similar period estimates to stable transgenic lines. We also show the expected circadian phenotypes in a short-period, long-period, and arrhythmic clock mutant. Although this technique cannot fully replace the use of stable luciferase reporter lines, it is well suited to rapidly test new reporter constructs or screening diverse genotypes for circadian period effects.

2 Materials

2.1 Plant Growth

1. Wild-type and mutant *A. thaliana* seeds.
2. 1/2 MS media: 0.215 g MS salts, 0.8–1 g agar per 100 mL deionized H₂O (*see Note 1*). Autoclave to sterilize.

3. 60 mm round petri plates (*see Note 2*).
4. 25-well 100 mm square petri plates.
5. Gas-permeable tape.
6. Black PVC insulation tape, 19 mm width.
7. Imaging rings: clear PVC tubing (6 mm external diameter), cut into <10 mm length, autoclaved to sterilize.
8. Forceps.

2.2 *Agrobacterium* Culture

1. *Agrobacterium tumefaciens* C58 transformed with binary luciferase constructs (*see Note 3*).
2. LB media with antibiotic: 10 g/L NaCl, 10 g/L tryptone, 5 g/L yeast extract, pH 7 (NaOH). Autoclave to sterilize and add antibiotic for the luciferase construct prior to use.
3. Shaking incubator.

2.3 Solutions

1. 100 mM acetosyringone stock: dissolve 196.2 mg 3',5'-dimethoxy-4'-hydroxyacetophenone in 10 mL DMSO. Store aliquots at -20°C .
2. 1 M MES buffer pH 5.7: dissolve 19.5 g 2-(*N*-morpholino)ethanesulfonic acid in 90 mL deionized H_2O . Adjust pH with KOH and add deionized H_2O to 100 mL. Autoclave.
3. 1 M MgCl_2 : dissolve 9.52 g $\text{MgCl}_2 \cdot 6\text{H}_2\text{O}$ in 100 mL deionized water. Autoclave.
4. 100 mM D-luciferin potassium salt stock solution: 100 mg in 3.14 mL sterile deionized H_2O . Prepare in dim light and store 50 μL aliquots wrapped in aluminum foil at -20°C .
5. Infiltration buffer: 5 mM MES pH 5.7, 10 mM MgCl_2 , 200 μM acetosyringone. Add 2 mL 1 M MES pH 5.7 and 4 mL 1 M MgCl_2 to 394 mL deionized water. Autoclave. Add 100 μL of 100 mM acetosyringone per 50 mL of buffer immediately before use.
6. 70% (v/v) ethanol.

2.4 Vacuum Infiltration

1. Vacuum pump (e.g., KNF Laboport N 840; 34 L min^{-1} , 99 mbar).
2. Vacuum desiccator with stopcock.
3. Laminar flow hood.
4. (Optional) 180 mm glass petri plates.

2.5 Luminescence Detection

1. A plant luminescence imaging system, consisting of a light-tight cabinet fitted with programmable LED arrays for blue (470 nm) and red (660 nm) light, and a CCD-camera, such as a

Photek HRPCS5. The imaging system should be placed in a temperature-controlled dark room with green lighting.

3 Methods

1. In a laminar flow, surface-sterilize and sow ~50–60 seeds on 1/2 MS media (1% agar) in 60 mm round petri dishes (*see Note 1*). Sow one genotype per plate and one plate per construct. Seal plates with gas-permeable tape. Chill plates in the dark at 4 °C for 2 days before transferring to growth cabinets with 12 h light/12 h dark at 20 °C and lights at 80–120 $\mu\text{mol m}^{-2} \text{s}^{-1}$.
2. Two days prior to infiltration, inoculate 5 mL of LB with antibiotic with *Agrobacterium* from a streaked LB plate carrying binary luciferase constructs. Incubate overnight at 30 °C, shaking at 200 rpm.
3. The day before infiltration, subculture *Agrobacterium* into 30 mL LB with antibiotic. Incubate overnight at 30 °C, shaking at 200 rpm.
4. On the day of infiltration, seedlings should be 5 days old (*see Note 4*). The OD₆₀₀ of the bacterial culture should be between 1.0 and 2.0. Centrifuge the culture at 4000 $\times g$ for 5 min and gently resuspend the bacterial pellet in infiltration buffer to a final OD₆₀₀ ~ 1.0 (*see Note 5*).
5. Clean the inside of the vacuum desiccator with ethanol. Working in a laminar flow hood, pour the bacterial infiltration mixture over the seedlings so that all are submerged (~10 mL per petri dish, Fig. 1) and place petri dishes with lids off in the desiccator (*see Note 1*).
6. Connect the desiccator to the pump and apply vacuum for 1 min. Air bubbles from seedlings should be visible. Turn off pump and release vacuum quickly by fully opening the valve (*see Note 6*). Repeat.
7. Pour off bacterial infiltration mixture. Replace lids of petri dishes, seal with gas-permeable tape, and return plates to the growth cabinet.
8. Prepare a 25-well plate for luciferase imaging. Mask well edges with black PVC tape and sterilize with ethanol in a laminar flow. Add 2 mL 1/2 MS (0.8% agar) to each well and insert four imaging rings per well (Fig. 1).
9. One or two days after infiltration, use forceps to collect ten infiltrated seedlings into a cluster and transfer into an imaging ring. For each genotype/construct combination, transfer one cluster into each of the four rings per well.

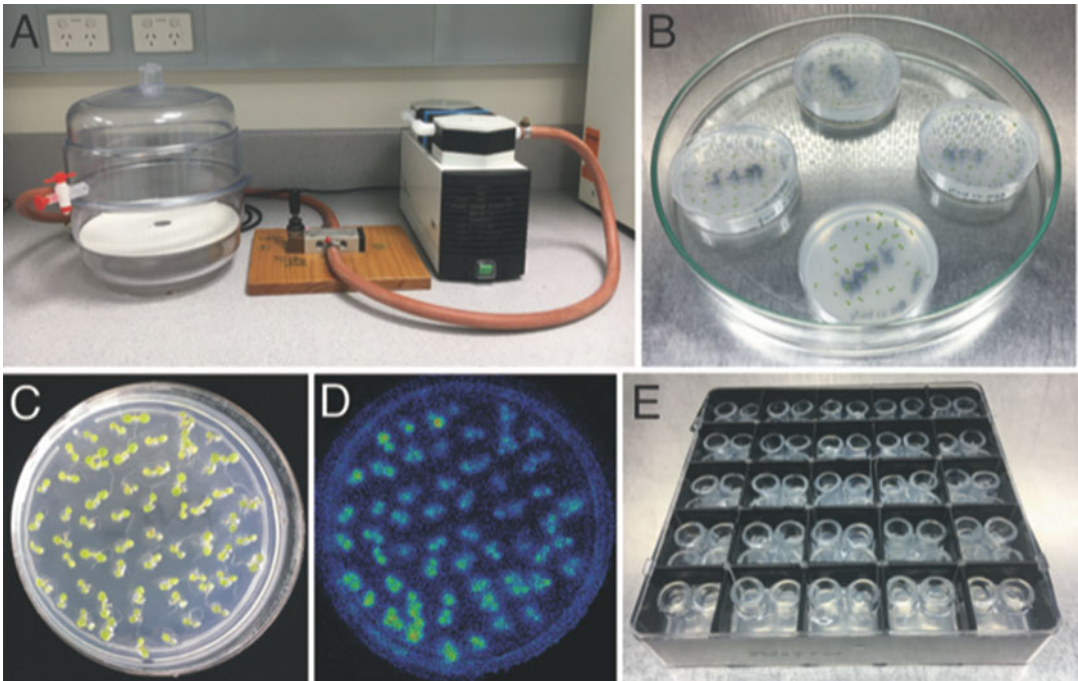


Fig. 1 *Agrobacteria*-mediated seedling transformation. (a) A vacuum desiccator connected to a laboratory vacuum pump. (b) Five d old *Arabidopsis* seedlings submerged in bacterial infiltration mixture, positioned in a 180 mm glass petri dish. (c) Seven d old Col-0 seedlings growing in a 60 mm petri dish, 2 days post-infiltration with *Agrobacterium* carrying *PRR7p:LUC2*. (d) Luminescence image of seedlings in (c). (e) 100 mm 25-well petri plate prepared for luminescence imaging

10. Prepare 1 mM D-luciferin in sterile deionized H₂O from stock solution and apply 25 μ L to each cluster in dim light. Return seedlings to the growth cabinet and repeat application of luciferin \sim 12 h later (*see Note 7*).
11. Place prepared 25-well plate into luminescence imaging system. Acquire luminescence images at 1 h intervals in continuous light for $>$ 96 h.
12. Perform circadian analyses of luminescence data (Fig. 2) using BioDare2 (<https://biodare2.ed.ac.uk>) [22].

4 Notes

1. We do not add sucrose to the plant growth media because this alters circadian rhythms in *Arabidopsis* [19–21] and promotes growth of *Agrobacterium* post-infiltration.
2. We find infiltration in multi-well plates produces non-uniform transformation efficiency. Small round petri dishes give even and consistent transformation. We place up to five small petri

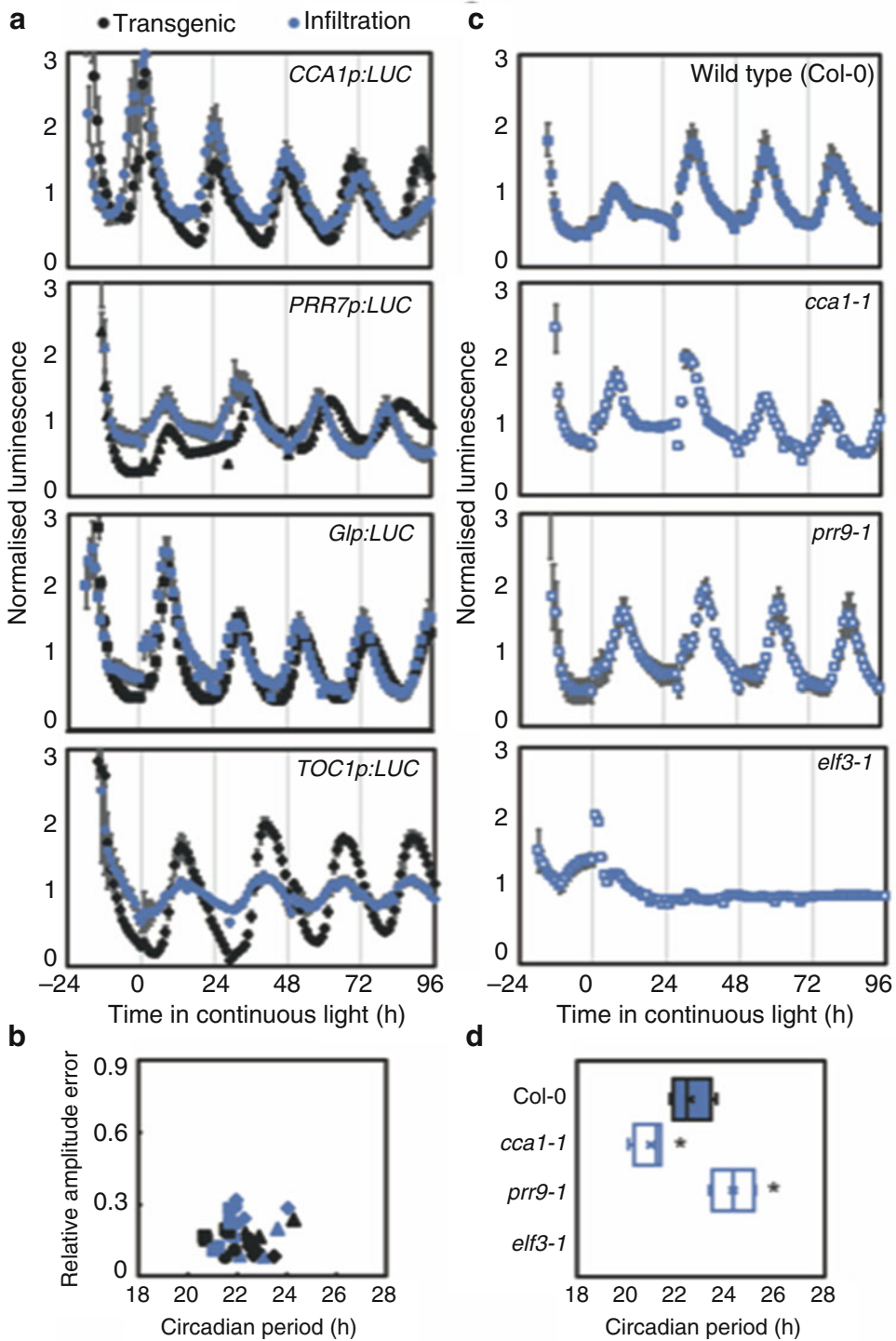


Fig. 2 Circadian rhythms of luciferase in infiltrated seedlings. **(a)** Luminescence in Col-0 seedlings infiltrated with *Agrobacterium* carrying *CCA1p:LUC2* (circles), *PRR7p:LUC2* (triangles), *Glp:LUC2* (squares), or *TOC1p:LUC2* (diamonds) compared to stable transgenic lines for each reporter. Data are means \pm SEM, $n = 4$. **(b)** Relative amplitude error and period estimates for luminescence data in **(a)**. Each marker represents an individual replicate. **(c)** Luminescence in Col-0, *cca1-1*, *prr9-1* and *elf3-1* infiltrated with *Agrobacterium*

dishes around the inside perimeter of 180 mm glass petri dishes to help maintain consistent position in the vacuum desiccator and ease handling.

3. We used binary constructs comprised of promoters of *CCA1* (1195 bp), *PRR7* (952 bp), *GI* (2519 bp), and *TOC1* (2068 bp) cloned into pEarlyGate301-LUC2 [23].
4. Highest seedling transformation efficiencies have been reported when using 3–4 days old seedlings grown in long-day conditions in media containing sucrose [16–18], but this should be adjusted according to photoperiod and light quantity. For seedlings grown in 12 h light/12 h dark without sucrose, we infiltrate 5 days old seedlings with good transformation efficiency and can detect signal >2 weeks after infiltration. Since immune responses in *Arabidopsis* are greatest around dawn [24, 25], we favor performing infiltration in the afternoon.
5. The OD₆₀₀ of the bacterial infiltration mixture is not critical. Similar transformation efficiencies are achieved between 0.5 and 2.0 OD₆₀₀ [17].
6. A fast release of vacuum pressure (over 15–20 s) results in better transformation efficiency compared with a slow vacuum release (2 to 5 min). We expect this is due to effective intercellular penetration of *Agrobacterium* into tissue. We also noted that extended periods of vacuum (>2 min) were deleterious for seedling growth. These timings may vary according to specific equipment components.
7. For our constructs, we consistently observed high luminescence immediately following luciferin application to infiltrated seedlings, which we confirmed was derived from the *Agrobacterium*. In sucrose-free media, this signal quickly decays, but we recommend to delay luciferase measurements for at least several hours after initial luciferin application.

References

1. Hsu PY, Harmer SL (2014) Wheels within wheels: the plant circadian system. *Trends Plant Sci* 19:240–249. <https://doi.org/10.1016/j.tplants.2013.11.007>
2. Haydon MJ, Li X, Ting MKY (2019) Temporal control of plant–environment interactions by the circadian clock. *Ann Plant Rev Online* 2:505–536. <https://doi.org/10.1002/9781119312994.apr0696>
3. Greenham K, Lou P, Remsen SE et al (2015) TRiP: tracking rhythms in plants, an automated leaf movement analysis program for circadian period estimation. *Plant Methods* 11:1–11. <https://doi.org/10.1186/s13007-015-0075-5>
4. Dornbusch T, Michaud O, Xenarios I, Fankhauser C (2014) Differentially phased leaf growth and movements in *Arabidopsis* depend

Fig. 2 (continued) carrying *GlpLUC2*. Data are means \pm SEM, $n = 4$. **(d)** Period estimates for luminescence data in **(c)**. Asterisks indicate significant difference by *t*-test ($p < 0.05$). No rhythms were detected for *elf3-1*

- on coordinated circadian and light regulation. *Plant Cell* 26:3911–3921. <https://doi.org/10.1105/tpc.114.129031>
5. Gould PD, Diaz P, Hogben C et al (2009) Delayed fluorescence as a universal tool for the measurement of circadian rhythms in higher plants. *Plant J* 58:893–901. <https://doi.org/10.1111/j.1365-313X.2009.03819.x>
 6. Litthauer S, Battle MW, Lawson T, Jones MA (2015) Phototropins maintain robust circadian oscillation of PSII operating efficiency under blue light. *Plant J* 83:1034–1045. <https://doi.org/10.1111/tpj.12947>
 7. Dakhiya Y, Green RM (2019) Thermal imaging as a non-invasive technique for analyzing circadian rhythms in plants. *New Phytol* 224 (4):1685–1696. <https://doi.org/10.1111/nph.16124>
 8. Millar AJ, Carre IA, Strayer CA et al (1995) Circadian clock mutants in *Arabidopsis* identified by luciferase imaging. *Science* 267:1161–1164
 9. Harmer SL, Hogenesch JB, Straume M et al (2000) Orchestrated transcription of key pathways in *Arabidopsis* by the circadian clock. *Science* 290:2110–2113. <https://doi.org/10.1126/science.290.5499.2110>
 10. Kim J, Somers DE (2010) Rapid assessment of gene function in the circadian clock using artificial MicroRNA in *Arabidopsis* mesophyll protoplasts. *Plant Physiol* 154:611–621. <https://doi.org/10.1104/pp.110.162271>
 11. Wenden B, Toner DLK, Hodge SK et al (2012) Spontaneous spatiotemporal waves of gene expression from biological clocks in the leaf. *Proc Natl Acad Sci U S A* 109:6757–6762. <https://doi.org/10.1073/pnas.1118814109>
 12. Endo M, Shimizu H, Nohales MA et al (2014) Tissue-specific clocks in *Arabidopsis* show asymmetric coupling. *Nature* 515:419–422. <https://doi.org/10.1038/nature13919>
 13. Takahashi N, Hirata Y, Aihara K, Mas P (2015) A hierarchical multi-oscillator network orchestrates the *Arabidopsis* circadian system. *Cell* 163:148–159. <https://doi.org/10.1016/j.cell.2015.08.062>
 14. Gould PD, Domijan M, Greenwood M et al (2018) Coordination of robust single cell rhythms in the *Arabidopsis* circadian clock via spatial waves of gene expression. *Elife* 7: e31700. <https://doi.org/10.7554/eLife.31700>
 15. Román Á, Golz JF, Webb AAR et al (2020) Combining GAL4 GFP enhancer trap with split luciferase to measure spatiotemporal promoter activity in *Arabidopsis*. *Plant J* 102:187–198. <https://doi.org/10.1111/tpj.14603>
 16. Li J, Park E, Von Arnim AG, Nebenführ A (2009) The FAST technique: a simplified *Agrobacterium*-based transformation method for transient gene expression analysis in seedlings of *Arabidopsis* and other plant species. *Plant Methods* 15:1–15. <https://doi.org/10.1186/1746-4811-5-6>
 17. Marion J, Bach L, Bellec Y et al (2008) Systematic analysis of protein subcellular localization and interaction using high-throughput transient transformation of *Arabidopsis* seedlings. *Plant J* 56:169–179. <https://doi.org/10.1111/j.1365-313X.2008.03596.x>
 18. Wu HY, Liu KH, Wang YC et al (2014) AGROBEST: an efficient *agrobacterium*-mediated transient expression method for versatile gene function analyses in *Arabidopsis* seedlings. *Plant Methods* 10:1–16. <https://doi.org/10.1186/1746-4811-10-19>
 19. Dalchau N, Baek SJ, Briggs HM et al (2011) The circadian oscillator gene *GIGANTEA* mediates a long-term response of the *Arabidopsis thaliana* circadian clock to sucrose. *Proc Natl Acad Sci U S A* 108:5104–5109. <https://doi.org/10.1073/pnas.1015452108>
 20. Haydon MJ, Mielczarek O, Robertson FC et al (2013) Photosynthetic entrainment of the *Arabidopsis* circadian clock. *Nature* 502:689–692. <https://doi.org/10.1038/nature12603>
 21. Haydon MJ, Mielczarek O, Frank A et al (2017) Sucrose and ethylene signaling interact to modulate the circadian clock. *Plant Physiol* 175:947–958. <https://doi.org/10.1104/pp.17.00592>
 22. Zielinski T, Moore AM, Troup E et al (2014) Strengths and limitations of period estimation methods for circadian data. *PLoS One* 9: e96462. <https://doi.org/10.1371/journal.pone.0096462>
 23. Rawat R, Schwartz J, Jones MA et al (2009) REVEILLE1, a myb-like transcription factor, integrates the circadian clock and auxin pathways. *Proc Natl Acad Sci U S A* 106:16883–16888. <https://doi.org/10.1073/pnas.0813035106>
 24. Bhardwaj V, Meier S, Petersen LN et al (2011) Defence responses of *Arabidopsis thaliana* to infection by *Pseudomonas syringae* are regulated by the circadian clock. *PLoS One* 6: e26968. <https://doi.org/10.1371/journal.pone.0026968>
 25. Wang W, Yang JB, Tada Y et al (2011) Timing of plant immune responses by a central circadian regulator. *Nature* 470:110–114. <https://doi.org/10.1038/nature09766>



Measurement of Luciferase Rhythms in Soybean Hairy Roots

Qiguang Xie, Yu Wang, Li Yuan, and Xiaodong Xu

Abstract

Firefly luciferase is widely used as a bioluminescence reporter, which is simple, high signal-to-noise ratio and especially suitable for the long-term analysis of circadian clock-regulated gene expression. Here, we report the method of tracking circadian rhythms in *Agrobacterium rhizogenes*-induced soybean hairy roots via TopCount™ Microplate Scintillation Counter or Deep-Cooled CCD camera. Using transgenic soybean hairy roots, we monitored the endogenous 24-h oscillations of clock genes expression and investigated the precise parameters of circadian rhythmicity. Researchers can easily analyze the circadian phenotype in legumes and non-legumes using bioluminescence reporters carried by the hairy roots, avoiding time-consuming transgenic work.

Keywords Circadian clock, Circadian rhythms, Firefly luciferase, Bioluminescence reporters, Hairy roots, Soybean (*Glycine max* (L.) Merr.), *Agrobacterium rhizogenes*

1 Introduction

Circadian clock is an evolutionary conserved time-keeping mechanism, which generates roughly 24-h self-sustained rhythms to regulate programs of molecular, metabolic, cellular, and physiological processes. Circadian rhythms are found in most living organisms, from prokaryotes to human beings. Like other organisms, circadian clock in plants spatial-temporally organizes growth and development to facilitate adaptation of environment [1, 2]. Circadian clock perceives cyclic changes of the external and internal cues, such as light, temperature, nutrition, humidity, abiotic stress and biotic stress, etc., and keeps in sync with the changes to confer organism a survival advantage [3–6]. Recent studies have demonstrated that the plant circadian clock contributes to multiple agronomic traits [7–10], suggesting that it can be applied to crop improvement.

Many high-throughput methods have been developed to investigate circadian clock in plants, such as leaf or cotyledon movement,

delayed fluorescence, and thermal imaging, suitable for measuring circadian rhythm phenotype in non-transgenic plants [11–13]. Another commonly used method is bioluminescence measurement based on constant or transient expression of the luciferase reporters in whole plants, tissues/organs, isolated cell line, or protoplasts, which is suitable for the accurate detection of autonomous circadian rhythm at the cellular and tissue level [14–18]. Firefly luciferase (*LUC*) is a sensitive and versatile reporter for the analysis of gene expression. Endogenous circadian rhythms in transgenic lines carrying *CLOCK GENE promoter:LUC* fusions, such as *CCA1:LUC* and *TOC1:LUC*, or *CLOCK OUTPUT GENE promoter:LUC* fusions, such as *CAB2:LUC*, *CCR2:LUC*, and *CAT3:LUC*, can be recorded by the PMT (photomultiplier tube) or CCD (charge-coupled device) with high temporal resolution.

In recent years, the field of plant research has shifted from model plants *Arabidopsis* to crops. The results show that the molecular architecture of circadian clock is more complicated in crops [7, 19, 20]. In particular, cross-cutting research interests, such as stress adaptation, domestication, photoperiodic flowering, etc., are worth exploring in depth, and the results will promote agricultural breeding and production applications.

Agrobacterium rhizogenes-mediated transformation of soybean was widely used to produce transgenic hairy roots [21, 22]. Here, with this method, we can simultaneously monitor the circadian oscillation of a large number of promoters of genes of interest in transgenic hairy roots, compared with the genetically modified soybean. The efficiency of the hairy roots induction with this method is as high as 90–99%; the final transformation efficiency for the constructs with *promoter:LUC* reporter in the hairy roots ranged from 30 to 60% (calculated based on the number of hairy roots produced and the final number of bioluminescent hairy roots obtained).

The accuracy and robustness of the *promoter:LUC* activity of this method allow researchers to elucidate the characteristics of circadian clock in soybean or other crops which can easily produce transgenic hairy roots.

2 Materials

2.1 Plasmids, Vectors, Strains, and Plants

1. Cloning donor vectors with firefly luciferase gene, *pENTR 1A LUC* which constructed based on gateway entry vector *pENTR 1A* (Thermo Fisher Scientific™), kanamycin resistance gene for selection in *E. coli*.
2. Destination vectors, *pH2GW7ΔP35S* which already deleted 35S promoter from *pH2GW7* [23], spectinomycin in *E. coli* and hygromycin in plants.

3. *Agrobacterium rhizogenes* (strain K599).
4. Soybean (*Glycine max* (L.) Merr., W82).

2.2 Media, Buffers, and Reagents

1. Commercial bleach.
2. HCl concentrated (37%).
3. Gamborg B-5 Basal Medium [24] (*see Note 1*).
4. YEP medium: 5 g/L yeast extract, 10 g/L peptone, 5 g/L NaCl. The pH is adjusted to 7, and medium can be autoclaved for 15 min at a maximum of 121 °C. After autoclaving, appropriate antibiotics (filter-sterilized) are added to select cells that contain the recombinant plasmid.
5. Liquid co-culture medium (LCCM): 0.32 g/L B-5 Basal Medium, 30 g/L sucrose, 3.9 g/L MES. The pH is adjusted to 5.4, and then be autoclaved at a maximum of 121 °C for 15 min. Add 40 mg/L acetosyringone before use.
6. Solid co-culture medium (SCCM): 0.32 g/L B-5 Basal Medium, 30 g/L sucrose, 3.9 g/L MES. The pH is adjusted to 5.4, and the medium is solidified with 4.5 g/L agar, and 121 °C 15 min autoclaving. Add 40 mg/L acetosyringone, 0.25 mg/L gibberellic acid (GA₃), 1.67 mg/L 6-benzylaminopurine, 400 mg/L L-cysteine, 154.2 mg/L DL-Dithiothreitol before use.
7. Root Medium (RM): 3.21 g/L B-5 Basal Medium, 30 g/L sucrose, 0.59 g/L MES. The pH is adjusted to 5.6, and the medium is solidified with 7.5 g/L agar, 121 °C 15 min autoclaving. After autoclaving, add 112 mg/L Gamborg Vitamin Powder, 200 mg/L cefotaxime, and 200 mg/L Timentin (filter-sterilized, select against residual *Agrobacterium*) before pour plate.
8. D-Luciferin (D-Luciferin, Potassium Salt, Gold Biotechnology): 2.5 mM in water. We refer to prepare a 100 mM stock solution, then make frozen aliquots, and dilute 1/40 for working solution (*see Note 2*).

2.3 Apparatus and Accessories

1. iKon-M Deep-Cooled CCD (Andor Technology™) (*see Note 3*).
2. TopCount™ Microplate Scintillation Counter (PerkinElmer™) (*see Note 3*).
3. White 96-well microtiter plates (we typically use white Optiplates; PerkinElmer) and also clear 96-well microtiter plates. TopSeal (PerkinElmer), a clear adhesive plastic sealant for the 96-well microtiter plates.

3 Methods

3.1 Hairy Roots Transformation Using *Agrobacterium rhizogenes* K599

1. Soybean seeds can be surface-sterilized by chlorine vapor. Place one layer of soybean seeds in the sterilized glass petri dish on a rack within a desiccator, and make sure the lid of the petri dish partially opened so that chlorine gas can reach the seeds. Place a 250 mL beaker containing 95 mL bleach into the desiccator jar, and apply enough Vaseline to the edge of the jar lid in advance, carefully add 5 mL concentrated HCl to the bleach, then immediately seal the jar very well. Allow sterilization by chlorine fumes to proceed for 12–16 h (we typically allow sterilization to continue overnight). Open container in a laminar flow hood, then seal petri dish with parafilm to keep the seed for future use.
2. Immerse the surface-sterilized seeds in an appropriate amount of sterile water (make sure the water surface just submerge the seeds) and leave them in the dark for 2 days at 25 °C. After imbibition, the seed coats are gently removed from the imbibed seeds, and the cotyledons and the connected 5 mm hypocotyls are detached for *Agrobacterium rhizogenes* infection. Hairy roots are induced as described in references [21, 22]. Place the soybean explants in *Agrobacterium rhizogenes* (strain K599) suspension (OD_{600 nm} of 0.5) for 30 min at 25 °C, use sterile 3 M filter paper to suck up the residual liquid on the explants, and then transfer the explants to the surface of SCCM medium; continue culturing for 3 days at 25 °C in the dark.
3. Before switching to RM medium, wash the explants with sterile water three times for 2 min each, and then continue the tissue culture for 14 days under 12 h light (white light 100 $\mu\text{mol m}^{-2} \text{s}^{-1}$)/12 h dark cycles at 25 °C.

3.2 Endogenous Circadian Rhythm Measurement and Data Assay

1. Cut the induced hairy roots from the explants and place in turn on the RM medium, and spray with 2.5 mM luciferin. Detect bioluminescence signals through highly sensitive CCD imaging system.
2. Select hairy roots with bioluminescence signals, cut the roots into small segments of 1 cm, transfer them to 96-well plates containing 200 μL RM medium plus 30 μL of 2.5 mM luciferin per well using sterilized long tweezers. The 96-well plate was sealed with clear sealing membranes, and two tiny holes were punched above each well using syringe needle for gas exchange. Put back the well-sealed plates to the original growth chamber to recover for 1 day in the same LD cycle, after that transfer the plates under free-running conditions to monitor the LUC activities with TopCountTM luminometer (see Notes 4 and 5).

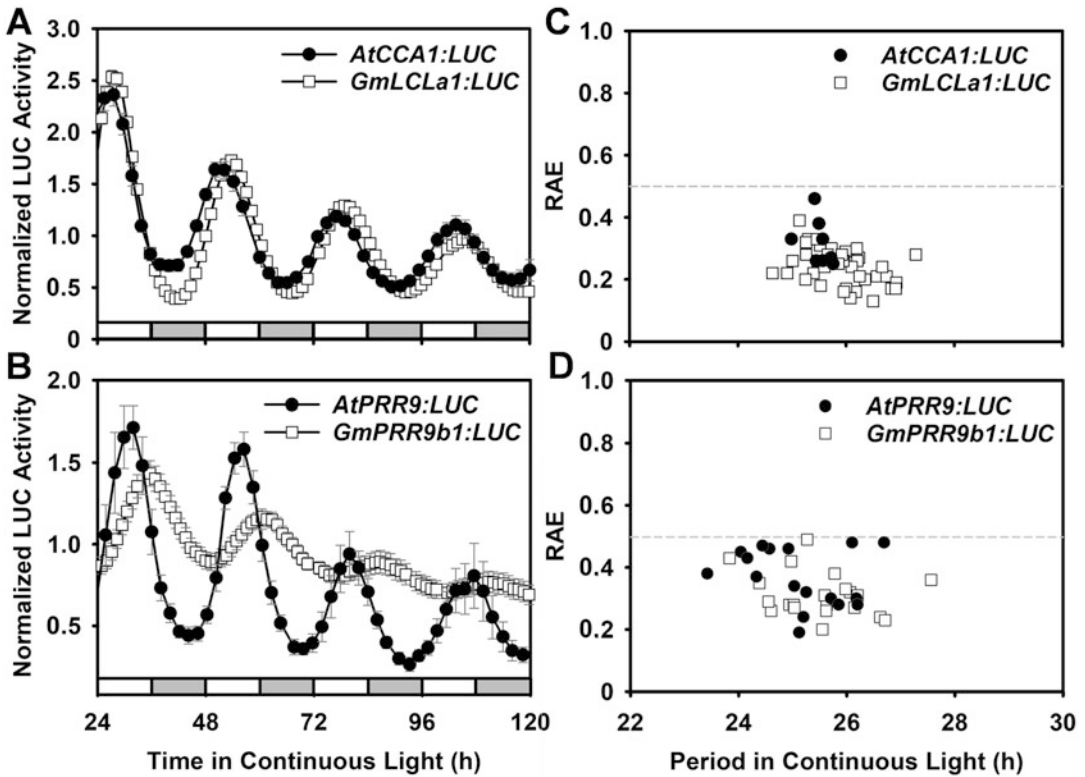


Fig. 1 Quantification of *AtCCA1*, *GmLCLa1*, *AtPRR9*, and *GmPRR9b1 promoter:LUC* activity in continuous light measured with a TopCount™. (a and b) Mean bioluminescence traces of luciferase activity from soybean hairy root. (c and d) Scatterplots of relative amplitude error (RAE) versus period length of circadian rhythms shown in (a and b)

3. Alternatively, the transgenic hairy roots carrying the *promoter:LUC* constructs can be placed on the surface of RM medium in the 90 mm disposable plastic petri dishes, and then 2.5 mM luciferin is applied to the roots before the bioluminescence measurement via photon-counting camera (*see Note 4*).
4. For tracking the self-sustained circadian rhythm, release the hairy roots into free-running conditions of constant white light, 25 °C, and 40–60% (humidity). Set up 2 min/plate delay time and 10 s/well measuring time before starting to collect data via the TopCount. Set the CCD camera to start taking pictures 2.5 min after turning off the light, and the exposure time is set to 25 min; the interval between each acquisition is 3 h. After 5 days of imaging, merge a series of frames into one, and then prefer to use the open architecture “ImageJ” program to analyze optical density of each well of all plates (*see Note 5*).
5. Circadian parameters of *LUC* expression are determined with BRASS 2.1.4, which employs fast Fourier transform-nonlinear

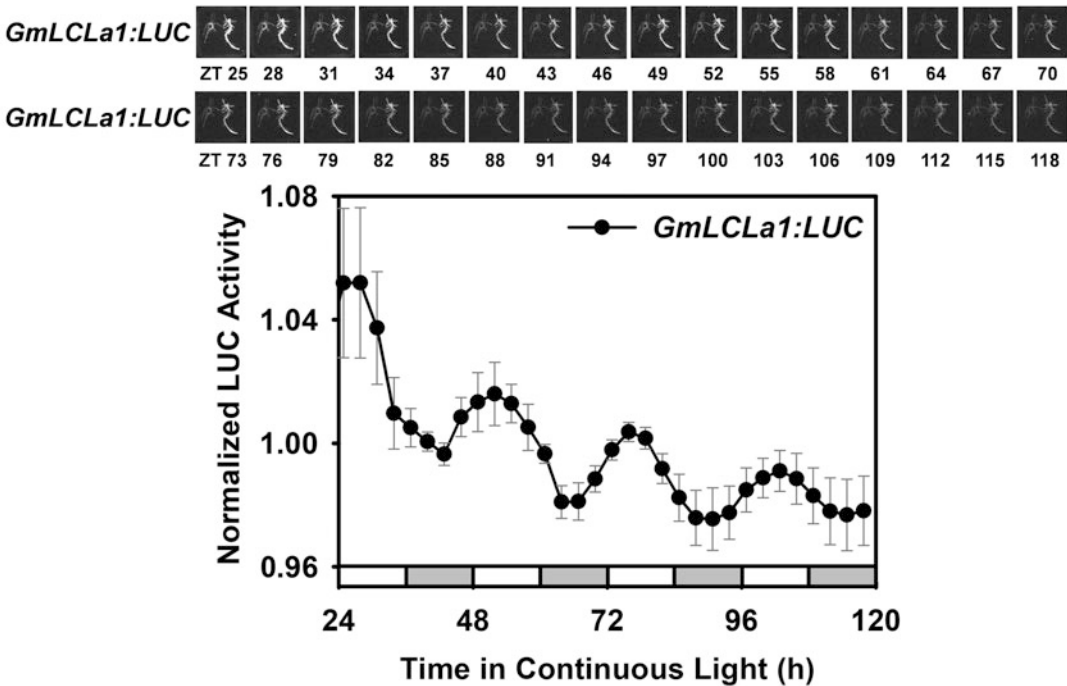


Fig. 2 Time series of images of soybean hairy roots taken with a CCD camera. Hairy roots were entrained to a 12-h light/12-h dark cycle and released into continuous light for imaging. Upper panel shows a time series of images of transgenic hairy roots which carrying *GmLCLa1:LUC*. The lower panel shows quantification of *promoter:LUC* activity. White bars indicate subjective day, and gray bars indicate subjective night

least squares (FFT-NLLS) [25, 26]. The range of relative amplitude error (RAE) is from 0 to 1, which is used to indicate the robustness of a circadian rhythm; RAE value approaching 0 means an ideal robust cosine wave, RAE value approaching 1 means the limit of statistical significance for any given rhythmic amplitude, and, in general, RAE values above 0.5 are considered to be arrhythmic (Figs. 1 and 2).

4 Notes

1. We purchased B5 medium premixed (G398) from PhytoTechnology Laboratories™.
2. We purchased D-Luciferin, Potassium Salt, from GoldBio™; after making 100 mM stock solution, aliquot 1 mL into 2 mL screw cap tubes, freeze at -20°C , and protect any unused stock solution from light. The 0.22- μm pore syringe filter was used for the sterilization of 2.5 mM D-luciferin (working concentration).

3. There are currently two main methods for high-throughput measurement of LUC activity. One is the PMT detector-based equipment, such as TopCount™ Microplate Scintillation Counter (PerkinElmer), and the other is Deep-Cooled CCD camera-based equipment; we put the CCD camera in a well-sealed growth chamber which contains computer-controlled LED lights, so various lighting conditions can be programmed. The lights will be turned off prior to imaging, and then be turned on again after imaging automatically, and one CCD camera can take picture of totally 16 petri dishes simultaneously. The TopCount™ uses PMT to detect bioluminescence signals that are more sensitive than Deep-Cooled CCD camera, so if the signal of transgenic hairy roots with reporter gene is weak, TopCount™ can be given priority, but if you want to see the spatiotemporal specificity of the experimental materials, CCD camera is the only choice.
4. If no enzyme reaction occurs, LUC protein will accumulate a lot till applying the substrate luciferin, so the first peak of *promoter:LUC* expression was very high; therefore, we initiate imaging typically 12–24 h after luciferin addition. The same thing happened when measuring LUC activities via TopCount™; to solve this problem, we could take another approach, just routinely entrained hairy roots within 96-well plates or in petri dishes when luciferin had been added for one more entraining cycle before released into continuous conditions.
5. The TopCount™ was programmed to load each successive plate into the sample chamber for luminescence measurement. Depending on the length of the delay time, it usually took about 1–2 h to complete a whole cycle; except for the 10-min measurement time, the plates were on the stacker most of the time. To permit light to reach the plates when loaded into the stacker, we had cut holes on all sides of the stacker without compromising its physical integrity. The stacker can hold up to 11 sample plates; between each sample plate, we interleave three clear 96-well plates to allow light to reach the hairy roots inside the sample plate; these clear plates must cycle through the sampling chamber but need not be read, and we could decide whether to measure the plate by setting program parameters.

Acknowledgments

This work was supported by grants from the National Natural Science Foundation of China to Q.X. (32170259, 31670285) and X.X. (U1904202, 32170275).

References

- Greenham K, McClung CR (2015) Integrating circadian dynamics with physiological processes in plants. *Nat Rev Genet* 16(10):598–610
- Sanchez SE, Kay SA (2016) The plant circadian clock: from a simple timekeeper to a complex developmental manager. *Cold Spring Harb Perspect Biol* 8(12):a027748
- Dodd AN, Salathia N, Hall A, Kveit E, Toth R, Nagy F, Hibberd JM, Millar AJ, Webb AA (2005) Plant circadian clocks increase photosynthesis, growth, survival, and competitive advantage. *Science* 309(5734):630–633
- Wang W, Barnaby JY, Tada Y, Li H, Tor M, Calderari D, Lee DU, Fu XD, Dong X (2011) Timing of plant immune responses by a central circadian regulator. *Nature* 470(7332):110–114
- Goodspeed D, Chehab EW, Min-Venditti A, Braam J, Covington MF (2012) Arabidopsis synchronizes jasmonate-mediated defense with insect circadian behavior. *Proc Natl Acad Sci U S A* 109(12):4674–4677
- Graf A, Schlereth A, Stitt M, Smith AM (2010) Circadian control of carbohydrate availability for growth in Arabidopsis plants at night. *Proc Natl Acad Sci U S A* 107(20):9458–9463
- Bendix C, Marshall CM, Harmon FG (2015) Circadian clock genes universally control key agricultural traits. *Mol Plant* 8(8):1135–1152
- Seo PJ, Mas P (2015) STRESSing the role of the plant circadian clock. *Trends Plant Sci* 20(4):230–237
- Mora-Garcia S, de Leone MJ, Yanovsky M (2017) Time to grow: circadian regulation of growth and metabolism in photosynthetic organisms. *Curr Opin Plant Biol* 35:84–90
- Shim JS, Kubota A, Imaizumi T (2017) Circadian clock and photoperiodic flowering in Arabidopsis: CONSTANS is a hub for signal integration. *Plant Physiol* 173(1):5–15
- Greenham K, Lou P, Remsen SE, Farid H, McClung CR (2015) TRiP: tracking rhythms in plants, an automated leaf movement analysis program for circadian period estimation. *Plant Methods* 11:33
- Rees H, Duncan S, Gould P, Wells R, Greenwood M, Brabbs T, Hall A (2019) A high-throughput delayed fluorescence method reveals underlying differences in the control of circadian rhythms in *Triticum aestivum* and *Brassica napus*. *Plant Methods* 15:51
- Dakhiya Y, Green RM (2019) Thermal imaging as a noninvasive technique for analyzing circadian rhythms in plants. *New Phytol* 224(4):1685–1696
- Millar A, Carre I, Strayer C, Chua N, Kay S (1995) Circadian clock mutants in Arabidopsis identified by luciferase imaging. *Science* 267(5201):1161–1163
- Kim J, Somers DE (2010) Rapid assessment of gene function in the circadian clock using artificial microRNA in Arabidopsis mesophyll protoplasts. *Plant Physiol* 154(2):611–621
- Wang Y, Yuan L, Su T, Wang Q, Gao Y, Zhang S, Jia Q, Yu G, Fu Y, Cheng Q, Liu B, Kong F, Zhang X, Song CP, Xu X, Xie Q (2019) Light- and temperature-entrainable circadian clock in soybean development. *Plant Cell Environ* 43(3):637–648
- Endo M, Shimizu H, Nohales MA, Araki T, Kay SA (2014) Tissue-specific clocks in Arabidopsis show asymmetric coupling. *Nature* 515(7527):419–422
- Román Á, Golz JF, Webb AAR, Graham IA, Haydon MJ (2019) Combining GAL4 GFP enhancer trap with split luciferase to measure spatiotemporal promoter activity in Arabidopsis. *Plant J* 102(1):187–198
- Lu S, Zhao X, Hu Y, Liu S, Nan H, Li X, Fang C, Cao D, Shi X, Kong L, Su T, Zhang F, Li S, Wang Z, Yuan X, Cober ER, Weller JL, Liu B, Hou X, Tian Z, Kong F (2017) Natural variation at the soybean J locus improves adaptation to the tropics and enhances yield. *Nat Genet* 49(5):773–779
- Muller NA, Wijnen CL, Srinivasan A, Rynagallo M, Ofner I, Lin T, Ranjan A, West D, Maloof JN, Sinha NR, Huang S, Zamir D, Jimenez-Gomez JM (2016) Domestication selected for deceleration of the circadian clock in cultivated tomato. *Nat Genet* 48(1):89–93
- Kereszt A, Li D, Indrasumunar A, Nguyen CD, Nontachaiyapoom S, Kinkema M, Gresshoff PM (2007) *Agrobacterium rhizogenes*-mediated transformation of soybean to study root biology. *Nat Protoc* 2(4):948–952
- Chen L, Cai Y, Liu X, Guo C, Sun S, Wu C, Jiang B, Han T, Hou W (2018) Soybean hairy roots produced in vitro by *Agrobacterium rhizogenes*-mediated transformation. *Crop J* 6(2):162–171
- Karimi M, Inze D, Depicker A (2002) GATEWAY vectors for agrobacterium-mediated plant transformation. *Trends Plant Sci* 7(5):193–195
- Gamborg OL, Miller RA, Ojima K (1968) Nutrient requirements of suspension cultures of soybean root cells. *Exp Cell Res* 50(1):151–158

25. Plautz JD, Straume M, Stanewsky R, Jamison CF, Brandes C, Dowse HB, Hall JC, Kay SA (1997) Quantitative analysis of drosophila period gene transcription in living animals. *J Biol Rhythm* 12(3):204–217
26. Southern MM, Millar AJ (2005) Circadian genetics in the model higher plant, *Arabidopsis thaliana*. *Methods Enzymol* 393:23–35



Chapter 7

ODE (Ordinary Differential Equation) Models for Plant Circadian Networks: What the Models Are and How They Should Be Used

Jonathan W. Pitchford and Paula Avello

Abstract

ODE models have been used for decades to help circadian biologists understand the rhythmic phenomena they observe and to predict the behavior of plant circadian rhythms under changed conditions such as genetic mutations or novel environments. The models vary in complexity, and for good reasons, but they share the same mathematical ingredients in their construction and the same computational methods in their solution. Here we explain the fundamental concepts which define ODE models. We sketch how ODE models can be understood, how they can be solved mathematically and computationally, and the important distinction between autonomous and non-autonomous phenomena. The concepts are illustrated with examples which illustrate the basic concepts and which may help to describe the strengths and limitations of these models and the computational investigations of their properties.

Keywords Circadian model, Periodic forcing, *Arabidopsis*, Mathematical simulation, MATLAB code, Systems biology

1 Fundamental Concepts: Models and ODEs

1.1 What Is a Circadian Model?

The celebrated phrase “all models are wrong” [1] is helpful only when accompanied by its more important sequel “but some models are useful”. Any mathematical model is an abstraction which tries to describe the vital components and interactions in the real world. In this sense, a model is a work of art: an attempt to distil the essence of the complex world in which we live into a form which the human mind can understand, can interpret, and can perhaps imagine manipulating.

We know that circadian rhythms exist in the real world, that they are important at scales ranging from the biochemical to the ecological, and that changes to external (e.g., environmental) and internal (e.g., genetic) processes can change the function of a clock

in various ways. We also know that mathematical equations can produce rhythmic outputs. It is natural to ask in what ways the biological reality of the former can be described by the simplicity of the latter, in the hope that such knowledge can be useful.

Here we describe one such approach, based on ODEs (ordinary differential equations), which is well suited to developing a useful understanding of the phenomena that experimentalists can observe and influence. It is not the most complicated, and it necessarily ignores factors (randomness, variability, and detailed spatial structure in particular) which we know are present in the real system. Nevertheless, ODEs can offer intuitive and practical insights and provide an adaptable conceptual framework to assimilate new empirical discoveries.

1.2 What Is an ODE? Some Mathematical Preliminaries

As alluded to above, “mathematical models” can mean many things, and their usefulness and complexity depend on their intended purpose. In contrast, an ODE is a mathematical object with a precise meaning [2]. Some careful definitions are necessary for a useful understanding of these models in the context of circadian networks.

For our purposes an *ODE model* is an equation, or a set of equations, which describe the rates of change of quantities of relevance to the circadian clock at a certain (possibly unspecified) location. These changing quantities are called *dynamic variables*, and the other numbers in the ODEs are called *parameters*. For example, a dynamic variable might be the concentration in the cytoplasm of a particular protein necessary to circadian function, whereas the constant degradation rate of that protein in the cytoplasm would be a parameter.

The *initial condition(s)* of the ODE model are the value(s) of the dynamic variables at some arbitrary starting time, usually time $t = 0$ for simplicity. The *solution* of the ODE model is generated by starting the system at its initial conditions and then allowing the dynamic variables to change according to the rules prescribed by the ODEs; in this sense the solution is simply the time-indexed list of the states of the dynamic variables as time progresses. In some (rare and simple) cases, the solution can be generated using pen and paper, but for all practical purposes, computational methods are necessary.

The word *ordinary* in ODE does not suggest simplicity; rather it means that any spatial structure in the biological system is either ignored or treated in a strictly compartmental manner. Spatial structure can be incorporated in ODEs by allowing separate differential equations to describe the states of dynamic variables in different locations (e.g., protein concentrations in the cytoplasm and nucleus, as in Locke et al. [3]). This is, of course, a simplification, but it can be a useful one. Models which allow dynamic variables to be represented in both time and continuous space are known as

partial differential equation models (PDEs). The mathematical theories describing and connecting PDEs and networks of ODEs are difficult and lie beyond the scope of this chapter. Like ODE models, such systems are known to exhibit a fascinating range of oscillatory and chaotic behavior.

1.3 A Useful

Example: Locke et al.

[3]

Work by Locke et al. [3] describes one of the simpler ODE models, chosen here for illustration thanks to its relative accessibility. The issues involved in understanding the model, and in computing and understanding its solutions, apply to more complex models. The model describes the rates of change in the concentrations of seven clock variables: $c_L^{(m)}$, $c_L^{(c)}$, and $c_L^{(n)}$ are the cellular concentrations of the products of the *LHY* gene as mRNA and protein in the cytoplasm and nucleus, respectively; $c_T^{(m)}$, $c_T^{(c)}$, and $c_T^{(n)}$ are corresponding concentrations for *TOC1*; and P is an additional light-sensitive protein. Mathematically these variables are referred to as *dynamic variables*, in contrast to a model's *parameters* which are (typically) fixed constants. An example ODE from this model is shown below:

$$\frac{dc_L^{(m)}}{dt} = L(t) + \frac{n_1 c_T^{(n)a}}{g_1^a + c_T^{(n)a}} - \frac{m_1 c_L^{(m)}}{k_1 + c_L^{(m)}}. \quad (1)$$

The ODE (1) is referred to as *coupled* because the dynamics of one variable is influenced by one or more other variable(s), e.g., $c_T^{(n)}$ affects the dynamics of $c_L^{(m)}$. Such coupling is natural in biological systems. The full model of Locke et al. [3] consists of seven coupled ODEs.

Equation 1 can be understood as follows: $c_L^{(m)}$ production is directly increased by some time-dependent amount $L(t)$ but also by the presence of $c_T^{(n)}$. This dependence on $c_T^{(n)}$ is nonlinear and saturates to a value of n_1 when $c_T^{(n)}$ is present in excess, and the parameter a captures the shape of this nonlinearity. Similarly, $c_L^{(m)}$ is reduced at a rate depending nonlinearly on $m_1 c_L^{(m)}$ and with a maximum loss rate of m_1 . (These latter nonlinear relationships are examples of a Hill function with coefficient a , and a Michaelis-Menten function, respectively [4].) In addition, the Locke et al. [3] model has an extra equation:

$$L(t) = q_1 c_P^{(n)} \theta_{\text{light}}, \quad (2)$$

which is not an ODE and which directly models the hypothesized effect of light. The parameter θ_{light} describes the light regime and changes in a circadian manner: $\theta_{\text{light}} = 1$ in daytime and $\theta_{\text{light}} = 0$ at night. Note that $L(t)$ appears in Eq. 1; the ODE (1) is therefore non-autonomous (see below).

The Locke et al. [3] model chooses to consider the interactions of only *TOC1* and *LHY* (modeling mRNA and protein for both)

and protein P , with spatial separation between nuclear and cytoplasmic components. Other models make different assumptions, e.g., suppressing spatial structure in the cell but accounting for mRNA and protein levels for a broader set of interacting genes [5] or considering only protein levels across a range of possible interaction networks [6]. In every case the emphasis has to be on “usefulness”—models are built for a purpose which can only be decided upon after collaboration with empirical scientists. One advantage of the ODE approach is that, for all such models, the mathematical and computational methods are essentially unchanged.

2 Qualitative Behavior of ODEs: Important Considerations for Circadian Biology

The preceding descriptions apply to any ODE model of a biological system. However, circadian systems are distinguished by the fact that the plant rhythm emerges in response to environmental signals, typically (but not exclusively) light-dark cycles. This makes a careful classification of the properties of the solutions, and their long-term behavior, especially important.

An ODE is *autonomous* if none of the parameters depend on time. Of crucial importance to circadian biology is the fact that, even though its parameters are constant, the solutions of an autonomous ODE model might not be: the solution might tend towards one of possibly many *stable steady states* and remain there for all time, its dynamic variables might oscillate indefinitely in some predictable fashion (called a *stable limit cycle*), or it might exhibit complex and seemingly unpredictable dynamics known as *chaos*. Changes in parameter values can cause the solutions of an ODE to change qualitatively, and such changes are called *bifurcations*. For example, a change in a reaction rate parameter might shift the ODE’s solution from a stable steady state to a stable limit cycle (such a transition is an example of a *Hopf bifurcation*). For a circadian model exhibiting stable limit cycle behavior, the *free-running period* refers to the time taken for the oscillation to repeat itself.

One might naively expect that any useful circadian model should show stable limit cycle behavior with a 24-h free-running period. Regular oscillations are, after all, a characteristic of a functional circadian clock. This is an oversimplification, however, because circadian systems in the real world are not autonomous—plant circadian rhythms emerge in response to periodic environmental signals, and our models must reflect this reality. In other words, any useful circadian model must respond to changing environmental factors (principally light, but also other factors such as temperature). Because this necessarily involves the models’

parameters changing with time, the resulting ODEs are *non-autonomous*. The mathematical theory of non-autonomous systems is much more complicated, and computational approaches are generally preferred.

Environmental conditions (typically changes in light) in ODE models have been modeled in a variety of ways. The simplest is binary variation, i.e., light is periodically “switched off” and “switched on” over a 24-h cycle, so that light-dark cycles are modeled as square waves. We say that an externally forced model exhibits *entrainment* if its outputs are themselves display a regular 24-h period [7]. Entrainment is clearly a necessary property for a useful circadian model. Mathematical and computational investigations allow the possible limits of entrainment to be explored, for example, imposing an overall period different to 24 h, or a different balance between light dark intervals [8].

3 Solving ODE Models Computationally

ODE models are used widely, and computational methods for their solution are well developed. Packages to implement their solution exist in a range of software environments (R, Python, and MATLAB are commonly used), and there is no need to reinvent the wheel. Different software packages may require the user to respect arcane linguistic peculiarities, but the basic protocol is as follows:

1. Set up parameter values (**Parameters.m**).
2. Define the ODE model (**Locke2005derivs.m**).
3. Decide an initial condition (**Locke2005.m line 5**).
4. Solve the dynamics and display the output (**Locke2005.m lines 7-9**).

The text in bold indicates the MATLAB example code, contained in Sect. 4. Note that three files (i.e., three separate, but linked, sets of computer code) are used: **Parameters.m** defines the parameter values, **Locke2005derivs.m** defines the ODE model, and the “driving” code **Locke2005.m** executes all the commands needed to combine them to produce an output. In other words, **Parameters.m** sets things up, **Locke2005derivs.m** is a “black box” where the mathematics is hidden, and **Locke2005.m** links these to do all the work. The reasons for splitting up the code in this way may become more apparent below, where a more realistic light-dark simulation can be run simply by modifying and replacing the original driving program **Locke2005.m** with **Locke2005forced.m**. An example of the outputs of this solution process is provided in Fig. 1.

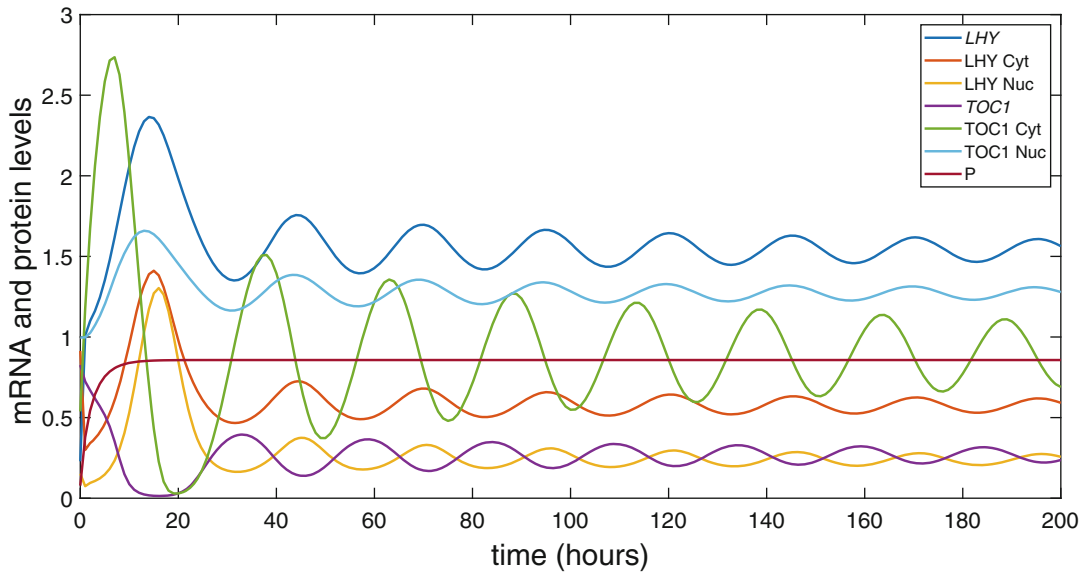


Fig. 1 A typical output from the autonomous Locke et al. [3] model under constant dark conditions. The horizontal axis is time (in hours); the vertical represents the concentration of the various clock components (arbitrary units). Outputs show stable limit cycle behavior, with *TOC1* and *LHY* clock components oscillating with a period of approximately 25 h after an initial burn-in from a random set of initial conditions. Note that the putative light-sensitive protein *P* (dark red) does not oscillate in constant dark

The problem comes when most numerical methods to solve ODEs, and the software built to implement these methods, relate to systems of autonomous ODEs. As explained above, this may be appropriate in finding the free-running period of a circadian system but is hardly sufficient for modeling the entrainment of circadian systems as is an intrinsically non-autonomous mechanism. The code `Locke2005forced.m` is an example of how to implement a numerical solution for a non-autonomous ODE. The code `Locke2005forced.m` simulates environmental light conditions as binary phases (light and dark, lines 30 and 22, respectively), and the transient effect of light on the clock component *LHY* is implemented via Eq. 2 (`Locke2005derivs.m` lines 6 and 7). To solve the dynamics of the forced model, we will use a modification of the protocol above, where step 4 is slightly more refined:

4. Solve the dynamics and display the output (`Locke2005forced.m`).
 - 4.1. Define the photoperiod (lines 16 and 17).
 - 4.2. Start an iterative process (line 21-37).
 - 4.3. Combine the solutions for light and dark phases (lines 22-36).

Note that the system is solved for light and dark phases separately and consecutively, but not independently; the initial conditions of the ODE model at the start of each light period are the values of the dynamic variables at time the system leaves previous dark phase (**Locke2005forced.m** lines **20**, **26**, and **34**), and vice versa for light-dark transitions.

Rather than a binary version of the external light cycle, other implementations consider the light-dark cycle as continuous changes in light levels, for example, by using a sinusoidal or a hyperbolic tangent function to cause smooth transitions between light and dark phases [9]. Because the environmental transitions in such cases are smooth, the computational solution methods (and sometimes the mathematical theory) are in many ways simpler than the binary forcing case. The details of their computational implementation, however, will depend on the software chosen (*see* [10] for examples of continuous transitions, and testing the effect of the detailed forcing regime, using MATLAB).

Figure 2 shows example output for (Fig. 2A) a constant light and (Fig. 2B) a forced light-dark implementation of Locke et al. [3] and raises two issues worthy of consideration. Firstly, Fig. 2A shows

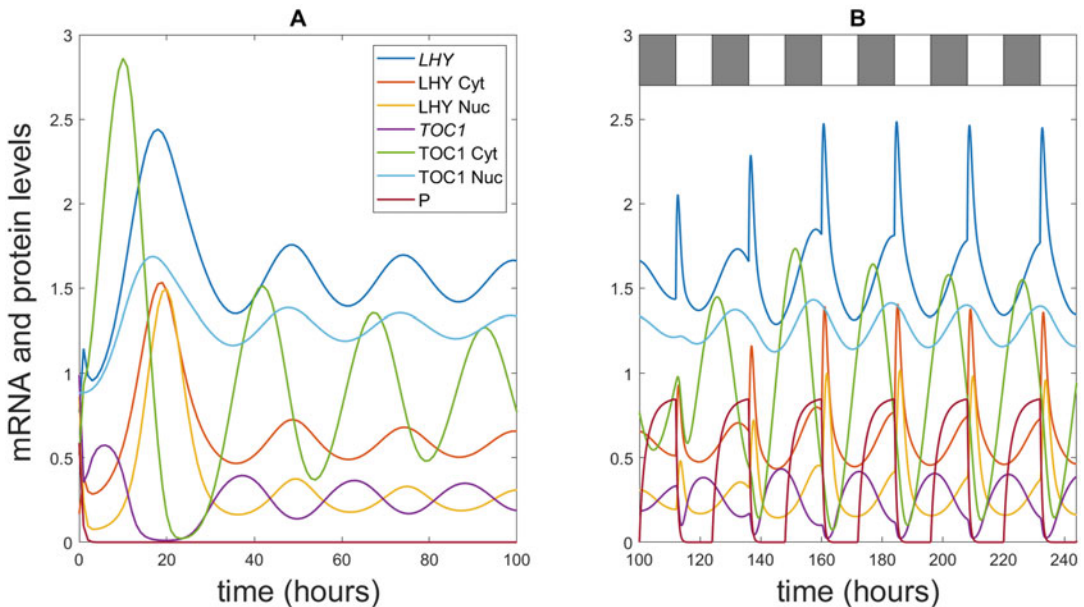


Fig. 2 Outputs from the Locke et al. [3] model under constant light conditions (A) and with photoperiods of 12-h dark and 12-h light (B). A shows that around 100 h of simulation burn-in are needed for the model's transients to decay and for the solution to reach a stable limit cycle. B shows the forced system; in this case the transients decay more rapidly. The resulting periodic solution (which cannot strictly be called a limit cycle) has a period of 24 h matching that for the dark-light forcing. The sharp peaks in the output signal are indicative of a stiff system and would make it advisable that the numerical solution is checked using an alternative solution method (see text)

initial behaviors which are not representative of the model's natural limit cycle behavior. This is not surprising, because the initial conditions are chosen at random (**Locke2005forced.m line 5**) and are unlikely to represent a realistic state of the system; instead, the user needs to wait for the transient dynamics to die out and for the natural limit cycle to be revealed. This process is known as “burn-in.” Secondly, in the forced system, (Fig. 2B) there are sharp peaks (spikes) in the output signal; the overall 24-h periodic dynamics have faster dynamics embedded within them. This is an example of a “stiff” system, a term used by mathematicians to describe systems with processes operating at disparate time scales. The numerical solution of stiff systems of ODEs is complicated and beyond the scope of this article. From a practical point of view, when confronted with a stiff system, most off-the-shelf software will either use its own internal procedures to solve the system (which might just mean that the computation takes more time), or give an error message, or both. Solution methods for stiff systems exist and should be used to check the accuracy of any solution. In the example here, the standard ODE solver (ode45) in **Locke2005-forced.m** would simply be replaced by a stiff solver (ode15s or ode23s in the code) and the solutions compared to check for consistency.

There is an elephant in the room: all the models discussed so far rely on “knowing” the values of parameters such as a , g_1 , k_1 , m_1 , and n_1 in Eq. 1. In a complex model, there may be many dozens of such unknown parameters, and their values may not be amenable to experimental estimation. The process of choosing the “correct” parameter values, and indeed the “correct” model, is beyond the scope of this account. In Locke et al. [3], the parameter values were estimated so that the outputs qualitatively match the period length, the phase of the peaks of *LHY* and *TOCI*, and the shape of the measured *LHY* mRNA expression profile, but several more complex alternative methods are available [11]. The fitting process is necessarily subjective and is again tied to the usefulness of an abstract model. A model with 100 unknown parameters can be made to fit 100 data points perfectly (and trivially), but such a modeling process will not have contributed any useful knowledge. Useful models are those which elucidate hidden mechanisms and inform new experiments and are best developed in close collaboration with empirical scientists.

4 Example MATLAB Code

`%Parameters.m`

```
% define global parameter values which can be used by all
programs

% sets the parameter values for the simulations

global q1 q2 n1 n2 g1 g2 m1 m2 m3 m4 m5 m6 m7 p1 p2 p3 r1
r2 r3 r4 k1 k2 k3 k4 k5 k6 k7 a b thetalight

q1 = 2.9741; q2 = 1.0; n1 = 16.9711; n2 = 1.3043; g1 =
3.0351;

g2 = 0.386; m1 = 9.3383; m2 = 16.9058;

m3 = 1.0214; m4 = 1.6859; m5 = 0.4212; m6 = 0.0484; m7 =
1.2; p1 = 4.9753; p2 = 1.2947;

p3 = 0.5; r1 = 1.4563; r2 = 0.8421; r3 = 0.0451; r4 =
0.0018; k1 = 1.3294;

k2 = 0.8085; k3 = 0.1445; k4 = 0.2089; k5 = 0.3187;

k6 = 0.3505; k7 = 1.2; a = 1; b = 2;
```

`%Locke2005derivs.m`

```
function F = locke2005derivs(t,y)

% extract dynamic variables from y vector

clm=y(1); clc=y(2); cln=y(3); ctm=y(4); ctc=y(5);

ctn=y(6); cpn=y(7);

% define global parameter values which can be used by all
programs

global q1 q2 n1 n2 g1 g2 m1 m2 m3 m4 m5 m6 m7 p1 p2 p3 r1
r2 r3 r4 k1 k2 k3 k4 k5 k6 k7 a b thetalight

L = q1*cpn*thetalight;
```

```

dclmdt = L + n1*((ctn.^a)/((g1.^a)+ctn.^a)) -
m1*clm/(k1+clm);
dclcdt = p1*clm - r1*clc + r2*cln - m2*clc/(k2+clc);
dclndt = r1*clc - r2*cln - m3*cln/(k3+cln);
dctmdt = n2*(g2.^b)/((g2.^b)+(cln.^b)) - m4*ctm/(k4+ctm);
dctcdt = p2*ctm - r3*ctc + r4*ctn - m5*ctc/(k5+ctc);
dctndt = r3*ctc - r4*ctn - m6*ctn/(k6+ctn);
dcpndt = (1-thetalight)*p3 - m7*cpn/(k7+cpn) -
q2*thetalight*cpn;
F = [dclmdt; dclcdt; dclndt; dctmdt; dctcdt; dctndt;
dcpndt];
end

```

%Locke2005.m

```

clear all;
% define global parameter values which can be used by all
programs
global q1 q2 n1 n2 g1 g2 m1 m2 m3 m4 m5 m6 m7 p1 p2 p3 r1
r2 r3 r4 k1 k2 k3 k4 k5 k6 k7 a b thetalight
run Parameters % sets the parameter values using the file
Parameters.m
ystart=rand(1,7); % random initial condition
ystart=[0.2290 0.9133 0.1524 0.8258 0.5383 0.9961
0.0782]; % randomly obtained and used in Figure 1
thetalight = 0; % dark
[t,ydark]=ode45(@locke2005derivs,[0:200],ystart);

```

```
plot(t,ydark,'linewidth',2);
set(gca,'FontSize',18);
ylabel('mRNA and protein levels ','fontSize',24)
xlabel('time (hours)','fontSize',24)
legend({'\itLHY', 'LHY Cyt', 'LHY Nuc', '\itTOC1', 'TOC1
Cyt', 'TOC1 Nuc', 'a protein P'},'fontSize',14)

%Locke2005forced.m

clear all;

% define global parameter values which can be used by all
programs

global q1 q2 n1 n2 g1 g2 m1 m2 m3 m4 m5 m6 m7 p1 p2 p3 r1
r2 r3 r4 k1 k2 k3 k4 k5 k6 k7 a b thetalight

run Parameters % sets the parameter values using the file
Parameters.m

ystart=rand(1,7); % random initial values
ystart=[0.7689 0.1673 0.8620 0.9899 0.5144 0.8843
0.5880]; % randomly obtained and used in Figure 2

% burn in in light conditions

thetalight = 1;

[t,y]=ode45(@locke2005derivs,[0:100],ystart);

subplot(1,2,1)

plot(t,y,'linewidth',1.5);

set(gca,'FontSize',13);

ylabel('mRNA and protein levels ','fontSize',24)
xlabel('time (hours)','fontSize',24)
```

```

title('A','fontSize',18)
legend({'\itLHY', 'LHY Cyt', 'LHY Nuc', '\itTOC1', 'TOC1
Cyt', 'TOC1 Nuc', 'P'},'fontSize',14)
lighttime=12; % duration for the light period
darktime=24-lighttime; % and the dark period
totaltime=150; % total time for forced simulation
elapsed=0;
ystart= y(end,:);
while elapsed<totaltime
    thetalight=0;

    [t,y]=ode45(@locke2005derivs,[elapsed:0.01:elapsed+darkti
me],ystart);
    elapsed=elapsed+darktime;
    ystart= y(end,:);
    subplot(1,2,2)
    plot(t,y,'linewidth',1.5);
    hold on
    thetalight=1;

    [t,y]=ode45(@locke2005derivs,[elapsed:0.01:elapsed+lightt
ime],ystart);
    elapsed=elapsed+lighttime;
    ystart= y(end,:);
    subplot(1,2,2)
    plot(t,y,'linewidth',1.5);

```

```

end

set(gca,'FontSize',13);

xlabel('time (hours)','fontSize',24)

title('B','fontSize',18)

my_labels=[{'100','120','140','160','180','200','220','240'}];

set(gca,'XTickLabel',my_labels);

days_plot=6;

T=24;

xlim([0 days_plot*T])

patch([0 T/2 T/2 0],[2.7 2.7 3 3],[0.5 0.5 0.5])

patch([T/2 2*T/2 2*T/2 T/2],[2.7 2.7 3 3],'w')

for i=2:2:2*(days_plot-1)

    patch([i*T/2 (i+1)*T/2 (i+1)*T/2 i*T/2],[2.7 2.7 3 3],[0.5 0.5 0.5])

    patch([(i+1)*T/2 (i+2)*T/2 (i+2)*T/2 (i+1)*T/2],[2.7 2.7 3 3],'w')

end

```

References

1. Box GEP (1976) Science and statistics. J Am Stat Assoc 71:791–799
2. Strogatz SH (2000) Nonlinear dynamics and chaos: with applications to physics, biology, chemistry and engineering (studies in nonlinearity). CRC Press, Boca Raton, FL
3. Locke JCW, Millar AJ, Turner MS (2005) Modelling genetic networks with noisy and varied experimental data: the circadian clock in *Arabidopsis thaliana*. J Theor Biol 234:383–393
4. Alon U (2006) An introduction to systems biology: design principles of biological circuits. Taylor & Francis, Boca Raton, FL
5. De Caluwé J, Xiao Q, Hermans C, Verbruggen N, Leloup JC, Gonze DA (2016) Compact model for the complex plant circadian clock. Front Plant Sci 7:1–15
6. Joanito I, Chu J-W, Wu S-H, Hsu C-P (2018) An incoherent feed-forward loop switches the Arabidopsis clock rapidly between two hysteretic states. Sci Rep 8:13944

7. Avello PA, Davis SJ, Ronald J, Pitchford JW (2019) Heat the clock: entrainment and compensation in *Arabidopsis* circadian rhythms. *J Circadian Rhythms* 17:5
8. De Caluwé J, de Melo JRF, Tosenberger A, Hermans C, Verbruggen N, Leloup JC et al (2017) Modeling the photoperiodic entrainment of the plant circadian clock. *J Theor Biol* 420:220–231
9. Pokhilko A, Hodge SK, Stratford K, Knox K, Edwards KD, Thomson AW et al (2010) Data assimilation constrains new connections and components in a complex, eukaryotic circadian clock model. *Mol Syst Biol* 6:416
10. Avello Fernández PA (2019) Modelling temperature dependence in the *Arabidopsis thaliana* circadian clock. PhD thesis, University of York, UK
11. Fogelmark K, Troein C (2014) Rethinking transcriptional activation in the *Arabidopsis* circadian clock. *PLoS Comput Biol* 10:e1003705



How to Detect QTLs in the Plant Circadian Clock

Muhammad Usman Anwer and Marcel Quint

Abstract

One of the most powerful methods to identify loci controlling complex quantitative traits has been the quantitative trait locus (QTL) mapping. The QTL mapping approach has proven immensely useful to improve our understanding of key pathways such as flowering time, growth, and disease resistance. Since major circadian clock parameters such as period, phase, and amplitude are quantitative in nature, the QTL mapping approach could also be used to study the complex genetic architecture of the circadian clock. Here, we describe a simple QTL mapping method to identify components controlling clock parameters in natural populations of *Arabidopsis thaliana*.

Keywords Circadian clock, Natural variation, Linkage map, QTL mapping, Luciferase assays

1 Introduction

Circadian clocks are essential components of most organisms that enable them to synchronize their internal cellular biology to the external environment. Under natural conditions, a robust oscillator ensures that important physiological and molecular processes happen at the most optimal time of the day-night cycle, resulting in an increased fitness [1, 2]. To achieve that, clock components known as *zeitnehmers* (time takers) receive the timing information from external environmental cues such as light and temperature (in a process known as entrainment) and convey it to the central oscillator [3, 4]. After setting the most optimal pace, the central oscillator then rhythmically regulates numerous output pathways, ensuring that the specific biological and developmental events only occur under the most suitable time of day [5, 6].

At the molecular level, the circadian clocks are comprised by transcriptional/translational feedback loops. For instance, in *Arabidopsis thaliana* (*Arabidopsis*), three such loops constitute a basic oscillator: a morning loop including CIRCADIAN CLOCK ASSOCIATED 1 (CCA1), LATE ELONGATED HYPOCOTYL (LHY),

and PSEUDO RESPONSE REGULATORS 7 and 9, an evening loop consisting of TIMING OF CAB EXPRESSION 1 (TOC1) and GIGANTEA (GI), and a core loop consisting of CCA1, LHY, and TOC1 [7, 8]. These three loops along with the components of the evening complex (EC), EARLY FLOWERING 3, EARLY FLOWERING 4, and LUX ARRHYTHMO (LUX), are collectively known as central oscillator or simply oscillator [9, 10]. Precise functioning of the central oscillator is essential to generate internal rhythms that are in sync with the external environment.

In *Arabidopsis*, two methods that are mostly used to monitor circadian rhythms are leaf movement analysis and, more recently, the luciferase-based reporter assay [11, 12]. The leaf movement analysis is based on the physiological change of the position of young leaves and cotyledons in seedlings and therefore does not require prior genetic manipulation of the plants. In luciferase reporter assays, the luciferase gene (LUC) is expressed under the promoter of *CLOCK CONTROL GENE* (CCG), and the construct (CCG::LUC) needs to be transgenically introduced into the plant genome before the plants can be used for clock assays. However, the luciferase reporter-based method is generally more accurate than the leaf movement assay and, in addition, allows high-throughput phenotyping of large numbers of seedlings [11, 12]. Nevertheless, both methods can be used to study the activity of the clock by analyzing the rhythms generated by the oscillator.

The circadian rhythms can be defined by no less than four parameters (Fig. 1, adopted from [6]): period, phase, amplitude, and robustness (also known as relative amplitude error (RAE)) [6]. Since these circadian traits are quantitative in nature, QTL mapping has been successfully used to map loci controlling these traits [6, 13–23]. Some of these studies have proven that geographically distinct *Arabidopsis* accessions provide a rich source of natural variations that could be utilized in QTL mapping to identify novel clock components [16, 19, 20, 23, 24]. Here, we describe how natural variations in *Arabidopsis* accessions can be used to identify loci in the circadian clock using QTL mapping.

2 Methods

2.1 QTL Mapping

QTL mapping comprises five basic steps that include (a) selection of appropriate parental accessions, (b) generation of suitable mapping populations, (c) construction of genetic maps by genotyping with polymorphic markers spanning the complete genome, (d) a phenotype for the trait of interest (such as period), and, finally, (e) statistical analysis to detect potential loci associated with the trait under study [6]. These steps are further elaborated below.

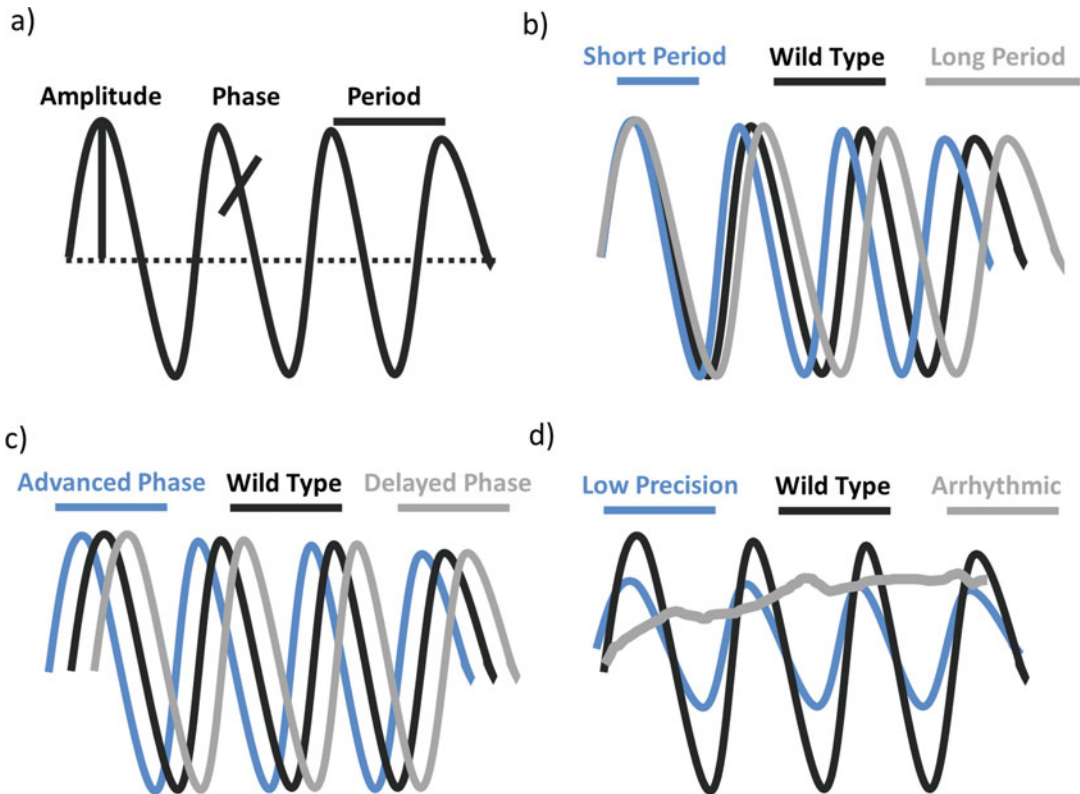


Fig. 1 Properties of a circadian rhythm. **(a)** Schematic diagram showing main parameters of a circadian rhythm. Amplitude is half the difference between the highest and the lowest value of the oscillation. Phase refers to the timing of a physiological event within the circadian cycle. Often, it refers to the highest rhythm value within the oscillation (peak). Period represents the time to complete one oscillation, which is normally taken as a time difference between two consecutive peaks. **(b–d)** shows the hypothetical period **(b)**, phase **(c)**, and precision **(d)** of three genotypes under free-running conditions. (Adopted from [6])

2.1.1 Selection of Parental Accessions

If possible, select *Arabidopsis* accessions that are/ or expected to be genetically different in clock traits (*see Note 1*). For example, accessions growing in different latitudes are expected to have genetically diverged because of adaptation to varying environmental conditions including photoperiod and temperature. Thus, genetic components controlling clock traits in a northern accession are potentially different from those regulating the clock in an equatorial accession [6].

At this stage, one of the parental accession (P_1) needs to be transformed with the *CCG::LUC* construct to enable high-throughput phenotyping (discussed in detail below; also *see Note 2*).

2.1.2 Generation of Suitable Mapping Populations

In principal, any segregating population can be used for QTL mapping (*see Note 4*). However, recombinant inbred lines (RILs) are the most commonly used segregating populations [13, 16, 19,

20]. RILs are immortal populations that could theoretically be used countless times for comparative analysis of multiple traits and environments [25]. RILs can be generated by following these steps:

1. Cross P_1 harboring *CCG::LUC* (see **Note 2**) with parental accession 2 (P_2 , without *CCG::LUC*) to obtain an F_1 . It makes sense to use P_1 as a pollen donor as an F_1 expressing *CCG::LUC* will confirm a successful cross.
2. Self-fertilize the F_1 (harboring *CCG::LUC*) to obtain a segregating F_2 population.
3. Select multiple F_2 lines and continue self-fertilization using single-seed descent (SSD) until F_7 seeds are obtained. Ensure during each generation that only plants expressing *CCG::LUC* are selected (see **Note 3**). The seeds from each line could now be labeled as individual RILs.
4. Bulk the seeds by growing multiple F_7 plants of each RIL. Each RIL should be >99% homozygous at this stage (see **Note 4**).

2.1.3 Genotyping and Phenotyping

There is no specific order in which genotyping and phenotyping should be performed. To save time, both can be carried out in parallel.

Genotyping

The objective of genotyping for QTL mapping is to determine the inheritance of the different parental alleles at regular intervals throughout the genome of each RIL. Although densely placed markers provide a slight advantage, evenly spaced markers located at every 10–20 centimorgan (cM) are sufficient to detect most QTLs [26, 27]. Any method of choice ranging from classic PCR based molecular markers to the recent genotyping by sequencing can be used for genotyping (reviewed in [28]). Once the genotyping is complete, calculate the genetic linkage maps using a linkage analysis software such as JoinMap[®] (<https://www.kyazma.nl/index.php/JoinMap/>) [29], as described briefly below:

1. Arrange the genotyping data in proper file format required by the software (see instructions for the selected software).
2. Create a “New project” and load the genotype data file into the project (data can also be pasted from an excel file).
3. Inspect the data under *Data* tab. If required, any markers or RILs could be excluded from the further analysis under the *Loci* or *Individuals* tabs (e.g., a marker or RIL with lots of missing data). Most of the other tabs would be empty at this stage.
4. Click on each tab and then click on the *calculate* button to perform the calculations. Each tab will provide some valuable information. For instance, under the *Similarity of Loci* tab, you can see if some of the loci are identical (with a similarity value

1000). These loci should be removed from further calculations as they will map at exactly the same position. However, they add to the calculation efforts. Identical RILs could also be identified and excluded under the *Similarity of Individuals* tab.

5. Inspect the marker grouping with different thresholds under the *Groupings (tree)* tab. Select the five groups with the markers belonging to same chromosome and with a minimum of 3.0 LOD threshold (if required adjust the grouping parameters available under *Calculation Options* button).
6. Apply the *Create Groups Using the Groupings Tree* function of the Population menu. This will open a new node with five sub-nodes (named Group 1 to Group 5) each corresponding to a group selected in the last step.
7. Select the first sub-node (named Group 1) and press the *Calculate* button. Most of the empty tab sheets will show different data now. Inspect the data and, if require, change the threshold in the *Group* tab within the *Calculation Options* menu.
8. Click on the *Calculate Map* button. This will open a new sub-node and display the linkage map of the group and other related data under different tabs. Inspect the position of the markers on the map. If required, modify the mapping options.
9. Repeat the **steps 7 and 8** after selecting the remaining four sub-nodes (Groups 2–5) created during **step 6**. This will generate the linkage maps of the five groups that correspond to the five chromosomes of *Arabidopsis*.
10. Use the *Combine Map* function under the *Join* menu to generate a single genetic linkage map.

Phenotyping

RILs carrying *CCG::LUC* can be phenotyped for clock traits using, for example, a TOPCOUNT[®] scintillation counter (PerkinElmer) as follows:

1. Surface-sterilize seeds using 95% ethanol and 5% bleach, followed by three to five times rinsing with sterile water.
2. Plate seeds on Murashige and Skoog (MS) medium supplemented with 1–3% sucrose (MS 1–3). Make sure that the seeds are separated well enough that the seedlings do not grow into each other.
3. Stratify for 3 days in darkness at 4 °C to synchronize germination.
4. Transfer the seedlings into entraining conditions (light-dark or warm-cool cycles) for 7 days.
5. On Day 7, transfer the seedlings to sterile black 96-well Microplates (OPTIPLATE[™] TM-96F, PerkinElmer) containing 200 µL of MS 1–3 agar.

6. Add 15 μL of 5 mM D-luciferin in each well.
7. Seal the plates with transparent film (Packard TopSeal) and perforate each well with a sterile needle.
8. Put the plates back into the same entraining conditions.
9. Next day at dusk, place the plates in the scintillation counter for luminescence measurement under free-running conditions (constant light or darkness and constant temperature).
10. Record the luminescence values every 30–40 min for 5 days.
11. Calculate the circadian clock parameters such as period, phase, amplitude, and RAE using rhythm analysis software such as Biological Rhythms Analysis Software System (BRASS: <http://millar.bio.ed.ac.uk/PEBrown/BRASS/BrassPage.htm>) (*see Note 5*).

2.1.4 Statistical Analysis to Detect QTLs

As a final step, statistical associations between the markers on the linkage map and the phenotypic data are calculated, which reveals the QTLs linked to the traits under study. Several software deploying different statistical approaches are available (*see Note 6*). Here, we briefly describe stepwise process to detect QTLs using MapQTL[®] (<https://www.kyazma.nl/index.php/MapQTL>) [30].

1. Create a *New Project* using the *File* menu.
2. Load properly formatted trait (containing phenotype data), locus (containing genotype data), and map (containing linkage map data) files into the project.
3. Select *Interval Mapping* (IM) from the drop-down menu in the *Analysis Selector* tool bar.
4. Using right click, select the linkage map under the *Maps* tab and the traits (for instance, period, phase, etc.) under the *Populations* tab.
5. Click on the *Calculate* button. This will automatically open the *Sessions* tab sheet. After calculations are completed, several tabs under the *Sessions* tab sheet will display important data. For instance, under the *Results* tab, IM results such as LOD score, variance, and % explained will be displayed. These results can be displayed as graphs by clicking the *Results Chart* tab.
6. Next, perform the permutation test to determine a LOD threshold. To perform a permutation test, select *Permutation Test* from the drop-down menu in the *Analysis Selector* tool bar. Then click on the *Analysis Options* tab and set *Number of Permutations* to 10,000. Make sure that the linkage map and the traits selected during **step 4** are still selected.
7. Click on the *Calculate* button and wait for the calculations to complete. A new session node will be opened under the *Sessions* tab sheet. Inspect the results in the *Results* tab and look up for a

genome-wide (GW) interval value in the “group column” at the relative cumulative value (Rel. cum. count column) of 0.9500 (or a value close). Take a note of the value.

8. Redo the permutation test for few more times with the same settings and record each time the estimated threshold value obtained. You will see that the threshold value is slightly different after each permutation test. Now take an average of all the values to get a final LOD threshold value. The regions of the chromosomes with a LOD score above this threshold will be designated as potential QTLs.

In MapQTL[®], the IM results can be further refined using the so-called multiple QTL mapping (MQM) model. In the MQM mapping, markers close to the QTLs detected in IM are used as cofactors, which increases QTL detection power by decreasing the residual variance. To perform MQM mapping,

9. Select the *Map* tab and check the boxes in the *Cofactor* column for the markers closest to the QTLs.
10. Select *MQM Mapping* from the drop-down menu in the *Analysis Selector* tool bar.
11. Click on the *Calculate* button and inspect the results of MQM mapping using the charts. The LOD significance threshold would be the same as determined by the permutation test.
12. In case new QTLs are detected or the markers closest to the previously detected QTLs are changed, modify the set of markers used as cofactor and repeat the MQM mapping until there is no change in the linked markers and a final set of QTLs is obtained (*see Note 7*).

3 Notes

1. Selection of parental accession with contrasting phenotypes should be preferred. However, because of transgressive segregation, periodicity QTLs have been detected in the populations where parental accessions did not show period differences.
2. Before proceeding further, the parental accession (P_1) harboring *CCG::LUC* should be backcrossed to the same parental accession (P_1 without *CCG::LUC*) to ensure a single copy of the *CCG::LUC* transgene in a homogenous genetic background.
3. Besides *CCG::LUC* presence, care should be taken that no other selection bias is introduced during SSD.

4. Already in the F_5 generation, RILs can be used for phenotyping without losing much of the computational power of the QTL mapping. The residual heterogeneity present in the F_5 -RILs provides an advantage as heterogeneous inbred families (HIFs) could be quickly generated to confirm the QTLs [31].
5. For online calculation of the circadian data, BioDare (<https://www.biodare.ed.ac.uk>) can also be used.
6. Several commercial (such as MapQTL, MultiQTL) and free (such as QTL cartographer, R/qTL) software packages are available for QTL mapping.
7. A potential QTL mapped around the location of the *CCG::LUC* transgene could be present in the final set of QTLs. This is not a bona fide QTL and should be removed from the list.

References

1. Salmela MJ, Weinig C (2019) The fitness benefits of genetic variation in circadian clock regulation. *Curr Opin Plant Biol* 49:86–93
2. Yerushalmi S, Yakir E, Green RM (2011) Circadian clocks and adaptation in *Arabidopsis*. *Mol Ecol* 20(6):1155–1165
3. Anwer MU et al (2020) Photoperiod sensing of the circadian clock is controlled by *EARLY FLOWERING 3* and *GIGANTEA*. *Plant J* 101:1397–1410
4. Inoue K, Araki T, Endo M (2017) Integration of input signals into the gene network in the plant circadian clock. *Plant Cell Physiol* 58(6):977–982
5. Mora-García S, de Leone MJ, Yanovsky M (2017) Time to grow: circadian regulation of growth and metabolism in photosynthetic organisms. *Curr Opin Plant Biol* 35:84–90
6. Anwer MU, Davis SJ (2013) An overview of natural variation studies in the *Arabidopsis thaliana* circadian clock. *Semin Cell Dev Biol* 24(5):422–429
7. McClung RC (2019) The plant circadian oscillator. *Biology* 8(1):14
8. Ronald J, Davis S (2017) Making the clock tick: the transcriptional landscape of the plant circadian clock. *Fl000Res* 6:951
9. Herrero E et al (2012) *EARLY FLOWERING4* Recruitment of *EARLY FLOWERING3* in the nucleus sustains the *Arabidopsis* circadian clock. *Plant Cell* 24:428
10. Nusinow DA et al (2011) The ELF4-ELF3-LUX complex links the circadian clock to diurnal control of hypocotyl growth. *Nature* 475(7356):398–402
11. Staiger D (2014) Plant circadian networks: methods and protocols. Springer, New York, NY
12. Edwards KD, Millar AJ (2007) Analysis of circadian leaf movement rhythms in *Arabidopsis thaliana*. In: Rosato E (ed) *Circadian rhythms: methods and protocols*. Humana Press, Totowa, NJ, pp 103–113
13. Rubin MJ et al (2019) QTL Underlying circadian clock parameters under seasonally variable field settings in *Arabidopsis thaliana*. *G3* 9(4):1131
14. Rubin MJ et al (2017) Circadian rhythms vary over the growing season and correlate with fitness components. *Mol Ecol* 26:5528
15. Raschke A et al (2015) Natural variants of *ELF3* affect thermomorphogenesis by transcriptionally modulating PIF4-dependent auxin response genes. *BMC Plant Biol* 15(1):197
16. Anwer MU et al (2014) Natural variation reveals that intracellular distribution of *ELF3* protein is associated with function in the circadian clock. *elife* 3:e02206
17. Lou P et al (2011) Genetic architecture of the circadian clock and flowering time in *Brassica rapa*. *Theor Appl Genet* 123(3):397–409
18. Edwards CE et al (2011) The genetic architecture of ecophysiological and circadian traits in *Brassica rapa*. *Genetics* 189(1):375–390
19. Boikoglou E et al (2011) Environmental memory from a circadian oscillator: the *Arabidopsis thaliana* clock differentially integrates perception of photic versus thermal entrainment. *Genetics* 189:655

20. Darrah C et al (2006) Analysis of phase of LUCIFERASE expression reveals novel circadian quantitative trait loci in Arabidopsis. *Plant Physiol* 140(4):1464–1474
21. Edwards KD et al (2005) Natural allelic variation in the temperature-compensation mechanisms of the Arabidopsis thaliana circadian clock. *Genetics* 170(1):387–400
22. Michael TP et al (2003) Enhanced fitness conferred by naturally occurring variation in the circadian clock. *Science* 302(5647):1049–1053
23. Swarup K et al (1999) Natural allelic variation identifies new genes in the Arabidopsis circadian system. *Plant J* 20(1):67–77
24. de Montaigu A et al (2014) Natural diversity in daily rhythms of gene expression contributes to phenotypic variation. *Proc Natl Acad Sci* 112:905
25. Takuno S, Terauchi R, Innan H (2012) The power of QTL mapping with RILs. *PLoS One* 7(10):e46545
26. Stange M et al (2013) High-density genotyping: an overkill for QTL mapping? Lessons learned from a case study in maize and simulations. *Theor Appl Genet* 126(10):2563–2574
27. Piepho H-P (2000) Optimal marker density for interval mapping in a backcross population. *Heredity* 84(4):437–440
28. Deschamps S, Llaca V, May GD (2012) Genotyping-by-sequencing in plants. *Biology* 1(3):460–483
29. Stam P (1993) Construction of integrated genetic linkage maps by means of a new computer package: join map. *Plant J* 3(5):739–744
30. Van Ooijen JW (1993) MapQTL, a computer program for mapping quantitative trait loci. Centre for Plant Breeding and Reproduction Research, Wageningen
31. Alonso-Blanco C, Koornneef M (2000) Naturally occurring variation in Arabidopsis: an underexploited resource for plant genetics. *Trends Plant Sci* 5(1):22–29



Measuring Hypocotyl Length in *Arabidopsis*

James Ronald and Seth Jon Davis

Abstract

Circadian clocks allow organisms to synchronize growth to occur at the most optimal time of the day. In plants, the circadian clock controls the timing of hypocotyl (seedling stem) elongation. The activity of the circadian clock subsequently results in hypocotyl elongation being restricted to a small window around dawn and the early morning. Measuring hypocotyl elongation has provided circadian biologists a quick and non-intensive experimental tool to understand the effect of a circadian mutation on plant growth. Furthermore, hypocotyl elongation is also independently regulated by light, temperature, and hormone signaling pathways. Thus, hypocotyl assays can be expanded to investigate the crosstalk between the circadian clock and other extrinsic and intrinsic signaling pathways in controlling plant development. In this chapter we describe the resources and methods required to set up and analyze hypocotyl elongation in *Arabidopsis*.

Key words Circadian clock, Growth, Hypocotyl, Circadian mutants, Light signaling, Hormone signaling

1 Introduction

The plant circadian clock integrates internal and external stimuli to synchronize internal physiological processes such as photosynthesis and growth to occur at the most optimal time of day [1]. One physiological process under the control of the circadian clock is hypocotyl elongation. Circadian control of hypocotyl elongation occurs primarily through the regulation of two transcription factors, *PHYTOCHROME INTERACTING FACTOR4* (*PIF4*) and *PHYTOCHROME INTERACTING FACTOR5* (*PIF5*) [2]. The circadian clock regulates *PIF4/5* expression so that hypocotyl elongation occurs during a restricted window of time. Under short-day photoperiods (8 h of light), *PIF4/5* expression occurs at dawn, while in long-day photoperiods, *PIF4/5* expression is shifted to early morning or midday [3]. The circadian clock also post-translationally controls *PIF4/5* activity to ensure that hypocotyl elongation is phased to the right time of day. Most circadian

mutants in *Arabidopsis* have defects in hypocotyl elongation; either hypocotyl elongation is not repressed (*elf3*, *elf4*, *lux* (*pcl*), and *gi*), or the hypocotyl is not elongated (*ztl*, *toc1*, *prr5/7/9*, and *cca1/lyy*) [4]. Separately of the circadian clock, hypocotyl elongation is also regulated by light, temperature, and internal signaling pathways such as metabolites and hormones [2, 5]. These pathways share overlap with the circadian clock, resulting in a complicated network of positive and negative interactions at the transcriptional and post-translational level to control the timing and extent of hypocotyl elongation.

Hypocotyl growth assays are relatively quick to set up and run, are inexpensive, and are not labor intensive. They can be simple experiments that only look at a single mutant line relative to wild type under a single photoperiod, or they can be expanded to incorporate multiple mutant lines, photoperiods, light wavelengths, temperature regimes, and hormone treatments to provide more detailed insights into how hypocotyl growth is being controlled. The ease and quick nature of the experiment can quickly provide an informative readout on circadian control of growth and the crosstalk between multiple signaling pathways. In this chapter we will describe how to set up a simple hypocotyl experiment and analyze the data and the experimental considerations that need to be incorporated into the design of a hypocotyl experiment.

2 Materials and Experimental Considerations

2.1 Equipment and Software Required

1. Clear, square vented petri dishes.
2. 100% ethanol.
3. Bleach/Triton X solution (per liter: 33% thin bleach, 200 μ L Triton X-100).
4. Select agar (*see Note 1*).
5. Growth media (*see Subheading 2.3*).
6. Flatbed scanner.
7. Reach-in growth cabinet or temperature-controlled room.
8. ImageJ (*see Note 2*).
9. Software to store generated data (Excel, Google Sheets, Numbers, etc.).
10. Statistical analysis software (Excel, R, MATLAB, etc.).

2.2 Growth Conditions

Hypocotyl length is sensitive to extrinsic and intrinsic factors. Therefore, the experimental design needs to be carefully considered so that robust and repeatable data is generated.

The duration, intensity, and wavelength of light all need to be considered in a hypocotyl experiment. Typically, measurements of

hypocotyl length with circadian mutants use short, neutral, or long days as under constant darkness or constant light circadian mutants have a weaker or no phenotype [6]. Alongside photoperiod, the intensity and wavelength of light need to be considered. Hypocotyl elongation is inversely correlated with light intensity. Therefore, if multiple growth chambers are being used, the light intensity needs to be similar across the chambers so that results can be comparable. Separately, it is important that all seedlings receive an equal amount of light within the growth chamber. To achieve this, all lines being used in the experiment should be plated onto the same plate, with a minimum of two plates per experiment. The two (or more) independent plates should be placed within the chamber so that they receive a similar intensity of light. The wavelength of light in the experiment can also be adjusted. Standard hypocotyl experiments will use white light, but monochromatic light or far-red supplementation can be added to investigate the crosstalk between a specific photoreceptor signaling pathway and the circadian clock in controlling hypocotyl growth.

The temperature of the growth chambers also needs to be considered as higher temperatures promote hypocotyl elongation [2]. It is therefore important to ensure that if multiple growth chambers are used, the temperature is identical or nearly identical across the two chambers unless temperature is a variable being investigated. The media (*see* Subheading 2.3) can also be supplemented with compounds such as hormones or pharmacological inhibitors such as geldanamycin. A range of concentrations should be tested prior to a full experiment to establish a dose-response curve. If the media is being supplemented with a compound, control plates should be supplemented with an equal volume of the solution used to dissolve the solute to confirm the observed response is specifically caused by the solute (*see* Note 3).

2.3 Growth Media

Standard hypocotyl measurements are carried out with Murashige and Skoog media (MS): 4.4 g/L MS basal salt, 0.5 g/L MES (2-*N*-morpholino-ethanesulfonic acid), and 1.5% (w/v) phytoagar. The pH of the medium should be adjusted to between 5.7 and 5.8 with 1 M KOH. Varying concentrations (0–3%) of sucrose can be added to the growth media; the concentration of sucrose should be kept consistent across an experiment unless sucrose is a variable being tested. Higher concentrations of sucrose can also increase the risk of mold contamination. Alternatively, media such as Hoagland's media can be used if specific concentrations of macro or microelements are needed or are being tested in the experiment. The choice and makeup of media should be kept the same across the experiment. All media should be autoclaved prior to use.

3 Experimental Setup and Data Analysis

1. Aliquot ~150 seeds for each genotype (enough for ~4 to 6 plates) to be investigated into a 1.5- or 2-mL microcentrifuge tube.
2. Under sterile conditions, add 1 mL of 100% ethanol and wash the seeds for 2 min. Spin the tubes down and remove the ethanol. Add 1 mL of bleach/Triton X and wash for 2 min. After 2 min, remove the bleach/Triton X solution and add 1 mL of sterile deionized water and spin down immediately. Repeat the wash step at least twice before resuspending the seeds in 1 mL of 0.1% agar water.
3. Carefully plate the seeds onto the appropriate plate, ensuring that seeds are evenly spaced apart and have minimal overlap (Fig. 1a, b) (*see Note 4*). Stratify seeds for 3–4 days at 4 °C (*see Note 5*).
4. After 3 or 4 days of stratification, transfer the plates to the appropriately set growth chamber and leave for between 5 and 7 days (*see Note 6*).
5. At the decided end point of the experiment, remove the plates from the growth chambers before the start of the dark phase. Using forceps (these do not need to be sterile), carefully lift the seedlings from the agar and lay horizontally onto the plate (Fig. 1c). Take care that seedlings are not crushed or damaged when initially removing them from the plate. The seedlings must also not cover each other when they are laid flat as this will make determining the start and end point of the hypocotyl more difficult.
6. Once all seedlings have been placed horizontally onto the plate, place the plate next to a ruler or scale bar on a flatbed scanner and scan the plate following the device instructions. Depending on the scanner, the contrast and brightness of the image may need to be adjusted post-scan to ensure that hypocotyls are clearly visible against the background.
7. Import all images to be analyzed into ImageJ (*see Note 3*).
8. The scale for the images needs to be set. Select the straight line tool on the floating ImageJ task bar and draw a known distance on your ruler or scale bar (Fig. 2a1). Then click on analyze and select set scale, a new ImageJ window will pop up. The known distance and unit measurement settings need to be changed to the decided values (Fig. 2a1, a3). The global button should be selected as this will ensure that the same aspect ratio is used across all scanned plates, resulting in more consistency in the measurements. The global setting is maintained until the ImageJ session is completely closed.

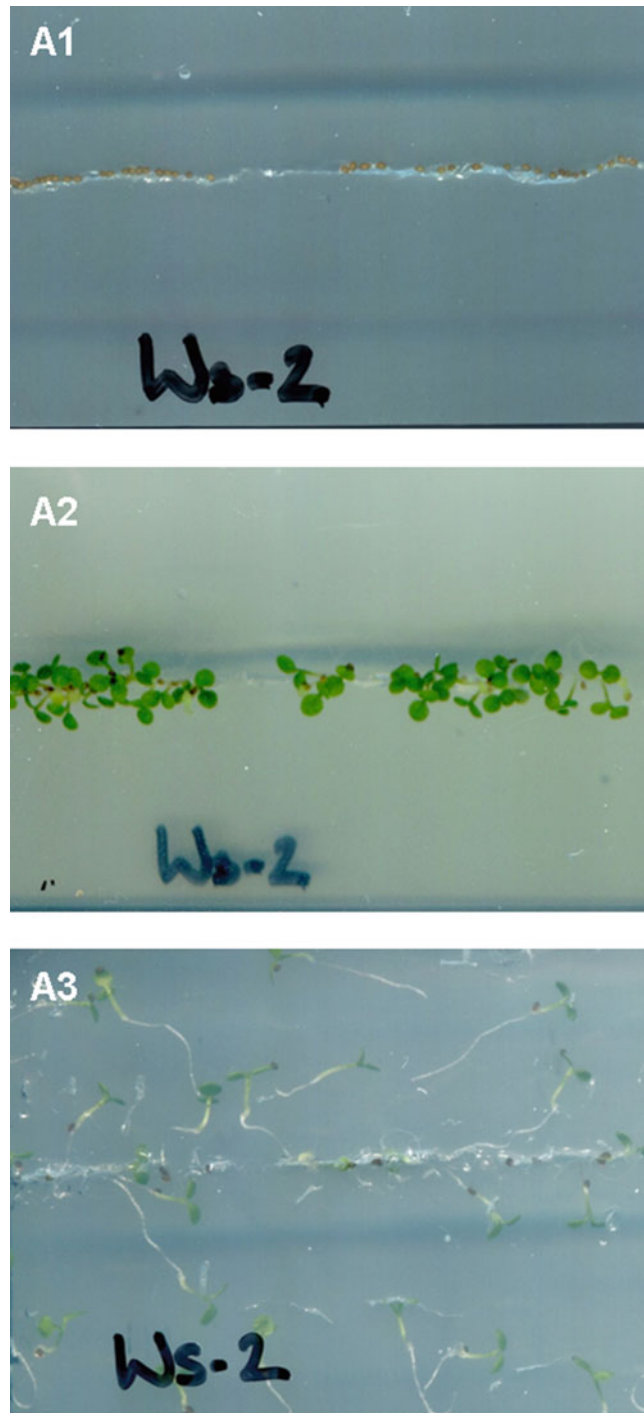


Fig. 1 Example of the plate **(A1)** Surface sterilized seeds are carefully plated to minimize overlap and overcrowding. **(A2)** Seedlings after 5 days of growth. **(A3)** Seedlings have been carefully lifted from the plate and laid flat on the agar, ready for analysis

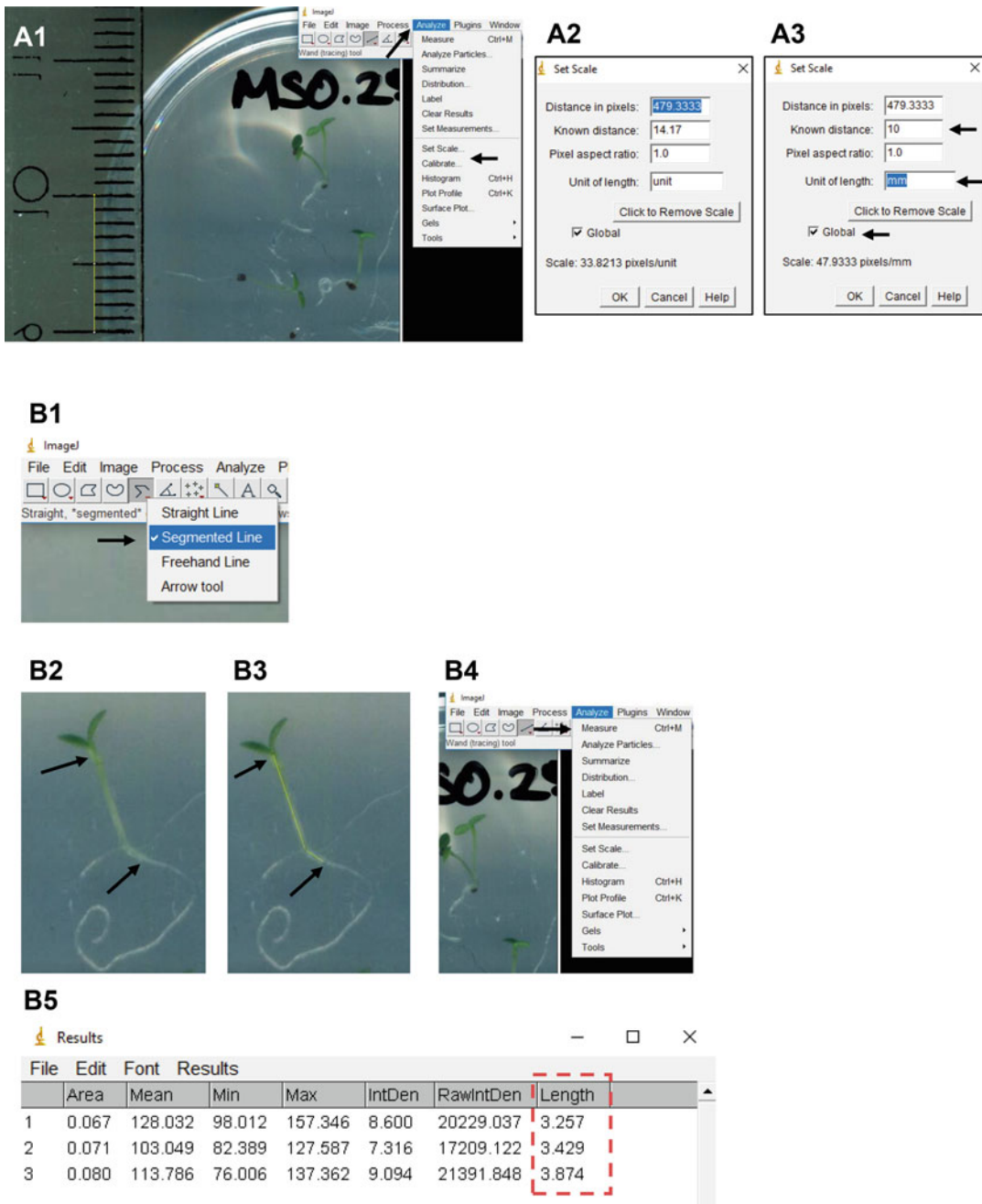


Fig. 2 Example of the imageJ analysis process. **(a)** Setting a scale prior to the analysis. **(b)** Using the segmented line tool to trace along the length of the hypocotyl, generating a measurement and the value table that is generated by imageJ

9. Once the scale has been set, the hypocotyl length can be measured. On the floating ImageJ task bar, right or double click the straight line tool and select segmented line (Fig. 2b1).

Starting from the region directly below the shoot apical meristem, click along the hypocotyl until the root/hypocotyl junction (*see Note 7*). To complete the line, double click at the end point (the hypocotyl-root junction). ImageJ will now produce a continuous straight line along the length of the hypocotyl (Fig. 2b3).

10. Once the line has been drawn, click on analyze and then measure to generate a measurement (Fig. 2b4).
11. The measurements will appear in a separate window. This window can be saved as csv file (click file and then save as or use the ctrl + s shortcut) or copied into a spreadsheet (Fig. 2b5) (*see Note 8*).
12. The measurements can then be analyzed and presented using the preferred data analysis package (Excel, R, MATLAB, etc.).

4 Notes

1. Alternative agar sources can be used such as agar-agar. Ensure that the 0.1% agar solution is autoclaved prior to use.
2. ImageJ is available to download for free from: <https://imagej.nih.gov/ij/download.html>.
3. A commonly used solvent for hormones is dimethyl sulfoxide (DMSO). DMSO can cause physiological effects at concentrations greater than 0.1% [7].
4. If seeds clump together on a plate, use a sterile toothpick or pipette tip to carefully separate the seeds.
5. Here, the start of the experiment is defined as the day of transfer to the growth chamber. It is therefore important to ensure that the plants receive a sufficient period of stratification so that seeds germinate synchronously.
6. The duration of hypocotyl experiment is not fixed, with most assays running between 5 and 7 days. Hypocotyl growth predominantly occurs in the first 3–5 days after germination [8], so the length of the experiment can be tailored as required.
7. The segmented line tool will allow you to trace along hypocotyls that are not completely straight; just follow the bend of the hypocotyl with the segmented line tool and ImageJ will generate a contiguous line once the measurement is complete.
8. The only data generated by ImageJ required for hypocotyl measurement is the length column (highlighted in the red box, Fig. 2b5). All other data columns can be discarded.

References

1. Ronald J, Davis S (2017) Making the clock tick: the transcriptional landscape of the plant circadian clock. *F1000Res* 6:951. (version 1; peer review: 2 approved)
2. Choi H, Oh E (2016) PIF4 integrates multiple environmental and hormonal signals for plant growth regulation in *Arabidopsis*. *Mol Cell* 39:587
3. Nomoto Y, Kubozono S, Yamashino T, Nakamichi N, Mizuno T (2012) Circadian clock- and PIF4-controlled plant growth: a coincidence mechanism directly integrates a hormone signaling network into the photoperiodic control of plant architectures in *Arabidopsis thaliana*. *Plant Cell Physiol* 53:1950
4. Nagel Dawn H, Kay Steve A (2012) Complexity in the wiring and regulation of plant circadian networks. *Curr Biol* 22:R648
5. Oakenfull RJ, Davis SJ (2017) Shining a light on the *Arabidopsis* circadian clock. *Plant Cell Environ* 40:2571
6. Anwer MU, Davis A, Davis SJ, Quint M (2020) Photoperiod sensing of the circadian clock is controlled by EARLY FLOWERING 3 and GIGANTEA. *Plant J* 101:1397
7. Hanano S, Domagalska MA, Nagy F, Davis SJ (2006) Multiple phytohormones influence distinct parameters of the plant circadian clock. *Genes Cells* 11:1381
8. Gendreau E, Traas J, Desnos T, Grandjean O, Caboche M, Hofte H (1997) Cellular basis of hypocotyl growth in *Arabidopsis thaliana*. *Plant Physiol* 114:295



High-Throughput Extraction and Enzymatic Determination of Sugars and Fructans in Fructan-Accumulating Plants

Kallyne A. Barros, Masami Inaba, Auxiliadora Oliveira Martins, and Ronan Sulpice

Abstract

Fructans are carbohydrates present in more than 15% of flowering plants. They represent the major pool of carbohydrates in some species, especially when facing cold or drought. However, the functions of fructans with high or low degrees of polymerization (DP), their diurnal use, and the regulation of their synthesis and degradation in response to stresses still remain unclear. Here we present an enzymatic protocol adapted to 96-well microplates that simultaneously allows the determination of fructans and glucose, fructose, and sucrose. Moreover, the protocol allows to estimate the average DP of the fructans in the samples. The protocol is based on the enzymatic degradation of fructans into glucose and fructose and their subsequent conversion into gluconate 6-phosphate concomitant with the formation of NADH in the presence of ATP.

Keywords Fructan determination, Enzymatic assay, Degree of polymerization, Sugar determination, Ethanolic extraction

1 Introduction

Starch and sucrose are primary products of photosynthesis and the most common reserve carbohydrates in plants. In some plants, including *Arabidopsis* where carbon (C) metabolism has been best studied, starch is the major transient C storage accumulated in chloroplasts during the day and consumed at night, while sucrose serves as an immediate C source for growth and maintenance in the light and is the main translocating form of carbohydrates. Other plants accumulate not only starch as transient C storage but also sucrose and hexoses [1–7] and possibly fructans [8]. Fructans, polymers of fructose, are found in about 15% of flowering plants. Fructans in plants are synthesized and accumulated in vacuoles and can represent a main pool of soluble carbohydrates [13]. In forage grasses and cereals of temperate climate regions, fructans have been

assigned roles as intermediate- or long-term reserves. These reserves are used for regrowth after defoliation [9] or in early spring [10] and for grain filling and seed development [11]. Fructans are also involved in the tolerance to abiotic stresses, such as cold and drought [12, 13].

The roles of fructans can vary depending on their structures, degree of polymerization (DP), and the tissues where they are accumulated. Although the terminology is not consensual, fructans are divided in low-DP fructans with two to ten fructosyl residues and high-DP fructans with more than ten fructosyl residues [14–18]. Low-DP fructans are usually found in leaves and have been suggested to function as membrane stabilizers [19], reactive oxygen species scavengers [18, 20, 21], and short-term reserves [22, 23]. In contrast, high-DP fructans are typically stored in specialized roots or stems and may serve as long-term reserves (reviewed by Versluys et al. [24]).

Despite the importance of fructans in fructan-accumulating plants, little is known about the diurnal regulation of fructan levels and their potential role as transient C storage for night usage [25]. In addition, the analysis of starch in fructan-accumulating plants is highly neglected, and it is not clear whether and how starch, sucrose, and fructans compete for trioses phosphates synthesized by the Calvin-Benson cycle [26–28]. Cairns et al. [4] demonstrated that in the annual ryegrass *Lolium temulentum*, the synthesis of starch is not stimulated when fructan synthesis is blocked, suggesting a limit for starch accumulation. Jin et al. [29] described a mechanism linking fructan and starch synthesis via two transcription factors SUSIBA (*sugar signalling in barley*) which are encoded by a single gene and transcribed from two different promoters. These two transcription factors respond to different sucrose concentrations and act in an antagonistic and auto-regulatory way, controlling the synthesis of starch and fructans in barley.

Fructan synthesis is stimulated by increases in sucrose content [23, 30–34], and it occurs particularly at the end of the day, when the rates of sucrose and starch synthesis are lower [1]. Using relatively artificial experimental setups such as detached leaves in order to induce fructans accumulation, it has been proposed that fructan synthesis is induced only after a certain concentration of sucrose is reached in the tissues [4, 27, 35–38].

Methods for fructan extraction and purification from plant tissues have been previously described. These methods consist of mainly two steps: (1) boiling plant tissues in water or ethanol to break membranes and (2) precipitation or filtering to separate fructans from other cellular components [15, 16]. However, these methods often require high amounts of plant materials, which can be hard to obtain from small tissues or specific sections of plants. Quantitative and qualitative determination of fructans is

usually performed by high-performance liquid chromatography (HPLC) or matrix-assisted laser desorption/ionization-time of flight (MALDI-TOF) [16, 39–41]. These methods are of relatively low throughput and high costs and not suitable for analyzing a large number of samples. Alternatively, fructan contents and average DP can be determined by enzymatic assays [14, 42] using the fructan assay kit from Megazyme International Ireland Ltd. (Bray, County Wicklow, Ireland), however without the possibility to determine at same time glucose, fructose, and sucrose.

Here we describe a high-throughput protocol for extraction and enzymatic determination of soluble carbohydrates, including glucose, fructose, sucrose, and fructans, in 96-well microplates. This is developed from the protocol for soluble sugars in non fructan-accumulating plants described by Stitt et al. [43] and the principle of fructan determination used for the fructan assay kit, with main modifications being (1) serial extraction in 100%, 80%, and 50% ethanol to separate low- and high-DP fructans by their precipitation properties [17], (2) use of nicotinamide adenine dinucleotide (NAD⁺) instead of more expensive nicotinamide adenine dinucleotide phosphate (NADP⁺), (3) use of maltase instead of less specific invertase for the hydrolysis of sucrose, and (4) additional steps for fructan determination directly following the determination of glucose, fructose, and sucrose.

2 Materials

Prepare all solutions and dilutions in deionized water, unless indicated otherwise. Use analytical grade reagents and follow manufacturers' instructions for handling and storage. Diligently follow all waste disposal regulations when disposing waste materials.

2.1 Equipment and Consumables

1. Block heater or heating cabinet.
2. Vortex mixer with microplate attachment.
3. Multi-channel pipettes.
4. Microcentrifuge.
5. Plate centrifuge.
6. UV plate reader.
7. Screw cap tubes set in 96-well rack.
8. Deep 96-well (1.2-mL) microplates.
9. 96-well microplates.
10. Adhesive aluminum sealing tapes.
11. Heat-resistant aluminum tapes.

2.2 Extraction of Soluble Compounds

1. 100% ethanol.
2. 80% (v/v) ethanol in 10 mM MES-KOH, pH 5.9.
3. 50% (v/v) ethanol in 10 mM MES-KOH, pH 5.9.

2.3 Determination of Soluble Carbohydrates

1. 0.1 M HEPES buffer: 0.1 M HEPES, pH 7, 3 mM MgCl₂. Store at -20 °C.
2. 0.5 M HEPES buffer: 0.5 M HEPES, pH 7, 3 mM MgCl₂. Store at -20 °C.
3. 0.1 M acetate buffer, pH 4.9. Store at -20 °C.
4. 100 mM (60 mg/mL) adenosine triphosphate ATP. Store in 2-mL aliquots at -20 °C.
5. 45 mM (28 mg/mL) NAD⁺. Store in 2-mL aliquots at -20 °C.
6. 1 M HCl (4.15 mL of 37% HCl in 50 mL). Store at 4 °C.
7. 1 M NaOH (0.2 g NaOH in 50 mL). Store at 4 °C.

Prepare 0.1 and 0.5 M HEPES buffers from 1 M HEPES-KOH, pH 7, and 300 mM MgCl₂. For 0.5 M acetate buffer, pH 4.9, prepare acetic acid solution (0.6010 mL of acetic acid in 50 mL) and sodium acetate solution (1.1894 g of sodium acetate in 50 mL) and combine the two solutions. Dilute fivefold to obtain 0.1 M acetate buffer.

2.4 Active Enzyme Solutions

The enzymes are provided as suspension in ammonium sulfate. To prepare an active enzyme solution, ammonium sulfate should be replaced by HEPES or acetate buffer as described below. Small volume of enzymes may be added directly to a reaction buffer without the replacement (e.g., G6PDH in 0.1 M HEPES buffer; *see* Subheading 3.2). Once prepared, keep active enzyme solutions on ice, or, if not immediately used, flash-freeze in liquid N₂ and store at -80 °C.

1. 900 U/mL hexokinase (HK EC 2.7.1.1). Transfer 140 µL of 1280 U/mL HK in a 1.5-mL tube. Spin down at the maximum speed (17,000 × *g*) for 2 min and remove the supernatant. Suspend the pellet in 200 µL of 0.1 M HEPES buffer.
2. 60 U/mL phosphoglucosomerase (PGI, EC 5.3.1.9), designated PGI-I. Transfer 12 µL of 1000 U/mL PGI in a 1.5-mL tube. Spin down and remove the supernatant. Suspend the pellet in 200 µL 0.1 M HEPES buffer.
3. 500 U/mL maltase/α-glucosidase (MAL, EC 3.2.1.20). Transfer 100 µL of 1000 U/mL MAL in a 1.5-mL tube. Spin down and remove the supernatant. Suspend the pellet in 200 µL 0.1 M HEPES buffer.

4. 100 U/mL endo-inulinase (EC 3.2.1.7) and exo-inulinases (EC 3.2.1.80/EC 3.2.1.26), designated FRU. Transfer 100 μ L of 200 U/mL endo-inulinase and 10 μ L of 2000 U/mL exo-inulinase into a 1.5-mL tube. Spin down and remove the supernatant. Suspend the pellet in 200 μ L of 0.1 M acetate buffer.
5. 140 U/mL glucose-6-phosphate dehydrogenase (G6PDH, EC 1.1.1.49) and 900 U/mL HK, designated G6PDH + HK. Transfer 14 μ L of 2000 U/mL G6PDH and 140 μ L of 1280 U/mL hexokinase. Spin down and remove the supernatant. Suspend the pellet in 200 μ L of 0.1 M HEPES buffer.
6. 300 U/mL PGI, designated PGI-II. Transfer 60 μ L of 1000 U/mL PGI in a 1.5-mL tube. Spin down and remove the supernatant. Suspend the pellet in 200 μ L of 0.1 M HEPES buffer.

3 Methods

The principle of the protocol for fructan determination involves enzymatic reactions of phosphorylation, oxidation, and isomerization in order to sequentially transform glucose, fructose, sucrose, and fructans into glucose-6-phosphate in the presence of ATP, the glucose-6-phosphate being further oxidized into gluconate-6-phosphate in presence of NAD^+ (Fig. 1). Glucose and fructose are phosphorylated by HK, and then glucose-6-phosphate is oxidized to gluconate-6-phosphate by G6PDH, with formation of NADH (Fig. 1a). Fructose-6-phosphate is isomerized to glucose-6-phosphate by PGI and oxidized by G6PDH, with formation of NADH (Fig. 1b). Sucrose is hydrolyzed by MAL to glucose and fructose, which in the presence of HK, PGI, and G6PDH from steps 1A and 1B will lead to the production of gluconate-6-phosphate and NADH (Fig. 1c). After glucose, fructose, and sucrose in the extracts have been determined, enzymes are denatured and NADH hydrolyzed by addition of HCl in order to decrease absorbance at 340 nm of the determination extracts. Then after neutralization of the extracts with NaOH and addition of acetate buffer to lower the pH to 4.5, fructans are hydrolyzed by FRU to fructose and glucose, which are phosphorylated, isomerized (for fructose), and oxidized (Fig. 1d). By stoichiometry, each 1 μ mol of NADH produced correspond to 1 μ mol of glucose-6-phosphate, thus allowing easy quantification of all compounds.

3.1 Extraction of Soluble Carbohydrates (and Other Soluble Compounds)

Prior to extraction, plant tissues should be finely powdered by grinding in a bead mill. Both fresh materials (grinded in liquid N_2) and freeze-dried materials can be used. Typically, 20 mg of fresh or 10 mg of dry powder is used as starting material. Serial

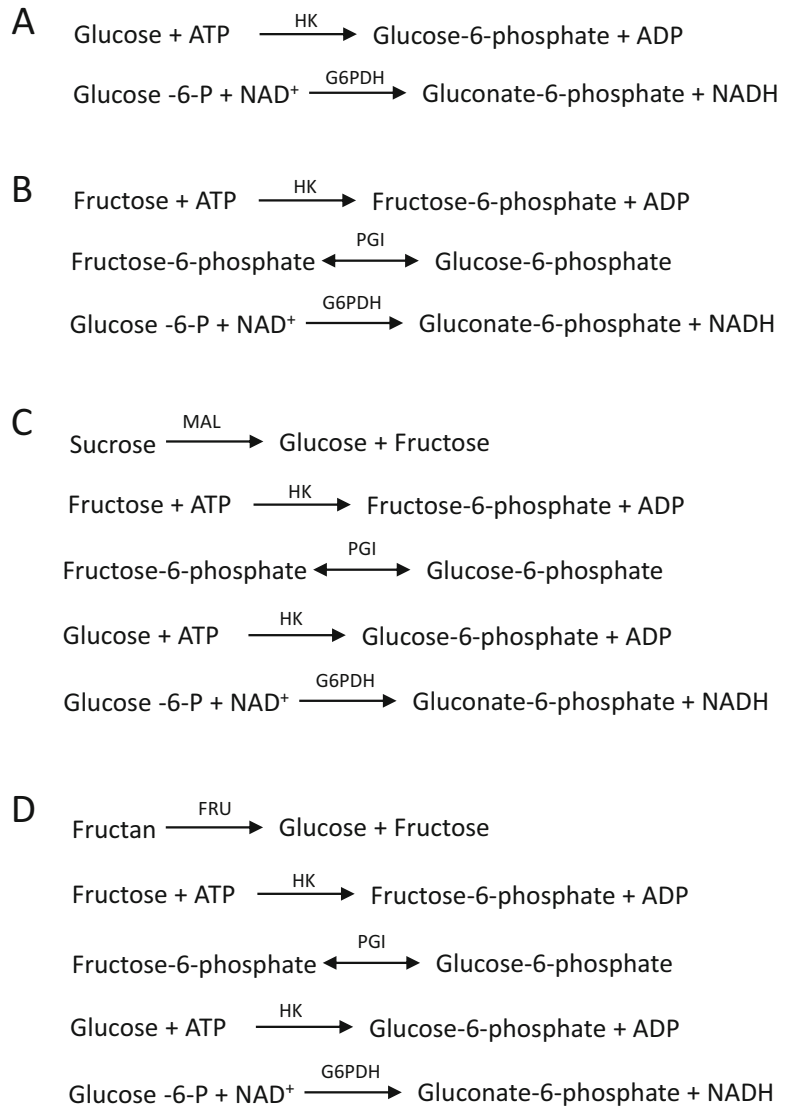


Fig. 1 Enzymatic reactions involved in the determination of glucose (a), fructose (b), sucrose (c), and fructans (d). *HK* hexokinase, *PGI* phosphoglucosomerase, *MAL* maltase (α -glucosidase), *FRU* a mixture of equal units of 1- β -D-fructan fructanohydrolase and β -D-fructofuranoside fructohydrolase; G6PDH, glucose-6-phosphate dehydrogenase

extraction in hot 100%, 80%, and 50% ethanol is performed [44]. Sugars and low-DP fructans will be extracted in 100% ethanol, while high-DP fructans are preferentially extracted in 80% and 50% ethanol. The ethanolic extracts can be combined if the aim is to obtain total fructans content and not to get information about the content of low- and high-DP fructans. The ethanolic extracts

contain pigments, soluble carbohydrates, amino acids, and organic acids.

1. Weigh fine-powdered plant tissues into screw cap tubes and set in a 96-well rack (*see Note 1*).
2. Add 500 μL of 100% ethanol into each tube. Shake vigorously on a vortex mixer to disperse power and incubate for 30 min at 95 $^{\circ}\text{C}$.
3. Centrifuge the tubes in a plate centrifuge at $3220 \times g$ for 10 min.
4. Transfer the supernatants to a deep 96-well microplate. Seal the plate with an aluminum sealing tape and keep at 4 $^{\circ}\text{C}$ (100% ethanolic extracts = E1).
5. Add 250 μL of 80% ethanol to the pellets, shake vigorously on a vortex, and incubate for 30 min at 95 $^{\circ}\text{C}$.
6. Centrifuge the tubes at $3220 \times g$ for 10 min.
7. Transfer the supernatants to a new deep 96-well microplate. Seal the plate with an aluminum sealing tape and keep at 4 $^{\circ}\text{C}$ (80% ethanolic extracts).
8. Add 250 μL of 50% ethanol to the pellets, shake vigorously on a vortex, and incubate for 30 min at 95 $^{\circ}\text{C}$.
9. Centrifuge the tubes at $3220 \times g$ for 10 min.
10. Transfer the supernatants to the deep 96-well microplate where 80% ethanol extracts are. Seal the plate with an aluminum sealing tape, homogenize the combined ethanolic extracts by inverting the plate a few times, and centrifuge briefly (30 s at $500 \times g$) in order to avoid the supernatant to freeze on aluminum sealing tape (combined 80% and 50% ethanolic extracts = E2).
11. The ethanolic extracts E1 and E2 can be kept at 4 $^{\circ}\text{C}$ for a few hours if they are used immediately. Otherwise store them at -20°C .

3.2 Determination of Glucose, Fructose, Sucrose, and Fructans

This protocol comprises four steps, i.e., (1) determination of glucose, fructose, and sucrose, (2) denaturation of the enzymes used and NADH generated and neutralization, (3) degradation of fructans, and (4) determination of fructan-derived glucose and fructose (Fig. 2).

3.2.1 Determination of Glucose, Fructose, and Sucrose

1. Prepare sugar determination mix: 7.5 mL of 0.1 M HEPES buffer, 240 μL of 100 mM ATP, and 240 μL of 45 mM NAD^{+} per microplate. Add 28 U of G6 PDH before use (0.28 U/reaction). You can add G6PDH suspension in ammonium sulfate (e.g., 14 μL of 2000 U/mL) directly into the mix.

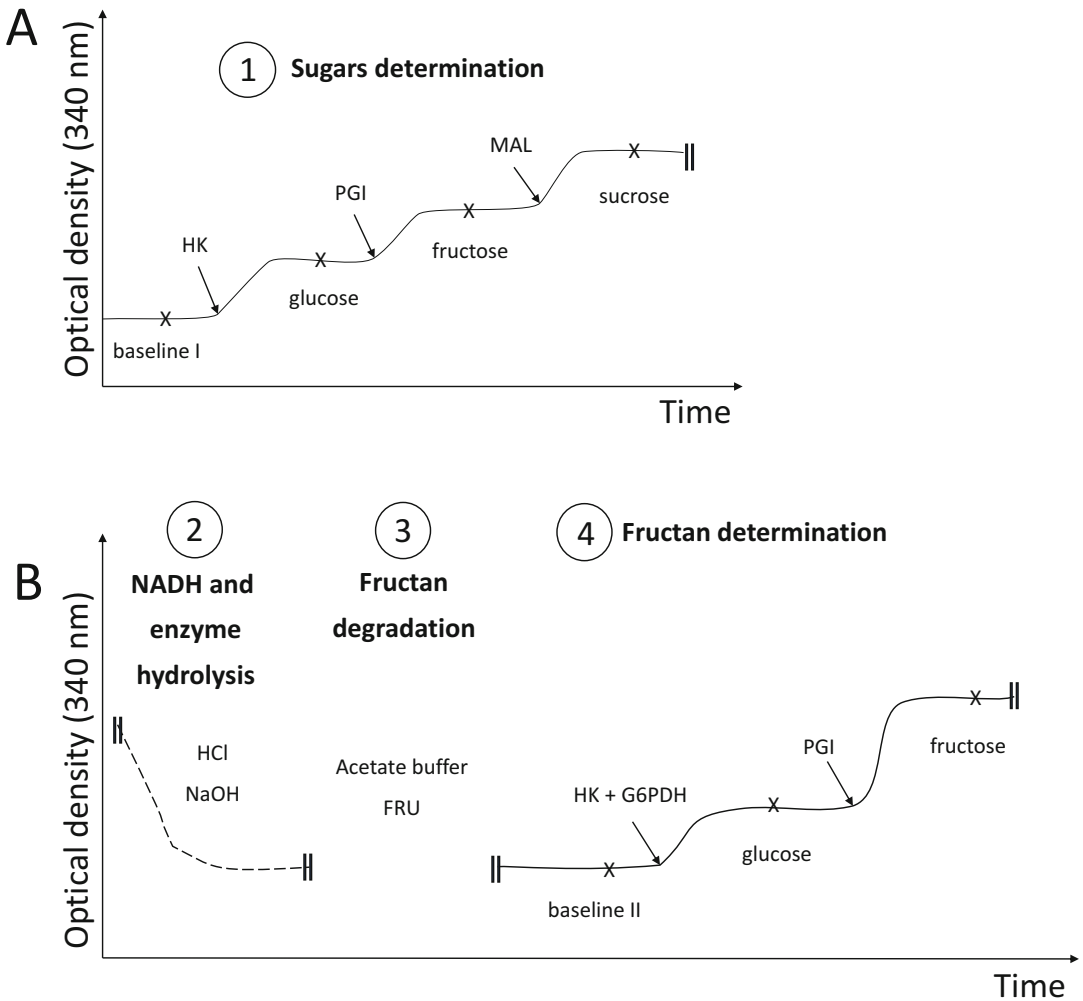


Fig. 2 (a, b) Schematic representation of the protocol for enzymatic determination of soluble carbohydrates. The protocol comprises four steps: (1) determination of glucose, fructose, and sucrose with HK, PGI, and MAL, (2) denaturation of the enzymes used in Part 1 and of the NADH which has been formed, (3) degradation of fructans with FRU, and (4) determination of fructan-derived glucose and fructose with HK, PGI, and G6PDH. Absorbance at 340 nm of each sample is recorded after the addition of each enzyme to the reaction mixes. X, optical density at 340 nm recorded when stabilized without enzymes (baseline) or after the addition of each enzyme; dashed line, representation of OD decrease during step 2; *HK* hexokinase, *PGI* phosphoglucoisomerase, *MAL* maltase (α -glucosidase), *FRU* enzyme mix of 1- β -D-fructan fructanohydrolase and β -D-fructofuranoside fructohydrolase, *G6PDH* glucose-6-phosphate dehydrogenase

2. Thaw and homogenize ethanolic extracts if they have been stored at -20°C . Mix well by inverting the deep-well plates a few times and centrifuge at $3200 \times g$ for 5 min.
3. In a 96-well microplate, pipette in each well 75 μL of the sugar determination mix and 5–50 μL of ethanolic extract (*see Note*

2). Shake the plate for a few min on a vortex mixer at a low speed to homogenize the mixtures without spilling.

4. Read the absorbance at 340 nm in a plate reader. Record the OD when stabilized as the baseline (*see Note 3*).
5. Add 1 μL of 900 U/mL HK (0.9 U/reaction) to each well, shake the plate for a few min, and read the absorbance at 340 nm until a plateau is reached. Record the OD.
6. Add 1 μL of 60 U/mL PGI (PGI-I, 0.06 U/reaction) to each well, shake the plate for a few min, and read the absorbance at 340 nm until a plateau is reached. Record the OD.
7. Add 1 μL of 500 U/mL MAL (0.5 U/reaction) to each well, shake the plate for a few min, and read the absorbance at 340 nm until a plateau is reached. Record the OD.

3.2.2 Denaturation of the Enzymes and NADH and Neutralization

1. Add 10 μL of 1 M HCl to each well, shake briefly, and seal the plate with heat-resistant aluminum tape.
2. Incubate the plate for 10 min at 95 °C. Let it cool. Spin down at $3200 \times g$ for 2 min.
3. Remove the tape carefully and add 10 μL of 1 M NaOH to each well to neutralize the reaction. Shake briefly.

3.2.3 Degradation of Fructans

1. Add 7 μL of 0.1 M acetate buffer, pH 4.9, to each well. Shake briefly.
2. Add 1 μL of FRU (0.1 U/reaction each of endo- and exo-inulinases) to each well. Seal the plate with aluminum sealing tape and incubate overnight at 37 °C.

3.2.4 Determination of Fructan-Derived Glucose and Fructose

1. Prepare fructan determination mix: 7.5 mL of 0.5 M HEPES buffer, 480 μL of 100 mM ATP, and 480 μL of 45 mM NAD^+ per microplate.
2. Centrifuge the plate briefly and remove the sealing tape (*see Note 4*). Add 75 μL of the fructan determination mix. Shake the plate for 5 min on a vortex mixer at a low speed.
3. Read the absorbance at 340 nm in a plate reader. Record the OD when stabilized as the baseline.
4. Add 1 μL of G6PDH + HK (0.14 U/reaction + 0.9 U/reaction) to each well, shake the plate for a few min, and read the absorbance at 340 nm until stabilized. Record the OD.
5. Add 1 μL of 300 U/mL PGI (PGI-II, 0.3 U/reaction) to each well, shake the plate for a few min, and read the absorbance at 340 nm until stabilized. Record the OD.

3.3 Calculation

The production of NADH is determined at 340 nm using a spectrophotometer. The calculation is based on the extinction

coefficient of NADH. To each metabolite, calculate the ΔOD , which is the difference between the plateau OD after enzyme addition and the previous OD. Apply to the Beer-Lambert law for units of molarity:

$$\Delta OD = \epsilon * l * c$$

where (ϵ) is the wavelength-dependent molar absorptivity coefficient; here the coefficient of extinction of NADH is 6.22 [45] given as $\mu\text{mol}/\text{mm}$, l is the light path length in mm, and c is the metabolite concentration in $\mu\text{mol}/\mu\text{L}$.

To calculate the concentration of NADH in your wells, if you work in microplates and the volumes in your wells are modified during the determination, you will then need to consider possible changes in path length for your calculation and change accordingly. It is because a plate reader reads OD from the top of the wells and then the path length will vary according to the total volume present in the wells.

As an alternative, you can also use external standards of the respective sugars you are measuring for calculations. Results are reliable when the ΔOD is higher than 0.01 and maximum OD lower than 1.8. Otherwise, it is recommended to modify the volume of extracts used.

The average DP for fructans is calculated based on the concentrations of glucose and fructose present in fructans:

$$\text{Average DP of fructan} = [\text{fructose}]/[\text{glucose}] + 1$$

Low concentrations of total fructans in samples may lead to issues for reliable determination of fructans average DP, especially if fructans have large DP to contain proportionally very low amounts of glucose.

4 Notes

1. Arrange the tubes in a 96-well rack. Do not use all the 96 positions but keep some for the standards to be used in determination steps. In addition we strongly suggest the addition of controls made of a master mix representative of the samples you are going to analyze. It will allow normalization between plates and the identification of potential biases between plates.
2. It is recommended to test run with various volumes of a representative subset of samples. It will allow for determining the optimal volume of extracts to use for being in the right range of OD.
3. Stable readings for the baseline are reached after 5–10 min. Plateaus for glucose and fructose are typically reached in 10–15 min after the addition of HK and PGI, respectively,

whereas sucrose plateau is reached in 30–40 min after the addition of MAL. Plateaus are reached faster if plates are shaken after the addition of each enzyme. It is recommended to use a plate reader/program that allows to access the plate anytime during the time course, as plateaus can be reached at different durations, depending on samples analyzed.

4. If the samples contain high levels of fructans and low levels of sugars, you might have to use only a portion, instead of the whole, of the reaction mixture used for the determination of sugars in the determination of fructans.

Acknowledgments

Kallyne Barros was supported by a postgraduate studentship funded by CNPQ (ID. 233005/2014-5) and Auxiliadora Oliveira Martins by CNPq (ID. 210299/2015-0). Ronan Sulpice and Masami Inaba were supported by a Research Stimulus Grant (VICCI—Grant No: 14/S/81) funded by the Irish Department of Agriculture, Food and the Marine (DAFM).

References

1. Sicher RC, Kremer DF, Harris WG (1984) Diurnal carbohydrate-metabolism of barley primary leaves. *Plant Physiol* 76(1):165–169
2. Farrar SC, Farrar JF (1986) Compartmentation and fluxes of sucrose in intact leaf blades of barley. *New Phytol* 103(4):645–657
3. Bihmidine S, Julius BT, Dweikat I, Braun DM (2016) Tonoplast Sugar Transporters (SbTSTs) putatively control sucrose accumulation in sweet sorghum stems. *Plant Signal Behav* 11(1):e1117721
4. Cairns AJ, Cookson A, Thomas BJ, Turner LB (2002) Starch metabolism in the fructan-grasses: patterns of starch accumulation in excised leaves of *Lolium temulentum* L. *J Plant Physiol* 159(3):293–305
5. van Arkel J, Sevenier R, Hakkert JC, Bouwmeester HJ, Koops AJ, van der Meer IM (2013) Tailor-made fructan synthesis in plants: a review. *Carbohydr Polym* 93(1):48–56
6. Larry MW (1973) Carbohydrate reserves of grasses: a review. *J Range Manag* 26(1):13–18
7. Lunn JE, Hatch MD (1995) Primary partitioning and storage of photosynthate in sucrose and starch in leaves of C-4 plants. *Planta* 197(2):385–391
8. Farrar SC, Farrar JF (1985) Carbon fluxes in leaf blades of barley. *New Phytol* 100(3):271–283
9. Meuriot F, Morvan-Bertrand A, Noiraud-Romy N, Decau ML, Escobar-Gutierrez AJ, Gastal F, Prud'homme MP (2018) Short-term effects of defoliation intensity on sugar remobilization and N fluxes in ryegrass. *J Exp Bot* 69(16):3975–3986
10. Yoshida M, Abe J, Moriyama M, Kuwabara T (1998) Carbohydrate levels among winter wheat cultivars varying in freezing tolerance and snow mold resistance during autumn and winter. *Physiol Plant* 103(1):8–16
11. Peukert M, Thiel J, Peshev D, Weschke W, Van den Ende W, Mock HP, Matros A (2014) Spatio-temporal dynamics of fructan metabolism in developing barley grains. *Plant Cell* 26(9):3728–3744
12. del Viso F, Puebla AF, Fusari CM, Casabuono AC, Couto AS, Pontis HG, Hopp HE, Heinz RA (2009) Molecular characterization of a putative sucrose: Fructan-6-fructosyltransferase (6-SFT) of the cold-resistant Patagonian grass *Bromus pictus* associated with fructan accumulation under low temperatures. *Plant Cell Physiol* 50(3):489–503
13. Vijn I, Smeekens S (1999) Fructan: more than a reserve carbohydrate? *Plant Physiol* 120(2):351–359

14. Muir JG, Shepherd SJ, Rosella O, Rose R, Barrett JS, Gibson PR (2007) Fructan and free fructose content of common Australian vegetables and fruit. *J Agric Food Chem* 55 (16):6619–6627
15. Livingston DP (1990) Fructan precipitation from a water/ethanol extract of oats and barley. *Plant Physiol* 92(3):767–769
16. Liu Z, Mouradov A, Smith KF, Spangenberg G (2011) An improved method for quantitative analysis of total fructans in plant tissues. *Anal Biochem* 418(2):253–259
17. Ku Y, Jansen O, Oles CJ, Lazar EZ, Rader JI (2003) Precipitation of inulins and oligoglucoses by ethanol and other solvents. *Food Chem* 81(1):125–132
18. Peshev D, Vergauwen R, Moglia A, Hideg E, Van den Ende W (2013) Towards understanding vacuolar antioxidant mechanisms: a role for fructans? *J Exp Bot* 64(4):1025–1038
19. Hincha DK, Livingston DP, Premakumar R, Zuther E, Obel N, Capela C, Heyer AG (2007) Fructans from oat and rye: composition and effects on membrane stability during drying. *Biochim Biophys Acta Biomembr* 1768 (6):1611–1619
20. Van den Ende W, Valluru R (2008) Sucrose, sacrosyl oligosaccharides, and oxidative stress: scavenging and salvaging? *J Exp Bot* 60 (1):9–18
21. Matros A, Peshev D, Peukert M, Mock H-P, Van den Ende W (2015) Sugars as hydroxyl radical scavengers: proof-of-concept by studying the fate of sucralose in *Arabidopsis*. *Plant J* 82(5):822–839
22. Roth A, Luscher N, Sprenger N, Boller T, Wiemken A (1997) Fructan and fructan-metabolizing enzymes in the growth zone of barley leaves. *New Phytol* 136(1):73–79
23. Cimini S, Locato V, Vergauwen R, Paradiso A, Cecchini C, Vandenpoel L, Verspreet J, Courtin CM, D'Egidio MG, Van den Ende W, De Gara L (2015) Fructan biosynthesis and degradation as part of plant metabolism controlling sugar fluxes during durum wheat kernel maturation. *Front Plant Sci* 6:89
24. Versluys M, Kirtel O, Toksoy Oner E, Van den Ende W (2018) The fructan syndrome: evolutionary aspects and common themes among plants and microbes. *Plant Cell Environ* 41 (1):16–38
25. Schnyder H (1993) The role of carbohydrate storage and redistribution in the source-sink relations of wheat and barley during grain filling — a review. *New Phytol* 123(2):233–245
26. Nagaraj VJ, Altenbach D, Galati V, Luscher M, Meyer AD, Boller T, Wiemken A (2004) Distinct regulation of sucrose: sucrose-1-fructosyltransferase (1-SST) and sucrose: fructan-6-fructosyltransferase (6-SFT), the key enzymes of fructan synthesis in barley leaves: 1-SST as the pacemaker. *New Phytol* 161 (3):735–748
27. Nagaraj VJ, Riedl R, Boller T, Wiemken A, Meyer AD (2001) Light and sugar regulation of the barley sucrose: fructan 6-fructosyltransferase promoter. *J Plant Physiol* 158(12):1601–1607
28. Ritsema T, Brodmann D, Diks SH, Bos CL, Nagaraj V, Pieterse CM, Boller T, Wiemken A, Peppelenbosch MP (2009) Are small GTPases signal hubs in sugar-mediated induction of fructan biosynthesis? *PLoS One* 4(8):e6605
29. Jin Y, Fei M, Rosenquist S, Jin L, Gohil S, Sandstrom C, Olsson H, Persson C, Hoglund AS, Fransson G, Ruan Y, Aman P, Jansson C, Liu C, Andersson R, Sun C (2017) A dual-promoter gene orchestrates the sucrose-coordinated synthesis of starch and fructan in barley. *Mol Plant* 10(12):1556–1570
30. Arkel V (2014) Fructan biosynthesis regulation and the production of tailor-made fructan in plants. In: *Polysaccharides: natural fibers in food and nutrition*. CRC Press, Boca Raton, FL, pp 1–29
31. Cairns AJ (2003) Fructan biosynthesis in transgenic plants. *J Exp Bot* 54(382):549–567
32. Chalmers J, Lidgett A, Cummings N, Cao Y, Forster J, Spangenberg G (2005) Molecular genetics of fructan metabolism in perennial ryegrass. *Plant Biotechnol J* 3(5):459–474
33. Apolinario AC, de Lima Damasceno BP, de Macedo Beltrao NE, Pessoa A, Converti A, da Silva JA (2014) Inulin-type fructans: a review on different aspects of biochemical and pharmaceutical technology. *Carbohydr Polym* 101:368–378
34. Xue GP, Drenth J, Glassop D, Kooiker M, McIntyre CL (2013) Dissecting the molecular basis of the contribution of source strength to high fructan accumulation in wheat. *Plant Mol Biol* 81(1–2):71–92
35. Obenland DM, Simmen U, Boller T, Wiemken A (1991) Regulation of sucrose-sucrose-fructosyltransferase in barley leaves. *Plant Physiol* 97(2):811–813
36. Suarez-Gonzalez EM, Lopez MG, Delano-Frier JP, Gomez-Leyva JF (2014) Expression of the 1-SST and 1-FFT genes and consequent fructan accumulation in *Agave tequilana* and *A. inaequidens* is differentially induced by diverse (a)biotic-stress related elicitors. *J Plant Physiol* 171(3–4):359–372

37. Wagner W, Wiemken A (1987) Enzymology of fructan synthesis in grasses: properties of sucrose-sucrose-fructosyltransferase in barley leaves (*Hordeum-vulgare*-L cv Gerbel). *Plant Physiol* 85(3):706–710
38. Wagner W, Wiemken A, Matile P (1986) Regulation of fructan metabolism in leaves of barley (*Hordeum vulgare* L cv Gerbel). *Plant Physiol* 81(2):444–447
39. Bohacenko J (2014) Fructan content determination by HPLC method with refractometric detection. *Listy Cukrov Repar* 130(1):28–32
40. Longland AC, Dhanoa MS, Harris PA (2012) Comparison of a colorimetric and a high-performance liquid chromatography method for the determination of fructan in pasture grasses for horses. *J Sci Food Agric* 92(9):1878–1885
41. Verspreet J, Hansen AH, Dornez E, Courtin CM, Harrison SJ (2014) A new high-throughput LC-MS method for the analysis of complex fructan mixtures. *Anal Bioanal Chem* 406(19):4785–4788
42. Rao RSP, Andersen JR, Dionisio G, Boelt B (2011) Fructan accumulation and transcription of candidate genes during cold acclimation in three varieties of *Poa pratensis*. *J Plant Physiol* 168(4):344–351
43. Stitt M, Lilley RM, Gerhardt R, Heldt HW (1989) Metabolite levels in specific cells and subcellular compartments of plant leaves. *Methods Enzymol* 174:518–552
44. Cross JM, von Korff M, Altmann T, Bartzetko L, Sulpice R, Gibon Y, Palacios N, Stitt M (2006) Variation of enzyme activities and metabolite levels in 24 *Arabidopsis* accessions growing in carbon-limited conditions. *Plant Physiol* 142(4):1574
45. McComb RB, Bond LW, Burnett RW, Keech RC, Bowers GN Jr (1976) Determination of the molar absorptivity of NADH. *Clin Chem* 22(2):141–150



Chapter 11

Simple Nuclei Preparation and Co-immunoprecipitation Procedures for Studying Protein Abundance and Interactions in Plant Circadian Time Courses

Akane Kubota, Young Hun Song, and Takato Imaizumi

Abstract

The plant circadian clock regulates multiple developmental and physiological events that occur at specific times and seasons. As many of the currently known clock proteins and clock-associated regulators are transcription factors, analyzing molecular events in the nuclei is crucial. In addition, long-time course analyses of protein abundance and interactions are often required to assess the role of the circadian clock on clock-regulated phenomena. Here we introduce a simple procedure to prepare nuclear-enriched tissues, which we routinely use to study time-resolved accumulation changes in low-abundance nuclear proteins (i.e., transcription factors). In addition to measuring changes in abundance, investigating the protein-protein interaction dynamics at specific times of day or under certain environmental conditions is needed for plant chronobiology studies. Therefore, we also present our co-immunoprecipitation method for studying diurnal/circadian protein-protein interactions, tailored to nuclear-localized proteins in *Arabidopsis* and tobacco.

Keywords Circadian rhythm, Nuclei purification, Time course analysis, Western blot, Co-immunoprecipitation, *Arabidopsis thaliana*, Tobacco (*Nicotiana benthamiana*)

1 Introduction

Various molecular events recur at nearly the same time from day to day in plants [1, 2]. These events are often under the control of the circadian clock. To elucidate the molecular networks underlying these daily time-specific activities, measuring the diurnal or circadian alteration of protein abundance as well as interaction dynamics is critical [3–15]. Most known clock genes encode transcription factors [16]. Also, many studies focus on transcriptional regulation to investigate clock-regulated output phenomena [17, 18], indicating the importance of establishing methods of studying molecular events in the nucleus. Often, transcription factors are low-abundance proteins, which are technically more challenging

to detect by western blot analysis using crude cell lysates. To detect changes in the abundance of transcription factors, isolating nuclei is effective. Many references are available to isolate nuclei from different tissues from various plant species [19–22]. In chronobiology, we often need to process a large number of time-course samples. Rapid and less complicated methods are preferable, as long as sample quality is not compromised. Here we describe a relatively simple and yet clear nuclei isolation method using *Arabidopsis* plants [23, 24]. Isolated nuclei samples can be utilized for western blot analysis as well as other assays to analyze protein-protein interactions (which we also describe here). For successful nuclei isolation, control of non-ionic detergents (such as Triton X-100 or Tween), which disrupt undesired cellular components, facilitates the release of nuclei. It is critically important to use certain organic reagents (such as sucrose or glycerol), which stabilize the nuclear membrane. Reducing compounds [dithiothreitol (DTT), β -mercaptoethanol] that maintain protein structure are crucial reagents in the isolation buffer, and supplements of protease inhibitors or phosphatase inhibitors are highly recommended depending on the protein of interest.

Investigating protein-protein interactions is a powerful approach to understanding protein molecular function. Although there are various methods available, here we describe how we carry out time-resolved protein-protein interaction assays using co-immunoprecipitation (Co-IP) techniques.

These two biochemistry methods are routinely used to describe the dynamics of nuclear protein abundance and the protein-protein interaction that often occurs at specific times of day or in certain environmental conditions.

2 Materials

2.1 *Plants for Nuclei Purification and Co-IP*

Plants can be grown in the same way for these two procedures. To obtain 70–100 μ g of protein from nuclei, approximately 150–250 14-day-old *Arabidopsis* seedlings (approximately 1–2 g) are used. For Co-IP, usually 0.3–1 g of plant tissue (*Arabidopsis* or tobacco *N. benthamiana*) is sufficient. Plate seeds less densely to avoid shading when plants are harvested onto the growth media [such as Murashige and Skoog (MS) or Linsmaier and Skoog (LS) media with/without sucrose] in small plastic plates (90 mm in diameter). Plants are grown under appropriate light conditions (such as long day, short day, 12 h light and 12 h dark, continuous light, or continuous dark conditions, etc.). Protein yields tend to be lower when using older seedlings, potentially due to the smaller number of cells compared to tissue weight. When samples are harvested, they need to be flash frozen in liquid N₂ (*see Note 1*). Harvest samples immediately after light on for dawn samples (such

as Zeitgeber time 0: ZT0) and a few minutes before light off for dusk samples (such as ZT16). Use a dim green safe light (avoid directly pointing the safe light at the plants) for harvesting during dark periods.

2.2 Reagents and Tools for Nuclei Purification

This procedure is a modification of the one supplied with Sigma CelLytic PM Plant Nuclei Isolation/Extraction Kit (cat# CEL-LYTPN1) [24]. However, information for alternative reagents (not relying on the kit) is also described (*see* **Notes 2, 4, and 5**).

1. NIB buffer (prepare reagents for the number of samples plus one extra): dilute 4× NIB buffer (supplemented in the kit) with sterile-deionized water and mix it well (*see* **Note 2**). Add 1 mM DTT (*see* **Note 3**) and protease/phosphatase inhibitors (optional).
2. NIBA buffer with or without Triton X-100: 1× NIB buffer, 100 μM MG-132, protease inhibitor cocktail, 1 mM Na₃VO₄, 2 mM NaF, 1 mM PMSF, 0.3% Triton X-100 (*see* **Note 4**).
3. Nuclei PURE storage buffer (*see* **Note 5**).
4. Nylon filter mesh (provided in the kit) or Miracloth (approximately 20–30 μm in pore size).
5. Mortar and pestle.
6. Mixer Mill (Retsch, MM400) or similar ball mills (such as TissueLyser II, Qiagen) for pulverizing tissues (*see* **Note 6**).
7. Stainless steel beads of approximately 3 mm in diameter, which are used to crush frozen tissues (*see* **Note 7**).
8. Bio-Rad Protein DC reagents (Cat# 5000116).
9. Spectrophotometer that can measure 650–750 nm range absorbance.

2.3 Reagents for Co-immunoprecipitation (Co-IP)

1. Co-IP buffer: Mix 50 mM Na-phosphate pH 7.4, 100 mM NaCl, 10% glycerol (vol/vol), 5 mM EDTA, 0.1% Triton X-100 (vol/vol), 1 mM DTT, 50 μM MG-132, 2 mM Na₃VO₄, 2 mM NaF, and Complete Protease Inhibitor Cocktail Tablets (Sigma or Pierce) (*see* **Note 8**).
2. Washing buffer: Mix 50 mM Na-phosphate pH 7.4, 100 mM NaCl, 10% glycerol (vol/vol), 5 mM EDTA, 0.1% Triton X-100 (vol/vol) (*see* **Note 9**).
3. Selection of beads for primary IP: IgG-binding Protein A-, G-, or A/G-conjugated magnetic beads (such as Dynabeads Protein A or Protein G, Life Technologies) are recommended (rather than sepharose/agarose beads) to minimize contamination from plant protein extract and to shorten overall experiment time. Depending on the animal species from which the

antibodies used for IP are derived, the appropriate Protein A-, G-, or A/G-coupled magnetic beads should be selected.

4. Mixer Mill (Retsch, MM400) or similar ball mill for pulverizing tissues (*see Note 6*).
5. Stainless steel beads of approximately 3 mm in diameter.
6. Sonicator equipped with a thin tip probe, which can be used in 1.5 mL tube.

3 Methods

3.1 Isolation of Nuclei for Western Blot Analysis

All operations should be carried out in the 4 °C cold room or on ice. Make sure to pre-chill all buffers and tubes on ice as well as the centrifuge rotors before starting.

1. Roughly break tissues in liquid N₂ using a mortar and pestle. Using an N₂-chilled spatula, transfer up to 1.0 mL of tissue powder in liquid N₂ (or dry ice)-chilled 2.0 mL tubes containing two to three stainless steel beads. Keep the samples either in liquid N₂, -80 °C or on dry ice. Pulverize the frozen samples using the Mixer Mill (*see Note 10*).
2. Put the pulverized frozen samples on ice, and immediately add 1.0 mL of ice-cold 1 × NIB buffer. Thaw and resuspend the frozen tissues well by pipetting, or vortex briefly. Keep the samples on ice.
3. Place either one layer of the filter mesh (about 3 cm × 3 cm) from the kit or four layers of Miracloth inside a 15 mL centrifuge tube (round bottom one is better) and pass the cell suspension through the filter by pipetting. Squeeze the filter with the tip of the P1000 pipette to remove as much as possible of the solution left on the filter (*see Note 11*).
4. Remove the filter from the tubes and centrifuge the tubes at 1260 × *g* at 4 °C for 10 min. During the centrifugation, pre-chill 1.5 mL tubes on ice (*see Note 12*).
5. Decant supernatant and remove any buffer by inverting the tubes on clean paper towel for a few seconds and tapping the tube. Put the tube back on ice and add 600 μL of ice-cold 1 × NIBA with Triton X-100 to all tubes. Resuspend the pellet (Fig. 1a) completely by pipetting or vortex well and transfer all resuspended samples into the chilled 1.5 mL tube.
6. Centrifuge the sample at 12,000 × *g* at 4 °C for 10 min (*see Note 13*).
7. Remove the supernatant by pipetting. Add 500 μL of ice-cold 1 × NIBA with Triton X-100 to all tubes. Break and resuspend the pellet by pipetting. Keep the remaining samples on ice (*see Note 14*).

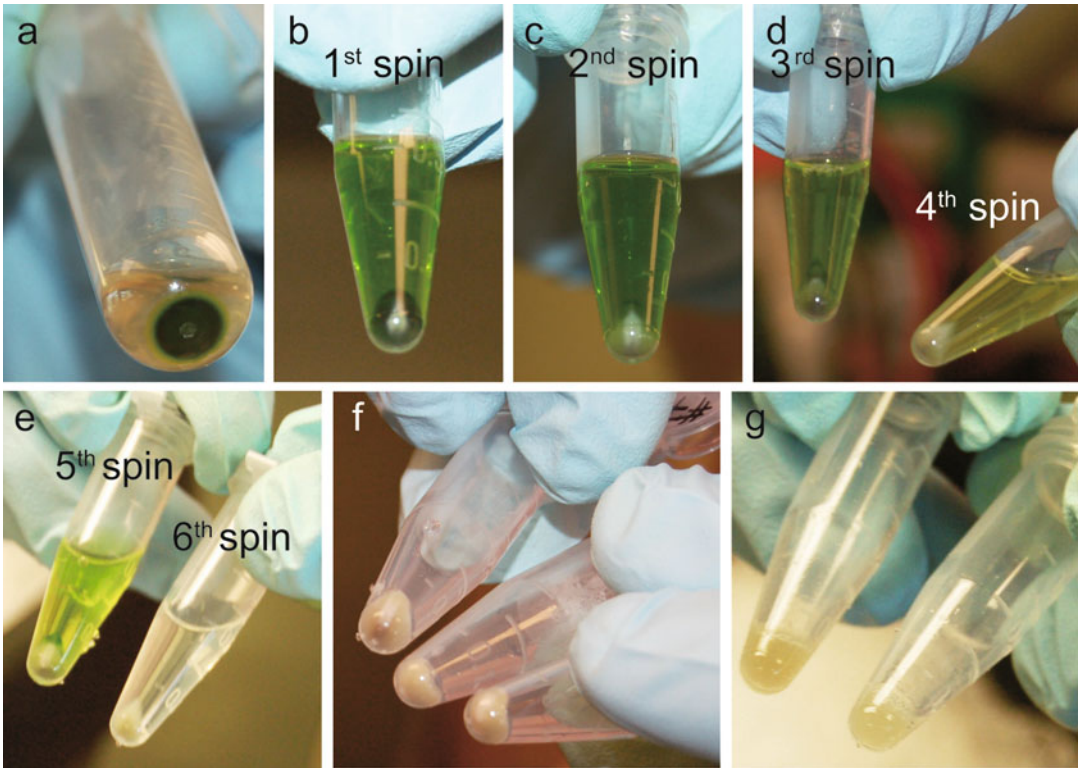


Fig. 1 Representative images of the supernatant and nuclei-containing pellets after each centrifugation during nuclei purification. **(a)** After the first centrifugation of NIB-resuspended tissues from step 4. **(b–e)** After the centrifugation of NIBA-resuspended nuclei pellet from each wash. Note that the white part of the pellet increases and the supernatant becomes colorless as you repeat the wash. **(f)** Nuclei-enriched pellet after the final centrifugation. **(g)** Nuclei pellet resuspended by PURE storage buffer

8. Centrifuge the sample at $12,000 \times g$ at 4°C for 5 min. Repeat **steps 7 and 8** four to six times until the pellet becomes white (sometimes, nuclei pellet is yellow or gray, depending on the growth conditions) and supernatant becomes clear (Fig. 1b–e, see **Note 15**).
9. Once the pellet and supernatant become colorless, add $500\ \mu\text{L}$ of ice-cold $1\times$ NIBA without Triton X-100. Resuspend the pellet and centrifuge the sample at $12,000 \times g$ at 4°C for 10 min.
10. Remove the supernatant completely. The pellet should not have any green color and should look like Fig. 1f. Add the same amount of Nuclei PURE Storage buffer as the volume of the nuclei pellet (Fig. 1g, see **Note 16**). Resuspend the pellet well by pipetting (see **Note 17**).
11. To analyze the protein concentration in the nuclei samples, use Bio-Rad Protein DC reagents. Mix Reagent A and Reagent S in 50:1 ratio to make Reagent A'. Mix $13\ \mu\text{L}$ of water and $2\ \mu\text{L}$ of

resuspended nuclei per tube and add 75 μL of Reagent A'. Add 600 μL of Reagent B, mix well by inverting samples, and wait for 10 min. Transfer mixtures to 1.0 mL cuvettes to measure OD_{650} to calculate the concentration.

12. For time-course analysis, use the same amount of protein across the time points. Mix the samples well with $2\times$ SDS sample buffer and then heat at 70 $^{\circ}\text{C}$ for 3 min, and centrifuge at maximum speed for 3–5 min to tightly precipitate debris. Load the supernatant on SDS-PAGE gel (*see Note 18*).

3.2 Preparation of Plant Tissues Expressing Potential Interacting Proteins for Co-IP

1. Use transgenic *Arabidopsis* plants or tobacco leaves transiently transfected with *Agrobacterium* harboring a protein expression binary plasmid (*see Note 19*). Harvest plant tissues and immediately freeze them in liquid N_2 .
2. Pulverize frozen tissues using the Mixer Mill equipped with liquid N_2 -chilled folders (*see Note 20*).
3. Aliquot 1.0 mL in volume (=0.5 g) of the frozen ground tissues into a liquid N_2 -chilled 2.0 mL tube (Fig. 2a) and store at -80°C (*see Note 21*). If the protein of interest is highly expressed, half of the tissue amount can be used.

3.3 Preparation of Antibody-Magnetic Bead Complex Prior to Co-IP

1. Take Co-IP buffer from -20°C freezer and let it thaw on ice before starting.
2. Take 10 μL of Dynabeads Protein G or Protein A (Invitrogen) for each Co-IP sample and transfer into a 1.7 mL tube. Insert the Dynabeads containing tube into a magnetic stand (i.e., DynaMag-2 Magnet, Invitrogen) and wait until the beads collect as a pellet on the magnetic side (*see Note 22*).
3. Discard the supernatant by pipetting. Take the tube out of the magnetic stand and put it on ice.
4. Add 250 μL of Co-IP buffer into the tube and resuspend the magnetic beads by gently tapping and inverting several times. Depending on the number of samples and the amount of beads prepared, add more Co-IP buffer if necessary.
5. Add the appropriate antibody (for immunoprecipitation of the target proteins) into the tube and mix briefly by tapping.
6. Incubate the tube in a rotator at 30–40 rpm at room temperature for 10 min to let Protein G (or A) bind to the antibodies (*see Note 23*).
7. After incubation, capture beads using the magnetic stand, and remove the supernatant by pipetting.
8. Wash the pellet once with 500 μL of Co-IP buffer by gently resuspending, and capture the beads again. Remove the supernatant by pipetting.

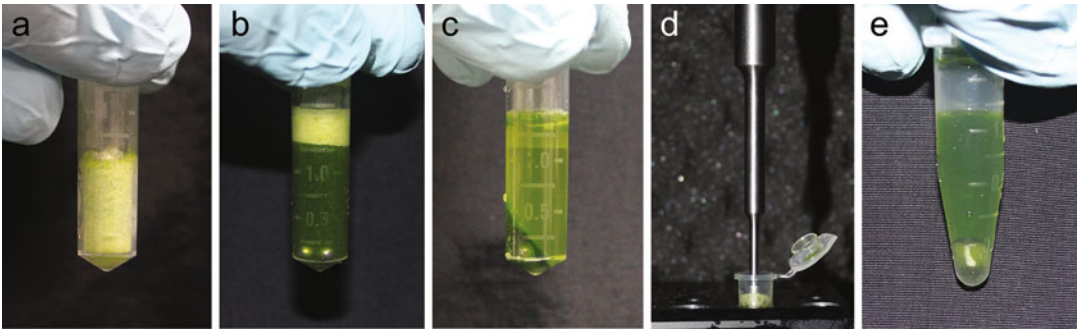


Fig. 2 Representative images of some protein extraction processes for Co-IP. **(a)** The amount of frozen pulverized tissues is shown. **(b)** The frozen tissues are resuspended in ice-cold Co-IP buffer and vortexed. **(c)** The supernatant, which is a cytosolic fraction, is usually colored a very faint green in this step. **(d)** To break organelles, we use a very thin tip sonication probe like the one shown in this picture. The tube is placed in an ice block. **(e)** This supernatant fraction contains proteins from nuclei and organelles

9. Transfer the tube with beads to ice, and add 50–100 μL of Co-IP buffer for each Co-IP sample and resuspend the beads by tapping or gentle short vortex. This can be kept on ice until cell lysate is ready.

3.4 Whole-Cell Protein Extraction

1. Take the pulverized tissues out of the $-80\text{ }^{\circ}\text{C}$ freezer (we recommend to minimize the storage time of the pulverized tissues in $-80\text{ }^{\circ}\text{C}$) and place it on ice. Add 1.0 mL of Co-IP buffer and make sure all tissues are resuspended in the buffer by pipetting. Once tissues are resuspended in the buffer, immediately vortex it vigorously for 1 min (Fig. 2b).
2. To disrupt organelles, sonicate 4–5 times with intermittent pulse sonication (i.e., repeat 15 s cycle with pulse on for 3 s and pulse off for 2 s at 10–30% amplitude, although this depends on the maximum power of the sonicator used) on an ice bath or a cooling block after vortexing the sample (*see Note 24*).
3. Centrifuge at $12,000 \times g$ at $4\text{ }^{\circ}\text{C}$ for 10 min. Transfer 1.0 mL of the supernatant into a pre-chilled 1.5 mL tube on ice.

3.5 Separate Cytosolic- and Nuclei-Enriched Fractions

Instead of using whole-cell extract, you can use different cell lysate fractions (i.e., cytosolic and/or nuclei enriched ones) (*see Note 25*).

1. Take the pulverized tissues out of the $-80\text{ }^{\circ}\text{C}$ freezer and place it on ice. Add 1.0 mL of Co-IP buffer and make sure all tissues are resuspended in the buffer by pipetting. Once tissues are resuspended in the buffer, immediately vortex it vigorously for 1 min, and then centrifuge at $12,000 \times g$ at $4\text{ }^{\circ}\text{C}$ for 10 min (Fig. 2c).

2. Transfer as much of the supernatant as possible to a new pre-chilled 1.5 mL tube placed on ice, and keep the original 2.0 mL tube with the pellet on ice. The supernatant is considered to be the cytosolic fraction in which the extract contains a majority of the cytosolic proteins.
3. Resuspend the pellet with 1.0 mL of ice-cold Co-IP buffer and sonicate four to five times with intermittent pulse sonication on ice or on a cooling block (Fig. 2d).
4. Centrifuge at $12,000 \times g$ at 4 °C for 10 min (Fig. 2e). Transfer 1.0 mL of the supernatant into a pre-chilled 1.5 mL tube on ice. The supernatant at this step is considered to be the protein extract from the nuclei-enriched fraction (*see Note 26*). The pellet color will turn pale green with an increased white portion as indication of nuclei enrichment.

3.6 Co-IP Procedure

Carry out all procedures in 4 °C cold room unless otherwise specified.

1. Before starting (*see Note 27*), aliquot 50 μ L of the supernatant in a different tube as input and mix it with 10 μ L of 6 \times SDS (or 50 μ L of 2 \times SDS) sample buffer by pipetting. Keep it on ice during the Co-IP process.
2. Add the prepared antibody-bound magnetic beads solution (Subheading 3.3, step 9) into the tube containing the rest of the supernatant. Make sure the beads in the solution are evenly dispersed (by pipetting) before it is added to the protein extract.
3. Rotate the tube at 30–40 rpm for 10–30 min under dark, dim light, or various light sources including blue, red, or far-red LEDs if applicable (*see Note 28*). Usually 30 min incubation is enough, but the time for the immune reaction may be adjusted based on protein stability, presence of nonspecific binding, etc. (*see Note 29*).
4. After incubation, transfer the tube to the magnetic stand to capture the beads. Once the solution becomes transparent (=all beads are captured), decant the supernatant by gently inverting and remove residual solution by pipetting.
5. Take the tube out of the stand and add 500 μ L of washing buffer. Resuspend the beads by inverting the tube about ten times.
6. Place the tube again in the magnetic stand to capture the beads. Remove the supernatant as much as possible by pipetting.
7. Repeat wash **steps 5** and **6** twice (in total wash the beads three times).
8. After removing the buffer by pipetting, centrifuge the tube for approximately 10–20 s at top speed to spin down any residual

buffer attached inside the tube. Then place the tube in the magnetic stand and completely remove any remaining buffer by pipetting. Transfer the tube to ice.

9. Add 30 μ L of 2 \times SDS sample buffer and resuspend the bead pellet by pipetting. The mixture of the beads and 2 \times SDS sample buffer is considered the immunoprecipitated sample.
10. Vortex very briefly both the input and the immunoprecipitated sample and incubate them at 70–80 °C on a heating block for 3–5 min to denature the proteins and dissociate the immune complex from the magnetic beads.
11. After heating the tubes, centrifuge briefly (less than a minute) to spin down all liquid at the bottom of the tube as well as precipitate the beads. By now, all samples are ready to run in a SDS-PAGE gel and subject to western blot assay.

4 Notes

1. Samples (intact, not pulverized) can be stored for a couple of months in –80 °C.
2. 1 \times NIB can be substituted with homemade buffer (see the following two options). If working with highly unstable proteins, adding protease inhibitors is recommended:
 - (a) 20 mM Tris-HCl, 20 mM MgCl₂, pH 6.8, 5% sucrose, 40% glycerol, 0.8% Triton X-100, 0.08% β -mercaptoethanol, protease inhibitor, 1 mM DTT, 1.3 mM PMSF [25].
 - (b) 20 mM Tris-HCl pH 7.4, 25% glycerol, 20 mM KCl, 2 mM EDTA, 12.5 mM MgCl₂, 0.25 M sucrose, 1 mM DTT, 1 mM PMSF [26].
3. DTT should be kept in –20 °C in a small aliquot and be freshly added before every extraction.
4. 1 \times NIBA with Triton X-100 can be substituted with homemade buffer with the following compositions (concentration of Triton X-100 can vary, depending on the tissue):
 - (a) 20 mM Tris-HCl, 20 mM MgCl₂, pH 6.8, 5% sucrose, 40% glycerol, 0.8% Triton X-100, 0.08% β -mercaptoethanol, protease inhibitor, 1 mM DTT, 1.3 mM PMSF [25].
 - (b) 20 mM Tris-HCl (pH 7.4), 25% glycerol, 2.5 mM MgCl₂, 0.2% Triton X-100 [26].
5. Nuclei PURE storage buffer can be substituted with homemade nuclei storage buffer (20 mM HEPES (pH 7.2), 5 mM MgCl₂, 2 mM DTT, 50% glycerol).

6. The pulverizing process can be done with liquid N₂-chilled mortars and pestles. However, clean mortars and pestles are required with each new sample. The Mixer Mill can process multiple samples simultaneously.
7. Optimal size of beads should be determined based on types of the grinder (i.e., Mixer Mill) and the tube used. We use two to three stainless steel beads in 2.0 mL tubes to grind up to approximately 1.0 mL volume of 14-day-old *Arabidopsis* seedlings.
8. 50 mM Tris-HCl or HEPES buffer can be used instead of the Na-phosphate buffer. The pH range should be 7.4–8.0. NaCl can be replaced with KCl. The concentration of NaCl/KCl is adjustable depending on the presence of nonspecific bindings. The mixed buffer can be stored at –20 °C.
9. The concentration of NaCl (or KCl) can be increased such as 150, 200, and 300 mM, when nonspecific bindings are visible, in order to reduce or eliminate background signals in western blot. This buffer can be stored at 4 °C.
10. The size of *Arabidopsis* leaf nuclei can be 5–20 μm. Too much or too little grinding decreases nuclei yield. We set the Mixer Mill at 25–30 frequency per min and run for 2 min to pulverize 1.0 mL volume of frozen leaf tissue. All tubes should be kept in liquid N₂-chilled tube holders while pulverizing samples.
11. Squeeze cell suspension trapped in the filter by pushing the filter using a clean pipet tip or your fingers. Wipe fingers with paper towels soaked with 70% ethanol every time after squeezing any suspension trapped in the filter into the tube to avoid sample cross-contamination. Multiple layers of nylon filter mesh with different pore sizes are also effective to remove debris [27]. The filter mesh that originally came with the kit can be reused, although Miracloth should not be reused. Used filter mesh should be washed with soap and rinsed well with deionized water, and stored in 70% ethanol.
12. After centrifugation, the pellet at the bottom of the tube (Fig. 1a, occasionally with a white ring around the pellet, made of precipitated nuclei) can be seen.
13. After the first centrifugation, the white pellet (in the middle) and the green pellet on top of the white pellet (Fig. 1b) should be visible. The white pellet contains nuclei.
14. After resuspending the supernatant, the samples can be kept on ice for 30 min or longer. In this case, you may obtain an increased amount of nuclei in the pellet with lighter green color.

15. When you remove the supernatant, if you have a good amount of nuclei pellet, you can gently remove the green pellet layer by pipetting (optional).
16. This method will give you 3–5 $\mu\text{g}/\mu\text{L}$ of nuclei-enriched protein solution. If you need a higher concentration of the solution, reduce the volume of the Nuclei PURE Storage buffer.
17. The nuclei solution is viscous. Be sure to resuspend the pellet by pipetting and vortex thoroughly. Isolated nuclei can be stored in $-80\text{ }^{\circ}\text{C}$ up to 3 months.
18. $4\times$ SDS sample buffer can be similarly used. Use at least the same volume of $2\times$ SDS sample buffer as the nuclei sample volume to ensure SDS binding to all proteins. Histone H3, which runs around 16 kDa, can be used as a loading control.
19. When the tobacco transient expression system is used, a technical issue frequently encountered is that the expression level of the protein of interest transiently induced varies from protein to protein. When this issue happens, there are two options. (1) Use different concentrations of *Agrobacterium* for each expression cassette. The standard concentration of *Agrobacterium* used to infect plants is an OD_{600} of approximately 1.0. It can go up to 2.5 with lower expression, while 0.25, 0.5, or 0.75 may be used for higher expressions. (2) Sequential agroinfiltration may also apply. Infiltrate *Agrobacterium* carrying a lower expression cassette first, and then infiltrate *Agrobacterium* with a higher expression cassette 1 or 2 days later. Harvest infiltrated leaf tissues on Day 3 after the first *Agrobacterium* injection. We usually harvest transfected samples on Day 3 post infection; however, if necrosis of the transfected areas is observed, the incubation time can be shortened to 1–2 days.
20. Compared with nuclei procedure, when we pulverize tissues for Co-IP or regular western blot analysis, we run the Mixer Mill longer (i.e., 3–4 min) to make sure all samples are finely pulverized. To extend running time for the Mixer Mill, we repeat a 1–2 min run several times, and before each run, tissue folders are briefly chilled in liquid N_2 to make sure samples won't thaw during this process. As soon as samples are pulverized, tubes are transferred back to liquid N_2 or dry ice to keep the samples completely frozen until extraction buffer is added.
21. This is a stopping point; however, we don't recommend keeping pulverized samples in $-80\text{ }^{\circ}\text{C}$ for a long time.
22. Also see the manufacturer protocol for details.
23. This incubation can exceed 10 min, although 10 min is usually sufficient.
24. Make sure that the pulse amplitude is not too strong. Place the tip of the probe near the bottom of the tube. This will prevent

spills and generating foam (the sample will foam with sonication). To avoid spilling samples by sonication, the cell suspension can be transferred to a bigger tube before sonication if necessary. Every time the sample is changed, the tip of the sonication probe should be rinsed thoroughly with deionized water. Without sonication, the supernatant after centrifugation is likely derived from mainly cytosol.

25. Once the fractionation is done, it is important to confirm whether the fractions used for Co-IP contain subcellular marker proteins, such as cytosolic markers [i.e., Thioredoxin X (Thx) [28]; note that Thx is localized in chloroplasts and cytosol] and nuclear markers (i.e., Histone H3) [24].
26. This extract contains proteins not only from nuclei but also from other organelles, although cytosolic proteins are mainly removed. If extract from purified nuclei is required, use the method for nuclei purification first and resuspend the purified nuclei with the Co-IP buffer once the nuclei are isolated. Then, sonicate and centrifuge in the way described in Subheading 3.5 to extract proteins from nuclei.
27. If the changes in the (co)immunoprecipitated proteins among samples are to be quantitatively compared, measure the protein concentrations in the extracts of all samples before Co-IP and adjust the concentrations until they are the same by adding the Co-IP buffer so that the same amount of total protein (within 1.0 mL of the extracts) is used for Co-IP across the samples.
28. If the interaction is light sensitive, avoid exposing samples to light as much as possible even during the preparation processes of protein extracts.
29. The incubation time for Co-IP should be determined by sampling immunoprecipitated proteins at different incubation times (for instance, 10, 30, 60, and 120 min). Changing the basal buffer (Na-phosphate, HEPES, or Tris-HCl of the same pH) can influence the stability/association of the protein complex. In our case (for our proteins of interest), a Na phosphate-based buffer seemed to be the most suitable.

Acknowledgments

This work was supported by NIH grant (GM079712) to TI, the National Research Foundation of Korea (NRF) grant (NRF-2020R1A2C1014655) to Y.H.S., JSPS KAKENHI (19K16170), Grant-in-Aid for Scientific Research on Innovative Areas (JP19H04866), Start-up Grant for Women Scientists from NAIST, and Lifescience Grant from Takeda Science Foundation to A.K.

References

- Harmer SL (2009) The circadian system in higher plants. *Annu Rev Plant Biol* 60:357–377
- Greenham K, McClung CR (2015) Integrating circadian dynamics with physiological processes in plants. *Nat Rev Genet* 16(10):598–610
- Sugano S, Andronis C, Green RM, Wang ZY, Tobin EM (1998) Protein kinase CK2 interacts with and phosphorylates the *Arabidopsis* circadian clock-associated 1 protein. *Proc Natl Acad Sci U S A* 95(18):11020–11025
- Más P, Devlin PF, Panda S, Kay SA (2000) Functional interaction of phytochrome B and cryptochrome 2. *Nature* 408(6809):207–211
- Más P, Kim WY, Somers DE, Kay SA (2003) Targeted degradation of TOC1 by ZTL modulates circadian function in *Arabidopsis thaliana*. *Nature* 426(6966):567–570
- Kim WY, Fujiwara S, Suh SS, Kim J, Kim Y, Han L, David K, Putterill J, Nam HG, Somers DE (2007) ZEITLUPE is a circadian photoreceptor stabilized by GIGANTEA in blue light. *Nature* 449(7160):356–360
- Fujiwara S, Wang L, Han L, Suh SS, Salome PA, McClung CR, Somers DE (2008) Post-translational regulation of the *Arabidopsis* circadian clock through selective proteolysis and phosphorylation of pseudo-response regulator proteins. *J Biol Chem* 283(34):23073–23083
- Para A, Farre EM, Imaizumi T, Pruneda-Paz JL, Harmon FG, Kay SA (2007) PRR3 is a vascular regulator of TOC1 stability in the *Arabidopsis* circadian clock. *Plant Cell* 19(11):3462–3473
- Yakir E, Hilman D, Kron I, Hassidim M, Melamed-Book N, Green RM (2009) Post-translational regulation of CIRCADIAN CLOCK ASSOCIATED1 in the circadian oscillator of *Arabidopsis*. *Plant Physiol* 150(2):844–857
- Baudry A, Ito S, Song YH, Strait AA, Kiba T, Lu S, Henriques R, Pruneda-Paz JL, Chua NH, Tobin EM, Kay SA, Imaizumi T (2010) F-box proteins FKF1 and LKP2 act in concert with ZEITLUPE to control *Arabidopsis* clock progression. *Plant Cell* 22(3):606–622
- Wang L, Fujiwara S, Somers DE (2010) PRR5 regulates phosphorylation, nuclear import and subnuclear localization of TOC1 in the *Arabidopsis* circadian clock. *EMBO J* 29(11):1903–1915
- Nusinow DA, Helfer A, Hamilton EE, King JJ, Imaizumi T, Schultz TF, Farré EM, Kay SA (2011) The ELF4-ELF3-LUX complex links the circadian clock to diurnal control of hypocotyl growth. *Nature* 475(7356):398–402
- Herrero E, Kolmos E, Bujdosó N, Yuan Y, Wang M, Berns MC, Uhlworm H, Coupland G, Saini R, Jaskolski M, Webb A, Goncalves J, Davis SJ (2012) EARLY FLOWERING4 recruitment of EARLY FLOWERING3 in the nucleus sustains the *Arabidopsis* circadian clock. *Plant Cell* 24(2):428–443
- Pudasaini A, Shim JS, Song YH, Shi H, Kiba T, Somers DE, Imaizumi T, Zoltowski BD (2017) Kinetics of the LOV domain of ZEITLUPE determine its circadian function in *Arabidopsis*. *eLife* 6:e21646
- Nohales MA, Liu W, Duffy T, Nozue K, Sawa M, Pruneda-Paz JL, Maloof JN, Jacobsen SE, Kay SA (2019) Multi-level modulation of light signaling by GIGANTEA regulates both the output and pace of the circadian clock. *Dev Cell* 49:840
- Hsu PY, Harmer SL (2014) Wheels within wheels: the plant circadian system. *Trends Plant Sci* 19(4):240–249
- de Montaigu A, Toth R, Coupland G (2010) Plant development goes like clockwork. *Trends Genet* 26(7):296–306
- Song YH, Shim JS, Kinmonth-Schultz HA, Imaizumi T (2015) Photoperiodic flowering: time measurement mechanisms in leaves. *Annu Rev Plant Biol* 66:441–464
- Folta KM, Kaufman LS (2000) Preparation of transcriptionally active nuclei from etiolated *Arabidopsis thaliana*. *Plant Cell Rep* 19(5):504–510
- Tan F, Li G, Chitteti BR, Peng Z (2007) Proteome and phosphoproteome analysis of chromatin associated proteins in rice (*Oryza sativa*). *Proteomics* 7(24):4511–4527
- Sikorskaite S, Rajamaki ML, Baniulis D, Stanys V, Valkonen JP (2013) Protocol: optimised methodology for isolation of nuclei from leaves of species in the *Solanaceae* and *Rosaceae* families. *Plant Methods* 9:31
- Yin X, Komatsu S (2016) Plant nuclear proteomics for unraveling physiological function. *New Biotechnol* 33(5, Pt B):644–654
- Song YH, Smith RW, To BJ, Millar AJ, Imaizumi T (2012) FKF1 conveys timing information for CONSTANS stabilization in photoperiodic flowering. *Science* 336(6084):1045–1049
- Song YH, Estrada DA, Johnson RS, Kim SK, Lee SY, MacCoss MJ, Imaizumi T (2014) Distinct roles of FKF1, GIGANTEA, and ZEITLUPE proteins in the regulation of

- CONSTANS stability in *Arabidopsis* photoperiodic flowering. *Proc Natl Acad Sci U S A* 111 (49):17672–17677
25. Hayama R, Sarid-Krebs L, Richter R, Fernandez V, Jang S, Coupland G (2017) PSEUDO RESPONSE REGULATORS stabilize CONSTANS protein to promote flowering in response to day length. *EMBO J* 36 (7):904–918
26. Xu F, Copeland C (2012) Nuclear extraction from *Arabidopsis thaliana*. *Bio Protoc* 2(24): e306
27. Goto C, Hashizume S, Fukao Y, Hara-Nishimura I, Tamura K (2019) Comprehensive nuclear proteome of *Arabidopsis* obtained by sequential extraction. *Nucleus* 10(1):81–92
28. Park SK, Jung YJ, Lee JR, Lee YM, Jang HH, Lee SS, Park JH, Kim SY, Moon JC, Lee SY, Chae HB, Shin MR, Jung JH, Kim MG, Kim WY, Yun DJ, Lee KO, Lee SY (2009) Heat-shock and redox-dependent functional switching of an h-type *Arabidopsis* thioredoxin from a disulfide reductase to a molecular chaperone. *Plant Physiol* 150(2):552–561



Chromatin Immunoprecipitation Protocol for Circadian Clock Proteins

Sally Adams and Isabelle A. Carré

Abstract

Chromatin immunoprecipitation, or ChIP, is a powerful experimental technique for probing protein-DNA interactions in vivo. This assay can be used to investigate the association of a protein of interest with specific target loci. Alternatively, it can be combined with high-throughput sequencing technology to identify genome-wide binding sites. Here, we describe a ChIP protocol that was optimized for low-abundance transcription factors in *Arabidopsis*, and provide guidance on how to adapt it for other types of plants and proteins.

Keywords Chromatin immunoprecipitation, Transcriptional regulation, Gene regulatory networks

1 Introduction

Chromatin immunoprecipitation or ChIP is a technique used to quantify protein-DNA interactions. The first step generally involves cross-linking live tissue, in order to introduce covalent bonds between proteins and the DNA that they are attached to. Chromatin is then extracted from the samples and sheared into 150–300 bp fragments, before immunoprecipitation (IP) using an antibody to the protein of interest. Finally, the cross-links are reversed, and the released DNA is assayed to identify the sequences bound by the protein. The abundance of specific DNA sequences can then be quantified in the immunoprecipitated sample by real-time PCR, in order to provide an estimate of the protein's binding to these loci. Alternatively, the immunoprecipitated DNA can be analyzed by high-throughput sequencing in an approach known as ChIP-seq, in order to reveal genome-wide binding interactions. Binding sites are then identified as segments of the genome where there is overrepresentation of sequence reads

relative to a control sample. These binding sites are visualized as peaks of read counts at the corresponding genomic position [1].

ChIP is a powerful tool for the study of transcriptional regulatory networks, because it allows investigations of direct regulatory interactions between transcription factors and their target promoters. This is particularly important in the context of circadian systems, which are composed of transcriptional-translational feedback loops and where core components of the oscillator are transcriptional regulators. Feedback within the system makes it particularly difficult to predict regulatory interactions from changes in gene expression levels in loss- or gain-of-function mutant backgrounds. However, ChIP analyses provide unambiguous answers and can uncover novel interactions. For example, in *Arabidopsis*, ChIP-seq analyses of binding sites for one of the evening components of the clock, known as TOC1, uncovered its interaction with *the* promoters of multiple clock genes including *CCA1*; *LHY*; *PRR5*, 7, and 9; *GI*; *TOC1*; *ELF4*; and *LUX* [2].

Analyses of genome-wide targets for core clock components via ChIP-seq can also be used to uncover the physiological processes that are directly influenced by these proteins. Thus, analysis of binding targets for the morning clock-component LHY revealed its direct influence on the biosynthesis of the stress response hormone abscisic acid (ABA) as well as on downstream signaling pathways [3].

ChIP can also be used to investigate chromatin structure through quantification of modified histones at specific loci. Core histones (H2A, H2B, H3, and H4) can be covalently modified at different positions of amino-terminal tails through acetylation, methylation, ubiquitination, phosphorylation, glycosylation, carbonylation, ADP ribosylation, sumoylation, or biotinylation, and these modifications, alone or in combination, can either restrict or promote accessibility of the transcription machinery to the DNA [4]. Time-course ChIP-seq studies in mammals have uncovered genome-wide rhythms of chromatin remodeling associated with binding of clock-associated transcription factors, RNA-polymerase II recruitment, and transcriptional initiation [5]. While no such genome-wide study has been carried out in plants, there is also evidence for rhythmic changes in histone H3 acetylation (histone 3 lysine 9 and 14 acetylation) and histone 3 lysine 4 trimethylation at multiple clock-associated loci, which are thought to enable rhythmic changes in transcriptional activity [6–10].

ChIP analyses have made a major contribution to our current understanding of regulatory connections within the plant circadian oscillator and of how individual oscillator components interface with downstream physiological processes. They have uncovered mechanisms by which clock components influence changes in chromatin structure to effect changes in transcriptional activity. However, much remains to be uncovered about how these regulatory

mechanisms are affected by different environment conditions or developmental stages, and ChIP will no doubt remain a key technique to address these questions.

Here we describe a ChIP protocol that was optimized for low-abundance transcription factors in *Arabidopsis* and provide guidance on how this protocol may be adapted for other types of plants and proteins.

2 Materials

2.1 Plant Material

You'll need sufficient plant material to yield the recommended amount of chromatin for immunoprecipitation. Twenty-five microgram of chromatin is recommended as starting material for immunoprecipitation of low-abundance transcription factors, but less may be required for high-abundance targets such as histones or RNA Polymerase II. Working with *Arabidopsis*, we sow approximately 400 μL of seed for each chromatin isolation and grow the plants for 14 days on MS-agar plates. This yields sufficient chromatin for two immunoprecipitations.

2.2 Equipment and Supplies

1. Desiccator.
2. Vacuum pump.
3. Nylon mesh.
4. Homogenizer: We use a Polytron Status X120. If not available, frozen tissue can be ground using a mortar and pestle and added to the extraction buffer.
5. Miracloth.
6. Funnel.
7. Sonifier: We use a Branson Digital probe Sonifier with a 1/8-in. Micro Tip. Bath sonifiers such as the Bioruptor (Diagenode) can also be used to shear chromatin. These offers the advantage of controlled cooling and that multiple samples can be processed in parallel.
8. Small artist paintbrush.
9. Magnetic separation racks for 2 and 50 mL tubes.
10. 2 mL microfuge tubes.
11. 50 mL conical centrifuge tubes (Falcon).
12. Polypropylene tubes suitable for high-speed centrifugation (Oak Ridge).
13. Rotating mixer wheel.
14. DNA clean up kit: We use the MinElute PCR Purification Kit (QIAGEN).

2.3 Solutions and Reagents

1. Cross-linking Solution: 1% formaldehyde.
2. Cross-linker Quenching Solution: 2 M glycine.
3. Extraction Buffer 1: 10 mM Tris-HCl (pH 8), 0.4 M sucrose, 5 mM 2 β -mercaptoethanol, 1 mM PMSF and protease inhibitors (we used either Roche complete cocktail or Sigma plant cocktail) (*see Note 1*).
4. Extraction Buffer 2: 10 mM Tris-HCl (pH 8), 0.25 M sucrose, 10 mM MgCl₂, 1% Triton X-100, 5 mM 2 β -mercaptoethanol, 1 mM PMSF and protease inhibitors (*see Note 1*).
5. Nuclei Lysis Buffer: 50 mM Tris-HCl (pH 8), 10 mM EDTA, 1% SDS, 5 mM 2 β -mercaptoethanol, 1 mM PMSF and protease inhibitors (*see Note 1*).
6. ChIP Dilution Buffer: 16.7 mM Tris-HCl (pH 8), 1.2 mM EDTA, 167 mM NaCl, 1.1% Triton X-100.
7. Low Salt Wash Buffer: 20 mM Tris-HCl (pH 8), 2 mM EDTA, 150 mM NaCl, 0.5% Triton X-100, 0.2% SDS.
8. High Salt Wash buffer: 20 mM Tris-HCl (pH 8), 2 mM EDTA, 500 mM NaCl, 0.5% Triton X-100, 0.2% SDS.
9. LiCl Wash Buffer: 10 mM Tris-HCl (pH 8), 1 mM EDTA, 0.25 M LiCl, 0.5% NP-40, 0.5% sodium deoxycholate.
10. TE buffer: 10 mM Tris-HCl (pH 8), 1 mM EDTA.
11. Protein A magnetic beads pre-equilibrated in ChIP dilution buffer: Aliquot Protein A beads into a fresh microfuge tube, allowing 100 μ L of beads per ChIP reaction. Place the tube into a magnetic separation rack to pellet the beads and remove the supernatant (*see Note 2*). Remove the tube from the magnet, add 1 mL of ChIP dilution buffer and mix. Replace the tube in the magnet and decant the supernatant. Repeat the wash twice more. After the final wash, adjust the Protein A bead slurry to 50% with ChIP dilution buffer (*see Note 3*).
12. 10% Chelex resin in water.
13. 20 mg/mL Proteinase K.

3 Methods

3.1 Experimental Design

3.1.1 Choice of Antibody

The quality of ChIP data depends crucially on the sensitivity and specificity of the antibody used. A good antibody will give a high level of enrichment for target loci relative to control samples, which makes it easier to detect binding events.

Antibodies may already be available to the protein of interest. ChIP-validated or ChIP-grade antibodies are recommended, but antibodies validated for immunoprecipitation (IP) or immunohistochemistry (IHC) experiments may work as well. Many antibodies

for modified histones are available commercially that have been validated for ChIP studies. We have had good success using a rabbit antiserum to the *Arabidopsis* LHY protein [3, 11]; however, few antibodies are available for plant transcription factors, and de novo antibody generation does not always yield an antibody that performs well in immunoprecipitations.

When no antibody is available, ChIP analyses may be carried out using antibodies to epitope tags such (YFP, FLAG, Myc, HA, or others). This requires of course the availability of transgenic plants expressing the epitope-tagged protein. The tagged protein should ideally be expressed under the control of its own promoter, in order to avoid binding to ectopic targets as a result of abnormal expression levels.

3.1.2 Control Samples

In ChIP analyses, binding of a protein to DNA is detected as increased abundance of the target sequence in the IP'd sample relative to a control sample. Different types of control samples can be used, and this depends largely on the type of antibody used for immunoprecipitations.

Comparison with mock ChIP DNA: i.e., DNA obtained from IP without antibodies, or *nonspecific ChIP DNA* performed using pre-immune serum corrects for nonspecific binding of DNA to sample tubes or protein A beads during the immunoprecipitation process. However very little material is pulled down in the absence of a specific antibody, and it is very difficult to retrieve sufficient material for sequencing, so these controls are not commonly used in ChIP-seq experiments.

Comparison with input DNA: i.e., DNA withdrawn from the sample prior to immunoprecipitation, corrects for biases in shearing of DNA and in PCR amplification during library preparation.

Comparison with ChIP DNA from samples lacking the target protein: is the most stringent control because this also allows correction for off-target binding of the antibody. Control samples may be generated from knockout mutant tissue, if using an antibody to the native protein, or from plants lacking the transgene, if using an antibody to an epitope tag.

3.1.3 Control Loci

Positive control: If possible, a known target locus should be examined by quantitative PCR. This should show significant enrichment in the ChIP sample relative to any of the controls described above.

Negative control: A genomic region where the protein of interest is not expected to bind should also be tested. If the ChIP experiment is specific, this will show no enrichment in the ChIP sample relative to control samples.

3.1.4 *Biological Replicates*

The preparation of ChIP samples is highly time-consuming (5 days overall), and the cost of sequencing remains high. Numbers of replicate experiments are therefore an important consideration. The Encyclopedia of DNA Elements (ENCODE) project, which aims to identify functional elements in the human genome and is the largest project of this type, recommends that all ChIP measurements would be performed on two independent biological replicates [12].

There is currently no consensus on how to combine data from these replicate experiments. Pooling all replicates is inappropriate because binding that is present in only one outlying replicate could be a false positive. On the other hand, only retaining information about binding sites that were identified in all samples may lead to discarding many real binding sites as false negatives.

3.2 *Protocol*

The protocol below was adapted from [13].

3.2.1 *Harvesting and Cross-Linking of Plant Tissue*

The initial step in ChIP experiments is the infiltration of live tissue with a cross-linking agent such as formaldehyde. This introduces covalent bonds between proteins and the DNA sequences that they are bound to and ensures that physical interactions are preserved during the subsequent steps of sample preparation. The cross-linking step may also be carried out on frozen tissue, providing that samples are kept on ice at all times and that the procedure is carried out quickly. While cross-linking is generally required for transcription factors, ChIP without cross-linking (also known as native ChIP) is also possible, however [14]. Histones, for example, don't need to be cross-linked as they bind DNA very tightly.

This part of the protocol can be carried out at room temperature.

1. Harvest plant tissue into a 50 mL conical centrifuge tube containing 20 mL of sterile ddH₂O. The total volume should rise to approximately 30 mL. Pack nylon mesh into the top of each tube to ensure that the seedlings stay immersed during the subsequent steps (*see* Fig. 1).
2. Using a needle, carefully make three holes in the cap of the tube (*see* Note 4).
3. Working in a fume hood, decant the ddH₂O from each tube into a suitable waste container, then add 20 mL of Cross-linking Solution (*see* Note 5).
4. Still in the fume hood, place the tubes containing the plant tissue into a desiccator attached to a vacuum pump (*see* Fig. 1), and apply a vacuum for 10 min. You should see tiny bubbles rising from the plant tissue. After 10 min, stop the pump and slowly open the outlet valve. The infiltrated seedlings should appear translucent. The cross-linking time may need

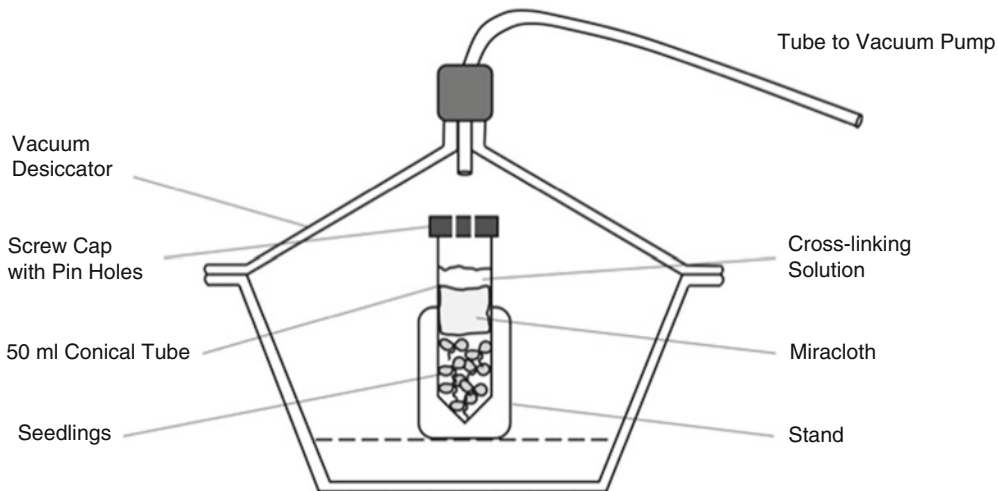


Fig. 1 Setup for vacuum infiltration of cross-linker into of plant tissue

optimization depending on plant tissue. Excessive cross-linking may result in chromatin that is resistant to fragmentation by sonication.

5. Add 1.3 mL of Cross-linker Quenching Solution to each tube. Apply a vacuum for a further 5 min and release as described above.
6. Wash the seedlings twice with 40 mL of sterile ddH₂O, decanting the supernatant into a suitable waste container (*see Note 5*). After the final wash, decant the supernatant and use a metal spatula to squeeze the material, in order to eliminate as much water as possible.
7. Remove the nylon mesh using forceps, ensuring that the plant material is left behind. Replace the conical tube lid with a new lid without needle holes and snap freeze the cross-linked material in liquid nitrogen. The material can be stored at -80°C until required.

3.2.2 Chromatin Isolation

All steps must be carried out at 4°C using pre-chilled solutions.

1. To each 50 mL tube containing frozen cross-linked material, add 30 mL of Extraction Buffer 1 (*see Note 1*). Once the sample is thawed, place the tube on ice and disrupt the material by blending with a suitable homogenizer for 30 s. Repeat the homogenization step twice more at 1 min intervals.
2. To remove unwanted plant debris, filter this solution through two layers of Miracloth. For each sample, cut two square pieces of Miracloth (Merck) approximately 14 cm by 14 cm. Fold each square twice, to make a smaller square, approximately 7 cm by 7 cm. Carefully open the squares to make a cone-like

shape and fit one Miracloth cone inside the other. Place the double-layered Miracloth cone in a funnel sitting in a polycarbonate screw cap (Oak Ridge) tube on ice. Filter your sample into the tube. The Miracloth can be gently squeezed to ensure as much liquid is harvested as possible.

3. Centrifuge samples for 20 min at 4000 rpm ($1940 \times g$) in a Beckman JA-20 rotor at 4 °C. This very gentle centrifugation will pellet the nuclei along with cellular debris. The pellet may be green due to chloroplast contamination, but this is not detrimental to downstream steps.
4. After centrifugation, remove the supernatant and add 1 mL of ice-cold Extraction Buffer 2 (*see Note 1*). To preserve intact nuclei, carefully resuspend the pellet using a small artist's paintbrush. Brush the pellet against the wall of the tube with gentle upward motions until the pellet is evenly resuspended in the buffer. Pour the sample into a 1.5 mL centrifuge tube and incubate on ice for 5–10 min. Do not use a pipette here as this may disrupt the nuclei.
5. Pellet the nuclei by centrifugation at top speed in a microfuge for 10 min at 4 °C (approximately $14,000 \times g$). Remove the supernatant and resuspend the nuclear pellet in 500 μ L of ice-cold Nuclear Lysis Buffer (*see Note 1*). As the nuclei will become disrupted after this step, there is no need to use a paintbrush.
6. Keeping your samples on ice at all times, fragment the chromatin by sonication. We typically sonicate samples five times for 10 s each at maximum amplitude, with 1-min pauses in between pulses (*see Notes 6 and 7*).
7. Pellet the cell debris by centrifugation at top speed in a microfuge (approximately $14,000 \times g$) for 10 min at 4 °C. Transfer the supernatant to fresh microfuge tube and repeat the sonication in **step 6**. In our hands, the repeated sonication step produced a more reproducible fragment size.
8. Once again, pellet the cell debris by centrifugation at top speed in microfuge (approximately $14,000 \times g$) for 10 min at 4 °C. Remove the supernatant (approximately 450 μ L) containing the fragmented chromatin to a fresh microfuge tube.

3.2.3 Quality Control of the Chromatin and Isolation of the Input DNA Sample

Before you proceed with the rest of the protocol, carry out the following quality control steps to ensure that the chromatin has been correctly fragmented.

1. To test the efficiency of fragmentation, run a small sample of the sheared chromatin on an agarose gel. Mix 10 μ L of each chromatin sample with 1 μ L of $10\times$ gel loading dye and 0.5 μ L of 10 μ g/ μ L RNase A solution, and run on a 1% (w/v) agarose

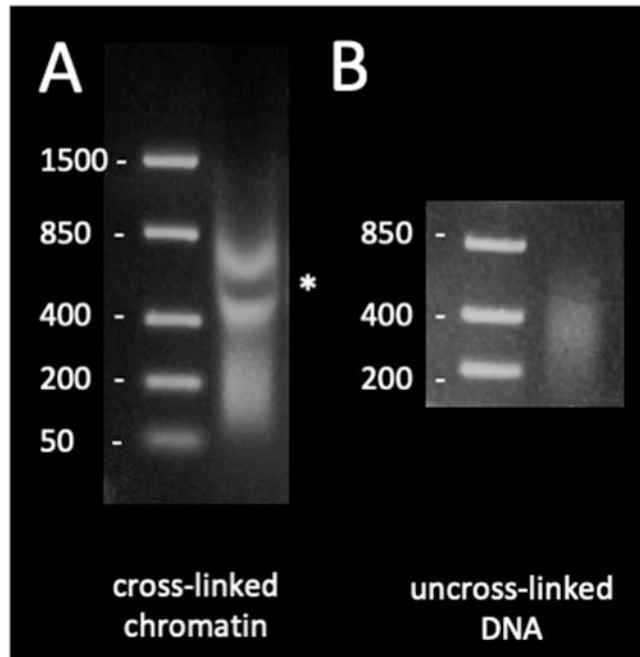


Fig. 2 Verification of chromatin fragmentation. To ensure that the sonication has produced fragments of the required size, samples are analyzed by agarose gel electrophoresis. **(a)** Before reversal of cross-links, chromatin fragments should run as a smear between 100 and 1000 bp, with the majority of fragments concentrated between 400 and 850 bp. Chlorophyll present in the chromatin sample may partially mask the smear, as indicated by *. **(b)** After protease treatment, reversal of cross-links, and purification, DNA fragments should appear as a smear between 200 and 400 bp

gel alongside a suitable DNA ladder. The chromatin should run as a distinct smear between 100 bp and 1 kb (Fig. 2a). Note that at this stage, the DNA is still cross-linked and that the chromatin smear will run at a higher molecular weight than the actual DNA fragments. It may also be partially masked due to contamination by chlorophyll, as indicated by * in Fig. 2a.

2. If the chromatin has been suitably fragmented, set aside at this stage to be used as “input DNA” control. Remove about 10% (50 μ L) of the chromatin and place in a separate microfuge tube. Add 50 μ L of sterile ddH₂O to this DNA sample to give a final volume of 100 μ L.
3. Reverse the cross-links and purify the input DNA as described either in Sect. 3.2.6 or 3.2.7, depending on whether the DNA is to be analysed via sequencing or PCR).
4. Optional: To determine the actual size range of the fragmented DNA, mix 10 μ L of purified input DNA with 1 μ L of 10 \times gel loading dye, and run on a 1% (w/v) agarose gel alongside a

suitable DNA ladder. The purified DNA should now run as a smear between 50 and 400 bp, with most DNA between 200 and 400 bp (Fig. 2b).

5. The input DNA sample and the remaining isolated chromatin can be stored at -80°C until used in immunoprecipitations and downstream analyses.

3.2.4 Immuno-precipitation (Day 1)

Immunoprecipitations are carried out over 2 consecutive days. We use magnetic beads because we find that it speeds up the process and minimizes contamination of samples. All steps must be carried out at 4°C , using pre-chilled solutions.

1. For each immunoprecipitation, transfer 190 μL of chromatin to a 2 mL centrifuge tube. This corresponds to approximately 25 μg of chromatin obtained from *Arabidopsis* seedlings according to this protocol. If a larger volume of chromatin is needed, use 50 mL tubes.
2. Dilute the sample tenfold with ChIP Dilution Buffer (*see Note 1*).
3. In order to remove any proteins from the sample that might bind nonspecifically to the Protein A beads, add 50 μL of beads pre-equilibrated in ChIP Dilution Buffer and incubate the tubes on a rotating mixer wheel at 4°C for 1 h.
4. Place the tubes in a magnetic separation rack to pellet beads, and transfer each pre-cleared chromatin sample to a fresh 2 mL tube.
5. Add the desired antibody (*see Note 8*) then incubate overnight (16 h) on a rotating mixer wheel at 4°C .

3.2.5 Immuno-precipitation (Day 2)

All steps must be carried out at 4°C and using pre-chilled solutions.

1. Add 50 μL of pre-equilibrated Protein A beads to each tube from step 28, and incubate on a rotating mixer wheel for 2–4 h at 4°C (*see Note 9*).
2. Pellet the beads with the magnet and remove the supernatant.
3. Recover the beads in 1 mL of ice-cold Low Salt Wash Buffer and transfer to a microfuge tube. Incubate the tube on a rotating mixer wheel at 4°C for 5 min. Apply the magnet and remove the supernatant.
4. Repeat this wash step four times with 1 mL of High Salt Wash Buffer.
5. Repeat this wash step with 1 mL of LiCl Wash Buffer (*see Note 10*).
6. Repeat this wash step twice with 1 mL of TE buffer.
7. After this final wash, recover the beads in 100 μL of TE buffer.

3.2.6 Reversal of Cross-Links and DNA Purification

This step must be carried out with both the immunoprecipitated samples from step 32 and with input DNA samples from step 17.

1. Add 1 μL of 10 $\mu\text{g}/\mu\text{L}$ RNase A solution to the sample and incubate at 37 °C for 20 min.
2. Add 5 μL of 10% SDS and 1 μL of $\mu\text{g}/\mu\text{L}$ proteinase K solution, and incubate for 2 h at 50 °C.
3. Add 8 μL of 5 M NaCl to the sample and incubate overnight at 65 °C.
4. Pellet the beads with the magnet, and retain the supernatant which contains the enriched DNA.
5. Purify and concentrate the DNA using the MinElute PCR Purification Kit (QIAGEN), as described in step 22.
6. Quantify the purified DNA as in step 23. Note that depending on the number of genome-wide targets for your transcription factor, the amount of DNA recovered may be too low for quantification. There may however be sufficient material for downstream analyses. Store at -80 °C or use directly in quantitative PCR analyses (*see* **Note 11**).

3.2.7 Alternative Protocol: Chelex Method

The following procedure replaces steps 33–38 and uses Chelex resin to purify DNA from samples. Chelex binds ions that are required for the action of nucleases and protects the DNA during boiling steps used to reverse cross-links [15]. This method saves time in the final stages of sample preparation and significantly improves DNA yield. However, it can only be used when ChIP samples are to be analyzed by PCR methods, because it produces single-stranded DNA which is not suitable for the linker addition step in ChIP-seq library construction.

1. Following step 17 or 32, add 100 μL of 10% Chelex resin to the input DNA sample, and vortex. Alternatively, following step 34, remove the residual TE and add 100 μL of 10% Chelex resin to washed protein A bead, and vortex.
2. Incubate at 100 °C for 10 min to reverse protein-DNA cross-links, then allow to cool to room temperature.
3. Optional: Add 1 μL of 20 mg/mL of Proteinase K and incubate 30 min at 50 °C. This step may improve recovery of DNA but in most cases is not essential.
4. Incubate at 100 °C for 10 min.
5. Centrifuge for 5 min at full speed, at room temperature. Collect the supernatant into a new tube.
6. Add 100 μL of TE to the pellet, vortex, and centrifuge again. Collect and combine both supernatants into a single tube. This elute is used directly in PCR reactions.

3.3 Downstream Analyses

3.3.1 Quantitative PCR

A successful ChIP procedure should result in specific enrichment for target sequences compared to control, non-target sequences (Fig. 3). This can be tested using quantitative, real-time PCR. Primers are designed to amplify 100–150 bp regions surrounding the sequences of interest. These primers are then used to quantify the abundance of the sequences in ChIP samples relative to input DNA samples.

This is calculated as follows:

$$\text{Relative abundance (\%of input)} = 100 * df * 2^{(CT_{\text{input}} - CT_{\text{ChIP}})}$$

where CT_{input} and CT_{ChIP} are the mean threshold cycles in real-time PCR reactions for input and ChIP samples and df corresponds to the dilution factor for the input DNA sample relative to the ChIP sample. Here, 50 μL of the chromatin was used towards the input DNA sample, and this was combined with 50 μL prior to reversal of cross-links and purification, so $df = 2$.

Additional controls should be performed to ensure the specificity of the assay.

1. When carrying ChIP experiments using antibodies to the endogenous protein, ChIP analyses should be carried out from knockout mutants lacking the protein of interest. This should reveal no significant enrichment for target sequences compared to control sequences (Fig. 3a).
2. When carrying ChIP experiments using antibodies to an epitope-tag, ChIP analyses should be carried out from plants lacking the transgene. This should reveal no significant enrichment for target sequences compared to control sequences (Fig. 3b).

3.3.2 High-Throughput Sequencing

High-throughput sequencing of ChIP samples allows mapping of genome-wide binding sites for proteins of interest. Binding sites for a given protein are identified as peaks of enriched sequence reads relative to a control sample (either an input DNA, a mock ChIP, or a no antibody sample). We won't describe the library preparation and sequencing steps here, as these stages of experiments are commonly outsourced to external services. Illumina sequencing is currently the most appropriate for doing ChIP-seq, because this method generates very high numbers of relatively short read. Single end, 36–100 bp reads are typically used in ChIP-seq experiments, and 50 bp single-end reads are sufficient for accurate mapping to the *Arabidopsis* genome.

The specific sequencing platform depends on the depth of sequence required and on whether samples will be analyzed in multiplex. The sensitivity of the technique for binding site identification increases with sequencing depth. A minimum of ten million reads per sample is recommended for mammalian transcription

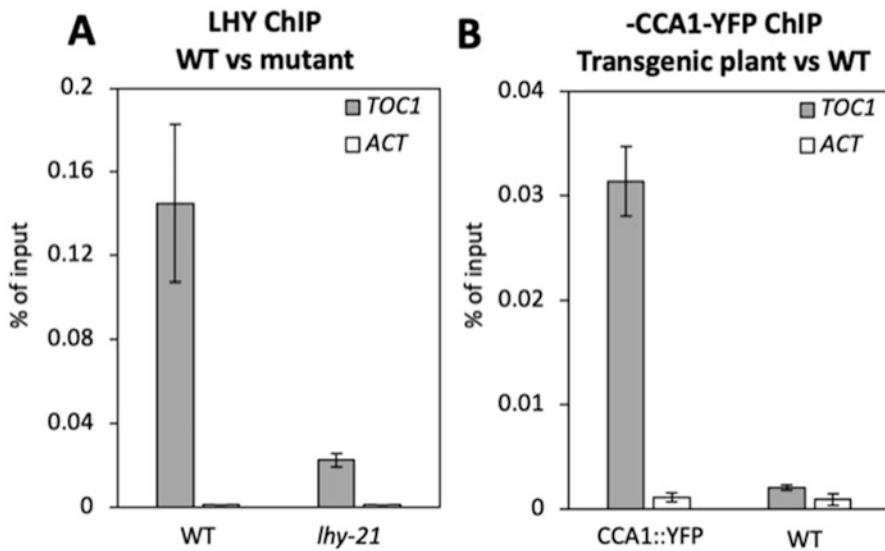


Fig. 3 Quality assessment of ChIP samples by quantitative PCR. In (a) ChIP was carried out using an antibody to the LHY protein. Enrichment for the known target *TOC1* relative to the control locus, *ACTIN* (*ACT*), in wild-type (WT) samples indicates successful immunoprecipitation. The lack of significant enrichment in the knockout mutant, *lhy-21*, demonstrates the specificity of the assay. In (b) binding of the CCA1 protein to the *TOC1* promoter was tested in transgenic plants expressing a CCA1-YFP fusion. ChIP was carried out using an antibody to YFP. Enrichment for *TOC1* sequences relative to the control locus, *ACTIN* (*ACT*), in CCA1:YFP samples indicates successful immunoprecipitation. The lack of significant enrichment in plants lacking the transgene demonstrates the specificity of the assay

factors, but this may be reduced to five million reads for smaller genomes [12]. The sequencing depth required will also be greater when investigating genome-wide binding sites for proteins that have larger numbers of binding sites. A pilot sequencing experiment may be required to evaluate the sequencing depth required for your specific experiments.

One major challenge is to obtain sufficient material for library preparation. It is generally recommended to use 50 ng of DNA as starting material, but this is often not possible when working with transcription factors. We found that quantitative PCR analysis of known binding target was a good test of whether samples contained sufficient target DNA for downstream sequencing analyses. For each library preparation, we routinely pooled five samples that contained undetectable amounts of DNA but amplified with a critical threshold (CT) value of less than 30.

Downstream analyses have been described in detail elsewhere [16]. For those who lack bioinformatics expertise, open-source web-based platforms such as Galaxy (<https://usegalaxy.org>) or CyVerse (<https://cyverse.org>) offer tutorials and established workflows with user-friendly graphical user interfaces that put these complex analyses within the reach of every biologist.

4 Notes

1. 2 β -mercaptoethanol, PMSF, and protease inhibitors must be added to the buffer immediately before use.
2. Beads may be pelleted by centrifugation if non-magnetic beads are used or if a magnetic system is not available.
3. While some protocols recommend blocking the beads with salmon sperm DNA, we found that this could cause issues in ChIP-seq experiments due to potential contamination of DNA sequences; therefore, we omitted a blocking step.
4. This is necessary in order for air to be allowed to escape during the vacuum infiltration step.
5. Formaldehyde causes skin, eye, and respiratory irritation. It is a sensitizing agent that can trigger an allergic reaction in normal tissue after single or repeated exposures. It is also classified as a known human carcinogen. Formaldehyde solutions should be disposed of as chemical hazardous waste only and not down the drain. Empty formaldehyde bottles or containers should not be discarded into biohazardous waste containers or broken glass boxes.
6. Conditions for optimal sonication will need to be optimized for your sample volume and/or equipment used. Optimal sonication conditions will generate chromatin in which 60–90% of the chromatin fragments are smaller than 400 bp. Over-sonication must be avoided because it can result in reduction or loss of signal due to harsh treatment of the chromatin.
7. In order to avoid formation of foam during sonication, do not allow the sonicator tip to touch the bottom or side of the microfuge tube. Foaming will reduce sonication efficiency.
8. The optimal concentration of antibody will need to be determined. The amount of antibody required per ChIP typically ranges from 1 to 10 μ g of antibody for every 25 μ g of chromatin. In order to determine the optimum concentration, perform a ChIP experiment using a range of antibody concentrations.
9. The incubation period should be optimized for each antibody. A longer incubation may result in better enrichment.
10. It is worth testing different washing conditions. The stringency of the last wash can be varied from 250 to 500 mM salt (usually NaCl or LiCl).
11. If carrying out PCR analyses of ChIP samples within a few days of preparation, do not freeze the precipitated DNA and store at 4 °C instead. This will avoid precipitation and poor

performance in PCR reactions. If DNA samples have been frozen, incubation at 37 °C for 30 min will result in improved PCR amplification. An alternative method is quantification relative to a mock ChIP sample. However, in our experience, insufficient DNA is recovered from such samples for accurate quantification.

Acknowledgment

This work was supported by BBSRC grant BB/F022832/1 to IAC.

References

1. Park PJ (2009) ChIP-seq: advantages and challenges of a maturing technology. *Nat Rev Genet* 10:669–680
2. Huang W, Pérez-García P, Pokhilko A, Millar AJ, Antoshechkin I, Riechmann JL, Mas P (2012) Mapping the core of the Arabidopsis circadian clock defines the network structure of the oscillator. *Science* 336:75–79
3. Adams S, Grundy J, Veflingstad SR, Dyer NP, Hannah MA, Ott S, Carré IA (2018) Circadian control of abscisic acid biosynthesis and signaling pathways revealed by genome-wide analysis of LHY binding targets. *New Phytol* 220:893–907
4. Bannister AJ, Kouzarides T (2011) Regulation of chromatin by histone modifications. *Cell Res* 21:381–395
5. Koike N, Yoo S-H, Huang H-C, Kumar V, Lee C, Kim T-K, Takahashi JS (2012) Transcriptional architecture and chromatin landscape of the core circadian clock in mammals. *Science* 338:349–354
6. Perales M, Mas P (2007) A functional link between rhythmic changes in chromatin structure and the Arabidopsis biological clock. *Plant Cell* 19:2111–2123
7. Hemmes H, Henriques R, Jang I-C, Kim S, Chua N-H (2012) Circadian clock regulates dynamic chromatin modifications associated with Arabidopsis CCA1/LHY and TOC1 transcriptional rhythms. *Plant Cell Physiol* 53:2016–2029
8. Song H-R, Noh Y-S (2012) Rhythmic oscillation of histone acetylation and methylation at the Arabidopsis central clock loci. *Mol Cell* 34:279–287
9. Malapeira J, Khaitova LC, Más P (2012) Ordered changes in histone modifications at the core of the Arabidopsis circadian clock. *Proc Natl Acad Sci U S A* 109:21540–21545
10. Baerenfaller K, Shu H, Hirsch-Hoffmann M, Fütterer J, Opitz L, Rehrauer H, Hennig L, Gruissem W (2016) Diurnal changes in the histone H3 signature H3K9ac|H3K27ac|H3S28p are associated with diurnal gene expression in Arabidopsis. *Plant Cell Environ* 39:2557–2569
11. Adams S, Manfield I, Stockley P, Carré IA (2015) Revised morning loops of the Arabidopsis circadian clock based on analyses of direct regulatory interactions. *PLoS One* 10:e0143943
12. Landt SG, Marinov GK, Kundaje A, Kheradpour P, Pauli F, Batzoglou S, Bernstein BE, Bickel P, Brown JB, Cayting P, Chen Y, DeSalvo G, Epstein C, Fisher-Aylor KI, Euskirchen G, Gerstein M, Gertz J, Hartemink AJ, Hoffman MM, Iyer VR, Jung YL, Karmakar S, Kellis M, Kharchenko PV, Li Q, Liu T, Liu XS, Ma L, Milosavljevic A, Myers RM, Park PJ, Pazin MJ, Perry MD, Raha D, Reddy TE, Rozowsky J, Shores N, Sidow A, Slattery M, Stamatoyannopoulos JA, Tolstorukov MY, White KP, Xi S, Farnham PJ, Lieb JD, Wold BJ, Snyder M (2012) ChIP-seq guidelines and practices of the ENCODE and modENCODE consortia. *Genome Res* 22:1813–1831
13. Gendrel A-V, Lippman Z, Yordan C, Colot V, Martienssem RA (2002) Dependence on heterochromatic Histone H3 methylation patterns on the Arabidopsis gene *DDMI*. *Science* 297:1871–1873
14. O’Neill LP, Turner BM (2003) Immunoprecipitation of native chromatin: NChIP. *Methods* 31:76–82

15. Nelson JD, Denisenko O, Bomszyk K (2006) Protocol for the fast chromatin immunoprecipitation (ChIP) method. *Nat Protoc* 1:179–185
16. Bailey T, Krajewski P, Ladunga I, Lefebvre C, Li Q, Liu T, Madrigal P, Taslim C, Zhang J (2013) Practical guidelines for the comprehensive analysis of ChIP-seq data. *PLoS Comput Biol* 9:e1003326



A High-Throughput 3'-Tag RNA Sequencing for Large-Scale Time-Series Transcriptome Studies

Xiaoyu Weng and Thomas E. Juenger

Abstract

RNA sequencing (RNA-seq) has proven invaluable for exploring gene expression variation under complex environmental cues. However, the cost of standard RNA-seq (e.g., Illumina TruSeq or NEBNext) remains a barrier for high-throughput applications. 3'-Tag RNA-seq (3'-TagSeq) is a cost-effective solution that permits large-scale experiments. Unlike standard RNA-seq, which generates sequencing libraries for full-length mRNAs, 3'-TagSeq only generates a single fragment from the 3' end of each transcript (a tag read) and quantifies gene expression by tag abundance. Consequently, 3'-TagSeq requires lower sequencing depth (~5 million reads per sample) than standard RNA-seq (~30 million reads per sample), which reduces costs and allows increased technical and biological replication in experiments. Because 3'-TagSeq is considerably cheaper than standard RNA-seq while exhibiting comparable accuracy and reproducibility, researchers focusing on gene expression levels in large or extensive time-series experiments might find 3'-TagSeq to be superior to standard RNA-seq. In this chapter, we describe 3'-TagSeq sequencing library preparation and provide example bioinformatics and statistical analyses of gene expression data.

Keywords 3'-TagSeq, Gene expression variation, Large-scale experiments

1 Introduction

Plants optimize their growth and development in response to complex environmental signals by fine-tuning gene expression. For example, a wide range of environmental signaling pathways are organized in a temporal manner through rhythmic regulation of gene expression, leading to a tight link between most physiological and biochemical events and the circadian clock [1, 2]. Time series of gene expression are thus essential to fully understand these environmental signaling pathways and their roles in developmental and adaptive environmental responses [3, 4].

Quantifying gene expression profiles with high-throughput RNA-sequencing (RNA-seq) has become indispensable to investigate the genomic function and regulatory mechanism in response

to various environmental cues [5, 6]. Given the importance of the circadian rhythm in regulating other responses, most recent transcriptome studies have incorporated time-series designs to improve our understanding of complex sensing and signaling processes [7, 8]. The standard RNA-seq approach sequences whole mRNA regions and requires a high read depth (~30 million reads per sample) for high-quality differential gene expression (DGE) analysis. This read depth limits researchers to a maximum of eight samples per lane (Illumina HiSeq 2500 platform) and has forced many studies to simplify the experimental design with limited sampling times, tissues, and experimental sizes. Given the high cost of library construction and sequencing depth requirements, the standard RNA-seq approach is often cost-prohibitive for large-scale experiments involving extensive sampling times or large number of replications.

To overcome these limitations, several cost-effective 3'-Tag RNA-seq (3'-TagSeq) techniques have been developed for researchers who focus on large-scale gene-level expression studies [9–12]. By focusing on the 3' end of transcripts, 3'-TagSeq usually requires fewer reads (~5 million reads per sample) for reliable DGE analysis, which reduces costs and allows many more libraries (~36 samples per lane on Illumina HiSeq 2500 platform) to be multiplexed for sequencing. This approach can be as sensitive as, or provide even more accurate measure of transcript abundance than commercially available standard RNA-seq kits, especially for moderate to low abundance transcripts [13, 14]. Moreover, data analysis of the 3'-TagSeq is also simplified because exon junction detection and the normalization of reads to gene length are not required. Hence, 3'-TagSeq is emerging as a compelling option for the transcriptome studies that require extensive time-series samplings and large biological replications.

In this chapter, we introduce complete 3'-TagSeq workflows with a recent example of a study exploring photoperiod responsive genes in *Panicum hallii* [15]. This 3'-TagSeq developed by Meyer et al. [9] has been successfully used for the transcriptome study in many species [15–19]. Our workflows contain both wet lab and computational aspects (Fig. 1). In the wet lab protocol, we start with sample collection and RNA extraction, followed by total RNA fragmentation, cDNA synthesis, and preparation of a barcoded sequencing library. In the computational pipelines, we provide bioinformatic and statistical code for quality control, read filtering, mapping and counting, and statistical modeling of significant changes in the gene expression level. Our workflows can be also applied to differential gene expression analysis in other kinds of treatments or genotype variation across multiple sampling times.

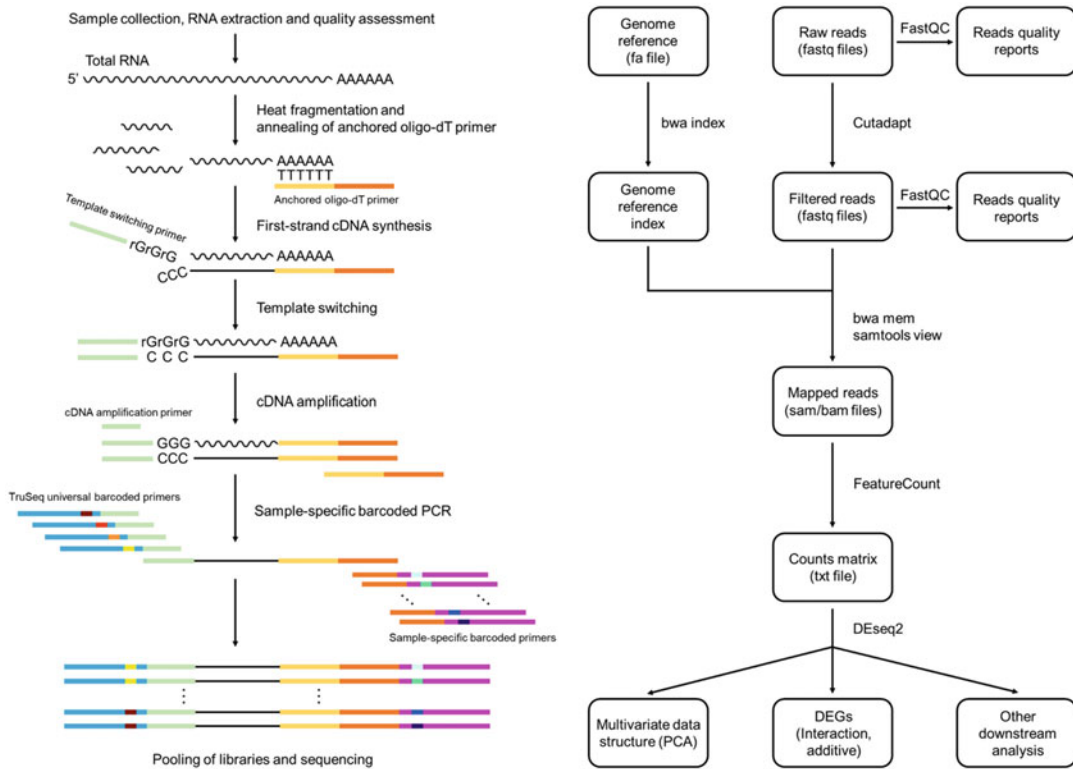


Fig. 1 Overview of 3'-TagSeq library preparation (left) and analysis pipeline (right)

2 Materials

2.1 Sampling of Plant Material and Grinding Tissues

1. Liquid nitrogen.
2. Ice pan.
3. 2.0 mL premium microcentrifuge tubes (Fisherbrand).
4. 3 mm steel beads.
5. Geno/Grinder 2000 (SPEX SamplePrep).
6. 96-well microcentrifuge tube rack.

2.2 RNA Extraction and Quality Assessment

1. TRIzol (Invitrogen).
2. 1.5 mL RNase-free tube.
3. Chloroform:Isoamyl alcohol 24:1 (Sigma).
4. Isopropanol.
5. Ethanol (EtOH).
6. 7.5 M ammonium acetate (Sigma).
7. 10× DNase buffer (Invitrogen).
8. DNaseI (Invitrogen).

9. Nuclease-free water.
10. Centrifuge.
11. Agarose powder (Molecular Biology Grade).
12. 1 × TAE buffer.
13. Gel documentation system.
14. Electrophoresis chamber and power supplier.
15. HydraGreen Safe DNA Dye.
16. NanoDrop (Thermo Scientific).
17. Bioanalyzer (Agilent).

2.3 Library Preparation

1. Anchored oligo dT primer (3ILL-30TV):
ACGTGTGCTCTTCCGATC-
TAATTTTTTTTTTTTTTTTTTTTTTTTTTTTTTTTTT.
2. Template switch primer (S-ILL-swMW) (*see Note 1*):
ACCCCATGGGGCTACACGACGCTCTTCC-
GATCTNNMWGGG.
3. cDNA amplification primer (5ILL):
CTACACGACGCTCTTCCGATCT.
4. TruSeq universal barcoded primers (i5-BC) (*see Note 2*):
AATGATACGGCGACCACCGAGATCTACAC
NNNNNN AACTCTTCCCTACACGACGCTCTTCC
GATCT.
5. Sample-specific barcoded primers (i7-BC) (*see Note 3*):
CAAGCAGAAGACGGCATAACGAGAT NNNNNNGTG
ACTGGAGTTCAGACGTGTGCTCTTCCGAT.
6. Barcode-specific primers:
i5: AATGATACGGCGACCACCGA.
i7: CAAGCAGAAGACGGCATAACGA.
7. Thermocycler.
8. 0.2 mL PCR-microtubes.
9. 10 mM dNTP mix.
10. 100 bp DNA ladder.
11. Titanium Taq polymerase (Clontech).
12. DTT (Invitrogen).
13. 5 × First Strand buffer (Invitrogen).
14. SMARTScribe Reverse Transcriptase (Clontech).
15. NucleoFast PCR Clean-up plates (MACHEREY-NAGEL).
16. Qubit dsDNA High Sensitivity Assay kit (Invitrogen).
17. PureLink Quick Gel Extraction and PCR Purification Combo kit (Invitrogen).

2.4 Analysis of 3-TagSeq Data

To perform Tag-seq data analysis, a laptop or computer with windows/Mac/UNIX operating system is required (minimum 8G RAM). Bioinformatic analysis is implemented using the Linux system (Ubuntu for windows/Mac users) and leverages conda environments. Software required for bioinformatic and statistical analyses are listed in below. The instruction on how to download and install these packages can be found via the provided URLs.

1. Miniconda3 (<https://docs.conda.io/en/latest/miniconda.html>).
2. FastQC (<https://www.bioinformatics.babraham.ac.uk/projects/fastqc/>).
3. Cutadapt (<https://cutadapt.readthedocs.io/en/stable/>).
4. BWA (<http://bio-bwa.sourceforge.net/index.shtml>).
5. Samtools (<http://www.htslib.org/>).
6. featureCounts (<http://subread.sourceforge.net/>).
7. R version 3.5.0 or higher (<https://www.r-project.org>).
8. RStudio version 1.1.463 or higher (<https://rstudio.com/>).
9. DESeq2 (<https://bioconductor.org/packages/release/bioc/html/DESeq2.html>).
10. edgeR (<https://www.bioconductor.org/packages/release/bioc/html/edgeR.html>).
11. ggplot2 (<https://cran.r-project.org/web/packages/ggplot2/index.html>).
12. tidyverse (<https://www.tidyverse.org/>).

3 Methods

3.1 Sampling of Plant Material

1. Add three steel beads to each 2.0 mL premium microcentrifuge tube and fill a Dewar flask with liquid nitrogen.
2. Cut the leaf tissue into ~1 cm pieces (*see Note 4*), transfer 4–6 pieces into the tube, and immediately shock-freeze in liquid nitrogen. Do not allow the tissue to thaw. Any thawing after initial freezing will lead to RNA degradation.
3. Either proceed to grind immediately or store tissue at -80°C for up to 6 months.

3.2 Grinding

1. Set up the ice pan with clean liquid nitrogen and place the 96-well microcentrifuge tube rack into the liquid nitrogen in the ice pan to deep freeze it.
2. Quickly transfer the 2.0 mL tubes to the 96-well microcentrifuge tube rack (Fig. 2).

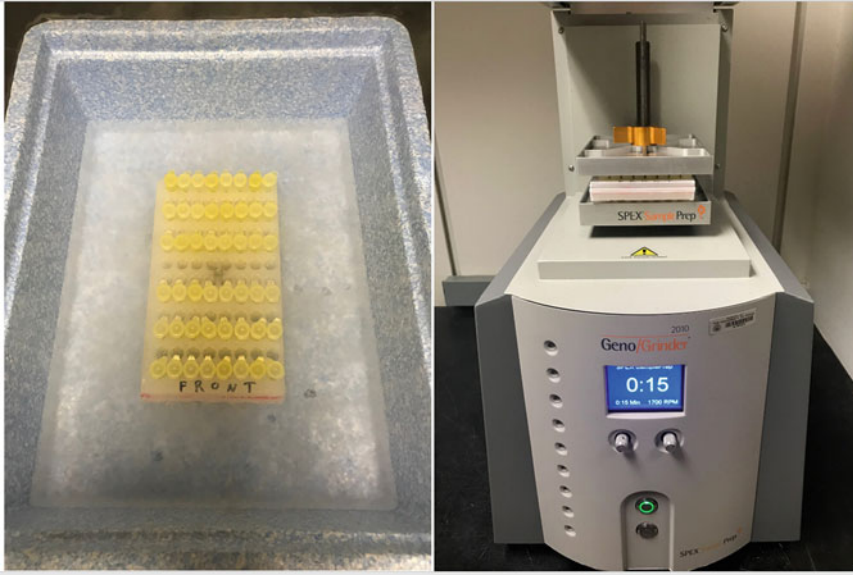


Fig. 2 Deep freeze the tissues and rack into the liquid nitrogen (left) and homogenize the tissues with Geno/Grinder 2000 (right)

3. Homogenize the tissues at 1700 spm (strokes per minute) for 15 s with Geno/Grinder 2000 (or similar bead beater) to a fine powder (Fig. 2).
4. Store tubes with tissue powder at -80°C or proceed immediately to RNA extraction.

3.3 RNA Extraction

Here we describe a standard RNA extraction using TRIzol (Invitrogen) protocol, but alternatives are available. This protocol usually allows the isolation of about 20–40 μg of total RNA from 100 to 200 mg of *P. ballii* leaves. These yields are usually sufficient to perform required RNA quality controls and to prepare libraries for 3'-TagSeq.

1. Add 1 mL of TRIzol reagent to the homogenized tissue powder and vortex immediately (*see Note 5*).
2. Add 200 μL of chloroform:isoamyl alcohol 24:1 and shake vigorously by hand for 1 min.
3. Let the tubes stand at room temperature for 10 min.
4. Centrifuge at $14,000 \times g$ for 10 min at 4°C to allow phase separation.
5. Carefully transfer 600 μL of the upper aqueous phase to a new tube. Ensure no interface debris is transferred.
6. Add 400 μL isopropanol and invert 3–4 times to mix well.
7. Centrifuge at $14,000 \times g$ for 15 min at 4°C . Carefully discard supernatant to obtain white RNA pellets.

8. Add 500 μL 75% EtOH and invert the tube to float the pellet. Centrifuge again at $14,000 \times g$ for 5 min at 4°C .
9. Discard the supernatant. Centrifuge again briefly and pipette off the residual supernatant.
10. Put the opened tube on the laminar flow bench and allow the pellet to air-dry for 10–20 min. When dry, the pellet will be transparent.
11. Resuspend the RNA in a mix of 26 μL RNase-free water, 3 μL $10\times$ DNase buffer, and 2 units of DNaseI (1 μL). Incubate 30 min at 37°C .
12. Add 70 μL RNase-free water to the $\sim 30 \mu\text{L}$ of RNA, 50 μL of 7.5 M ammonium acetate, and 400 μL 100% EtOH and mix well. Centrifuge at $14,000 \times g$ for 20 min at 4°C and carefully pour off the supernatant.
13. Add 500 μL 75% EtOH and invert the tube to float the pellet. Centrifuge again at $14,000 \times g$ for 5 min at 4°C .
14. Discard the supernatant. Centrifuge again briefly and pipette off the residual supernatant.
15. Dissolve the pellet in 30 μL of RNase-free water and incubate at 55°C for 5 min. RNA is now ready for downstream quantification or storage at -80°C .

3.4 Quality Assessment of RNA

1. Determine the RNA concentration and sample contamination (protein/carbohydrate or ethanol occurrence) using a NanoDrop instrument (<http://www.nanodrop.com/>). The 260/230 nm absorbance represents carbohydrate or ethanol contaminations, and the 260/280 nm represents protein contamination. Clean RNA ranges above 1.8–2.0 in both ratios. Values of the 260/230 and 260/280 nm ratios below 1.6 indicate poor quality extraction, and it is not recommended to use this material for library preparation and subsequent sequencing.
2. Load 1 μg of RNA on an agarose gel (or Bioanalyzer machine, Agilent) to test the integrity of the RNA (*see Note 6*). The RNA should show clear sharp bands of 28S and 18S after agarose gel electrophoresis; 23S and 16S RNA bands can be seen clearly in leaf RNA extract (Fig. 3).

3.5 Library Preparation

3.5.1 RNA Fragmentation

The first step in 3'-TagSeq workflows is to fragment total RNA to an appropriate size range prior to reverse transcription. To avoid poly-A contamination, 3'-TagSeq library insert should be slightly larger than 300 bp.

1. Total RNA (1 μg) from each sample is mixed with anchored oligo dT primer (3ILL-30TV) and RNase-free water to a 10 μL final volume in PCR tubes as follows:

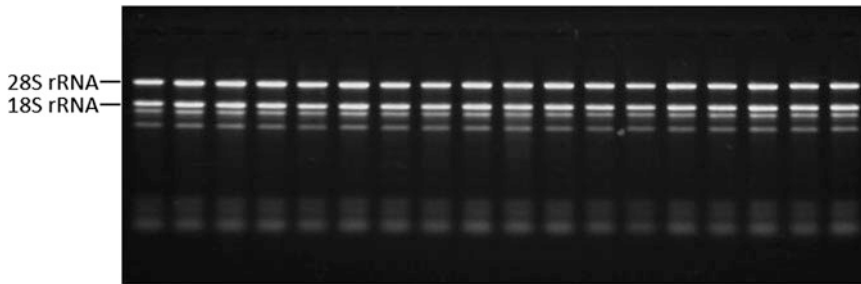


Fig. 3 Agarose gel electrophoresis of total RNA isolated. Each lane contains 1 μg of total RNA from *P. hallii* leaves

Total RNA	1 μg
10 μM 3ILL-30TV	1 μL
Add RNase-free water to	10 μL

- Incubate PCR tubes in a thermocycler at 95 $^{\circ}\text{C}$ for 12 min to fragment RNA to a desired size range (300–600 bp) and immediately cool on ice to terminate the fragmentation and denature the anchored oligo dT primer (Fig. 4) (*see Note 7*).

3.5.2 First-Strand cDNA (FS-cDNA) Synthesis

Reverse transcribe fragmented RNA with a denatured anchored oligo dT primer, which is complementary to the 3' end poly-A tail of the mRNA, to direct the synthesis of the FS-cDNA. The template switch primer (S-ILL-swMW) will hybridize to untemplated C nucleotides at the 5' end of full-length cDNA during reverse transcription.

- Prepare cDNA synthesis mix as follows:

10 mM dNTP mix	1 μL
20 mM DTT	2 μL
5 \times First Strand buffer	4 μL
10 μM S-ILL-swMW	1 μL
SMARTScribe Reverse Transcriptase	1 μL
Add RNase-free water to	10 μL

- Add 10 μL of cDNA synthesis mix to above fragmented RNA sample.
- Incubate FS-cDNA synthesis reaction in a thermocycler at 42 $^{\circ}\text{C}$ for 60 min followed by 70 $^{\circ}\text{C}$ incubation for 10 min to inactivate the reverse transcriptase.
- Store FS-cDNA on ice or at -20°C until ready to proceed to the next step.

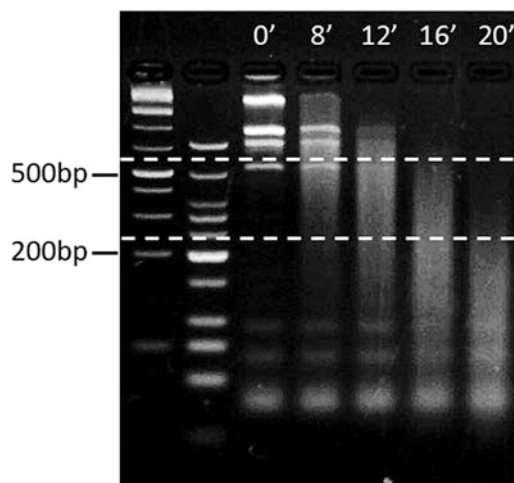


Fig. 4 Optimization of fragmentation times for 3'-TagSeq analysis of *P. hallii* total RNA. The appropriate size range should be 300–600 bp (between two dash lines)

3.5.3 cDNA Amplification

Construction of 3'-TagSeq libraries is accomplished in two rounds of PCR amplification. The first round of cDNA amplification is performed using primers 5ILL and 3ILL-30TV and FS-cDNA as the template.

1. Assemble the PCR reaction as follows:

FS-cDNA template	10 μ L
10 \times PCR buffer	5 μ L
2.5 mM dNTP mix	5 μ L
10 μ M 5ILL	1 μ L
10 μ M 3ILL-30TV	1 μ L
Titanium Taq polymerase	1 μ L
Add RNase-free water to	50 μ L

2. Perform the PCR reaction in a thermocycler using the following program. Generally, 14–16 cycles yield sufficient production (Fig. 4) (*see Note 8*).

Cycle	Denature	Anneal	Extend	Hold
1	95 $^{\circ}$ C for 5 min	–	–	–
14–16	95 $^{\circ}$ C for 40 s	63 $^{\circ}$ C for 2 min	72 $^{\circ}$ C for 2 min	–
1	–	–	72 $^{\circ}$ C for 3 min	–
1	–	–	–	4 $^{\circ}$ C

3. Confirm the cDNA amplification efficiency by running 5 μL of PCR production in a 1.5% agarose gel. A smear cDNA (300–600 bp) should be faintly visible (Fig. 5).
4. Purify the remaining cDNA (~45 μL) using NucleoFast PCR Clean-up plates (MACHEREY-NAGEL) according to the manufacturer's instructions. Use 30 μL of RNase-free water to elute the cDNA production.
5. Quantify the purified product by Qubit dsDNA High Sensitivity Assay kit (Invitrogen) or PicoGreen assay using microreader.
6. Dilute the purified cDNA amplified production to 5 ng/ μL as the template for the second round of barcoding PCR or store at $-20\text{ }^{\circ}\text{C}$ until ready to proceed to the next step.

3.5.4 Sample-Specific Barcoded PCR

The second round of PCR is performed using unique 3' and 5' barcoded primers and purified cDNA amplified product as the template. Each library to be pooled for sequencing should be amplified with a pair of different barcoded primers. We designed 4 different variations of TruSeq universal barcoded primers at 3' end (i5-BC) and 36 sample-specific barcoded primers at 5' end (i7-BC) (*see* **Notes 2** and **3**). More barcode sequences can be found elsewhere.

1. Individual DNA libraries were re-amplified with 4 PCR cycles using i5-BC and i7-BC as primers and 50 ng of purified cDNA as the template.

Purified cDNA amplified production (5 ng/ μL)	10 μL
10 \times PCR buffer	5 μL
2.5 mM dNTP	5 μL
10 μM i5-BC primer	1 μL
10 μM i7-BC primer	1 μL
Titanium Taq polymerase	1 μL
RNase-free water	27 μL
Total volume	50 μL

2. Perform the PCR reaction with four cycles in a thermocycler using the following program.

Cycle	Denature	Anneal	Extend	Hold
1	95 $^{\circ}\text{C}$ for 5 min	–	–	–
4	95 $^{\circ}\text{C}$ for 40 s	63 $^{\circ}\text{C}$ for 2 min	72 $^{\circ}\text{C}$ for 1 min	–
1	–	–	72 $^{\circ}\text{C}$ for 2 min	–
1	–	–	–	4 $^{\circ}\text{C}$

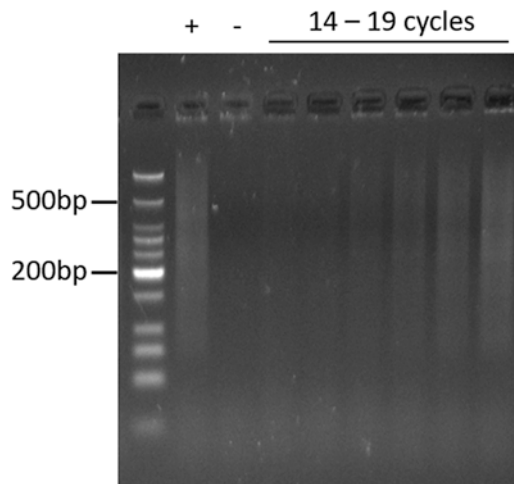


Fig. 5 Optimization of the full-length cDNA amplification

3. Run 5 μL of each PCR production on 1.5% agarose gel to confirm that amplification across all samples was successful and uniform (Fig. 6).

3.5.5 Pool Samples and Size Selection

1. Pool equal volume from each individually barcoded 3'-TagSeq library (*see Note 9*). Purify and concentrate the pools into 60 μL using PureLink Quick Gel Extraction and PCR Purification Combo kit (Invitrogen) according to the manufacturer's instructions.
2. Prepare a 1.5% $1\times$ TAE agarose gel with HydraGreen Safe DNA Dye added (4 μL per 100 mL buffer) and pour in an appropriate gel chamber tray. Add 10 μL of $6\times$ Loading Dye to the 50 μL of sample and load the entire volume onto the gel. We usually use the 100 bp (or 1 kb) DNA ladder as the marker. Then run the gel in $1\times$ TAE buffer at 5 V/cm (i.e., at 100 V if the distance between electrodes is 20 cm) for 70–90 min until marker bands in the 100–500 bp size range are well separated.
3. Use a blue-light gel illuminator to safely cut out the required size range (400–500 bp). Cut only the middle of the lane, and leave the edges (Fig. 7). Turn off the UV light and carefully cut out the marked region, transferring it into a 2 mL premium microcentrifuge tubes.
4. Extract DNA from the gel slice using PureLink Quick Gel Extraction and PCR Purification Combo kit (Invitrogen) according to the manufacturer's instructions.

3.5.6 Quantification for Mixing on the Same HiSeq2500 Lane

Finally, we perform a PCR amplification to confirm the quality and the size selection using barcode-specific primers i5 and i7. Run 5 μL of each PCR production on 1.5% agarose gel. A smear cDNA (300–600 bp) should be faintly visible (Fig. 7). Prepared libraries

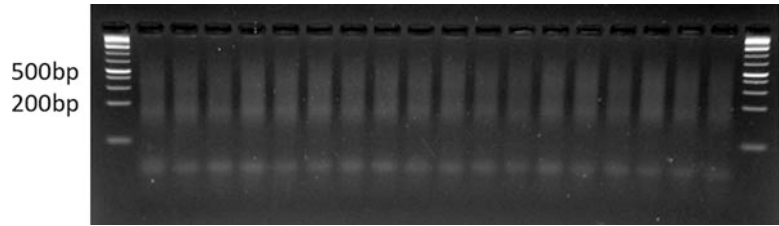


Fig. 6 Sample-specific barcoded PCR

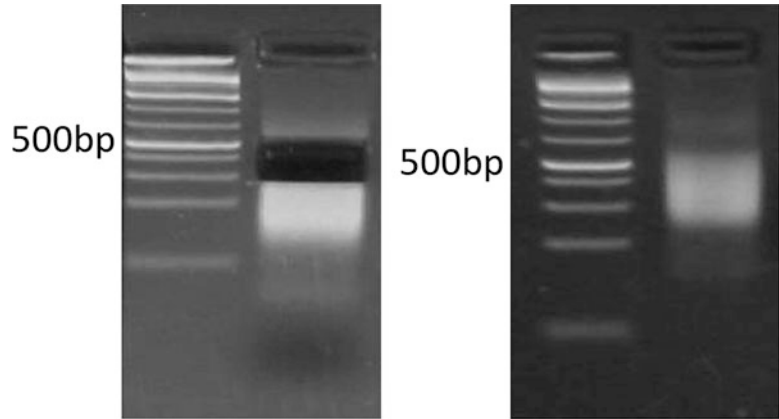


Fig. 7 Gel extraction (left) and quality assessment PCR of library (right)

are ready to run in a single Illumina HiSeq 2500 lane, aiming to obtain at least five million reads per sample (single end, 100 bp) (*see Note 10*).

3.6 Bioinformatics Analysis of 3'- TagSeq Data

The 3'-TagSeq selects molecules using a poly-A capture and utilizes a designed inline adapter on the 5' end of the molecule. We therefore have four steps for bioinformatics analysis: (1) reads quality assessment; (2) reads filtering with poly-A tails and 5' adapter; (3) reads mapping to the assembly reference genome; and (4) counting reads associated with genes.

We apply our recently published data in *Panicum hallii* (*P. hallii*) as an example [15]. These single-end 3'-TagSeq Illumina datasets are available in the Sequence Read Archive (SRA) database with accession number SRP144094, including 36 libraries in the experiment. Before starting the analysis, we create the following folders ordered by number: <01-sra>, <02-fastq>, <03-QC>, <04-filtered-fastq>, <05-reference>, <06-sam>, <07-bam>, and <08-counts>. We assume that all 36 files named from SRR7085479.sra to SRR7085514.sra are stored in the folder <01-sra> and the reference genome sequence file (e.g., Phallii_495_v3.0.fa) and corresponding gene annotation file (e.g., Phallii_495_v3.1.gene.gff3) are stored in the folder <05-reference>.

3.6.1 Data Preparation

Transfer all 36 *.sra files to *.fastq files by using the fasterq-dump tool. You can ignore this step if you already have your own .fastq files.

1. Basic usage:

```
fasterq-dump <path> [options]
```

2. Input: 36 *.sra files named from SRR7085479 to SRR7085514 in the folder <01-sra>.

3. Optional: To make a loop for 36 files

```
for id in `seq 479 514`
do fasterq-dump -p -O 02-fastq/ 01-sra/SRR7085${id}.sra
done
```

The -p tag will show progress. The -O tag stands for output directory.

4. Output: The fasterq-dump will deliver *.fastq files into the folder <02-fastq>.

3.6.2 Read Quality Assessment

Evaluate the quality of raw reads using the FastQC tool.

1. Basic usage:

```
fastqc seqfile1 seqfile2 .. seqfileN
```

2. Input: All 36 *.fastq files from the last step in the folder <02-fastq>.

3. Optional:

```
fastqc -o 03-QC 02-fastq/*.fastq
```

The -o tag stands for output directory.

4. Output: All output files will be created in the folder <03-QC>.

3.6.3 Read Filtering with Poly-A Tails and 5' Adapters

Trim the 5' end adapters and 3' poly-A tails using the Cutadapt tool.

1. Basic usage (for single-end reads):

```
cutadapt -a ADAPTER [options] [-o output.fastq] input.fastq
```

2. Input: All 36 *.fastq files created from Subheading 3.6.1 in the folder <02-fastq>.
3. Optional: To make a loop for 36 files

```
for id in `seq 479 514`
do cutadapt -a "A{15}" -u 8 -m 25 -e .2 02-fastq/SRR7085
${id}.sra.fastq -o 04-filtered-fastq/SRR7085${id}.filtered.
fastq
done
```

The -a tag indicates trimming the sequence of an adapter ligated to the 3' end. Here we searched for a 15-mer poly-A sequence of length. The -u tag indicates removal of bases from the beginning. Here the first eight bases were removed to filter the 5' adapter. The -m tag indicates discard reads shorter than a minimum length. Default is 0, and here sequences of length greater than 25 base pairs were retained. The -e tag stands for maximum allowed error rate as value between 0 and 1. Default is 10% (0.1), and here we allow an error rate of 20% (0.2). The -o tag stands for output directory.

4. Output: All *.filtered.fastq files will be deliver into the folder <04-filtered-fastq>.

Evaluate the quality of filtered reads using the FastQC tool.

1. Input: All 36 *.filtered.fastq files from the last step in the folder <04-filtered-fastq >.
2. Optional:

```
fastqc -o 03-QC 04-filtered-fastq/*.fastq
```

The -o tag stands for output directory.

3. Output: All output files will be created in the folder <03-QC>.

3.6.4 Reference Index Building

Use the index command from BWA tool to generate the genome reference index:

1. Basic usage:

```
bwa <command> [options]
```

2. Input: The genome reference file (Phallii_495_v3.0.fa) in the folder <05-reference>.
3. Optional

```
bwa index 05-reference/Phallii_495_v3.0.fa
```

4. Output: Five reference index files will be generated in the folder <05-reference>, which are Phallii_495_v3.0.fa.amb, Phallii_495_v3.0.fa.ann, Phallii_495_v3.0.fa.bwt, Phallii_495_v3.0.fa.pac, and Phallii_495_v3.0.fa.sa.

3.6.5 Reads Mapping

Align the filtered reads to the *P. ballii* genome using the BWA-mem tool (*see Note 11*).

1. Basic usage:

```
bwa mem [options] <idxbase> <in1.fq>
```

2. Input: All 36 *.filtered.fastq files created from Subheading 3.6.3 in the folder <04-filtered-fastq > and index reference files created from Subheading 3.6.4 in the folder <05-reference>.
3. Optional: To make a loop for 36 files

```
for id in `seq 479 514`
do bwa mem -M -t 4 -o 06-sam/SRR7085${id}.sam
05-reference/Phallii_495_v3.0.fa 04-filtered-fastq/SRR7085
${id}.filtered.fastq
done
```

The -t tag stands for number of threads. Here we set the thread as 4, which can handle by most of laptop. The -o tag indicates .sam file to output results.

4. Output: All *.sam files will be deliver into the folder <06-sam>.

To retain reliable alignments, filter the .sam files by Samtools view and transfer the outputs as .bam files.

1. Basic usage:

```
samtools view [options] <in.bam>
```

2. Input: All 36 *.sam files created from the last step in the folder <06-sam>.
3. Optional: To make a loop for 36 files

```
for id in `seq 479 514`
```

```
do samtools view -b -q 10 -o 07-bam/SRR7085${id}.bam
06-sam/SRR7085${id}.sam
done
```

The `-b` tag stands for output as `.bam` file. The `-q` tag indicates the threshold of reads mapping quality. Here we set as 10 to retain high-quality aligning reads.

4. Output: All `*.bam` files will be deliver into the folder `<07-bam>`.

3.6.6 Reads Counting

Use the `featureCounts` tool to extract read counts information from all `.bam` files.

1. Basic usage:

```
featureCounts [options] -a <annotation_file> -o
<output_file> input_file1 [input_file2] ...
```

2. Input: All 36 `*.bam` files created from the Subheading 3.6.5 in the folder `<07-bam>` and the annotation file (`Phallii_495_v3.1.gene.gff3`) in the folder `<05-reference>`.
3. Optional:

```
featureCounts -a 05-reference/Phallii_495_v3.1.gene.gff3
-t gene -g ID --readExtension5 0 --readExtension3 0 -s 1 -T
4 -primary -o 08-counts/expr_matrix.txt 07-bam/*.bam
```

The `-a` tag stands for the name of the annotation file (GTF/GFF format by default). The `-t` tag stands for specify feature type in GTF/GFF annotation file (“exon” by default but “gene” in *P. ballii* annotation file). The `-g` tag stands for specify attribute type in GTF/GFF annotation file (“gene_id” by default but “ID” in *P. ballii* annotation file). The `-s` tag indicates perform strand-specific read counting. Possible values include 0 (unstranded), 1 (stranded), and 2 (reversely stranded). Default value is 0 but 1 for 3'-TagSeq. The `-T` tag indicates the number of threads, which are setting as 4 here. The `-o` tag indicates the name of output file including read counts. The flag `--readExtension5 <int>` stands for reads are extended upstream by `<int>` bases from their 5' end. The flag `--readExtension3 <int>` stands for reads are extended upstream by `<int>` bases from their 3' end.

4. Output: An `expr_matrix.txt` matrix file including read counts for all genes will be deliver into the folder `<08-counts>`.

3.7 Statistical Analysis of Transcriptome Data

In our example, we have two conditions (long day and short day) and six sampling times in the experiment. For statistical analysis, we use DESeq2 to build factorial linear models and test for differential expressed genes with photoperiod interaction and additive photoperiod effects of day length and sampling time. Here DESeq2 fits a negative binomial model to untransformed transcript counts and conducts statistical testing via likelihood ratio tests. For more information about DESeq2: (<http://bioconductor.org/packages/devel/bioc/vignettes/DESeq2/inst/doc/DESeq2.html>).

1. Package library.

```
library(tidyverse)
library(DESeq2)
library(edgeR)
library(ggplot2)
```

2. Set your working environment in RStudio and import the expression matrix data from the output of Subheading 3.6.6.

```
setwd("~/")
countsdata <- read.table(file = "expr_matrix.txt", header = T, sep = "\t",
                          quote = "", check.names = F)
```

3. Construct count data.

```
countdata <- countsdata[,7:42]
rownames(countdata) <- countsdata[,1]
```

4. Construct coldata.

```
coldata <- colnames(countdata) %>% as.data.frame() %>%
rename(samples = ".") %>%
  separate(samples, c('folder', 'daylength', 'time', 'replicate', "file")) %>%
  rowwise() %>% mutate(id=paste(daylength,time,
replicate, sep = "_")) %>%
  select(id, daylength, time) %>% ungroup() %>%
  mutate_at(vars(matches('daylength|time')), funs
(as.factor)) %>%
  as.data.frame()
```

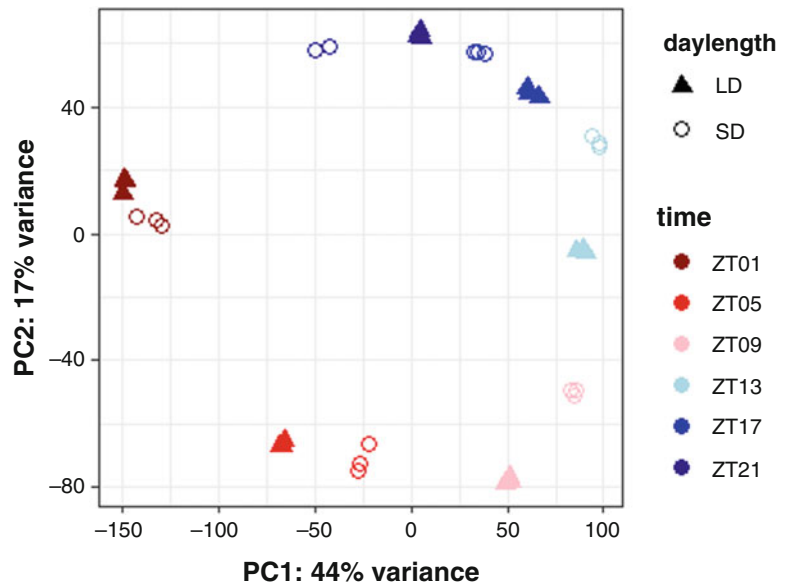


Fig. 8 PCA of 36 samples showing the diurnal signatures and photoperiod effects

5. Construct dds.

```
dds_full = DESeqDataSetFromMatrix(countData = countdata,
                                   colData = coldata,
                                   design = ~ daylength + time +
daylength:time)
```

6. Principal component analysis (PCA) with variance stabilizing transformations (VST) normalized expression counts (Fig. 8). VST normalization for count data.

```
vsd <- vst(dds_full)
```

Principal component plot of samples.

```
pcaData <- plotPCA(vsd, intgroup=c("daylength", "time"),
                   ntop = 37232, returnData=TRUE)
```

Customize the PCA plot using the ggplot function.

```
percentVar <- round(100 * attr(pcaData, "percentVar"))
ggplot(pcaData, aes(PC1, PC2, color = time, shape =
daylength)) +
  geom_point(size = 3) + scale_shape_manual(values = c
```

```
(17,1)) +
  scale_color_manual(values = c("darkred", "red", "pink",
                                "lightblue", "blue", "navyblue"))
+
  xlab(paste0("PC1: ", percentVar[1], "% variance")) +
  ylab(paste0("PC2: ", percentVar[2], "% variance")) +
  theme_bw()
```

7. To determine photoperiod interaction genes, we compare the difference in deviance between the full model (daylength + time + daylength \times time) and an additive reduced model (daylength + time) formula.

```
dds_int = DESeq(dds_full, test='LRT', reduced = ~
daylength + time)
res_int = results(dds_int)
```

Select significant interaction effect DEGs ($q < 0.05$) and save in a csv.file.

```
sum(res_int$padj < 0.05, na.rm=TRUE)
[1] 8462
res_int_sig = subset(res_int, padj < 0.05)
write.csv(res_int_sig, 'diff_gene_int_sig.csv', row.names
= T)
```

8. To determine additive photoperiod effect genes, we compare the difference in deviance between the two-factor additive model (daylength + time) and a reduced model (time) formula.

```
dds_drop = DESeqDataSetFromMatrix(countData = countdata,
                                   colData = coldata,
                                   design = ~ daylength + time)
dds_DL = DESeq(dds_drop, test='LRT', reduced = ~ time)
res_DL = results(dds_DL)
```

Select significant daylength effect DEGs ($q < 0.05$) and save in a csv.file.

```
sum(res_DL$padj < 0.05, na.rm=TRUE)
[1] 1666
res_DL_sig <- subset(res_DL, padj < 0.05)
write.csv(res_DL_sig, 'diff_gene_DL_sig.csv', row.names =
```

T)

9. We can also test the effect across sampling times by comparing the difference in deviance between the two-factor additive model (daylength + time) and a reduced model (daylength) formula.

```
dds_ZT = DESeq(dds_drop, test='LRT', reduced = ~
daylength)
res_ZT = results(dds_ZT)
```

Select significant timing effect DEGs ($q < 0.05$) and save in a csv.file.

```
sum(res_ZT$padj < 0.05, na.rm=TRUE)
[1] 16024
res_ZT_sig <- subset(res_ZT, padj < 0.05)
write.csv(res_ZT_sig, 'diff_gene_ZT_sig.csv', row.names =
T)
```

4 Notes

1. The template switch primer should be stored in multiple aliquots at -80°C to prevent degradation.
2. TruSeq universal barcoded primers are also known as i5 barcoded primers (i5-BC, BC = *NNNNNN*). N's with underline indicate the 6-base index sequence. We designed four different variations of i5 barcode oligo, and their sequences are given in the Table 1. More barcode sequences can be found elsewhere.
3. Sample-specific barcoded primers are also known as i7 barcoded primers (i7-BC, BC = *NNNNNN*). N's with underline indicate the 6-base index sequence. We used 36 different variations of i7 barcode oligo in the *P. hallii* photoperiod experiment. Their sequences given in the Table 2 below are a selection of standard illumine TruSeq barcodes that have the best hamming distance. More barcode sequences can be found elsewhere.
4. This protocol has been mainly optimized for lead tissue but could be applied in different type of tissues.
5. Do not let the ground plant tissue thaw until in the presence of TRIzol.

Table 1
Barcode sequences

ATCACG	ACTTGA	TAGCTT	GGCTAC
--------	--------	--------	--------

Table 2
Standard illumine TruSeq

CGATTA	ATTATA	GAATGA	TCGGGA	CTTCGA	GTGTTT
CCTTCA	CACACC	CTCGCT	AAAGCT	AGACCA	CAAGGG
GCCGGT	ACTTTT	AGATGT	CCACTC	CCGGTG	AACTTC
TCCTGC	TAATAC	ATGTGA	TATAGA	TTTGCA	GTGCCA
CTAACA	AGCATT	TGTGTC	GCCTAA	TCAAGT	GGACGG
TTTCAC	TAGTTG	TCCCTT	GGGTGC	CGCGGC	CACGTA

6. Running RNA on normal agarose gel is usually enough to test the integrity of the RNA in our experiment (Fig. 3). For a better detection sensitivity and accuracy, we recommend to analyze RNA with Agilent 2100 Bioanalyzer (<https://www.agilent.com/>).
7. Prior to working with important experimental samples, we recommend testing a range of different incubation temperatures (e.g., 95 °C or 70 °C) and times (e.g., 8, 12, 16, and 20 minutes) to identify the duration that produces the appropriate size range (300–600 bp) in your samples (Fig. 4).
8. It is important not to over-amplify the cDNA at this step, to avoid artifacts and distortion of expression ratios. We usually see a smear on a gel after 14 cycles. We do not use more than 16 cycles if at all possible. If no smear is detected in control reactions with 17–19 cycles, this indicates a problem with the first-strand cDNA synthesis.
9. Pooling equal amounts of library is important and determines how even the reads are among pooled samples. In this protocol, we quantify and adjust cDNA templates at the beginning of Subheading 3.5.4. This usually produces uniform PCR productions for each library, which then allows pooling by equal volume. If PCR products from each library are not uniform as expect at the end of Subheading 3.5.4, then quantify and adjust PCR products again before pooling. We suggest pooling 32–36 libraries for one lane of HiSeq 2500.
10. The protocol described here is customized for Illumina HiSeq 2500 sequencing platform but could be applied in other Illumina sequencing platforms.

11. In this protocol, we align the reads to *P. hallii* annotated genome sequence. However, researchers could map to different reference resources (e.g., assembled transcriptome) using the same tools. Depending on quality of reference, a buffering of mapping locations could be useful. For example, if the gene model is incorrect in three prime annotations, then reads will not be counted.

References

1. Harmer SL (2009) The circadian system in higher plants. *Annu Rev Plant Biol* 60:357–377
2. Greenham K, McClung CR (2015) Integrating circadian dynamics with physiological processes in plants. *Nat Rev Genet* 16(10):598–610
3. Lopez-Maury L, Marguerat S, Bahler J (2008) Tuning gene expression to changing environments: from rapid responses to evolutionary adaptation. *Nat Rev Genet* 9(8):583–593
4. Doherty CJ, Kay SA (2010) Circadian control of global gene expression patterns. *Annu Rev Genet* 44:419–444
5. Barah P, Naika BNM, Jayavelu ND et al (2016) Transcriptional regulatory networks in *Arabidopsis thaliana* during single and combined stresses. *Nucleic Acids Res* 44:3147–3164
6. Coolen S, Proietti S, Hickman R et al (2016) Transcriptome dynamics of *Arabidopsis* during sequential biotic and abiotic stresses. *Plant J* 86:249–267
7. Wilkins O, Hafemeister C, Plessis A et al (2016) EGRINs (Environmental gene regulatory influence networks) in rice that function in the response to water deficit, high temperature, and agricultural environments. *Plant Cell* 28:2365–2384
8. Calixto CPG, Guo W, James AB et al (2018) Rapid and dynamic alternative splicing impacts the *Arabidopsis* cold response transcriptome. *Plant Cell* 30:1424–1444
9. Meyer E, Aglyamova GV, Matz MV (2011) Profiling gene expression responses of coral larvae (*Acropora millepora*) to elevated temperature and settlement inducers using a novel RNA-Seq procedure. *Mol Ecol* 20:3599–3616
10. Moll P, Ante M, Seitz A et al (2014) QuantSeq 3' mRNA sequencing for RNA quantification. *Nat Methods* 11:972
11. Kremling KAG, Chen SY, Su MH et al (2018) Dysregulation of expression correlates with rare-allele burden and fitness loss in maize. *Nature* 555:520–523
12. Tzfadia O, Bocobza S, Defoort J et al (2018) The 'TranSeq' 3'-end sequencing method for high-throughput transcriptomics and gene space refinement in plant genomes. *Plant J* 96:223–232
13. Lohman BK, Weber JN, Bolnick DI (2016) Evaluation of TagSeq, a reliable low-cost alternative for RNAseq. *Mol Ecol Resour* 16:1315–1321
14. Ma FY, Fuqua BK, Hasin Y et al (2019) A comparison between whole transcript and 3' RNA sequencing methods using Kapa and Lexogen library preparation methods. *BMC Genomics* 20:9
15. Weng XY, Lovell JT, Schwartz SL et al (2019) Complex interactions between day length and diurnal patterns of gene expression drive photoperiodic responses in a perennial C-4 grass. *Plant Cell Environ* 42:2165–2182
16. Des Marais DL, Skillern WD, Juenger TE (2015) Deeply diverged alleles in the *Arabidopsis* AREB1 transcription factor drive genome-wide differences in transcriptional response to the environment. *Mol Biol Evol* 32:956–969
17. Lovell JT, Shakirov EV, Schwartz S et al (2016) Promises and challenges of eco-physiological genomics in the field: tests of drought responses in switchgrass. *Plant Physiol* 172:734–748
18. Gordon SP, Contreras-Moreira B, Woods DP et al (2017) Extensive gene content variation in the *Brachypodium distachyon* pan-genome correlates with population structure. *Nat Commun* 8:2184
19. Razaque S, Haque T, Elias SM et al (2017) Reproductive stage physiological and transcriptional responses to salinity stress in reciprocal populations derived from tolerant (Horkuch) and susceptible (IR29) rice. *Sci Rep* 7:46138



Experimental Design for Time-Series RNA-Seq Analysis of Gene Expression and Alternative Splicing

Nikoleta A. Tzioutziou, Allan B. James, Wenbin Guo,
Cristiane P. G. Calixto, Runxuan Zhang, Hugh G. Nimmo,
and John W. S. Brown

Abstract

RNA-sequencing (RNA-seq) is currently the method of choice for analysis of differential gene expression. To fully exploit the wealth of data generated from genome-wide transcriptomic approaches, the initial design of the experiment is of paramount importance. Biological rhythms in nature are pervasive and are driven by endogenous gene networks collectively known as circadian clocks. Measuring circadian gene expression requires time-course experiments which take into account time-of-day factors influencing variability in expression levels. We describe here an approach for characterizing diurnal changes in expression and alternative splicing for plants undergoing cooling. The method uses inexpensive everyday laboratory equipment and utilizes an RNA-seq application (3D RNA-seq) that can handle complex experimental designs and requires little or no prior bioinformatics expertise.

Keywords Time course, Experimental design, RNA-seq, Data validation, Primer design

1 Introduction

Circadian clocks are the intrinsic and the entrainable time-keeping mechanisms that have evolved in most organisms. For plants, the circadian clock synchronizes external cues (such as light/dark and temperature cycles) with internal physiological processes such as photosynthesis, leaf movement, flowering time, stress responses, hormone synthesis, and metabolism. The circadian clock is composed of complex networks of genes that follow self-sustained rhythmic patterns of expression with a period of approximately 24 h. Characteristically, clock genes, and clock-regulated genes, oscillate—displaying peaks and troughs at different times (or phases) throughout the day. In *Arabidopsis*, the circadian

clock is responsible for daily changes in the transcriptome, affecting the expression of around one third of genes [1–3].

Several factors such as temperature, day length, light intensity, and light quality influence time-keeping by the circadian clock. Designing and conducting circadian time-course experiments therefore require careful planning and a clear vision of the hypothesis. Most of these physical parameters can be controlled by growing plants under strictly defined laboratory conditions (e.g., in environmentally controlled growth cabinets) while appreciating that plants in the wild experience highly fluctuating environmental conditions. Experimental parameters, reproducibility, and overall number of samples will impact downstream handling and analysis and resolution of rhythmic expression by sampling times (e.g., every 3, 4, or 6 h). To exploit the potential of RNA-seq data and minimize the experimental and environmental error, appropriate controls should be used such as non-treated vs. treated, wild-type vs. mutant, and negative and positive controls. Another consideration is randomization of the samples in the growth cabinets due to potential uneven distribution of temperature or light intensity within the growth cabinet. In particular, due to the effect of the circadian clock, gene expression can vary at different times of the day. For time-course experiments, harvesting the same time points (phase) for distinct days with different treatments (e.g., temperature) provides controls for time-of-day variation in expression in the downstream analysis (Fig. 1). This approach has recently been used to identify the very early changes occurring at the level of gene expression and alternative splicing for plants undergoing low-temperature transition [4] (Fig. 1).

Microarrays [5–12] or, more recently, RNA-seq [13–15] have been employed to measure differential expression at the gene level. However, RNA-seq contains additional information on the expression of distinct transcripts allowing analysis of not only gene level differential expression but also differential transcript expression and alternative splicing (AS) [16]. The value of studying gene expression at the individual transcript level has recently been demonstrated [4, 17]. Transcript-specific expression (1) improves the accuracy of gene level expression estimates [18, 19] and (2) identifies changes in AS of genes that can impact protein function or transcript levels and ultimately plant response to environmental signals. AS is highly prevalent in plants with RNA-seq analysis showing that more than 60% of the *Arabidopsis* intron-containing genes code for multiple transcript isoforms [4, 20–22]. Changes in AS are triggered during development and in response to biotic and abiotic stresses [20, 21, 23–26]. Transcript-specific RNA-seq analysis opens up the opportunity to study dynamic changes in the transcriptome to capture different aspects of gene expression both at the transcriptional and post-transcriptional levels.

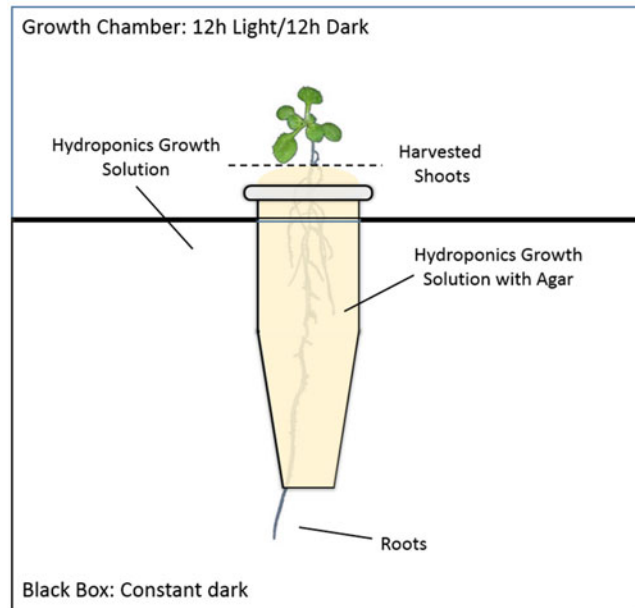


Fig. 1 Schematic diagram of *Arabidopsis* plants growing in hydroponic solution in the black boxes

Due to the large number of samples required in time-course experiments, an RNA-seq time course typically involves a trade-off between biological replication and cost. To ensure high power for the statistical analysis of RNA-seq data and to ensure adequate sequencing depth of the samples, several biological replicates of the entire time course are required [14]. The ability to detect significant differences in gene and transcript expression and AS depends on the number of biological replicate samples of the same time point and the depth of sequencing. Although the popular number of biological replicates is 3, 4–6 or even more replicates significantly increase the quality of the data and the number of differences detected between treatments [27]. In our experience and based on the premise that it is extremely important to include the routine analysis of AS, 3–4 biological replicates giving a total of 100–120 M paired-end reads provide enough data for a thorough analysis of differential expression and AS while considering available resources. Algorithms have been developed for the calculation of replication and cost [13].

The methods of analysis of RNA-seq data are extremely important and have improved immensely in the last 3–4 years. Different software packages use different algorithms and methods to count reads, assemble and quantify transcripts, and perform statistical analysis for differential expression. Several studies have shown that commonly used programs suffer from low precision (<50%) and recall (<50%) by generating misassembled transcripts and missing

bona fide transcripts which impact the accuracy of transcript quantification and downstream analysis of differential expression [28–31]. On the other hand, more recently developed programs using lightweight algorithms such as Salmon and Kallisto produce rapid and highly accurate transcript quantifications. A second limitation of many commonly used RNA-seq analysis programs is the restriction to pair-wise comparisons and inability to handle complex experimental designs. Limma-voom and edgeR [32, 33] have overcome this limitation by providing much greater flexibility in number and types of comparisons that can be made [4, 17, 34]. The 3D RNA-seq program (<https://ics.hutton.ac.uk/3drnaseq/>) has been designed to analyze RNA-seq data, including time-course and developmental series data [35]. It is very flexible, allowing multiple different comparisons to be made by setting up contrast groups. It delivers differential gene and transcript expression, differential AS, and differential transcript usage of the data. It is rapid and accurate and ideal for circadian experiments. Finally, validation of the results of RNA-seq data analysis remains important to provide confidence in the final results and methods used.

Here we detail a hydroponics-based system that utilizes inexpensive laboratory equipment for the preparation of mature (5-week-old) *Arabidopsis* plants that is applicable for harvesting distinct tissue types (shoots and roots) and has been used for multi-time point circadian analyses. We also outline a novel RNA-seq analysis pipeline as well as approaches for validation of expression and AS.

2 Materials

2.1 Seed Sterilization Solution (*Arabidopsis*)

1. Dissolve one chlorine tablet in 35 mL of distilled sterile water and add four drops of Triton X-100 (approximately 200 μ L).
2. Mix 5 mL of the chlorine solution with 45 mL of 70% ethanol and allow to sit for 5 min in the fridge. A precipitate will form. Spin at 4,000 rpm ($1,699 \times g$) for 5 min to fully pellet the precipitate.
3. Use the supernatant immediately without autoclaving, do not store.

2.2 Hydroponic Growth Solution

1. Modified protocol from Arteca and Arteca [36] to optimize *Arabidopsis* growth. Prepare the macronutrient (Table 1) and micronutrient (Table 2) stocks and dilute them 1000 \times into distilled H₂O to obtain the hydroponic growth solution.
2. Adjust the pH of the hydroponic solution to pH 5.7 with 1 M NaOH and top up with distilled H₂O to the desirable final volume of the solution.

Table 1
Macronutrient solution composition

Macronutrient stock solutions	Stock concentration	Final concentration
KNO ₃	1.25 M	1.25 mM
Ca(NO ₃) ₂ ·4H ₂ O	0.5 M	0.5 mM
MgSO ₄ ·7H ₂ O	0.5 M	0.5 mM
FeNaEDTA	42.5 mM	42.5 μM
KH ₂ PO ₄	0.625 M	0.625 mM
NaCl	2 M	2 mM
Micronutrients	1000×	1×

Table 2
Micronutrient solution composition

Reagent	Stock concentration (μM)	Final concentration (μM)
CuSO ₄ ·5H ₂ O	160	0.16
ZnSO ₄	380	0.38
MnSO ₄	1.8	1.8
H ₃ BO ₃	45	45
(NH ₄) ₆ Mo ₇ O ₂₄	15	0.015
CoCl ₂	10	0.01

2.3 Isoform-Specific Primer Design for Expression/AS Validation

1. To validate transcripts of interest, use the most updated reference transcriptome available for *Arabidopsis* or your species of interest. Incomplete or inaccurate transcriptomes can lead to incorrectly designed primers that will affect downstream applications, especially when transcript-specific amplification is required.
2. Use an online tool that offers the option of adjusting the primer design parameters. Such freely available tools are primer3 [37–39], PrimerQuest [40], OligoPerfect (Thermo Fisher Scientific; www.thermofisher.com), and others.
3. Primer design for total gene expression analysis: Align all transcripts coded by the gene of interest and design both the forward and reverse primers from the sequence of constitutively expressed exons (exons present in all alternative transcripts). Transcript alignment can be done using available tools such as the Clustal suite (www.ebi.ac.uk/Tools/msa), MUSCLE [41], T-COFFEE [42], MAFFT [43], etc.
4. Primer design for amplifying a single transcript of interest: Align all transcripts coded by your gene of interest and design

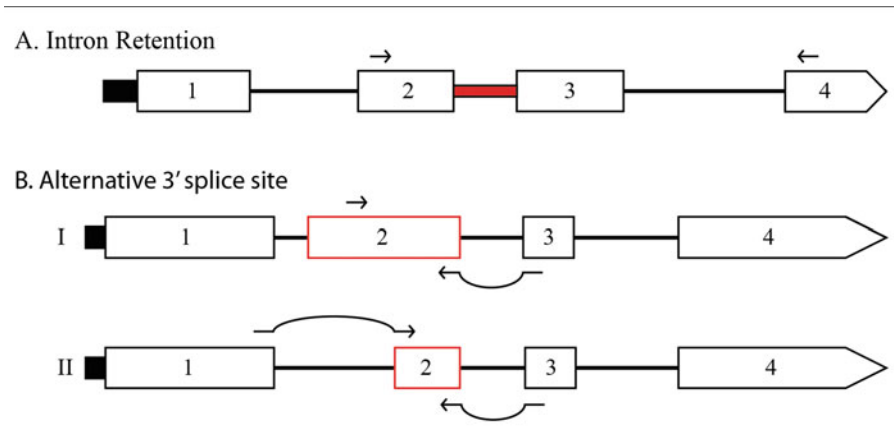


Fig. 2 Primers can be designed to unique regions of transcripts to distinguish transcript isoforms and AS events. **(a)** Gene structure with four exons, having one intron retention (red). Primers are designed to cover at least two introns to distinguish between genomic DNA amplification and the intron retention. **(b)** Transcript structures with four exons, having exon 2 alternatively spliced with a 3' splice site event. It is necessary to use two different primer pairs to distinguish between transcripts. Common primers can be used, and primers spanning a splice junction are effective (I and II); transcript-specific primers can be designed to an exon region unique to one transcript (I) or which span a splicing event/splice junction unique to one transcript (II)

the forward and/or reverse primer on the alternatively spliced region that is unique to that transcript or across the alternative splicing junction (Fig. 2).

5. Primer design for amplifying an AS event of interest: Align all transcripts coded by your gene of interest and identify the transcripts that contain the AS event. Design the forward and reverse primer to flank the region containing the AS event to produce distinct RT-PCR products which reflect the AS change (Fig. 2).
6. Calculate the size of expected amplification products for all transcripts to make sure that they will have a good separation if run on a gel. The optimal size for the PCR products ranges from 200 to 1200 bp.
7. Design the primers to be 18–22 nt long, have a melting temperature of 55–60 °C, GC content of 40–60%, while at the same time avoid repeats, runs of single nucleotides, and GC-rich 3' ends.
8. Check the quality of the designed primers using tools such as NetPrimer (<http://www.premierbiosoft.com/>). Look at the ΔG value of predicted hairpins, self-dimers, and cross-dimers of the designed primer pairs. Stable, undesirable structures have larger negative ΔG values. Choose pairs of primers with ΔG values above -2 kcal/mol for 3' ends and -5 kcal/mol for both self-dimers and cross-dimers.

9. BLAST all designed primers back to the *Arabidopsis* (or species of interest) genome to ensure that they are unique, thus avoiding unspecific priming.

3 Methods

3.1 *Arabidopsis* Seed Sterilization and Stratification

Sterilize seeds in the laminar flow under sterile conditions (*see* **Note 1**).

1. Add *Arabidopsis* seeds to a microfuge tube (20 mg \approx 1000 seeds).
2. Treat the seeds with 1 mL of 70% ethanol for 2 min while shaking gently. Allow the seeds to sink and remove the ethanol.
3. Treat the seeds with 1 mL of the sterilizing solution for 5–8 min while shaking gently. Allow the seeds to sink and remove the sterilizing solution.
4. Treat the seeds with 1 mL of 70% ethanol for 2 min while shaking gently. Allow the seeds to sink and remove the ethanol.
5. Wash the seeds five times with 1 mL distilled sterile H₂O by shaking. Between washes allow the seeds to sink to the bottom of the tube.
6. Add the same volume of water to the seeds as their volume.
7. Keep in the fridge in the dark at 4 °C for 3–4 days in order to stratify prior to sowing.

3.2 *Hydroponic Growth of Arabidopsis Plants*

Plants are grown in two stages.

Stage 1: Seed to 2-week-old seedling

1. Prepare 1/2 hydroponic solution complemented with 0.7% agar and sterilize by autoclaving.
The following steps are carried out in a laminar flow under sterile conditions.
2. Pour the sterile solution into microfuge tubes making sure that the top of the medium creates a curved surface at the top.
3. Score the top of the curved surface with a sterile blade. This is thought to provide the emerging root a convenient route into the agar medium.
4. Draw around 10 μ L of the previously prepared sterile seed-water mix using a pipette and a sterile pipette tip and sequentially pipette one or two *Arabidopsis* seeds per microfuge tube.
5. Place microfuge tubes in sterile boxes, seal with tape, and place in a growth cabinet. Grow for 10 days in 12 h light (150 μ E/m²/s) and 12 h dark.

6. On day 10, prepare 1/2 hydroponic solution and sterilize by autoclaving.
7. Thin out the seedlings to only one per microfuge tube.
8. Cut the bottom of the microfuge tubes with a microfuge tube cutter (Sigma-Aldrich) and fill the box with enough hydroponic solution to cover the bottom of the cut tubes. Allow seedlings to grow for another 4 days.

Stage 2: 2-week-old seedlings to maturity

1. Prepare growth boxes that protect roots from being exposed to light. For our experiments we used widely available and inexpensive polystyrene storage boxes (Fisher Scientific) with push fit lids (approximately 6 cm × 17 cm × 11 cm). Cover the boxes with black PVC electrical insulation tape and drill holes in the lids with sufficient diameter to house the microfuge tubes (e.g., 13 plants per box) in order that only the top of the microfuge tube is exposed to light.
2. Place the cut microfuge tubes in the boxes to grow the plants hydroponically. Due to small technical variation in the hydroponic growth of *Arabidopsis* plants, biological averaging is preferred in these experiments, and for this reason, the plants grown in each box will be pooled upon harvesting to form one sample. The number of plants per sample can vary based on the needs of the experiment and the amount of tissue that will be needed for the downstream processes (we generally harvest around 13 plants per box).
3. Prepare 1/2 hydroponic solution (do not autoclave) and fill the boxes with enough solution (around 550–600 mL) to just cover the bottom of the tubes.
4. Grow plants to the desirable growth stage in a growth cabinet (e.g., in 12 h light (150 $\mu\text{E}/\text{m}^2/\text{s}$) and 12 h dark), maintaining the desired conditions of temperature and humidity (e.g., 20 °C and 55% relative humidity).
5. Change the hydroponic solution every 10 days to ensure that there is adequate supply of fresh nutrients to the plants.
6. To minimize negative effects from the possible microclimates within the growth cabinet (small differences in temperature and light availability), move the black boxes randomly around every 2–3 days. During harvesting, randomly choose a box of plants for every time point.

3.3 Time-Course Harvesting

The circadian clock operates differently in shoots and roots [44]. Hydroponics allows straightforward harvesting of shoot and/or root material.

1. Grow *Arabidopsis* plants until they reach the desirable growth stage. Harvest the rosettes by gently lifting the leaves to reveal the roots, use a pair of scissors to separate the upper body of the plant from the roots, freeze the samples rapidly in liquid N₂, and store at -80 °C until further processing.
2. Clean, excellent quality root tissue can be obtained if desired: pull the roots gently from the bottom of the microfuge tube and dry on a piece of paper before freezing in liquid nitrogen. For high-resolution RNA-seq experiments, sample collection every 3–4 h provides adequate information on changes in rhythmicity at the transcript level.
3. Generate biological replicates for each time point in independent experiments. It is recommended to use the same growth cabinet for all repeats to eliminate the potential effects of minor changes in light intensities and light quality on gene expression.

3.4 RNA Isolation

1. Isolate the total RNA from 100 mg of ground frozen *Arabidopsis* tissue using the Qiagen RNeasy Plant Mini kit following the manufacturer's instructions.
2. Remove residual co-isolated genomic DNA using commercially available DNase treatments (e.g., TURBO DNA-free, Thermo Fisher Scientific).
3. Assess RNA sample quality and concentration spectrophotometrically. An A₂₆₀/A₂₈₀ ratio of >1.8 is indicative of highly purified RNA. In the absence of a spectrophotometer, RNA quality can be assessed by running aliquots of the RNA sample on denaturing agarose gels to visualize intact rRNA bands. However, typically around 200 ng of RNA is required to be loaded on the gel to visualize the RNA in ethidium bromide-stained gels.
4. The integrity of the RNA prior to RNA-seq analysis can also be assessed by performing RNA Integrity Number (RIN) analysis [45]. This is often a prerequisite quality control step for submission of RNA samples to RNA-seq facilities and providers.

3.5 Library Preparation and RNA Sequencing

Usually, the sequencing provider is responsible for constructing the RNA-seq libraries, prepare the samples and run them on the high-throughput sequencing platform of your choice. Paired-end, strand-specific RNA sequencing is recommended since long paired-end reads (125–150 bp) improve the accuracy of AS analysis [46, 47].

3.6 RNA-Seq Analysis Pipeline

The 3D RNA-seq analysis program takes transcript quantifications from Salmon and Kallisto. Raw RNA-seq reads must be processed

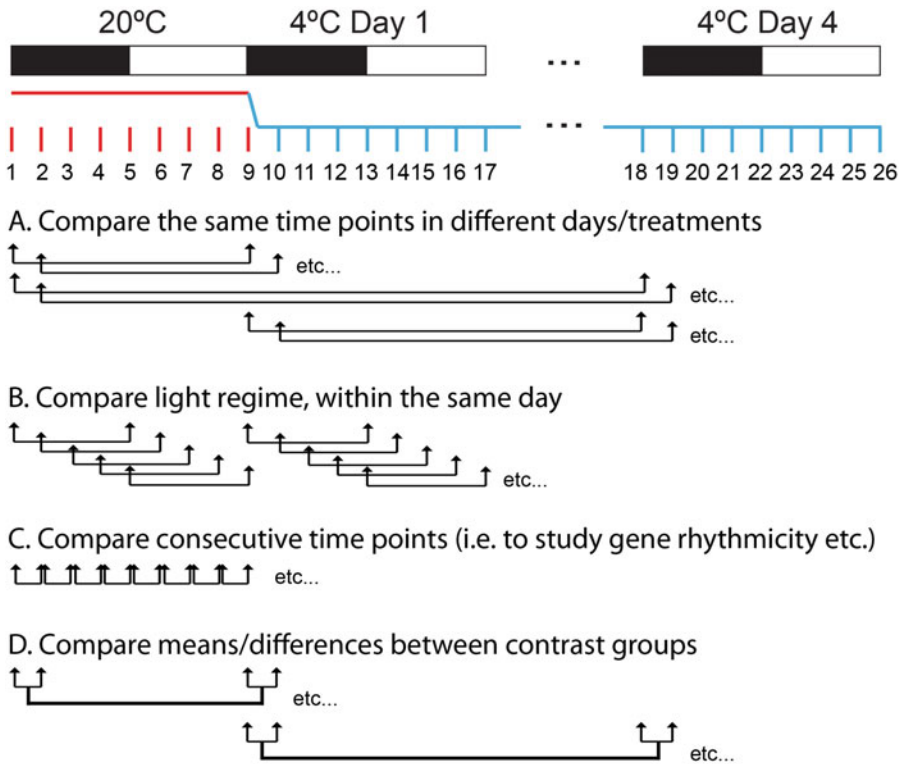


Fig. 3 Flexibility of contrast group comparisons feasible with 3D RNA-seq. Experiment example is from [4]. Rosettes were harvested every 3 h beginning with the last 24 h at 20 °C and on days 1 and 4 after transfer to 4 °C. The switch to 4 °C from 20 °C was initiated at dusk, and the air temperature reached 4 °C after 2 h. In total, a time-course experiment consisting of 26 time points was harvested. 3D RNA-seq allows multiple different comparisons to be set up. (a) Comparisons can be set up to compare day 1 at 4 °C and day 4 at 4–20 °C or day 1 to day 4 at 4 °C to examine effects of lowering temperature, as in [4, 17]. The same time-of-day samples are compared to control for studying time-of-day variation in expression. (b) Comparison of light and dark samples across each 24 h period allows to study night/day variation in gene expression. (c) Comparison of consecutive time points (particularly useful for studying gene rhythmicity, developmental series, or treatment dosage experiments). (d) Comparison of the means or differences between samples allows for more complex investigations to be set up

prior to analysis by 3D RNA-seq. Currently, these steps are performed as described below:

1. Remove residual adaptor sequences at both 5' and 3' ends from raw reads using cutadapt (version 1.4.2 or newer) (<https://pypi.python.org/pypi/cutadapt/1.4.2>) with quality score threshold set at 20 and minimum length of the trimmed read kept at 20. The "--paired-output" option should be included to keep the two paired read files synchronized and avoid unpaired reads.
2. The sequencing files should be examined before and after the trimming using fastQC version 0.10.0 or newer.

3. Transcript quantification from RNA-seq data can be performed with Salmon version 0.82 or newer [48] in conjunction with a reference transcript dataset (for *Arabidopsis*, this is AtRTD2-QUASI [49]). For indexing in Salmon, use the quasi-mapping mode to build an auxiliary k-mer hash over k-mers of length 31 (“--type quasi -k 31”).
4. When running Salmon, the option to correct for the sequence-specific bias (“--seqBias”) should be included. The number of bootstraps can be set to 30, and all other parameters could be on default settings, if your analysis allows it (Fig. 3).

3.6.1 Validation of Gene and Transcript Expression with Reverse Transcription Quantitative PCR (RT-qPCR)

1. Typically RT-qPCR can be performed as described previously [50]. Synthesize complementary DNA (cDNA) from 2 µg of total RNA using oligo dT primers and commercially available reverse transcriptase (e.g., SuperScript II reverse transcriptase, Thermo Fisher Scientific).
2. Perform RT-qPCR reactions using 10–20-fold dilutions of cDNA and commercially available fast QPCR master mixes (e.g., Brilliant III SYBR Green QPCR Master Mix, Agilent) on real-time PCR instruments (e.g., the StepOnePlus Real-Time PCR System, Thermo Fisher Scientific).
3. Use the average Ct values of reference genes as internal controls of expression levels. In our hands, expression levels of *PP2A* (AT1G13320) and *IPP2* (AT3G02780) provide reference expression levels; however, the choice of reference gene(s) should be determined empirically.
4. Relative changes in gene expression for the gene of interest (GOI) can be determined using the Ct values for the reference gene(s) and the GOI and employing the delta-delta Ct algorithm [51].

3.6.2 Validation of AS with High-Resolution RT-PCR

Validation of AS results from RNA-seq analysis is performed essentially as described previously [52].

1. To avoid DNA contamination of RNA samples, apply an on-column DNase treatment during RNA isolation following the manufacturer’s instructions.
2. Synthesize the cDNA from 4 µg of total RNA using the RNA to cDNA EcoDry (Double Primed) kit (Clontech Laboratories, Takara Bio) in a final volume of 20 µL according to manufacturer’s instructions. The kit contains a dry master mix of SMART™ MMLV Reverse Transcriptase, dNTPs, buffer and both random hexamer, and oligo(dT)18 primers. Incubate at 42 °C for 1 h and stop the reaction by heating at 70 °C for 10 min. Store at –20 °C until further use.

3. Use gene-specific primers to amplify the total expression of gene- or transcript-specific primers to amplify specific transcript isoforms.
4. Note: If high-resolution RT-PCR is used for data validation, ensure that the forward primer is fluorescently labeled, i.e., 6-carboxyfluorescein, or ROX, etc.
5. For the PCR reaction, prepare a mix of 3 μL of diluted cDNA (1:10) as a template, 0.1 μL of each of the forward and reverse primers (100 mM), 2 μL of 10 \times PCR buffer, 0.2 μL of Taq polymerase (5 units/ μL ; Roche), 1 μL of 10 mM dNTPs (Invitrogen, Life Technologies), and RNase-free water (Qiagen) up to a final volume of 20 μL .
6. Perform RT-PCRs under the following conditions: initial denaturation at 94 °C for 2 min, followed by 28–35 cycles (for RT-PCR) or 24–26 cycles (for high-resolution RT-PCR) of denaturation at 94 °C for 15 s, annealing at 50 °C for 30 s, and extension at 70 °C for 1 min (for fragments smaller than 1000 bp) or 1.5 min (for fragments between 1000 and 1200 bp), followed by a final extension at 70 °C for 10 min.
7. Visualize the amplified products in a 1.5–2% agarose gel stained with an intercalating agent (e.g., ethidium bromide).
8. Note: In the case of high-resolution RT-PCR, mix 1.5 μL of RT-PCR product with 8.5 μL of Hi-Di formamide (Applied Biosystems) and 0.01 μL of GeneScan 500 LIZ dye or 0.04 μL of GeneScan 1200 LIZ dye size standard and run on a fragment DNA analyzer such as the ABI 3730 (Applied Biosystems, Life Technologies). PCR products are separated to single base-pair resolution and are quantified by measuring the intensity of the fluorescence (relative fluorescence units). Analyze the data generated by the fragment DNA analyzer using the appropriate tool (e.g., GeneMapper software from Applied Biosystems, Life Technologies).
9. During data validation use appropriate negative and positive controls in order to have a better control over the analysis and data interpretation. In addition, select a couple of housekeeping genes to run with all the samples and use the data to perform data normalization.

4 Note

1. Autoclave buffers, tips, and tubes before use.

Acknowledgments

This work was supported by funding from the Biotechnology and Biological Sciences Research Council (BBSRC) [BB/P009751/1 to JWSB; BB/K006835/1 to HGN] and the Scottish Government Rural and Environment Science and Analytical Services division (RESAS) [to JWSB and RZ].

References

1. Harmer SL, Hogenesch JB, Straume M, Chang HS, Han B, Zhu T, Wang X, Kreps JA, Kay SA (2000) Orchestrated transcription of key pathways in Arabidopsis by the circadian clock. *Science* 290(5499):2110–2113
2. Michael TP, McClung CR (2003) Enhancer trapping reveals widespread circadian clock transcriptional control in Arabidopsis. *Plant Physiol* 132(2):629–639. <https://doi.org/10.1104/pp.021006>
3. Covington MF, Maloof JN, Straume M, Kay SA, Harmer SL (2008) Global transcriptome analysis reveals circadian regulation of key pathways in plant growth and development. *Genome Biol* 9(8):R130. <https://doi.org/10.1186/gb-2008-9-8-r130>
4. Calixto CPG, Guo W, James AB, Tzioutziou NA, Entizne JC, Panter PE, Knight H, Nimmo HG, Zhang R, Brown JWS (2018) Rapid and dynamic alternative splicing impacts the Arabidopsis cold response transcriptome. *Plant Cell* 30(7):1424–1444. <https://doi.org/10.1105/tpc.18.00177>
5. Breeze E, Harrison E, McHattie S, Hughes L, Hickman R, Hill C, Kiddle S, Kim YS, Penfold CA, Jenkins D, Zhang C, Morris K, Jenner C, Jackson S, Thomas B, Tabrett A, Legaie R, Moore JD, Wild DL, Ott S, Rand D, Beynon J, Denby K, Mead A, Buchanan-Wollaston V (2011) High-resolution temporal profiling of transcripts during Arabidopsis leaf senescence reveals a distinct chronology of processes and regulation. *Plant Cell* 23(3):873–894. <https://doi.org/10.1105/tpc.111.083345>
6. Carvallo MA, Pino MT, Jeknic Z, Zou C, Doherty CJ, Shiu SH, Chen TH, Thomashow MF (2011) A comparison of the low temperature transcriptomes and CBF regulons of three plant species that differ in freezing tolerance: *Solanum commersonii*, *Solanum tuberosum*, and Arabidopsis thaliana. *J Exp Bot* 62(11):3807–3819. <https://doi.org/10.1093/jxb/err066>
7. Leviatan N, Alkan N, Leshkowitz D, Fluhr R (2013) Genome-wide survey of cold stress regulated alternative splicing in Arabidopsis thaliana with tiling microarray. *PLoS One* 8(6):e66511. <https://doi.org/10.1371/journal.pone.0066511>
8. Mockler TC, Michael TP, Priest HD, Shen R, Sullivan CM, Givan SA, McEntee C, Kay SA, Chory J (2007) The DIURNAL project: DIURNAL and circadian expression profiling, model-based pattern matching, and promoter analysis. *Cold Spring Harb Symp Quant Biol* 72:353–363. <https://doi.org/10.1101/sqb.2007.72.006>
9. Schaffer R, Landgraf J, Accerbi M, Simon V, Larson M, Wisman E (2001) Microarray analysis of diurnal and circadian-regulated genes in Arabidopsis. *Plant Cell* 13(1):113–123. <https://doi.org/10.1105/tpc.13.1.113>
10. Tikkanen M, Gollan PJ, Mekala NR, Isojarvi J, Aro EM (2014) Light-harvesting mutants show differential gene expression upon shift to high light as a consequence of photosynthetic redox and reactive oxygen species metabolism. *Philos Trans R Soc Lond Ser B Biol Sci* 369(1640):20130229. <https://doi.org/10.1098/rstb.2013.0229>
11. Vogel JT, Zarka DG, Van Buskirk HA, Fowler SG, Thomashow MF (2005) Roles of the CBF2 and ZAT12 transcription factors in configuring the low temperature transcriptome of Arabidopsis. *Plant J* 41(2):195–211. <https://doi.org/10.1111/j.1365-3113X.2004.02288.x>
12. Windram O, Madhou P, McHattie S, Hill C, Hickman R, Cooke E, Jenkins DJ, Penfold CA, Baxter L, Breeze E, Kiddle SJ, Rhodes J, Atwell S, Kliebenstein DJ, Kim YS, Stegle O, Borgwardt K, Zhang C, Tabrett A, Legaie R, Moore J, Finkenstadt B, Wild DL, Mead A, Rand D, Beynon J, Ott S, Buchanan-Wollaston V, Denby KJ (2012) Arabidopsis defense against Botrytis cinerea: chronology and regulation deciphered by high-resolution temporal transcriptomic analysis. *Plant Cell* 24

- (9):3530–3557. <https://doi.org/10.1105/tpc.112.102046>
13. Gehan MA, Park S, Gilmour SJ, An C, Lee CM, Thomashow MF (2015) Natural variation in the C-repeat binding factor cold response pathway correlates with local adaptation of *Arabidopsis* ecotypes. *Plant J* 84(4):682–693. <https://doi.org/10.1111/tpj.13027>
 14. Jia Y, Ding Y, Shi Y, Zhang X, Gong Z, Yang S (2016) The cbfs triple mutants reveal the essential functions of CBFs in cold acclimation and allow the definition of CBF regulons in *Arabidopsis*. *New Phytol* 212(2):345–353. <https://doi.org/10.1111/nph.14088>
 15. Zhao C, Zhang Z, Xie S, Si T, Li Y, Zhu JK (2016) Mutational evidence for the critical role of CBF transcription factors in cold acclimation in *Arabidopsis*. *Plant Physiol* 171(4):2744–2759. <https://doi.org/10.1104/pp.16.00533>
 16. Stephan-Otto Attolini C, Pena V, Rossell D (2015) Designing alternative splicing RNA-seq studies. Beyond generic guidelines. *Bioinformatics* 31(22):3631–3637. <https://doi.org/10.1093/bioinformatics/btv436>
 17. Calixto CPG, Tzioutziou NA, James AB, Hornyk C, Guo W, Zhang R, Nimmo HG, Brown JWS (2019) Cold-dependent expression and alternative splicing of *Arabidopsis* long non-coding RNAs. *Front Plant Sci* 10:235. <https://doi.org/10.3389/fpls.2019.00235>
 18. Rapazote-Flores P, Bayer M, Milne L, Mayer C-D, Fuller J, Guo W, Hedley PE, Morris J, Halpin C, Kam J, McKim SM, Zwirek M, Casao MC, Barakate A, Schreiber M, Stephen G, Zhang R, Brown JW, Waugh R, Simpson CG (2019) BaRTv1.0: an improved barley reference transcript dataset to determine accurate changes in the barley transcriptome using RNA-seq. *bioRxiv*:638106. <https://doi.org/10.1101/638106>
 19. Sonesson C, Love MI, Robinson MD (2015) Differential analyses for RNA-seq: transcript-level estimates improve gene-level inferences. *F1000Research* 4:1521. <https://doi.org/10.12688/f1000research.7563.2>
 20. Marquez Y, Brown JW, Simpson C, Barta A, Kalyna M (2012) Transcriptome survey reveals increased complexity of the alternative splicing landscape in *Arabidopsis*. *Genome Res* 22(6):1184–1195. <https://doi.org/10.1101/gr.134106.111>
 21. Syed NH, Kalyna M, Marquez Y, Barta A, Brown JW (2012) Alternative splicing in plants—coming of age. *Trends Plant Sci* 17(10):616–623. <https://doi.org/10.1016/j.tplants.2012.06.001>
 22. Filichkin SA, Priest HD, Givan SA, Shen R, Bryant DW, Fox SE, Wong WK, Mockler TC (2010) Genome-wide mapping of alternative splicing in *Arabidopsis thaliana*. *Genome Res* 20(1):45–58. <https://doi.org/10.1101/gr.093302.109>
 23. Carvalho RF, Feijao CV, Duque P (2013) On the physiological significance of alternative splicing events in higher plants. *Protoplasma* 250(3):639–650. <https://doi.org/10.1007/s00709-012-0448-9>
 24. Drechsel G, Kahles A, Kesarwani AK, Stauffer E, Behr J, Drewe P, Ratsch G, Wachter A (2013) Nonsense-mediated decay of alternative precursor mRNA splicing variants is a major determinant of the *Arabidopsis* steady state transcriptome. *Plant Cell* 25(10):3726–3742. <https://doi.org/10.1105/tpc.113.115485>
 25. Chamala S, Feng G, Chavarro C, Barbazuk WB (2015) Genome-wide identification of evolutionarily conserved alternative splicing events in flowering plants. *Front Bioeng Biotechnol* 3:33. <https://doi.org/10.3389/fbioe.2015.00033>
 26. Mastrangelo AM, Marone D, Laido G, De Leonardis AM, De Vita P (2012) Alternative splicing: enhancing ability to cope with stress via transcriptome plasticity. *Plant Sci* 185–186:40–49. <https://doi.org/10.1016/j.plantsci.2011.09.006>
 27. Schurch NJ, Schofield P, Gierlinski M, Cole C, Sherstnev A, Singh V, Wrobel N, Gharbi K, Simpson GG, Owen-Hughes T, Blaxter M, Barton GJ (2016) Erratum: how many biological replicates are needed in an RNA-seq experiment and which differential expression tool should you use? *RNA* 22(10):1641. <https://doi.org/10.1261/rna.058339.116>
 28. Hayer KE, Pizarro A, Lahens NF, Hogenesch JB, Grant GR (2015) Benchmark analysis of algorithms for determining and quantifying full-length mRNA splice forms from RNA-seq data. *Bioinformatics* 31(24):3938–3945. <https://doi.org/10.1093/bioinformatics/btv488>
 29. Kanitz A, Gypas F, Gruber AJ, Gruber AR, Martin G, Zavolan M (2015) Comparative assessment of methods for the computational inference of transcript isoform abundance from RNA-seq data. *Genome Biol* 16:150. <https://doi.org/10.1186/s13059-015-0702-5>
 30. Perteau M, Perteau GM, Antonescu CM, Chang TC, Mendell JT, Salzberg SL (2015) StringTie enables improved reconstruction of a transcriptome from RNA-seq reads. *Nat Biotechnol* 33

- (3):290–295. <https://doi.org/10.1038/nbt.3122>
31. Steijger T, Abril JF, Engstrom PG, Kokocinski F, Consortium R, Hubbard TJ, Guigo R, Harrow J, Bertone P (2013) Assessment of transcript reconstruction methods for RNA-seq. *Nat Methods* 10(12):1177–1184. <https://doi.org/10.1038/nmeth.2714>
32. Law CW, Alhamdoosh M, Su S, Dong X, Tian L, Smyth GK, Ritchie ME (2016) RNA-seq analysis is easy as 1-2-3 with limma, Glimma and edgeR. *F1000Research* 5:1408. <https://doi.org/10.12688/f1000research.9005.3>
33. Law CW, Chen Y, Shi W, Smyth GK (2014) Voom: precision weights unlock linear model analysis tools for RNA-seq read counts. *Genome Biol* 15(2):R29. <https://doi.org/10.1186/gb-2014-15-2-r29>
34. Gloss BS, Signal B, Cheetham SW, Gruhl F, Kaczorowski DC, Perkins AC, Dinger ME (2017) High resolution temporal transcriptomics of mouse embryoid body development reveals complex expression dynamics of coding and noncoding loci. *Sci Rep* 7(1):6731. <https://doi.org/10.1038/s41598-017-06110-5>
35. Guo W, Tzioutziou N, Stephen G, Milne I, Calixto C, Waugh R, Brown JWS, Zhang R (2019) 3D RNA-seq—a powerful and flexible tool for rapid and accurate differential expression and alternative splicing analysis of RNA-seq data for biologists. *bioRxiv:656686*. <https://doi.org/10.1101/656686>
36. Artega RN, Artega JM (2000) A novel method for growing *Arabidopsis thaliana* plants hydroponically. *Physiol Plantarum* 108(2):188–193. <https://doi.org/10.1034/j.1399-3054.2000.108002188x/>
37. Koressaar T, Lepamets M, Kaplinski L, Raime K, Andreson R, Remm M (2018) Primer3_masker: integrating masking of template sequence with primer design software. *Bioinformatics* 34(11):1937–1938. <https://doi.org/10.1093/bioinformatics/bty036>
38. Koressaar T, Remm M (2007) Enhancements and modifications of primer design program Primer3. *Bioinformatics* 23(10):1289–1291. <https://doi.org/10.1093/bioinformatics/btm091>
39. Untergasser A, Cutcutache I, Koressaar T, Ye J, Faircloth BC, Remm M, Rozen SG (2012) Primer3—new capabilities and interfaces. *Nucleic Acids Res* 40(15):e115. <https://doi.org/10.1093/nar/gks596>
40. Thornton B, Basu C (2015) Rapid and simple method of qPCR primer design. *Methods Mol Biol* 1275:173–179. https://doi.org/10.1007/978-1-4939-2365-6_13
41. Edgar RC (2004) MUSCLE: multiple sequence alignment with high accuracy and high throughput. *Nucleic Acids Res* 32(5):1792–1797. <https://doi.org/10.1093/nar/gkh340>
42. Notredame C, Higgins DG, Heringa J (2000) T-Coffee: a novel method for fast and accurate multiple sequence alignment. *J Mol Biol* 302(1):205–217. <https://doi.org/10.1006/jmbi.2000.4042>
43. Katoh K, Standley DM (2013) MAFFT multiple sequence alignment software version 7: improvements in performance and usability. *Mol Biol Evol* 30(4):772–780. <https://doi.org/10.1093/molbev/mst010>
44. James AB, Monreal JA, Nimmo GA, Kelly CL, Herzyk P, Jenkins GI, Nimmo HG (2008) The circadian clock in *Arabidopsis* roots is a simplified slave version of the clock in shoots. *Science* 322(5909):1832–1835. <https://doi.org/10.1126/science.1161403>
45. Schroeder A, Mueller O, Stocker S, Salowsky R, Leiber M, Gassmann M, Lightfoot S, Menzel W, Granzow M, Ragg T (2006) The RIN: an RNA integrity number for assigning integrity values to RNA measurements. *BMC Mol Biol* 7:3. <https://doi.org/10.1186/1471-2199-7-3>
46. Chang Z, Wang Z, Li G (2014) The impacts of read length and transcriptome complexity for de novo assembly: a simulation study. *PLoS One* 9(4):e94825. <https://doi.org/10.1371/journal.pone.0094825>
47. Hara Y, Tatsumi K, Yoshida M, Kajikawa E, Kiyonari H, Kuraku S (2015) Optimizing and benchmarking de novo transcriptome sequencing: from library preparation to assembly evaluation. *BMC Genomics* 16:977. <https://doi.org/10.1186/s12864-015-2007-1>
48. Patro R, Duggal G, Love MI, Irizarry RA, Kingsford C (2017) Salmon provides fast and bias-aware quantification of transcript expression. *Nat Methods* 14(4):417–419. <https://doi.org/10.1038/nmeth.4197>
49. Zhang R, Calixto CPG, Marquez Y, Venhuizen P, Tzioutziou NA, Guo W, Spensley M, Entzine JC, Lewandowska D, Ten Have S, Frei Dit Frey N, Hirt H, James AB, Nimmo HG, Barta A, Kalyna M, Brown JWS (2017) A high quality *Arabidopsis* transcriptome for accurate transcript-level analysis of alternative splicing. *Nucleic Acids Res* 45(9):5061–5073. <https://doi.org/10.1093/nar/gkx267>

50. James AB, Syed NH, Bordage S, Marshall J, Nimmo GA, Jenkins GI, Herzyk P, Brown JW, Nimmo HG (2012) Alternative splicing mediates responses of the Arabidopsis circadian clock to temperature changes. *Plant Cell* 24 (3):961–981. <https://doi.org/10.1105/tpc.111.093948>
51. Livak KJ, Schmittgen TD (2001) Analysis of relative gene expression data using real-time quantitative PCR and the $2^{-\Delta\Delta C_T}$ method. *Methods* 25(4):402–408. <https://doi.org/10.1006/meth.2001.1262>
52. Simpson CG, Fuller J, Maronova M, Kalyna M, Davidson D, McNicol J, Barta A, Brown JW (2008) Monitoring changes in alternative precursor messenger RNA splicing in multiple gene transcripts. *Plant J* 53(6):1035–1048. <https://doi.org/10.1111/j.1365-313X.2007.03392.x>



Using Tandem Affinity Purification to Identify Circadian Clock Protein Complexes from *Arabidopsis*

Maria L. Sorkin and Dmitri A. Nusinow

Abstract

Identification of protein-protein interactions is an effective method of elucidating new roles for circadian clock-associated proteins that can expand beyond the information collected from transcriptional studies and genetic screens. Tandem affinity purification coupled with liquid chromatography mass spectrometry (APMS) utilizes epitope-tagged versions of your protein of interest to co-precipitate direct and indirect protein partners. Here, we provide a protocol and suggestions for proper design of 6x-His-3x-FLAG-tagged clock proteins and isolation of protein-protein interactions using two immunoprecipitation steps for increased specificity.

Keywords Affinity purification, Mass spectrometry, Protein-protein interactions, Circadian clock

1 Introduction

Tandem affinity purification coupled with mass spectrometry (APMS) is a powerful method to identify protein-protein interactions on a proteomic level. While most clock proteins have been identified via forward and reverse genetic screens, taking a proteomic approach to studying the clock may illuminate novel clock components and roles for clock proteins that were overlooked previously. By engineering a plant with an affinity-tagged version of a protein of interest, one can effectively capture near-native, direct, and indirect protein interactions with the tagged protein *in vivo*.

One challenge of APMS is the difficulty of identifying and eliminating false positive proteins that are co-precipitated with the protein of interest. Co-precipitation of false positives is often due to the abundance of the contaminating protein or the native affinity of that protein for the antibody or resin you are using during the protocol. The protocol supplied here includes two immunoprecip-

itation steps for each epitope tag in the purification of a 6x-His-3x-FLAG tandem affinity-tagged bait protein in *A. thaliana*. The use of two different affinity tags significantly reduces the number of false positives, as it is increasingly unlikely that a contaminating protein has high affinity for two different antibodies or resins. We also recommend using both (1) a GFP-6x-His-3x-FLAG and (2) a wild-type no-tag background as negative controls. Any protein co-precipitated in these control immunoprecipitations can likely be deprioritized as a true interacting partner of the bait protein of interest. One may also use localization data to deprioritize proteins that are located in a separate compartment from the protein of interest; for example, a chloroplast-localized protein that is co-precipitated with a nuclear-localized transcription factor could be a false positive. Lastly, several datasets including Van Leene et al. [1] and Besbrugge et al. [2] contain lists of common contaminants in APMS experiments and can also be used to filter out nonspecific binding proteins.

The circadian clock is made up of approximately 25 core oscillator proteins that participate in interlocking transcription-translation feedback loops to regulate numerous and diverse physiological outputs [3]. Identification and compilation of protein-protein interactions for circadian clock-associated proteins will be a useful resource for understanding how the clock connects to environmental input pathways and how it coordinates appropriate physiological responses in the plant. APMS is an ideal method for probing complex signaling networks such as the circadian clock because of its effective capture of direct and indirect interacting proteins on a proteomic scale. Additionally, APMS is conducted *in vivo* in an engineered plant that can be grown under specific environmental conditions that are known to affect clock activity. Thus, APMS allows for identification of protein-protein interactions in physiologically relevant conditions for the plant and is higher throughput compared to other techniques such as the yeast 2-hybrid system.

Our method effectively captures protein-protein interactions *in vivo* and has been used to identify both established and novel protein interactions [4] (*see Note 1* for details on designing and characterizing engineered bait proteins). Additionally, we detail a cost-effective method for cross-linking an antibody of interest to Protein G Magnetic Beads from scratch, eliminating the need to buy expensive pre-cross-linked antibody beads.

2 Materials

Prepare all solutions using ultrapure deionized water (18 MPa at 25 °C).

2.1 Cross-Linking Antibodies to Protein G Beads

1. Dynabeads™ Protein G for Immunoprecipitation (Thermo Fisher Scientific, catalog number: 10003D).
2. Monoclonal ANTI-FLAG M2 antibody produced in mouse (Sigma-Aldrich, catalog number: F1804).
3. Magnetic stand for microcentrifuge tubes.
4. Protein G Wash Buffer: 0.1 M $\text{Na}_3\text{C}_6\text{H}_5\text{O}_7$ pH 5.0, 0.01% NP-40.
5. Cross-linking Sensitization Buffer: 0.2 M triethanolamine, pH 8.2.
6. Cross-linking Buffer: 10 mM dimethyl pimelimidate (DMP) in 0.2 M triethanolamine, pH 8.2. Prepare fresh.
7. Cross-linking Quench Buffer: 0.2 M ethanolamine, pH 8.2.
8. Tris-Buffered Saline: 50 mM Tris-HCl, pH 7.5, 150 mM NaCl, 0.01% Triton X-100.
9. Dynabeads™ Storage Buffer: 50% Glycerol, 50 mM Tris-HCl, pH 8.0, 150 mM NaCl, 0.01%, Triton X-100, 0.03% Na-Azide.
10. 4× SDS-PAGE Sample Buffer: For 10 mL of sample buffer, mix 5 mL 0.5 M Tris-HCl pH 6.8, 1.0 g SDS, 0.8 mL 0.1% bromophenol blue, and 4 mL of 100% glycerol. Adjust the final volume to 10 mL with ultrapure water. Aliquot into 10 tubes containing 950 μL of this solution. When ready to use an aliquot, add 2-mercaptoethanol to a final concentration of 5%; so add 50 μL . Heat and mix tube to dissolve mixture if necessary.

2.2 Plant Growth and Tissue Homogenization

1. MS agar medium: Add 2.205 g Murashige and Skoog medium and 7.0 g agar to ~500 mL of water. Add water to a volume of 1 L. Autoclave and dispense ~40 mL per 15 cm dish.
2. 15 cm petri dish.
3. Filter paper.
4. Gas sterilization chamber.
5. Liquid N_2 .
6. Mixer Mill MM 400 Tissue Homogenizer (Retsch).
7. 35 mL stainless steel grinding jar (Retsch, catalog number: 01.462.0214).
8. 3.2 mm stainless steel balls (BioSpec Products, catalog number: 11079132ss).
9. Dry ice.

2.3 Affinity Purification

1. Magnetic stand for microcentrifuge tubes.
2. Magnetic stand for 15-mL conical tubes.

3. Sonic Dismembrator.
4. Low protein-binding microcentrifuge tubes.
5. 50-mL round-bottom tube.
6. Dynabeads™ His-Tag Isolation and Pulldown (Thermo Fisher Scientific, catalog number: 10104D).
7. 3× FLAG peptide (Sigma-Aldrich, catalog number: F4799).
8. Dry ice.
9. SII buffer: 100 mM Na-phosphate, pH 8.0, 150 mM NaCl, 5 mM EDTA, 5 mM EGTA, 0.1% Triton X-100 (*see Note 2*). Filter through a 0.22 μm filter syringe to sterilize and store at 4 °C.
10. SII buffer plus inhibitors: Make just before use. Use filter-sterilized SII buffer made in the previous step. Add phenylmethylsulfonyl fluoride (PMSF) to a final concentration of 1mM (*see Note 3*), 1× protease inhibitor tablet (EDTA-free) (Thermo Fisher Scientific, catalog number: 88266), 1× phosphatase inhibitor cocktail II (Sigma-Aldrich, catalog number: P5726), 1× phosphatase inhibitor cocktail III (Sigma-Aldrich, catalog number: P0044), and MG-132 to a final concentration of 50 μM.
11. Protein concentration assay that is compatible with detergent, such as the Bio-Rad DC Protein Assay (Bio-Rad, catalog number: 5000111).
12. His Immunoprecipitation (IP) Buffer (*see Note 4*): 100 mM Na-phosphate, pH 8.0, 150 mM NaCl, 0.025% Triton X-100 (*see Note 2*). Filter through a 0.22 μm filter syringe to sterilize. Store at 4 °C.
13. 3× FLAG peptide: 50 mg/mL MDYKDHDGDYKDHDIDYKDDDDK resuspended in 100 mM Na-phosphate, pH 8.0. Store at –80 °C.
14. FLAG Elution Buffer: 500 μg/mL 3× FLAG peptide in His IP Buffer.
15. Ammonium bicarbonate buffer: Make fresh the day of purification. Solution is 25 mM ammonium bicarbonate in ultrapure deionized water. Filter through a 0.22 μm filter syringe to sterilize.

3 Methods

3.1 Cross-linking Antibody to Protein G Beads (See Notes 5 and 6)

1. Rotate Dynabeads™ Protein G to fully resuspend beads in solution (*see Notes 7 and 8*).
2. Pipette 1.2 mL of resuspended Protein G Dynabeads™ into a microcentrifuge tube. Place tubes on a magnetic stand to

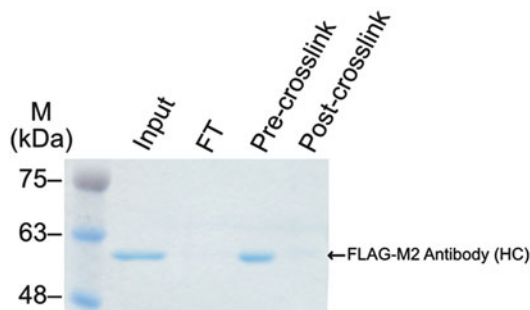


Fig. 1 Coomassie blue stain of quality control samples from crosslinking FLAG-M2 antibody to Protein G Dynabeads™. Samples have been boiled; therefore, the antibody will dissociate from the beads and will result in a ~60 kDa band representing the heavy chain of the antibody unless effectively crosslinked. *HC* heavy chain, *FT* flow through

collect beads for 1 min. Remove supernatant with a pipette and discard.

3. Add 900 μL of protein G wash buffer to beads and rotate to wash for 5 min. Spin down the tube briefly in a microcentrifuge to collect liquid from cap, place in magnetic stand for 1 min, and remove wash without disturbing beads. Repeat this wash step once for a total of two washes to complete buffer exchange of the bead solution.
4. Add 700 μL of protein G wash buffer to washed beads and then add exactly 200 μL of anti-FLAG M2 antibody to the tube (*see Note 9*).
5. Rotate tube at 4 $^{\circ}\text{C}$ for 1 h to allow antibody to bind to Dynabeads™ (*see Note 10*).
6. After the 1 h incubation, remove 1% (9 μL) of resuspended bead solution for the “input” control sample that will be analyzed via SDS-PAGE gel (Fig. 1).
7. Spin down tube to gather all liquid from cap and place on magnetic stand for 1 min. Remove 1% (9 μL) of supernatant for “flow-through” control sample that will be analyzed via SDS-PAGE gel (Fig. 1). Remove remaining flow through from beads and discard.
8. Wash beads by adding 900 μL of protein G wash buffer and rotating for 5 min at room temperature. All following steps are performed at room temperature.
9. Repeat wash once for a total of two washes.
10. Wash beads twice with 900 μL 0.2 M NaBorate, pH 8.0. Rotate each wash for 3 min.
11. Wash beads 3 times with 900 μL 0.2 M triethanolamine, pH 8.2 (cross-linking sensitization buffer), to sensitize beads

for cross-linking. Rotate each wash for 3 min. On the last wash, save 1% (9 μ L) of resuspended beads in a microcentrifuge tube for the pre-cross-link control sample.

12. Cross-link antibody to beads by adding 900 μ L of freshly prepared 0.015 M dimethyl pimelimidate (DMP) in 0.2 M triethanolamine, pH 8.2 (cross-linking buffer). Incubate with rotation for 30 min at room temperature (*see Note 11*).
13. Spin down tube to capture liquid from cap, then place tube on magnetic stand for 1 min to capture beads. Remove supernatant.
14. Add 900 μ L of 0.2 M ethanolamine, pH 8.2 (cross-linking quench buffer), to quench DMP cross-linker. Incubate with rotation for 30 min at room temperature.
15. Spin down tube to capture liquid from cap, then place tube on magnetic stand for 1 min to capture beads. Remove ethanolamine supernatant and discard.
16. Wash beads twice with 900 μ L of 0.1 M glycine, pH 2.5, to strip off non-covalently linked antibody. Invert by hand for exactly 1 min each time to wash beads quickly (*see Note 12*).
17. Wash twice with 900 μ L of 1 \times Tris-buffered saline to neutralize pH. Rotate each wash for 3 min. During the second saline wash, fully resuspend beads and remove 1% (9 μ L) as the post-cross-link control sample.
18. Remove saline wash and resuspend beads in 1.2 mL DynabeadsTM storage buffer. Beads can be stored at -20°C for at least 1 year.
19. Add 4 \times SDS sample buffer to quality control samples (input, flow through, pre-cross-link, post-cross-link) and boil for 10 min to denature.
20. Test for effective cross-linking by running an SDS-PAGE gel of the input, flow through, pre-cross-link, and post-cross-link control samples taken. Stain the SDS-PAGE gel with Coomassie blue to show abundance of antibody in each sample. An example of successful cross-linking is shown in Fig. 1 (*see Notes 10 and 11*).

3.2 Plant Growth and Tissue Collection

1. For each genotype, gas sterilize 18 tubes containing ~ 50 μ L of seeds. Spread 2 tubes of seed evenly per 15-cm diameter plates, totaling 9 plates per genotype. This should be enough seed to collect 3 \times ~ 5 g of tissue from 10-day-old *A. thaliana* seedlings expressing the 6x-His-3x-FLAG-tagged protein of interest in the null mutant background. Three packets of 5 g of tissue will serve as 3 biological replicates. Tubes containing ~ 50 μ L of seed can be gas sterilized in 1.5 mL tubes for 4–5 h in a

sterilization chamber after adding 3 mL of hydrochloric acid to 100 mL of bleach.

2. Scatter seeds evenly on 15-cm diameter round plates with 15-cm round filter paper placed on top of 1/2× Murashige and Skoog media containing 1% sucrose. Seal plates with micropore tape to allow gas exchange and place in darkness at 4 °C for 2–3 days.
3. Transfer plates to the appropriate growth conditions. Typical collections are grown under 12-h light, 12-h dark photoperiods (12:12) at 22 °C. Grow plants under white light at 100 μmol/m²/s (*see Note 13*).
4. On the 10th day of growth, collect 5 g of tissue into tin foil packets at the peak time of protein expression or at the zeitgeber time of interest (*see Notes 14 and 15*). Five grams of tissue can typically be obtained from collecting tissue from two to three plates. Flash freeze tissue in tinfoil in liquid N₂.
5. Tissue packets can be stored at –80 °C for at least 6 months.

3.3 Tissue Homogenization

1. Cool steel grinding jars in liquid nitrogen. Each jar can hold up to 5 g of tissue.
2. Pre-crush 5 g packets of tissue as much as possible in tin foil while frozen before transferring into pre-cooled 35-mL steel grinding jars compatible with a Retsch Mixer Mill 400 or other similar ball mill. Ensure O-ring and stainless steel ball are in place before sealing jar. Use sterile, liquid nitrogen-cooled spatulas to help transfer tissue. Keep grinding cassettes cold.
3. The first set of grinding is performed for 45 s at 25 s⁻¹ frequency. Then, repeat grinding 3× at 45 s at 30 s⁻¹ frequency. Cool steel grinding jars in liquid nitrogen in between each set of tissue homogenization to ensure tissue remains frozen.
4. After a total of four rounds of homogenization, open steel jars and use a liquid nitrogen pre-cooled spatula to transfer powdered tissue to a pre-labeled, pre-cooled, and sterile 50-mL conical tube on dry ice.
5. Store 50-mL conical tube containing tissue powder at –80 °C for up to 1 month, if necessary.

3.4 Protein Extraction and Sonication (See Note 16)

All subsequent steps should be performed in a 4 °C cold room unless otherwise noted.

1. Add ~12 mL of SII buffer plus inhibitors to 5 g of frozen tissue powder in a 50-mL conical tube on dry ice. Remove the tube from dry ice. Allow bubbles to release before closing the lid of the 50-mL conical.

2. Incubate frozen tissue in SII buffer for 10–15 min with rotation, or until all ground powder is in solution and there are no chunks.
3. Use a Fisherbrand Model 505 Sonic Dismembrator probe sonicator with micro tip or similar to break up material and lyse cells using a duty cycle for 20 s (2 s on, 2 s off, total of 40 s, to prevent heat generation) at 50% power. Place sample on ice to cool, then repeat sonication.

3.5 Extract Clarification

1. Transfer extract to a clean, 50-mL round-bottom centrifuge tube and centrifuge for 10 min at $\geq 20,000 \times g$ at 4 °C.
2. Transfer supernatant to a second clean 50-mL round-bottom centrifuge tube by using a serological pipet, avoiding disturbing the pellet.
3. Repeat the centrifugation step, spinning for 10 min at $\geq 20,000 \times g$ at 4 °C.
4. Remove and save the green supernatant using a 10 mL serological pipette tip with a p1000 pipette tip attached to the end while avoiding disturbing the pellet. Filter the clarified lysate through a 0.45 μm syringe filter into a sterile 15 mL conical tube. Save 90 μL of clarified extract for the “total input” quality control sample that will be analyzed via Western blot (Fig. 2).
5. Measure protein concentration of clarified extract (*see Note 17*).

3.6 Pre-wash Anti-FLAG Dynabeads™

1. For 5 g of tissue from 10-day-old plants, use 250 μL of cross-linked anti-FLAG Dynabeads™ (*see Note 18*).
2. During the centrifugation steps, fully resuspend cross-linked anti-FLAG Dynabeads™ (made in Subheading 3.1) with rotation at 4 °C.
3. Add 500 μL of SII buffer without inhibitors to a microcentrifuge then add exactly 250 μL of cross-linked anti-FLAG Dynabeads™ to the buffer (*see Note 18*).
4. Spin down tube to collect any liquid from cap and place on magnetic stand for 1 min to capture beads. Remove supernatant.
5. Complete buffer exchange by washing beads twice more for 3 min in 900 μL SII buffer without inhibitors in a microcentrifuge tube. Always spin down tubes to collect liquid from caps then place tubes on the magnetic stand to capture beads for 1 min before removing washes, making sure to not disturb the beads.
6. After 2 washes, resuspend beads in 400 μL of SII buffer and keep on ice until ready for the immunoprecipitation step.

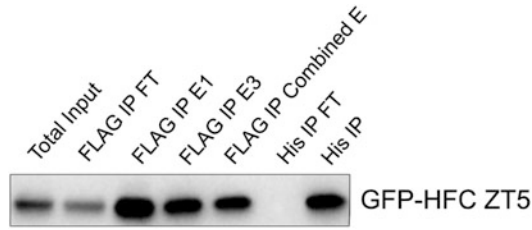


Fig. 2 Immunoblot treated with anti-FLAG antibody at 1:10,000 concentration. Figure shows quality control samples from a tandem affinity purification of 35S::GFP-6x-His-3x-FLAG (HFC). Ideally, there is little HFC-fusion protein observed in the flow through samples, and the final His IP sample contains the majority of the original input. The presence of a band in the FLAG IP FT sample indicates that, for this overexpressed protein, we should increase the number of FLAG beads used or increase the time of the FLAG IP incubation to further deplete the tagged protein. *FT* flow through, *E* elution, *IP* immunoprecipitation

3.7 FLAG Immunoprecipitation

1. Place pre-washed anti-FLAG Dynabeads™ (made in Subheading 3.7) on magnetic stand for 1 min and remove supernatant.
2. Use ~500 μ L of extract to resuspend and transfer all washed anti-FLAG Dynabeads™ back into the clarified extract in the 15 mL conical tube.
3. Rinse the 1.5 mL tube that contained washed anti-FLAG Dynabeads™ twice with ~500 μ L extract to ensure that all beads have been transferred to the 15 mL conical tube.
4. Incubate extract with anti-FLAG beads for 60 min with rotation at 4 °C (*see Note 19*).
5. Prepare the FLAG elution buffer during the IP. A volume of 3.6 mL of FLAG elution buffer should be enough for two samples.

3.8 Bead Capture and Washes

1. Spin down 15 mL tubes to collect liquid from caps at $1000 \times g$ at 4 °C for 10 s.
2. Place 15 mL conical tube on a magnetic stand to capture beads.
3. Remove flow through using a 10 mL serological pipette tip with a p1000 pipette tip attached to the end to reduce flow rate and chance of disturbing beads. Save 90 μ L of the depleted extract for the “FLAG IP flow through” quality control sample.
4. Wash Dynabeads™ with 10 mL of His IP buffer without inhibitors for 5 min with rotation (*see Note 4*).
5. Spin down 15 mL tube at $1000 \times g$ at 4 °C for 10 s and place on magnetic stand to capture beads. Remove wash using a 10 mL serological pipette tip with a p1000 tip attached to the end.
6. Repeat wash once more with 10 mL of His IP buffer.

7. On the third wash, use 900 μL of His IP buffer to wash beads off the side of the 15 mL tube and transfer to a 1.5 mL low protein-binding tube. Repeat the wash to transfer all magnetic beads from the 15 mL conical tube to the 1.5 mL tube. Discard wash each time.
8. Wash one more time with 900 μL of His IP buffer in the 1.5 mL tube for a total of three 900 μL washes.

3.9 Elution of Immunoprecipitated Proteins Off Anti-FLAG Beads

1. After removing the last wash from beads, add 400 μL of FLAG elution buffer to beads. Rotate at 4 °C for 15 min.
2. Spin down tubes briefly to collect liquid from caps. Place tubes in magnetic stand to capture beads for 1 min. Remove 1/10th of elution (40 μL) and save in a tube labeled “Elution 1” for quality control. Pipette remaining elution into a low-protein-binding 1.5 mL tube labeled “Combined Elution.”
3. Repeat **steps 1 and 2** at 4 °C one more time, each time saving 1/10th of elution (Elutions 1 and 2) and transferring the remaining elution into the “Combined Elutions” tube.
4. Repeat **steps 1 and 2** at 30 °C twice. Each time save 1/10th of elution (Elutions 3 and 4) and transferring the remaining elution into the “Combined Elutions” tube.
5. After all elution steps, remove 1/20th (~72 μL) of the “Combined Elutions” for the “Combined Elutions” quality control sample.

3.10 Wash His-Tag Isolation Dynabeads™

1. Fully resuspend the Dynabeads™ His-Tag Isolation and Pull-down magnetic beads by rotating bottle at 4 °C.
2. During the elution incubation steps, begin performing wash steps for the Dynabeads™ His-Tag Isolation and Pulldown magnetic beads. For 5 g tissue sample, use 90 μL of His Dynabeads™ (*see Note 20*).
3. Add exactly 90 μL of His Dynabeads™ to 500 μL of His IP buffer in a low-protein-binding microcentrifuge tube that is well labeled (this is the final tube) and pipette up and down to wash all beads from the pipette tip.
4. Place the tube on the magnetic stand to capture beads for 1 min. Remove wash, making sure not to disrupt beads.
5. Complete buffer exchange by washing beads with 500 μL of His IP buffer for 5 min with rotation. Remove wash.
6. Add 500 μL of His IP buffer to beads and let sit on ice until ready for use.

3.11 His Immunoprecipitation and Washes

1. Once all elutions are combined into one tube, remove the supernatant from the washed His Dynabeads™ (prepared in Subheading 3.11) and add the combined eluate to beads.

2. Incubate eluate with His beads for 20 min at 4 °C with rotation.
3. Place tube on magnetic stand to capture beads for 1 min. Remove 1/20th of His IP flow through (~72 µL) for quality control. Remove and discard remaining flow through from beads.
4. Wash beads with 900 µL of His IP buffer for 5 min with rotation at 4 °C.
5. Spin down tube to collect liquid from the lid. Place tube on magnetic stand for 1 min to capture beads. Remove wash, making sure not to disrupt beads.
6. Repeat wash two more times for a total of three 900 µL washes in His IP buffer.
7. For the fourth wash, add 900 µL of sterile-filtered 25 mM ammonium bicarbonate and rotate for 3 min at 4 °C.
8. Repeat ammonium bicarbonate wash three more times, for a total of four washes in ammonium bicarbonate.
9. On the fourth ammonium bicarbonate wash, completely resuspend beads in the buffer. Remove 1/10th of bead suspension (90 µL) for quality control.
10. Spin down tube for 1 min to collect liquid from the lid. Place tube on magnetic stand for 1 min to capture beads. Remove wash.
11. Spin down tube for 1 min a second time, place on magnetic stand, and remove any remaining ammonium bicarbonate buffer from tube.
12. Flash freeze tube in liquid N₂. Samples can be stored at –80 °C for up to 1 year. Samples are now ready for digestion and analysis by LC-MS.

3.12 Quality Control Western Blot

1. Before sending samples for LC-MS analysis, it is good practice to perform a Western blot on quality control samples to ensure bait proteins were effectively immunoprecipitated.
2. We recommend running the following samples for the quality control gel: total input, FLAG IP flow through, FLAG elutions 1–4, combined FLAG eluate, His IP ammonium bicarb suspension, and His IP flow through. For the His IP suspension sample, spin down tube and remove supernatant from beads. Resuspend beads in 30 µL of 2× SDS sample buffer. Add 4× SDS sample buffer to all other quality control samples to 1× concentration and boil for 10 min to denature.
3. Run the quality control samples on an SDS-PAGE gel and transfer to nitrocellulose membrane. Probe for your bait protein using either a native antibody, anti-His antibody, or anti-

FLAG antibody. If possible, use another antibody to detect a known protein interactor to ensure protein-protein interactions were maintained and co-precipitated throughout procedure.

4. Figure 2 shows a sample Western blot from a successful tandem affinity purification using this protocol.

4 Notes

1. Recommendations for the design of affinity-tagged proteins:
 - (a) We recommend using a 6x-His-3x-FLAG tandem affinity tag at the C-terminus of your protein unless the modification of the C-terminus will likely result in functional disruption.
 - (b) Transform your affinity-tagged protein into a null mutant background so that the native protein is absent to maximize interaction between your tagged protein and its partners.
 - (c) Expression level of the transgene can affect the level of nonspecific binding in your immunoprecipitation; we recommend testing the ability of the affinity-tagged plant in rescuing the mutant background. Ideally, the tagged protein should rescue mutant phenotypes back to wild-type levels.
2. Use of detergents in buffers used for sample preparation for mass spectrometry can cause damage to mass spectrometer equipment and interfere with proper quantification of peptides. Conversely, complete removal of detergents from these buffers inhibits immunoprecipitation of bait proteins and co-immunoprecipitation of interacting proteins using Dynabeads™ in our experience. The detergent concentrations used in these buffers have yielded effective protein extraction and binding to affinity beads without causing damage or interference while using the LTQ-Velos Pro Orbitrap LC-MS/MS.
3. Once dissolved in isopropanol solution, PMSF has a short half-life. Use within 1 h.
4. The His IP buffer does not contain chelating agents EDTA and EGTA as these agents can chelate the cobalt from the His-isolation Dynabeads™ and render them inactive. Do not use chelating agents in any steps involving the His-isolation Dynabeads™. Thus, SII buffer cannot be used in any of the steps involving His Dynabeads™.
5. Instead of cross-linking your antibody to Protein G beads from scratch, you may purchase Dynabeads™ that are pre-cross-linked to the antibody. If purchasing pre-cross-linked beads,

avoid beads made of or coated in sepharose, amylose, or any other carbohydrate. Many plant proteins will bind to carbohydrate resins, which will increase nonspecific binding.

6. The cross-linking protocol takes approximately 2.5 h to complete, not including running the SDS-PAGE quality control gel.
7. A regular scale preparation is 1.2 mL cross-linked bead solution per tube. Therefore, 200 μ L of 1 μ g/mL anti-FLAG M2 antibody will be added to 1.2 mL of Protein G beads.
8. For affinity purification using antibodies generated in rabbits, Protein A Dynabeads™ can be substituted. For Protein A cross-linking, replace Na-citrate pH 5.0 with Na-phosphate pH 8.0 buffer in the Protein A Wash Buffer.
9. It is important to add exactly 200 μ L of antibody to each tube to maintain an identical background of cross-linked beads for all immunoprecipitations.
10. If you are seeing flow through of antibody after incubation with Protein G beads (as determined by Coomassie stain of an SDS-PAGE gel), you may need to decrease the amount of antibody added or increase the time of incubation with the beads. See Fig. 1 for an example of a successful cross-linking quality control gel.
11. If antibody is dissociating from Protein G Dynabeads™ (there is a heavy chain band in the post-cross-link sample on the Coomassie stain of the quality control SDS-PAGE gel), increase cross-linking time with DMP or purchase new DMP if stock is old. See Fig. 1 for an example of a successful cross-linking quality control gel.
12. Do not incubate cross-linked Dynabeads™ in 0.2 M glycine for more than 1 min. Overexposure to glycine can cause the cross-linked antibody to strip off the beads.
13. Expression and stability of clock-associated proteins are often modulated by the intensity, wavelength, and duration of light as well as temperature. Consider these factors when selecting growth conditions.
14. If collecting tissue at a dawn or dusk transition, collect the tissue under the light condition prior to the transition. For example, if collecting at dawn—the time of the dark-light transition—then collect tissue under darkness. This will prevent accumulation of light-induced or light-stabilized proteins that would normally be absent. Alternatively, take additional time points before and after the environmental transition to capture any dynamic interactions.
15. If collecting during the dark period, tissue may be collected under dim green light. Ensure that all other sources of light are

blacked out to ensure full darkness and to avoid activation of photoreceptor light-signaling pathways.

16. The affinity purification protocol starting from the protein extraction and sonication step typically takes between 6 and 9 h to complete.
17. For 5 g of tissue resuspended in 12 mL of SII buffer, we typically measure between 2 and 5 mg/mL of total protein content. You can measure protein concentration using a detergent-compatible method such as the DC Protein Assay from Bio-Rad.
18. You may need to optimize the volume of beads used during the IPs. If there is a high amount of flow through of the tagged bait protein observed in the quality control immunoblot, we recommend increasing the bead volume from 250 μ L. You may also experiment with using fewer beads to find the lowest bead input you can use to deplete your bait protein.
19. You may need to optimize the incubation time of your extract with the anti-FLAG beads. We recommend incubation for 60 min to capture your bait protein and any interacting proteins. However, if you notice there is high flow through of your bait protein after a 60-min incubation (as determined in your quality control Western blot (Fig. 2)), you may want to increase the time of your FLAG IP.
20. The binding capacity of the His Dynabeads™ is listed as 40 μ g of a 28 kDa histidine-tagged protein/mg (25 μ L) of beads. You may want to adjust the volume of His beads used depending on the total protein content measured from the extract and your estimates of total His-tagged bait protein.

Acknowledgments

M. L. Sorkin is supported by NSF GRF award number DGE-1745038. This protocol is based upon material analyzed using an Orbitrap Fusion Lumos LC-MS/MS supported by the National Science Foundation under Grant No. DBI-1827534.

References

1. Van Leene J, Eeckhout D, Cannoot B et al (2015) An improved toolbox to unravel the plant cellular machinery by tandem affinity purification of Arabidopsis protein complexes. *Nat Protoc* 10:169–187. <https://doi.org/10.1038/nprot.2014.199>
2. Besbrugge N, Van Leene J, Eeckhout D et al (2018) GSyellow, a multifaceted tag for functional protein analysis in monocot and dicot plants. *Plant Physiol* 177:447–464. <https://doi.org/10.1104/pp.18.00175>
3. Creux N, Harmer S (2019) Circadian rhythms in plants. *Cold Spring Harb Perspect Biol* 11(9): a034611. <https://doi.org/10.1101/cshperspect.a034611>
4. Huang H, Alvarez S, Bindbeutel R et al (2016) Identification of evening complex associated

proteins in Arabidopsis by affinity purification and mass spectrometry. Mol Cell Proteomics

15:201–217.

<https://doi.org/10.6019/PXD002606>.Each



Firefly Luciferase Complementation-Based Analysis of Dynamic Protein-Protein Interactions Under Diurnal and Circadian Conditions in *Arabidopsis*

Qiguang Xie, Qiao Wang, and Xiaodong Xu

Abstract

Split firefly luciferase complementation assay (FLCA) is one of the most widely used sensitive and reliable methods for the analysis of constitutive and dynamic protein-protein interactions (PPIs). Here, we report a method for long-term in vivo detects plant protein-protein interactions in *Arabidopsis* F1 hybrids via Topcount™ Microplate Scintillation Counter or Deep-Cooled CCD camera. Following these protocols, we successfully detected time-dependent PPIs of EARLY FLOWERING 3 (ELF3) and EARLY FLOWERING 4 (ELF4); both of them with LUX ARRHYTHMO (LUX) belong to an evening complex which has been found to play a key role in circadian rhythms, flowering, and growth.

Key words Dynamic protein-protein interactions, Firefly luciferase complementation, Bioluminescence, Diurnal rhythm, Circadian rhythm

1 Introduction

Circadian (~24-h) clocks enable organisms to coordinate with diurnal cycles of light (photoperiod) and temperature (thermoperiod); it constitutes essential timing mechanisms regulating almost all of the physiological processes [1, 2]. According to the global transcriptome analysis, there are about 89% of *Arabidopsis* transcripts which show rhythmic expression patterns in at least one condition (thermocycles, photocycles, or circadian conditions) [3]. Protein-protein interactions (PPIs) are critical for gene expression, signal transduction, metabolic pathways, intracellular transport pathways, etc. [4]. These suggest that if just focusing on constitutive or static protein-protein interactions, we must lose a lot of important time-related information.

There are many methods to investigate PPIs: some of them are in vitro methods like affinity purification or tandem affinity

purification (TAP), co-immunoprecipitation (co-IP), cross-linking protein interaction analysis, etc.; some of them are *in vivo* methods, such as yeast two hybrid (Y2H), bimolecular fluorescence complementation (BiFC), fluorescence resonance energy transfer (FRET), bioluminescence resonance energy transfer (BRET), etc.; and the others are *in silico* [5]. Each of them has its own strengths and weaknesses, and sensitivity and specificity are the main criteria for judging a method's quality. Luciferase complementation assays (LCAs) are one of the most powerful approaches for visualizing PPIs in cells and living organism nowadays.

Luciferase is a generic term for the class of oxidative enzymes that produces bioluminescence [4, 6]. There are two types of luciferase grouped by their substrates. Type I are firefly luciferase (FLuc) and other beetle luciferases oxidize D-luciferin, and type II are Renilla luciferase (RLuc), Gaussia luciferase (GLuc), and Nano-Luc (NLuc) which oxidize coelenterazine or its analogues. Although there is no amino acid sequence similarity between these two types of luciferases, they all can be used as LCA by splitting into two subunits [7–14]. In the LCA, complementary DNA (cDNA) of luciferases is first split into the N- and C-terminal fragments and then fused to cDNAs of a protein pair of interest; when the fusion proteins interact with each other, making the N- and C-terminal luciferase close enough, the enzyme activity of luciferase could be recovered at the same time. Compared with type II luciferases, FLCA has a long-lived glow kinetics and low background; the signals of FLCA are still strong enough after a week, even if one single seedling moves to each well of 96-well plates which is measured by Topcount™ multi-detector microplate scintillation counter [15]. For these reasons, FLCA is better for detecting long-term PPIs over few days.

We cloned two full-length genes, *ELF3* and *ELF4*, which belong to the evening complex (EC) and peak at dusk in *A. thaliana*, and then generated two transgenic lines which carry N-terminal or C-terminal LUC fusion constructs fusion constructs, *ELF3:ELF3-nLUC* or *ELF4:ELF4-cLUC*. After harvesting the F1 crossed seeds, use young F1 hybrids with both constructs to detect long-term bioluminescence signals under light/dark cycles or continuous light conditions. The interaction of *ELF3* and *ELF4* shows robust rhythm phenotype which suggests that split firefly luciferase should become the preferred reporter for investigating dynamic PPIs in circadian or other time-specific studies in plants.

2 Materials

2.1 Plasmids, Vectors, Strains, and Plants

1. Cloning donor vectors (pENTR™ 1A, kanamycin resistance gene for selection in *E. coli*, and pCR8/GW/TOPO TA Cloning Vector, spectinomycin resistance gene for selection in *E. coli*).

2. Destination vectors (pH2GW7ΔP35S, spectinomycin in *E. coli* and hygromycin in plants; pMDC123, kanamycin in *E. coli* and BASTA in plants).
3. *Agrobacterium tumefaciens* (strain GV3101) cells.
4. *Arabidopsis* seedlings (*A. thaliana*, ecotype Col-0) (*see Note 1*).

2.2 Media, Buffers, and Reagents

1. 95% or 100% Ethanol.
2. Bleach.
3. Luria-Bertani (LB) medium containing appropriate antibiotics (filter-sterilized).
4. Half-strength Murashige and Skoog medium (*see Note 2*) with 0.8% agar and 2% sucrose. The pH is adjusted to 5.8. Appropriate antibiotics (filter-sterilized) are added to select for the plasmid. We also add 500 μg/mL carbenicillin to select against residual *Agrobacterium*.
5. D-luciferin (potassium salt): 2.5 mM in water. We typically make a 100 mM stock solution which we store frozen and dilute 40-fold for use (*see Note 3*).

2.3 Apparatus

1. iKon-M Deep-Cooled CCD (Andor Technology) (*see Note 4*).
2. Topcount™ Microplate Scintillation Counter (PerkinElmer) (*see Note 5*).
3. White 96-well microtiter plates (we typically use white Opti-plates; PerkinElmer) and also clear 96-well microtiter plates (*see Note 6*). TopSeal (PerkinElmer), a clear adhesive plastic sealant for the 96-well microtiter plates.

3 Methods

3.1 Full-Length Gene Cloning, Vector Construction, and Transformation

1. PCR products of full-length genomic DNA of candidate genes (*ELF3* and *ELF4*) including promoter and 3' untranslated region (UTR) were amplified from *Arabidopsis* Col-0 genomic DNA with appropriate primer pairs and then cloned into Gateway™ pENTR™ or pCR8/GW/TOPO TA Cloning Vectors. The stop codons of target genes were then replaced with paired SfiI restriction sites (GGCCGTCAAGGCC and GGCCTCATGGGCC) through PCR amplification, and then a modified *nLUC* or *cLUC* fragment flanked by SfiI sites was inserted to in-frame of target genes translational fusions (Fig. 1).

Primers (5' to 3') used to amplify *ELF3*, *ELF4*, *nLUC*, and *cLUC*:

ELF3-Locus-F, GATAACCGCAACTAGATTCTTCCTGAG.

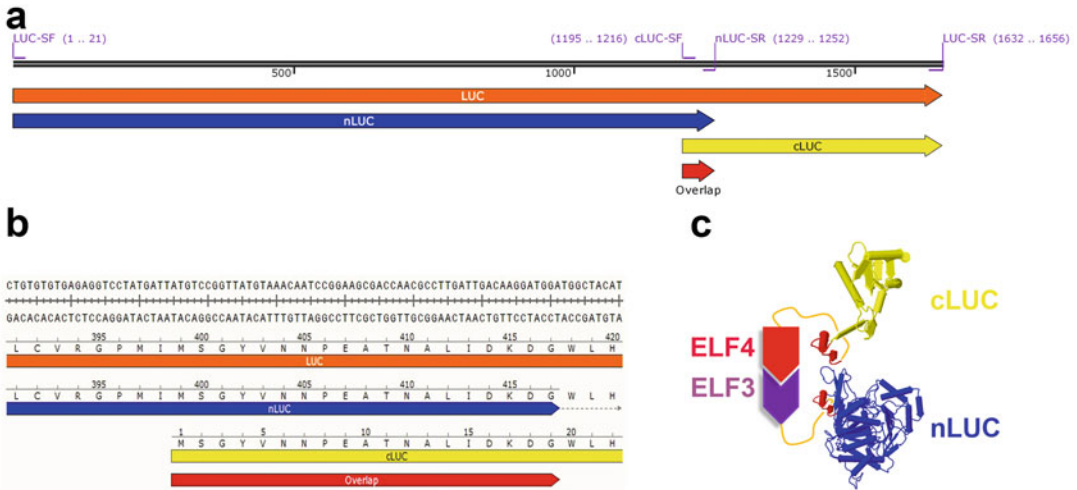


Fig. 1 The principle of FLCA technology. **(a)** Schematic representation of the position of PCR primers which are used to amplify the *nLUC* and *cLUC*. **(b)** The DNA coding sequence and translated amino acid sequence of overlapping region in both *nLUC* and *cLUC*. **(c)** N- or C-terminal firefly luciferase fusing with ELF3 (purple) and ELF4 (red), respectively. N-terminal, overlap region, and C-terminal of LUC which are shown as blue, dark red, and yellow

ELF3-Locus-R, CGTCTCCGCCCTATATTAATCGA
TGTC.

ELF3-SfiI-F, GCTGGCCTTGACGGCCAGGCTTAGAG
GAGTCATAGCGTTTAC.

ELF3-SfiI-R, GCTGGCCTCATGGGCCTAATCCTCTC
TATGCGTATTGTACTTG.

ELF4-Locus-F, CTA CGT TGT GTT TTC TAG AAA
AAG AG.

ELF4-Locus-R, CTGGACTGGTACCTAATGTGTTATC.

ELF4-SfiI-F, GCTGGCCTTGACGGCCAGCTC
TAGTTCGGCAGCACCAC.

ELF4-SfiI-R, GCTGGCCTCATGGGCCTAATGAACCG
GAATCAAATTGTTTC.

LUC-SF, GACGGCCGTCAAGGCCACATGGTCACC
GACGCCAAAAC.

nLUC-SR, CGGCCATGAGGCCTTATC
CATCCTTGTCAATCAAGGCGT.

cLUC-SF, CGGCCGTCAAGGCCACATGTCCGGT
TATGTAAACAATC.

LUC-SR, GTCGGCCATGAGGCCTTACACGGC
GATCTTCCGCCCTTC.

- The donor constructs were then recombined into pH2GW7ΔP35S (deleted p35S region from pH2GW7) [16] or pMDC123 [17] (Fig. 2).

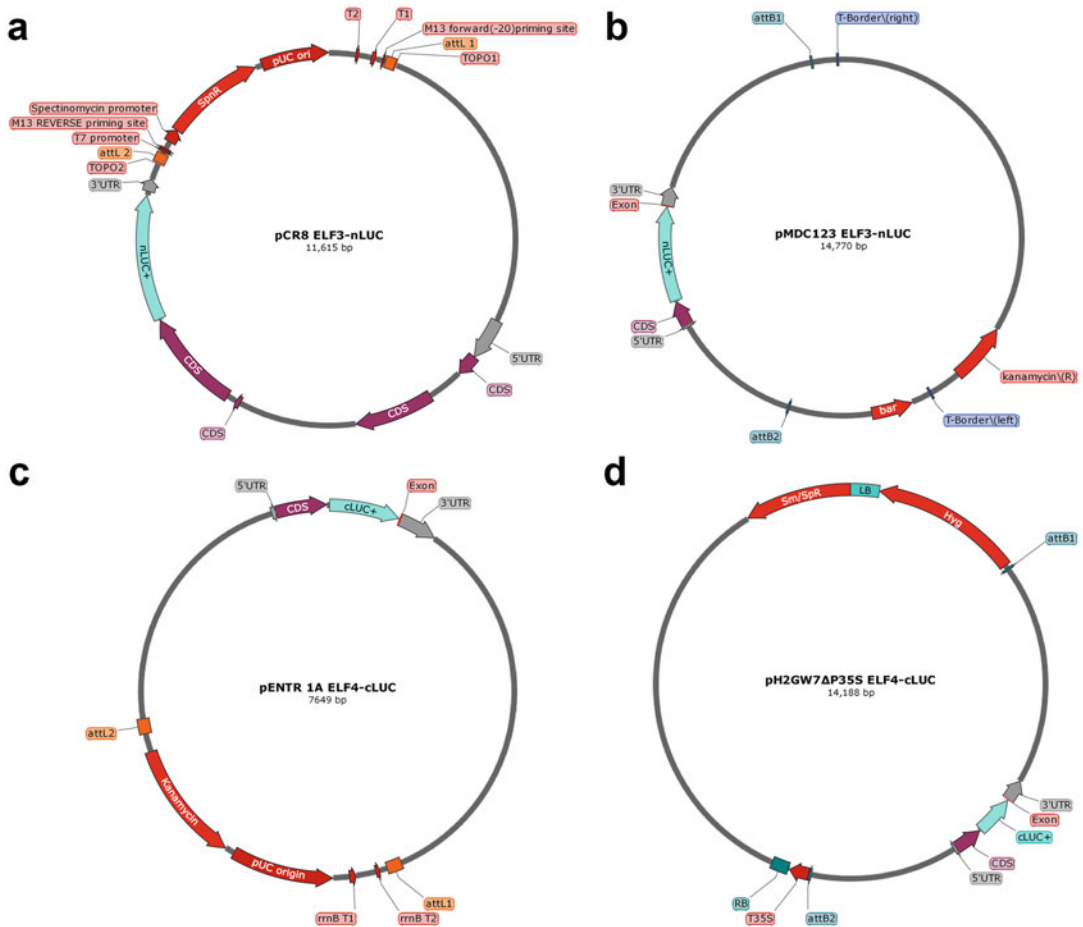


Fig. 2 Generating *ELF3* and *ELF4* *nLUC/cLUC* fusion constructs; four panels show the circular maps of pCR8 *ELF3-nLUC* (a), pMDC123 *ELF3-nLUC* (b), pENTR 1A *ELF4-cLUC* (c), and pH2GW7ΔP35S *ELF4-cLUC* (d). Full-length *ELF3* and *ELF4* genes and C-terminal *nLUC/cLUC* fusion donor constructs had been recombined into the binary vector pMDC123 or pH2GW7 from which the CaMV 35S promoter had been deleted (pH2GW7ΔP35S) by Gateway LR recombination

3. Full-length gene C-terminal *nLUC/cLUC* fusion constructs were independently transformed into *Arabidopsis Col-0* to yield stable transgenic lines, and then two transgenic lines which carry *ELF3:ELF3-nLUC* and *ELF4:ELF4-cLUC* were crossed; F1 hybrids seeds were harvested for the measurement of LUC complementary activity.

3.2 Split-LUC Complementation Assay

1. Soak seeds of F1 hybrids in sterile water for 3 min, and then soak in 70% ethanol for 3 min. Decant. Soak in 10% bleach for 10 min (shaking a few times). Decant. Rinse five times (3 min per rinse) in sterile distill water.

2. Germinate sterilized F1 hybrids seeds on one-half strength MS medium plus 2% sucrose and 0.8% agar in petri dishes. Stratify for 3 days at 4 °C cold room to synchronize germination.
3. Take out the plates and put them into growth chamber under entraining conditions (light-dark cycles, constant temperature, such as 12L/12D, 22 °C) for 7–10 days or until primary true leaves are emerging.
4. Carefully transfer seedlings using sterilized long tweezers into white 96-well plates pre-filled with 180 µL solid medium described above (*see Note 7*), add 30 µL fresh D-luciferin solution (2.5 mM), and then apply plate seals (TopSeal; PerkinElmer) to the top surface of the plates; 2 holes should be punched in the area just above each plant/well with a smallest size syringe needle to allow gas exchange.
5. All plates should be put back into the growth chamber under the entraining conditions described above for one more LD cycle/day.
6. After one day recovery, plates were transferred onto the Topcount™ (very sensitive, suitable for any signal strength of LCA) or CCD camera (only suitable for brighter signal strength of LCA) to collect data (We typically image for 10 min at 2-h intervals via CCD, and 30-min to 2-h intervals via TopCount depends on how many plates we measuring) (*see Notes 8 and 9*) (Fig. 3).

4 Notes

1. Although we describe methods in F1 hybrids transgenic Arabidopsis seedlings, these protocols should also be adapted for Arabidopsis or tobacco protoplasts, callus or tissue culture from other plant species which transformed with plasmids expressing split FLuc fusion proteins.
2. We ordered dry powder MS medium premixed from Phyto-Technology Laboratories. Usually, we add 2% sucrose to the one-half strength MS medium as this permits sustained robust rhythmicity especially for experiments running in continuous dark (no less than 1% sucrose). However, it is important to note that sucrose should not be added over 3% that may affect circadian rhythms [18, 19].
3. We ordered D-Luciferin, Potassium Salt from GoldBio; after making 100 mM stock solution, aliquot 1 mL into 2 mL screw cap tubes, freeze at –20 °C, and protect any unused stock solution from light. We use a syringe-driven Filter Unit (0.22 µm) to sterilize D-luciferin working solution (2.5 mM).

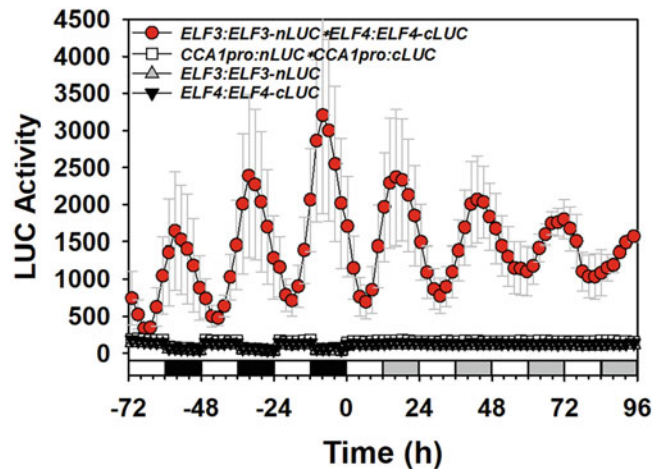


Fig. 3 Application of split luciferase complementation assay (LCA) to study the ELF3 and ELF4 interaction. ELF3 showed dynamic interactions with ELF4 in seedlings under diurnal (12 h light/12 h dark, white and black bars) and free-running (continuous light, white and gray bars) conditions (continuous light, white and gray bars) conditions. Endogenous full-length *ELF3:ELF3* fused to the N-terminal half of firefly *LUC* (*nLUC*) and *ELF4:ELF4* fused to the C-terminal half of firefly *LUC* (*cLUC*). Constructs were independently transformed into *Arabidopsis* to yield stable transgenic lines that were crossed, and LUC activity was measured in F1 heterozygotes. Individual seedlings expressing *ELF3:ELF3-nLUC*, *ELF4:ELF4-cLUC*, and F1 heterozygotes which carry both *CCA1pro:nLUC* and *CCA1pro:cLUC* (*CCA1* promoter driving *nLUC* or *cLUC*) were used as control. Data collected with a TopCount™ luminometer are presented as absolute LUC activities (means \pm SE, $n = 12$)

4. We put Deep-Cooled CCD camera in a well-sealed growth chamber which contains computer-controlled LED lights, so various light regimes and light/dark cycles can be programed. The lights will be turned off prior to imaging and then be turned on again automatically.
5. The TopCount™ Microplate Scintillation Counter (PerkinElmer) with 12 Photomultiplier Tubes (PMT) detectors permits high-sensitivity and high-throughput analyses. The TopCount™ can run completely automatically according to the pre-programed parameters through the software. All sample plates can be loaded in order and in cycles for several days. The TopCount™ produces a TXT file of tab-delimited values for each reading of a plate (the position of each well and photon counts per second of each well with the time it was taken). For experiments in continuous light or in light-dark cycles, we inserted three clear microtiter plates between two sample plates to permit light reaching to the sample plates (TopCount™ should be programed to skip the clear plates and only read sample plates). To permit enough light to reach the plates

inside the stacker, we cut holes on left and right sides of the stacker without compromising its physical integrity and then put LED lights which are controlled by a timer affixed to both sides of the stacker and that allowed us to set the appropriate light-dark cycles, continuous light, or even red and blue light in particular intensity.

6. The 96-well plates for samples must be opaque to avoid bioluminescence contamination between neighboring wells.
7. We prepare the TopCount™ plates 2 days before transferring seedlings; the 96 wells must be filled with 180 µL of solid MS medium supplemented with 2% sucrose. We use a multichannel pipette to load hot medium into the wells row by row. Once the MS medium of each well has solidified, we wrap the plates with aluminum foil and keep them at 4 °C. We took out the plates 3 h ahead of experiment, let them get warm to room temperature, and then add 30 µL fresh D-luciferin working solution.
8. Autofluorescence is the natural emission of plant cellular components, such as chlorophylls and phenolic compounds. For imaging with a CCD camera, we usually set 10 min delay when LED light is off and then start to imaging. For reading plates with TopCount™, we usually set 2 min delay before reading the loaded plate.
9. We first merge a series of LCA frames into one, and then prefer to use the open architecture “ImageJ” program to analyze optical density inside of each well. There are also other commercially available programs that work well, such as “Image-Pro Plus” or “Metamorph.”

Acknowledgments

This work was supported by grants from the National Science Foundation of China (Grant 31670285) and the Hebei Province Science Foundation (Grants 17966304D and E2016100018).

References

1. Greenham K, McClung CR (2015) Integrating circadian dynamics with physiological processes in plants. *Nat Rev Genet* 16(10):598–610. <https://doi.org/10.1038/nrg3976>
2. Nohales MA, Kay SA (2016) Molecular mechanisms at the core of the plant circadian oscillator. *Nat Struct Mol Biol* 23(12):1061–1069. <https://doi.org/10.1038/nsmb.3327>
3. Michael TP, Mockler TC, Breton G, McEntee C, Byer A, Trout JD, Hazen SP, Shen R, Priest HD, Sullivan CM, Givan SA, Yanovsky M, Hong F, Kay SA, Chory J (2008) Network discovery pipeline elucidates conserved time-of-day-specific cis-regulatory modules. *PLoS Genet* 4(2):e14. <https://doi.org/10.1371/journal.pgen.0040014>
4. Wiens MD, Campbell RE (2018) Surveying the landscape of optogenetic methods for detection of protein-protein interactions. *Wiley Interdiscip Rev Syst Biol Med* 10(3): e1415. <https://doi.org/10.1002/wsbm.1415>

5. Rao VS, Srinivas K, Sujini GN, Kumar GN (2014) Protein-protein interaction detection: methods and analysis. *Int J Proteomics* 2014:147648. <https://doi.org/10.1155/2014/147648>
6. Zhou Z, Bi G, Zhou JM (2018) Luciferase complementation assay for protein-protein interactions in plants. *Curr Protoc Plant Biol* 3(1):42–50. <https://doi.org/10.1002/cppb.20066>
7. Ozawa T, Kaihara A, Sato M, Tachihara K, Umezawa Y (2001) Split luciferase as an optical probe for detecting protein-protein interactions in mammalian cells based on protein splicing. *Anal Chem* 73(11):2516–2521
8. Kim SB, Ozawa T, Watanabe S, Umezawa Y (2004) High-throughput sensing and noninvasive imaging of protein nuclear transport by using reconstitution of split Renilla luciferase. *Proc Natl Acad Sci U S A* 101(32):11542–11547. <https://doi.org/10.1073/pnas.0401722101>
9. Paulmurugan R, Gambhir SS (2003) Monitoring protein-protein interactions using split synthetic renilla luciferase protein-fragment-assisted complementation. *Anal Chem* 75(7):1584–1589
10. Kaihara A, Kawai Y, Sato M, Ozawa T, Umezawa Y (2003) Locating a protein-protein interaction in living cells via split Renilla luciferase complementation. *Anal Chem* 75(16):4176–4181
11. Remy I, Michnick SW (2006) A highly sensitive protein-protein interaction assay based on Gaussia luciferase. *Nat Methods* 3(12):977–979. <https://doi.org/10.1038/nmeth979>
12. Dixon AS, Schwinn MK, Hall MP, Zimmerman K, Otto P, Lubben TH, Butler BL, Binkowski BF, Machleidt T, Kirkland TA, Wood MG, Eggers CT, Encell LP, Wood KV (2016) NanoLuc complementation reporter optimized for accurate measurement of protein interactions in cells. *ACS Chem Biol* 11(2):400–408. <https://doi.org/10.1021/acscchembio.5b00753>
13. Kim SB, Otani Y, Umezawa Y, Tao H (2007) Bioluminescent indicator for determining protein-protein interactions using intramolecular complementation of split click beetle luciferase. *Anal Chem* 79(13):4820–4826. <https://doi.org/10.1021/ac0621571>
14. Chen H, Zou Y, Shang Y, Lin H, Wang Y, Cai R, Tang X, Zhou JM (2008) Firefly luciferase complementation imaging assay for protein-protein interactions in plants. *Plant Physiol* 146(2):368–376. <https://doi.org/10.1104/pp.107.111740>
15. Xie Q, Wang P, Liu X, Yuan L, Wang L, Zhang C, Li Y, Xing H, Zhi L, Yue Z, Zhao C, McClung CR, Xu X (2014) LNK1 and LNK2 are transcriptional coactivators in the Arabidopsis circadian oscillator. *Plant Cell* 26(7):2843–2857. <https://doi.org/10.1105/tpc.114.126573>
16. Karimi M, Inze D, Depicker A (2002) GATEWAY vectors for Agrobacterium-mediated plant transformation. *Trends Plant Sci* 7(5):193–195
17. Curtis MD, Grossniklaus U (2003) A gateway cloning vector set for high-throughput functional analysis of genes in planta. *Plant Physiol* 133(2):462–469. <https://doi.org/10.1104/pp.103.027979>
18. Haydon MJ, Mielczarek O, Robertson FC, Hubbard KE, Webb AA (2013) Photosynthetic entrainment of the Arabidopsis thaliana circadian clock. *Nature* 502(7473):689–692. <https://doi.org/10.1038/nature12603>
19. Dalchau N, Baek SJ, Briggs HM, Robertson FC, Dodd AN, Gardner MJ, Stancombe MA, Haydon MJ, Stan GB, Goncalves JM, Webb AA (2011) The circadian oscillator gene GIGANTEA mediates a long-term response of the Arabidopsis thaliana circadian clock to sucrose. *Proc Natl Acad Sci U S A* 108(12):5104–5109. <https://doi.org/10.1073/pnas.1015452108>



Monitoring Seasonal Bud Set, Bud Burst, and Cold Hardiness in *Populus*

Mikael Johansson, Naoki Takata, Cristian Ibáñez, and Maria E. Eriksson

Abstract

Using a perennial model plant allows the study of reoccurring seasonal events in a way that is not possible using a fast-growing annual such as *A. thaliana* (*Arabidopsis*). In this study, we present a hybrid aspen (*Populus tremula* × *P. tremuloides*) as our perennial model plant. These plants can be grown in growth chambers to shorten growth periods and manipulate day length and temperature in ways that would be impossible under natural conditions. In addition, the use of growth chambers allows easy monitoring of height and diameter expansion, accelerating the collection of data from new strategies that allow evaluation of promoters or inhibitors of growth. Here, we describe how to study and quantify responses to seasonal changes (mainly using *P. tremula* × *P. tremuloides*) by measuring growth rate and key events under different photoperiodic cycles.

Key words Photoperiod, *Populus*, Perennial, Critical day length, Bud set, Bud burst, Freezing tolerance, Cold acclimation

1 Introduction

This protocol describes in detail how to grow, measure, and sample *Populus* trees to study their responses under different seasonal cycles. *Populus*, a temperate woody perennial with a life span of many years, has been established as a model plant for deciduous tree species [1]. These growth characteristics mean a very long time is required to follow responses to seasonal changes in natural conditions. By artificially inducing seasonal changes in a growth chamber, researchers can study these processes in a shorter time frame and identify plausible triggering factors that cannot be distinguished under field conditions. Specifically, we use environmentally controlled growth chambers to manipulate day length and temperature to trigger seasonal responses in *Populus*.

As an example, we use data previously published by Ibáñez et al. [2] where wild-type lines and lines with downregulated levels of core clock genes were grown and examined for almost 14 weeks (*see* Fig. 1).

Plants are initially grown under long day, growth-promoting conditions (4 weeks). The long days are of critical importance for perennial species, since they become dormant and thus do not grow under short day conditions. The plants are then shifted to 15 h photoperiods (6 weeks), below the wild-type critical day length (CDL), which is defined as the day length under which at least 50% of the trees stop growing and start the entry into dormancy (*see* **Note 1**). Next, the plants are shifted to a 14 h photoperiod (~7.5 weeks) to capture the difference between the genotypes. After the bud set is scored, the plants are moved to artificial winter conditions (18 weeks at 6 °C and short day (SD) of 8 h light and 16 h dark, 8:16). For instance, plant lines with downregulated levels of circadian gene expression clearly have a CDL shorter than wild type (*see* Fig. 1a). After the artificial winter period, the plants are transferred to warm long days again, and bud burst is scored (*see* Fig. 1b). For bud burst to be scored, plants need their chilling requirement fulfilled, and in our hands, 6 weeks of chilling appear too short, while 8 weeks or more will promote a normal bud burst. Figure 2 shows an example of the frequency of bud burst in plants that have received less or more chilling.

2 Materials

1. Environmentally controlled growth chambers: As *Populus* is a fast-growing tree species that can grow to considerable heights, use growth chambers with ample head room and a light intensity of about 200 $\mu\text{mol photons/m}^2/\text{s}$ and the possibility to freely manipulate light and temperature periods (*see* **Note 2**).
2. Substrate: To accommodate growth of *Populus* trees, use a mix of perlite and fertilized peat (1:3 perlite:peat) as the soil medium, for example, P-jord (Hasselfors, Sweden).
3. Pots: *Populus* trees require plenty of space for their roots to develop normally, so use large pots (height 11 cm \times width 10 cm \times radius 10 cm). During their initial growth, protect the trees using plastic bag coverings supported by plastic or wooden sticks.
4. Tools: Carpenter's ruler to measure height.
5. Digital caliper to measure diameter.
6. Colored stickers to tag leaves, branches, or any other part of the plants when they need to be marked to follow growth (e.g., the

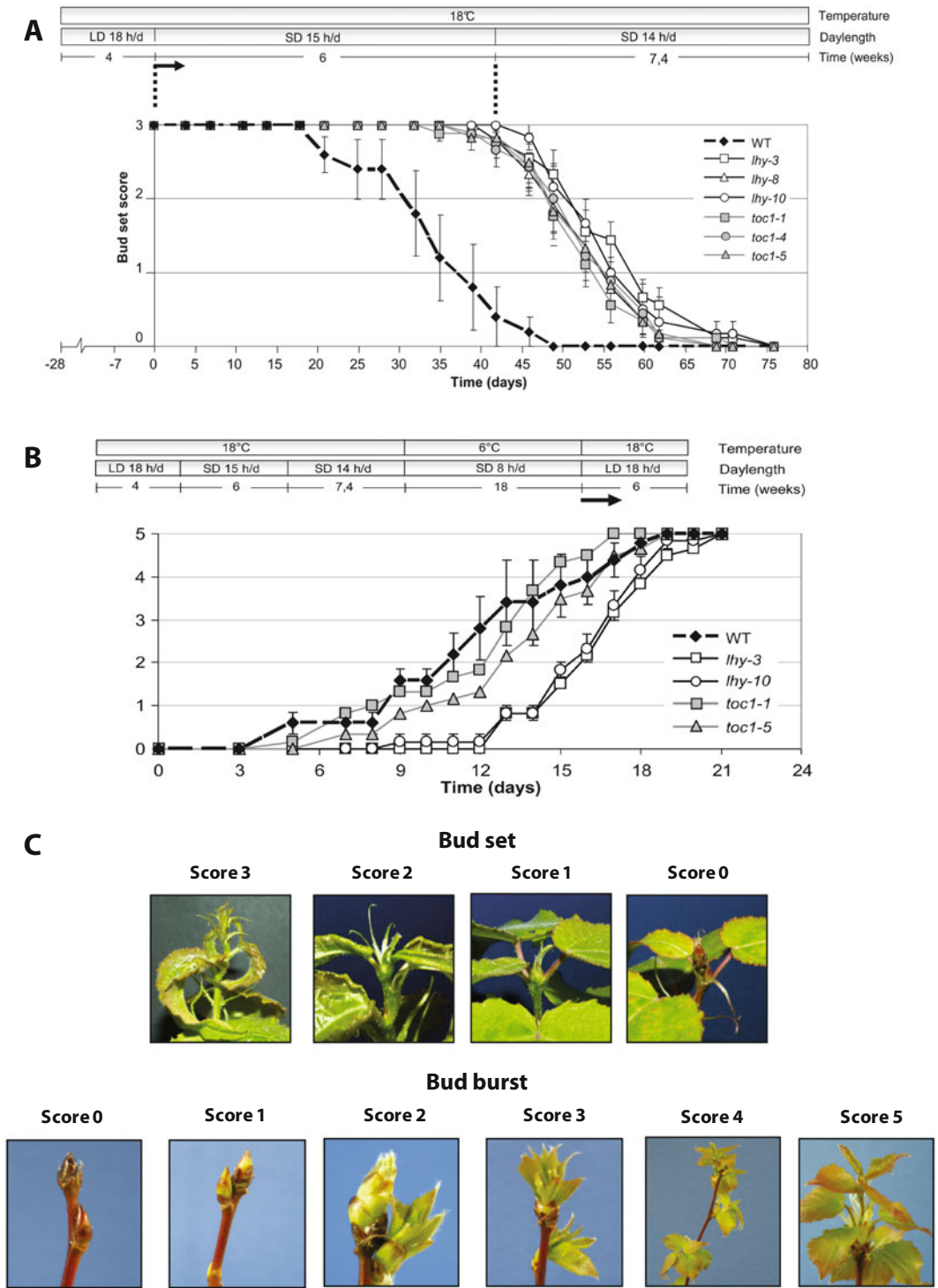


Fig. 1 (a) Bud set and (b) bud burst in *Populus* trees with reduced clock gene expression. (c) Bud score images for bud set and bud burst, showing typical buds at the different growth stages. (Ibáñez et al, *Plant Physiol* 2010;153:1823-1833. Copyright 2010 by American Society of Plant Biologists)

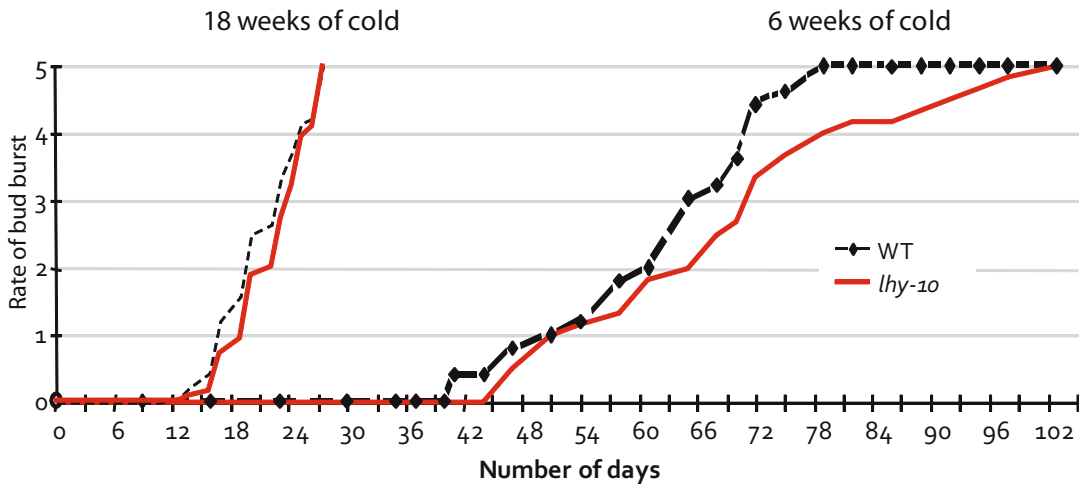


Fig. 2 Illustration of how the response of bud burst is depending on the length of the cold treatment in *Populus*. (Ibáñez et al, *Plant Physiol* 2010;153:1823-1833. Copyright 2010 by American Society of Plant Biologists)

number of internodes produced during a certain time) or marked for sampling.

7. Fertilizer: To ensure optimal growth, use a good quality fertilizer such as Weibulls Rika S NPK 7-1-5 and dilute 1–100.
8. Freezing tests: Freezing cabinet to maintain temperatures below -70°C (e.g., 500/80–180DU, Weiss Umwelttechnik GmbH, Germany).
9. Electro-conductivity meter (B-173, Horiba Ltd., Japan) to test freezing tolerance.

3 Methods

3.1 Propagation/ Initiation

1. Propagate the plant material for the study. This protocol was originally based on work with cultured plants [3, 4], but the procedure is the same if the plants are propagated from cuttings (or seeds) [5].
2. Before transferring cultured plants to soil in individual pots, prepare all the pots with well-watered soil and gather all other necessary equipment. The plants are sensitive to dehydration and other environmental disturbances when removed from their culturing conditions, so transplant the trees in a timely manner (*see Note 3*).
3. Open the container with the plants, measure their initial height, and swiftly move them to the soil (*see Note 4*). The final samples should be at least 10 cm at initial height. Then cover the pots with transparent plastic bags (usually supported by two plastic or wooden sticks placed in the soil).

4. One week after planting, cut the corners of the plastic bags. After 2 weeks, remove the plastic bags entirely and start measuring height. Fertilization of the plants should occur once a week and be started at the beginning of the second week.
5. Randomize the plants and then rotate once a week to ensure each plant is grown under similar light, temperature, humidity, and air flow conditions (*see Note 5*). This control for consistent conditions is done by moving each plant three to five steps to the left, depending on the sample size and area constraints.

3.2 Growth

1. Initially, grow the trees under growth-promoting long day conditions: typically 18 h days and 6 h nights with a temperature of 18 °C and light intensity of about 200 $\mu\text{mol photons/m}^2/\text{s}$. In our study, the *Populus* wild type has a CDL of about 15.5 h. When handling light signaling and clock component RNAi or overexpressing trees, their CDL conditions may require a much longer day length (*see Note 1*).
2. Measure growth, from soil to shoot apex, at least once a week with an accuracy of 0.5 cm. When the plants have a stem diameter of at least 2 mm, measure stems width 10 cm above soil every week (*see Note 6*). These measurements reflect how the trees grow under “optimal” growth conditions (*see Note 7*). For many studies of growth, it may be important to use a developmentally scaled measure such as the plastochron index. See Erickson and Michelini [6] for details.

3.3 Winter Dormancy Measurements

3.3.1 Critical Day Length (CDL), Growth Cessation, and Bud Set

1. When the trees reach a desirable size and/or when sufficient data is gathered to compare growth under long days, shorten the day length below the CDL, taking specific genotypic requirements into account. Usually the time of lights on is kept constant, and the photoperiod is shortened from the point of lights off. Plants re-entrain in about 3 days. Such day-length shortening will induce growth cessation and bud set. At this point fertilization of the trees is stopped. To compare the response of trees, the growth of the trees is measured until they stop growing in order to capture the cessation of the reduced growth increment over time and the average number of days needed by each plant to complete bud set. In addition, further statistical analyses can be performed (*see below*). Measuring twice a week during this phase gives a good resolution.
2. Score bud set concomitantly with height, and any other measurements should be conducted twice a week according to the predefined scale [7] (three for vegetative growth and zero for bud set) (*see Note 8*) (Fig. 1c). If more precision is desirable, see Rohde et al. [8] for a more detailed scale.

3. At this stage, it may be beneficial to estimate the CDL by setting the day length to a desirable period, the period when CDL is estimated to begin. If the trees do not respond to this after 4 weeks by stopping growth and setting buds, the day light period can be shortened. When about 50% of the trees stop growth and set buds, the CDL is reached. For detailed information, see Olsen et al. [9].
4. After all plants (or a sufficient number, *see Note 9*) set buds completely and are dormant, grow them under artificial winter conditions for about 8 weeks: short day conditions (8 h light, 16 h dark); light intensity of about 20 $\mu\text{mol photons/m}^2/\text{s}$; and at a constant low temperature (+6 °C). These conditions and period ensured that the plants fulfil their chilling requirement and are responding to external conditions in an “online” or “eco-dormant” state [10], ready to restart their growth. Temperatures between 0 and 15 °C are effective for breaking dormancy, with the optimum generally around 5 °C [11, 12].

Figure 2 illustrates the importance of proper chilling: plants were maintained at +6 °C for 6 weeks compared to 18 weeks.

3.3.2 Freeze Test

To probe the trees’ resistance to cold and thus their ability to survive a cold winter period, a freeze test of the stem material is performed. We do this by measuring the electrolyte leakage [8, 10] as well as by using a visual score [2].

1. Cut stem sections of about 20–60 cm beneath the shoot tip into small pieces (1 mm in the tangential direction \times 5 mm in the radial direction \times 15 mm in the axial direction).
2. Place 3 or 4 pieces in a test tube containing 0.5 mL of distilled water. Maintain several test tubes, at least three, at 4 °C in the dark. The fresh, unfrozen samples are used as a baseline to estimate injury or no injury.
3. Keep the test tubes at -2 °C for 30 min in a programmable freezer.
4. Freezing of samples in the test tubes is uniformly initiated by seeding with ice chips, and samples are kept at -2 °C for an additional hour.
5. Cool samples at a rate of 2 °C/h to the given temperatures.
6. Soon after reaching the given temperatures, withdraw the test tubes from the freezer and thaw them overnight at 4 °C in the dark.
7. Add 2.5 mL aliquot of distilled water to each test tube and incubate the tubes at room temperature for 6 h with gentle shaking in the dark.

8. Measure the electrolytes in the distilled water released from the frozen-thawed tissues (C_T) by using the electro-conductivity meter.
9. After measurement, boil the tubes containing the samples for 10 min to induce complete injury.
10. Again gently shake the tubes for 2 h at room temperature in the dark, and measure the amount of electrolytes in distilled water (C_{Tk}).
11. The percentage of freezing injury is calculated as $100 \times (C_T / C_{Tk} - C_0 / C_{0k}) / (1 - C_0 / C_{0k})$, where C_0 is determined as the amount of electrolytes from fresh tissues and C_{0k} is determined as the amount of electrolytes after boiling the fresh tissues.
12. By plotting the percentage of freezing injury at different freezing temperatures, the temperature at which 50% of the cells were injured (LT_{50}) can be determined (*see* Fig. 3a).

3.3.3 Visual Score of Freeze Injury

In addition to measuring electrolyte leakage as an indicator for freezing resistance, you can score the injury visually as follows.

1. After trimming the remaining tree segments for electrolyte analyses, they can be assessed for visual injury after 3 weeks of storage at about 10 °C and 100% relative humidity.
2. The photosynthetic parenchyma cells ≥ 5 mm away from the segment ends are examined under bright white light for signs of discoloration. Indices of injury of 0%, 25%, 50%, 75%, and 100% are assigned to no discoloration, initial and final discoloration of the inner parenchyma, and initial and final discoloration of the outer parenchyma, respectively (discoloration of inner parenchyma is completed before discoloration of outer parenchyma starts). This is quantified in Fig. 3b, c illustrates the visual difference in injury between wild type and plants with reduced *LHY1* and *LHY2* expression.

3.3.4 Bud Burst

1. By increasing the temperature and day lengths (e.g., 18 h light, 6 h dark at 18 °C), you induce a “spring” response and evoke bud burst. Also, using constant light is an established method to force bud burst [13].
2. The rate of bud burst is followed by a scoring system according to the six developmental stages of bud burst (stage 0–5) developed by UPOV [14] and applied to hybrid aspen in Ibáñez et al. [2] (Fig. 1c). Score bud burst three times a week because it is a very fast phenological change given the chilling requirement has been fulfilled. The buds typically need less than 3 weeks to resume elongation growth.
3. After all (or a majority, *see* Note 9) of the trees start to grow again, you can assume that an artificial seasonal growth cycle of

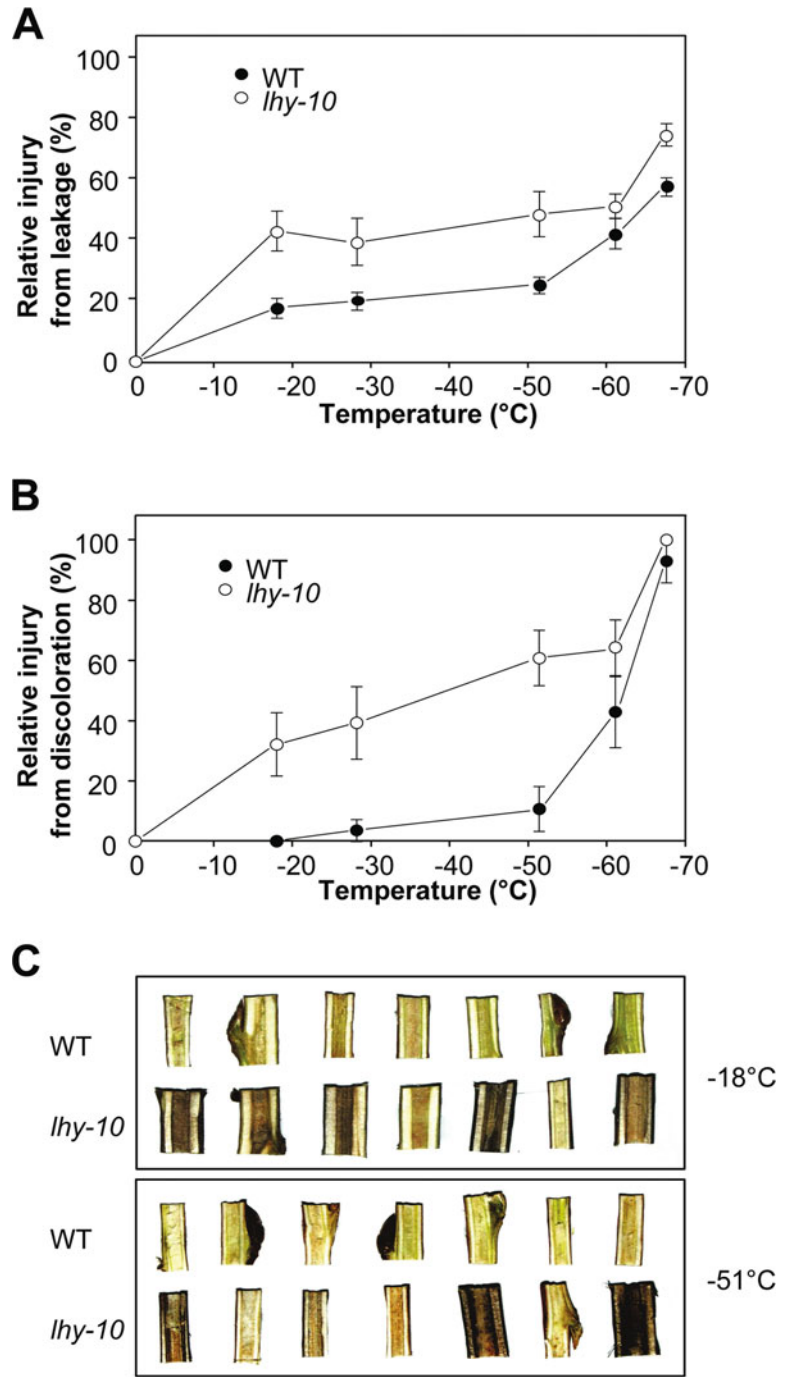


Fig. 3 (a) is relative injury as assayed by electrolyte leakage, (b) is relative injury as assayed by visual scoring, and (c) is photo of stem pieces used to score injury

Populus is achieved, allowing you to measure one season's growth (*see* Note 10).

3.4 Statistical Processing of Data

To confirm differences between lines, two-way ANOVA or paired *t*-tests can be used, but there are also more exhaustive ways to describe the results, as described in the following example from Kalcsits et al. [15].

Days of induction treatment until growth cessation can be calculated using a curve fitting software, for example, TableCurve 2D (SPSS Inc., Chicago, IL, USA), which helps find the best fitting equation [15]. Regression curves can then be created using the best-fit equation: in this example, $y = a + bx^3$, where y is growth increment, x days of induction, and a and b best fit constants derived from the equation and growth data [15]. By fitting regression curves to each plant, the date of growth cessation can be estimated by finding the x -intercept point ($x = 0$). Rate of growth cessation (cm per week) can then be determined by calculating the slope of the linear part of the growth curve.

Longer time to bud break can be interpreted as a higher level of dormancy. Bud break/depth of dormancy can be calculated as the difference between the days to bud break (DBB) at the final day of measurements and days to bud break at day 0 [15]. Rate of bud break can then be determined from the slope of the dormancy induction curve: $y = a + b/[1 + \exp(-(x - c)/d)]$, where a is the minimum DBB, b the depth of dormancy [maximum DBB (y) - minimum DBB (y)], c the center point (x , days) of inflection, and d a constant derived from the data. An alternative treatment can be studied in Ghelardini et al. [11].

3.5 Sampling of Material for Transcript or Protein Analysis

During these growth cycles, it may make sense to sample leaves, stems, buds, or other parts to examine transcript and/or protein levels (*see* Note 11). As the size of the trees often limits the amount of replicates, randomize sampling such that individual trees do not bias the results. Ideally, sample leaves in the same developmental stage. This is done by counting from the apex the number of leaf primordia equal to or exceeding 1 cm in length (*see* Fig. 4). The internode below that leaf is the first counted internode. We typically used the leaves growing on internodes 8–11, as defined in Fig. 4, which provides young, expanded leaf and internode material for transcript and protein analysis. Preferably, a pool of at least three leaves (from different trees) for each sample should be used.

If collecting a time series requires many replicates, consider to take leaf number 8–10 in a random manner or internode number 8 from the first, number 9 from the second, and number 10 from the third tree to establish a pool of material that is “developmentally averaged.” Also, especially for time series, do not overharvest leaves; we sample random trees but ensure that any one tree is not

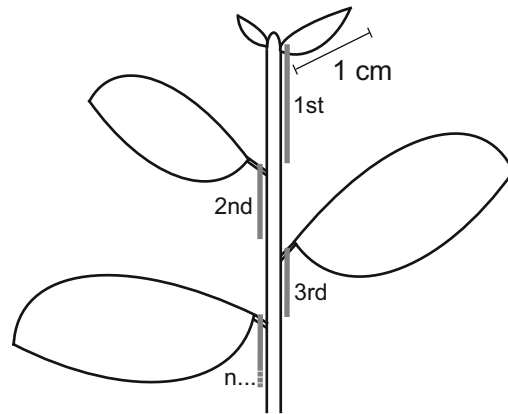


Fig. 4 Illustration of how to count the internodes on a *Populus* plant. The first counted internode is the one starting under the first primordial leaf exceeding 1 cm in length. Then the internodes are counted down the stem as illustrated

sampled at the next sampling (after 2 or 4 h), so they are available from the next third time point.

If the stem is sampled for analysis, other than the fact that this is the last sampling of the trees, the part of the stem that is used should be considered. Tissue above the tenth internode from the bud consists mainly of primary tissue. Material older/growing below the tenth internode constitutes secondary tissues (i.e., phloem, cambium, and xylem). The 20th internode is usually a good area to sample, as it contains mature phloem, cambium, and xylem.

4 Notes

1. CDL greatly varies depending on what latitude the ecotype originates from. For example, the hybrid aspen T89 genotype, a common wild-type control, has a critical day length of 15.5 h [16], which means that day lengths at and below 15.5 h will induce bud set in 50% of the tested population [9, 15, 17].
2. Remember that as the trees grow closer to the light sources, the light intensity received by them will increase. This effect can be limited by initially growing the trees on tables and subsequently moving them to the floor as they grow.
3. Survival rate of plants moved from culturing conditions to soil is >95% for the hybrid aspen T89 wild type.
4. Avoid potting plants that are too small as their roots are easily damaged during transplanting. The plants to be transplanted should have a height of around 10 cm and have well-developed roots. If using in vitro cultured plants, also avoid potting plants

that are so large that they have grown into the lid of the propagation container, as this may result in disturbed growth at later stages.

5. Avoid crowding the plants as this may impair growth and make it difficult to make measurements inside the chamber.
6. Do not measure the diameter at the actual nodes, as this will skew your measurements.
7. Expected growth rate of *Populus* trees is around 10–20 cm, or around 10% per week under optimal growth conditions.
8. When buds reach a bud score of 0, they are hard and have a prickly and shiny appearance.
9. As some plants may refuse to enter dormancy or resume growth due to unknown internal factors, when at least 6 plants or preferably 90% or more of the population has set bud, it is reasonable to proceed with further treatments.
10. This protocol describes the study of certain seasonal key events and provides ample room for additional treatments during other growth studies. It could, for example, be used when studying specific wavelengths of light, during the dark period, or when studying growth under suboptimal temperature conditions as when working with light receptor RNAi or over-expressor trees [18].
11. Use a green light when samples are collected during the night, as other wavelengths are more likely to trigger a light response [19].

Acknowledgments

The authors are grateful for financial and other support from various funding bodies and institutions. MJ is supported by a scholarship from the Alexander von Humboldt Foundation and through SPP1530 (DFG). CI is supported by FONDECYT grant no. 1110831 (CONICYT—Chile).

MEE is a VINNMER Marie Curie International Qualification Fellow funded by the Swedish Governmental Agency for Innovation Systems (VINNOVA) and the European Union, with current support from the Swedish Research Council (VR), Umeå University Career Grant, and Carl Trygger Foundation for Scientific Research. Further MEE would like to acknowledge the Department of Plant Sciences and Churchill College at Cambridge University and Umeå Plant Science Centre and the support from the VR- and VINNOVA-funded Berzelii Centre of Forest Biotechnology, FORMAS, the Kempe Foundation, and Stiftelsen Nils och Dorte Troëdssons forskningsfond.

References

1. Jansson S, Douglas CJ (2007) *Populus*. A model system for plant biology. *Annu Rev Plant Biol* 58:435–458
2. Ibáñez C, Kozarewa I, Johansson M, Ögren E, Rohde A et al (2010) Circadian clock components regulate entry and affect exit of seasonal dormancy as well as winter hardiness in populus trees. *Plant Physiol* 153:1823–1833
3. Nilsson O, Aldén T, Sitbon F, Anthony Little CH, Chalupa V et al (1992) Spatial pattern of cauliflower mosaic virus 35S promoter-luciferase expression in transgenic hybrid aspen trees monitored by enzymatic assay and non-destructive imaging. *Transgenic Res* 1:209–220
4. Eriksson ME, Israelsson M, Olsson O, Moritz T (2000) Increased gibberellin biosynthesis in transgenic trees promotes growth, biomass production and xylem fiber length. *Nat Biotechnol* 18:784–788
5. Dickmann DI, Isebrands JG, Eckenwalder JE, Richardson J (eds) (2002) *Poplar culture in North America*. NRC Research Press, Ottawa
6. Erickson RO, Michelini FJ (1957) The plastochron index. *Am J Bot* 44:297–305
7. Rohde A, Prinsen E, de Rycke R, Engler G, van Montagu M et al (2002) PtABI3 impinges on the growth and differentiation of embryonic leaves during bud set in poplar. *Plant Cell* 14:2975
8. Rohde A, Bastien C, Boerjan W (2011) Temperature signals contribute to the timing of photoperiodic growth cessation and bud set in poplar. *Tree Physiol* 31:472–482
9. Olsen JE, Junttila O, Moritz T (1997) Long-day induced bud break in *Salix pentandra* is associated with transiently elevated levels of GA1 and gradual increase in indole-3-acetic acid. *Plant Cell Physiol* 38:536–540
10. Rohde A, Bhalerao RP (2007) Plant dormancy in the perennial context. *Trends Plant Sci* 12:217–223
11. Ghelardini L, Santini A, Black-Samuelsson S, Myking T, Falusi M et al (2010) Bud dormancy release in elm (*Ulmus* spp.) clones—a case study of photoperiod and temperature responses. *Tree Physiol* 30:264–274
12. Perry TO (1971) Dormancy of trees in winter. *Science* 171:29–36
13. Welling A, Rinne P, Viherä-Aarnio A, Kontunen-Soppela S, Heino P et al (2004) Photoperiod and temperature differentially regulate the expression of two dehydrin genes during overwintering of birch (*Betula pubescens* Ehrh.). *J Exp Bot* 55:507–516
14. UPOV (1981) Guidelines for the conduct of tests for distinctness, homogeneity and stability in Poplar (*Populus* L). International Union for the Protection of New Varieties of Plant, Geneva
15. Kalcits LA, Silim S, Tanino K (2009) Warm temperature accelerates short photoperiod-induced growth cessation and dormancy induction in hybrid poplar (*Populus* × spp.). *Trees Struct Funct* 23:971–979
16. Olsen J, Junttila O, Nilsen J, Eriksson M, Martinussen I et al (1997) Ectopic expression of oat phytochrome A in hybrid aspen changes critical daylength for growth and prevents cold acclimatization. *Plant J* 12:1339–1350
17. Tanino KK, Kalcits L, Silim S, Kendall E, Gray GR et al (2010) Temperature-driven plasticity in growth cessation and dormancy development in deciduous woody plants: a working hypothesis suggesting how molecular and cellular function is affected by temperature during dormancy induction. *Plant Mol Biol* 73:49–65
18. Kozarewa I, Ibáñez C, Johansson M, Ögren E, Mozley D et al (2010) Alteration of PHYA expression change circadian rhythms and timing of bud set in *Populus*. *Plant Mol Biol* 73:143–156
19. Arana MV, La Marin-de Rosa N, Maloof JN, Blazquez MA, Alabadi D et al (2011) Circadian oscillation of gibberellin signaling in *Arabidopsis*. *Proc Natl Acad Sci U S A* 108:9292–9297



Chapter 18

The Perennial Clock Is an Essential Timer for Seasonal Growth Events and Cold Hardiness

Mikael Johansson, Cristian Ibáñez, Naoki Takata, and Maria E. Eriksson

Abstract

Over the last several decades, changes in global temperatures have led to changes in local environments affecting the growth conditions for many species. This is a trend that makes it even more important to understand how plants respond to local variations and seasonal changes in climate.

To detect daily and seasonal changes as well as acute stress factors such as cold and drought, plants rely on a circadian clock. This chapter introduces the current knowledge and literature about the setup and function of the circadian clock in various tree and perennial species, with a focus on the *Populus* genus.

Key words Circadian clock, Perennial plants, *Populus*, Seasonal regulation, Cold tolerance, Bud set, Bud burst, Growth

Abbreviations

8:16	8-h light: 16-h dark daily cycle
ABA	Abscisic acid
BOA	BROTHER OF LUX ARRHYTHMO
CCA1	CIRCADIAN CLOCK ASSOCIATED1
CDL	Critical day length
CHE	CCA1 HIKING EXPEDITION
CO	CONSTANS
EBI	EARLY BIRD
EC	Evening complex
ELF	EARLY FLOWERING
FKF1	FLAVIN BINDING, KELCH REPEAT, F-BOX1
FT	FLOWERING LOCUS T
GA	Gibberellic acid
GI	GIGANTEA
HY5	ELONGATED HYPOCOTYL 5
IAA	Indole-3-acetic acid
JMJD5	JUMONJI DOMAIN CONTAINING 5

LHY	LATE ELONGATED HYPOCOTYL
LKP2	LOV KELCH PROTEIN2
LUX	LUX ARRHYTHMO
PRR	PSEUDO RESPONSE REGULATOR
SD/LD	Short day/long day
TOC1	TIMING OF CAB2 EXPRESSION 1
ZTL	ZEITLUPE

1 Introduction

Most of what is known about the circadian clock in higher plants is derived from the model plant *A. thaliana* (Arabidopsis), where extensive studies on the molecular level have been performed. The MYB transcription factors CIRCADIAN CLOCK ASSOCIATED1 (CCA1) and LATE ELONGATED HYPOCOTYL (LHY), together with the PSEUDO RESPONSE REGULATOR family members PRR1/TIMING OF CAB2 EXPRESSION 1 (TOC1), PRR3, PRR5, PRR7, PRR9 as well as the GIGANTEA (GI) protein have been shown to be core regulators of circadian rhythm, forming at least three interconnected transcriptional-translational feedback loops [1, 2]. CCA1, LHY, and TOC1 form a core loop of the clock, repressing each other's expression [3, 4]. CCA1 and LHY regulate *TOC1*, *LUX ARRHYTHMO* (*LUX*), *GI*, *EARLY FLOWERING 3* (*ELF3*), *ELF4*, *CCA1 HIKING EXPEDITION* (*CHE*), *JUMONJI DOMAIN CONTAINING 5* (*JMJD5*), and *BROTHER OF LUX ARRHYTHMO* (*BOA*), also known as *NOX*, to repress their expression [3, 4]. TOC1 not only influences expression of *CCA1* and *LHY* but also of *PRR7*, *PRR9*, *GI*, and the Evening Complex (EC) components—*ELF3*, *ELF4*, and *LUX* [5–7]. The EC binds to the promoters of several other clock-related components and represses the expression of *ELF4*, *GI*, *LUX*, *TOC1*, and *PRR9* [1]. *BOA/NOX* activates *CCA1* by binding to its promoter, and *CHE* and *JMJD5* repress the expression of *CCA1* [5, 8–10].

TOC1 levels, which are inversely proportional to the speed of the clock [11], are regulated by ZEITLUPE (ZTL). ZTL and GI control the degradation of the TOC1 protein [11, 12]. ZTL has two additional members in its protein family—FLAVIN BINDING, KELCH REPEAT, F-BOX1 (FKF1), and LOV KELCH PROTEIN2 (LKP2)—that are involved in regulation of the clock, at least in the absence of ZTL [13–15]. ZTL interacts with the transcription factor EARLY BIRD (EBI), but does not control its degradation as with TOC1 [16]. Instead, it modulates the effect of EBI to fine-tune the expression of clock components, linking transcriptional regulation with the ZTL-mediated ubiquitination pathway. GI is a large protein that is involved in the temperature

compensation mechanism of the clock and has a role in photoperiodic flowering by regulating *CONSTANS* (*CO*) [17–19]. It has also been described to have roles in cold tolerance and in salt tolerance responses [20, 21].

PRR9, *PRR7*, and *PRR5* are expressed in sequence, starting with light activation of *PRR9* in the morning and subsequent expression of the other members repressing the expression of *CCA1* and *LHY*, forming what is sometimes referred to as the morning loop [22–24]. *PRR5* regulates phosphorylation and nuclear import of *TOC1* and is targeted for degradation by *ZTL* [25, 26]. *PRR3* is only expressed in vascular tissues and is involved in controlling the stability of *TOC1* [27]. This rather complex network of interactions has recently been described in more detail by Nagel and Kay [1], Troncoso-Ponce and Mas [28], and Nakamichi et al. [29].

2 Perennial Clocks

To study seasonal regulation as well as the role of the circadian clock, researchers use a perennial plant species with a long life-span, as in the *Populus* genus. This model species belongs to the Rosids, like *Arabidopsis* [30, 31] and allows researchers to perform comparative studies to elucidate the function(s) of clock-related components in a perennial woody plant. Such comparative studies of transcriptomes have shown that cyclic patterns of many clock genes are conserved in different plant species including *Populus* [32], providing some evidence of the need of an endogenous timer through evolution. The importance of an inner, functional clock that matches and resets to environmental conditions has been experimentally shown in cyanobacteria [33], *Arabidopsis* [34–37], and *Populus* trees [38, 39]. In *Populus*, the circadian clock involves setting the proper phase of *CO* and *FT* expression [40, 41] and proper growth cessation also depends on important regulators of cell division activity such as *AINTEGUMENTALIKE 1* [42, 43]. For a recent review, see Singh et al. [42].

3 The *Populus* Clock

The importance of a properly functional endogenous clock to detect seasonal events has been demonstrated by studying *Populus* trees with downregulated core clock proteins [39]. Downregulation by RNAi of *LHY1* and *LHY2* genes together or of *TOC1* led to a shorter circadian period, evidence that they are involved in regulating the speed of the clock.

The *LHY* and *CCA1* genes are highly conserved among plant species. Phylogenetic studies in the woody model plant species *P. trichocarpa* have shown that two *LHY* genes have been created through duplication events, *LHY1* and *LHY2* [44], where *LHY2* has significantly higher expression levels than *LHY1*. The high expression may be due to activation of *LHY2* by *LHY1* and/or *LHY2*, as the promoter of *LHY2* contains four *CCA1* binding elements that promote activation of the Arabidopsis light-harvesting chlorophyll a/b protein gene *LHCBI*3* and *CCA1* itself [45]. The *LHY1*'s promoter reveals no such binding elements when querying the 2.5 kbp sequence upstream translational start of these genes using the SoGoDB database [46]. In Arabidopsis, the progenitors of *CCA1* and *LHY* were duplicated in the whole genome duplication event that occurred in *Brassica* species and separately from the *LHY* duplication in *Populus* species, although they all share a common ancestor [44]. Thus, the two *LHY* genes may share the roles that *CCA1* and *LHY* play in other plants. However, *Populus* contains only one *TOC1* gene orthologue, which is expressed at an earlier phase than its Arabidopsis counterpart [39]. In addition, *TOC1* has also been shown to repress *LHY1* and *LHY2* expression under constant dark and cold conditions [39].

Interestingly, as the *LHY* genes have been shown to be targets of natural selection, they may play an important role in environmental adaptation [47]. Furthermore, circadian clock associated genes in *P. tremula* show elevated protein evolution rates, which indicate rapid evolution in these genes [48].

Clock associated *PRR* genes are conserved among many angiosperm species, with seven copies existing in *P. trichocarpa* (including *PRR1/TOC1*), compared to five in Arabidopsis [49], exhibiting the loss of *PRR3* and duplications of *PRR5(a and b)*, *PRR7(a and b)*, and *PRR9(a and b)*. This loss of *PRR3* in *Populus* might indicate a different setup of the circadian clock in *Populus* species due to a different regulation of posttranslational events, as the vascularly expressed *PRR3* in Arabidopsis affects protein stability of *PRR1/TOC1* [27]. Absence of *PRR3* has also been suggested in chestnut [50]. The duplication and deletion of clock components through plant evolution may be due to altered dosages of the different genes involved in the regulation of the clock. Expression of other clock associated/regulated genes, such as *PRR5*, *FKF1*, and *GI*, has a similar pattern in *Populus* as in Arabidopsis (and rice) [32], with their expression peaks in *Populus* showing an advance in phase in *LHY1* and *LHY2* RNA interference (RNAi) lines, indicating that they are under control of *LHY1* and/or *LHY2* [32, 39]. *ZTL* genes, *ZTL1* and *ZTL2*, are also present in the *Populus* clock, and, as with its Arabidopsis homologue, no obvious cycling in gene expression pattern has been reported [51, 52].

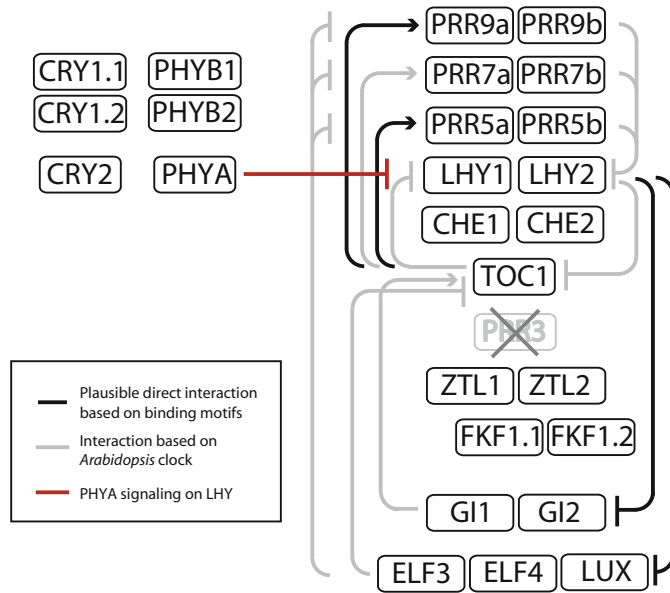


Fig. 1 Predicted setup of photoreceptors and circadian clock components in *Populus* based on knowledge of gene orthologues to their counterparts in *Arabidopsis* and their possible interactions/connections. Black arrows indicate possible direct interaction

In addition *ELF3*, *ELF4*, and *LUX* are found in *Populus*, perhaps playing roles in the clock [51, 52]. Figure 1 describes the putative setup of the circadian clock in *Populus* species, including apoproteins for photoreceptors/putative receptors in the red and blue wavelengths phytochromes (PHYs), cryptochromes (CRYs), ZTLs, and FKF1s [42].

4 Seasonal Regulation by the Clock

Temperate tree species stop growing and initiate bud set and dormancy when the length of day is below a critical value, the critical day length (CDL) [53]. CDL was shortened in trees with lower expression levels of either *LHYs* or *TOC1*, prompting them to grow when wild-type trees stopped, indicating that it is the circadian clock that is setting the CDL in *Populus* trees [39]. Hence, the clock is acting downstream of photoperiod perception involving photoreceptors, such as phytochrome A (phyA) [38, 54]. Another important aspect mediated of phyA perception [38, 54] is short-day-induced cold acclimation in hybrid aspen trees [55]. This cold tolerance is reduced in trees with lower levels of *LHY1* and *LHY2*, while it is increased in trees with lower *TOC1* levels because of their increased *LHY1* and *LHY2* expression. These results show the importance of proper detection of day length and action of the

clock components LHY1 and LHY2, where TOC1 inhibits *LHY* expression. A functional clock (with its genes' expression kept intact) is crucial for survival since it synchronizes growth cessation, cold, and freezing tolerance with the onset of winter conditions [39].

As mentioned previously, photoreceptors are essential for the plant's ability to measure light and thus day length [56]. In *Populus* three phytochromes have been described: *PHYA*, *PHYB1*, and *PHYB2* [57].

Studies with increased and reduced levels of heterologous oat *PHYA* in *Populus* indicate that *phyA* plays a role in growth cessation, bud set, and cold response [54, 58, 59]. Plants with reduced *PHYA* gene expression show lengthening of circadian clock controlled gene expression, and *LHY2* expression is up-regulated by far-red light pulses in trees with reduced levels of *PHYA*, suggesting that the period lengthening is due to modulated *LHY1* and *LHY2* levels [38]. Therefore, it can be concluded that light input through *phyA* is involved in setting the correct phase and pace of the clock. In addition, the flowering-related genes—*PttCO1* and *PttCO2* as well as *FLOWERING LOCUS T1 (FT1)* and *T2 (FT2)*—have been implicated in seasonal regulation in *Populus* as their phases of expression correlate with the bud set behaviour of photoperiodic ecotypes over a latitudinal range [40, 60]. The two FT proteins control the transition from juvenile to reproductive stages during growth and the CO/FT module is involved in growth cessation and bud set. *FT1* and *FT2* are differentially expressed with *FT1* suggested to be a regulator of reproductive onset and *FT2* of vegetative growth [48].

5 Clocks in Other Perennial Plant Species

Circadian output rhythms have been observed in many tree species with the first notable examples in classical times from the army of Alexander the Great [61]. Even if little is known about their molecular mechanisms there are some studies that have addressed this issue.

In the ancient gymnosperm *Ginkgo biloba* *LHCB* gene, mRNA continues to cycle under constant conditions, a clock-modulated response that is also seen in flowering plants [62].

Putative orthologues of Arabidopsis *CCA1* and *GI* with cycling expression patterns have been observed in *Eucalyptus* hybrids [63]. Ectopic expression of clock homologues from Norway spruce (*Picea abies*), *PaCCA1*, *PaGI*, *PaZTL*, and *PaPRR1* in Arabidopsis suggest that protein function of these gene products are at least partly preserved compared to its Arabidopsis counterparts [64]. It also suggests that the three-loop network setup of the clock was present before plants evolutionary split between angiosperms and

gymnosperms. Several putative circadian gene orthologues have been described in grapevines—*CCA1*, *ELF4*, *GI*, *ELONGATED HYPOCOTYL 5* (*HY5*), *LHY*, *PRR7*, *PRR9*, and *ZTL*—and are also believed to be involved in floral transition [65]. *CCA1* and *PRR7* have expression peaks similar to its Arabidopsis counterparts in studies performed during berry development [66]. Intriguingly, the authors of this paper do not report a *TOC1* gene. Papaya circadian genes cycle with the same phase as Arabidopsis genes, although the clock setup seems to differ slightly [67]. There is only one *ZTL* family member in papaya, compared to three in Arabidopsis, and there is only one *LHY* homologue of *CCA1/LHY* and five *PRRs* in papaya, the same number of *PRRs* as in Arabidopsis.

In *Castanea sativa* and *Populus*, the circadian rhythms are disrupted by cold winter periods [68, 69]. Interestingly, mRNA levels of *CsLHY*, *CsTOC1*, *CsPRR5*, *CsPRR7*, and *CsPRR9* are constantly elevated in chestnut during prolonged cold [68, 69]. A similar expression in response to cold can also be observed for the *Populus* clock genes *LHY1*, *LHY2*, and *PRR5* [39]. In Arabidopsis, however, the amplitude of clock component cycles is dampened or disrupted during diurnal cold conditions after a short initial cold response [70]. It has been shown that Arabidopsis mutants of *CCA1* and *LHY* are impaired in cold hardiness because these MYB factors bind to and induce the expression of *C-REPEAT BINDING FACTOR 1* (*CBF1*), *CBF2*, and *CBF3* during cold response [70–72]. There are also clear differences in regulation of *CCA1* and *LHY* gene expression with respect to amplitudes suggesting there are putative differences in how the cold affects central clock gene expression in Arabidopsis and hardy boreal plants.

Leafy spurge (*Euphorbia esula*) is another species with a perennial life cycle that has been developed as a model system for studying herbaceous perennial plants [73, 74]. Circadian clock genes of Leafy spurge have been described as key regulators of physiological activity, dormancy, and flowering [75, 76].

6 Seasonal Processes: Bud Set, Dormancy, and Bud Burst

A widely studied process of seasonal growth is bud set—the end of the growth period and the initiation of bud dormancy [77, 78]. The timing of bud set is important because it initiates the end of the growing season and the beginning of dormancy, a strategy that allows the plant to survive winter. Through its control of the CDL, the circadian clock has an important role in controlling this balance [39]. There are, however, differences in responses, depending on species and latitude. The ability to sense photoperiod and adapt to the local environment is highlighted in studies that focus on latitudinal responses of various tree species [79–84]. For example, northern (northern Sweden) and southern (Romania)

populations of *Picea abies* respond differently to short days: only one night of 16 h is needed to induce bud set in the northern population, whereas four nights of 16 h are needed to induce bud set in the southern population [85]. Different factors seem to have different weight over latitude: for woody species, night length is more important in southern than northern populations and light quality is more important in northern than southern populations [78].

Dormancy is the inability to initiate growth during favourable conditions [86]. In the early or very late dormant stages, plants will respond with growth when moved to favourable conditions, so the dormancy at this stage is reversible. When plants enter dormancy, they need their chilling requirement to be fulfilled before responding to favourable growth conditions [87]. Another aspect influencing seasonal responses is the age of the tree. Short days induce growth cessation and dormancy in young *Salix pentandra* and *Salix caprea* seedlings, whereas older trees growing under natural conditions in high latitudes do not seem to be regulated by photoperiod [88]. In addition, some temperate tree species (e.g., apple and pear) are insensitive to the photoperiod, but instead respond to low temperature [89]. However, over-expression of a *CBF* gene has been reported to result in short-day induced dormancy and increased cold hardiness in apple trees [90]. This suggests that there is a complex interaction between day length and temperature requirements, likely balanced by the circadian clock, which play important roles in both.

7 The Role of Phytohormones in Seasonal Regulation

Different hormones are also involved in the regulation of seasonal processes; an important factor of photoperiodic control of dormancy and bud break is the hormone gibberellic acid (GA) [91]. GA biosynthesis is involved in the photoperiodic control of growth in hybrid aspen. That is, increased levels of bioactive GA affect transcript levels of genes such as *LHY1*, *LHY2*, and *TOC1* [92]. In addition, ethylene has been shown to be involved in terminal bud formation of birch [93]. An increase of ABA levels precedes development of bud dormancy and cold hardiness, while the auxin indole-3-acetic acid (IAA) decreased with increasing cold hardiness and dormancy, suggesting a role for several hormones in photoperiodic control of growth and dormancy [42, 94, 95]. In cotton and the flower *Stellaria longipes*, a daily rhythmicity of ethylene-related genes under different photoperiodic conditions has been demonstrated [96–98]. In *Populus*, photoperiod, ABA and ethylene control bud formation, growth cessation, and dormancy acquisition in response to short days [99]. In Arabidopsis,

the connection between hormones and the circadian clock has been well established [100–103]. Thus are further studies likely to reveal a more expanded role for hormones in perennial clocks.

8 Temperature Effects in Dormancy

As briefly described above, another important factor is temperature. Presumably, temperature responses may help short-term acclimatization for trees [83]. Warmer temperatures also hasten bud formation. In fact, the bud formation process is mainly influenced by temperature and not by shortening photoperiod [83], with the winter chilling requirement of buds as a way to ensure that trees do not resume growth too early and suffer damage due to unfavourable conditions. The role of the endogenous clock is probably to signal that the environment is suitable for resumed growth, depending on a fulfilled chilling requirement, but the mechanism is currently not understood.

On the other end of the seasonal spectrum, the clock ensures that the tree starts growth cessation *in time* to fulfil the chilling requirement during winter dormancy [104]. Also, the dormancy process is likely to be under epigenetic control [105], reviewed in [42]. Plants can thus resume bud growth when they have received a sufficient chilling period, but they wait until the temperature is favourable [86]. Although temperature has a strong influence, *LHY1* and *LHY2* expression are essential for the timing of this reactivation emanating in bud burst [39]. Additionally, the timing of bud burst in Norway spruce seedlings is affected by temperature during bud set and dormancy induction [106, 107].

Recently the apricot *SOCI-like* gene (*ParSOCI*), closely related to *SOCI* which acts downstream of the circadian clock in setting flowering time in *Arabidopsis*, has been shown to have a diurnal expression pattern and is linked to chilling requirements for apricot dormancy break [108].

While oak species have also been studied for their molecular regulation of bud burst, clock genes were not specifically addressed [109]. Further, studies on timing of bud burst using grape wine, black currants and raspberries offer insight to dormancy release [110, 111].

It is possible to override winter and induce dormancy release by treating plants with heat shocks or hydrogen cyanamide to force them respond to oxidative or respiratory stress [110, 112]. As metabolic clocks respond to redox cycles and include hyperoxidized peroxiredoxins [113, 114], it appears likely that the circadian clock's performance would be affected by these treatments that advances the timing of bud burst.

Extended growing seasons due to climate warming have been shown to trigger a counter-intuitive phenology-driven response in many plants. For example, *P. balsamifera* has recently been shown to exhibit both bud set and bud burst earlier in the season, advancing the active growth period [115]. Fitter and Fitter [116] found that 385 plants growing in Oxfordshire, England, exhibited significant changes in their flowering time (16% of them had advanced their flowering). Interestingly, the perennial shrub *Buddleja davidii* showed the reverse phenotype, exhibiting delay in its flowering by 36 days. Under these conditions, *Buddleja* would need a longer chilling requirement and thus would delay flowering. This suggests that dormancy and aspects of it, such as the chilling requirement, is of particular interest for understanding the mechanisms plants might use to counteract the effects of temperature changes. Improper chilling fulfillment can lead to reduced growth and survival as well as creates mismatch between organisms such as plants and their pollinators, thereby affecting ecosystems more widely. Although genetic variation may be able to compensate for climate changes to a certain extent, there are some northern ecotypes of *P. balsamifera* harbouring unique variation associated with early bud set that is not found elsewhere and may be at risk of disappearing [117].

9 Outlook

It is clear that the endogenous circadian clock is important for seasonal regulation, but how it acts to mediate environmental signals and influence downstream processes is still largely unknown. The setup of the clock in trees is likely to be somewhat different than the setup in *Arabidopsis*, presumably due to differences in their ecological niches and habitats (see Fig. 1). Trees are long-lived and need to accurately predict and respond to seasonally-related changes in day length and temperature to time their growth accordingly. This is particularly important either at high latitudes where mismatches in timing will result in impaired growth or death or in the arid and semi-arid regions where regulation of stress responses to drought and salinity might be also controlled by the clock [21, 118]. Such stressful conditions might occur more frequently due to changes in climate and result in fast, unanticipated environmental changes. Future mechanistic studies should therefore focus on clock mediated regulation of responses to environmental changes and regulation of tree growth.

Acknowledgements

The authors are grateful for financial and other support from various funding bodies and Institutions. M.J. was supported by a scholarship from the Alexander von Humboldt Foundation and through SPP1530 (DFG). C.I. was supported by FONDECYT grant no. 1110831 (CONICYT—Chile). M.E.E. was supported by a VINNMER Marie Curie International Qualification Fellowship funded by The Swedish Governmental Agency for Innovation Systems (VINNOVA) and the European Union, with additional support from the Swedish Research Council (VR), Umeå University Career Grant, Carl Trygger's Foundation for Scientific Research. Further M.E.E. would like to acknowledge the Department of Plant Sciences and Churchill College at Cambridge University, Umeå Plant Science Centre and support from the VR and VINNOVA funded Berzelii Centre of Forest Biotechnology, FORMAS, the Kempe Foundation, and Stiftelsen Nils och Dorti Troëdssons forskningsfond.

References

1. Nagel DH, Kay SA (2012) Complexity in the wiring and regulation of plant circadian networks. *Curr Biol* 22:R648–R657
2. Dodd AN, Gardner MJ, Hotta CT, Hubbard KE, Dalchau N et al (2007) The Arabidopsis circadian clock incorporates a cADPR-based feedback loop. *Science* 318:1789–1792
3. Huang W, Perez-Garcia P, Pokhilko A, Millar AJ, Antoshechkin I et al (2012) Mapping the core of the Arabidopsis circadian clock defines the network structure of the oscillator. *Science* 336:75–79
4. Gendron JM, Pruneda-Paz JL, Doherty CJ, Gross AM, Kang SE et al (2012) Arabidopsis circadian clock protein, TOC1, is a DNA-binding transcription factor. *Proc Natl Acad Sci U S A* 109:3167–3172
5. Chow BY, Helfer A, Nusinow DA, Kay SA (2012) ELF3 recruitment to the PRR9 promoter requires other evening complex members in the Arabidopsis circadian clock. *Plant Signal Behav* 7:170–173
6. Nusinow DA, Helfer A, Hamilton EE, King JJ, Imaizumi T et al (2011) The ELF4-ELF3-LUX complex links the circadian clock to diurnal control of hypocotyl growth. *Nature* 475:398–402
7. Herrero E, Kolmos E, Bujdoso N, Yuan Y, Wang M et al (2012) EARLY FLOWERING4 recruitment of EARLY FLOWERING3 in the nucleus sustains the Arabidopsis circadian clock. *Plant Cell* 24:428–443
8. Dai S, Wei X, Pei L, Thompson RL, Liu Y et al (2011) BROTHER OF LUX ARRHYTHMO is a component of the Arabidopsis circadian clock. *Plant Cell* 23:961–972
9. Pruneda-Paz JL, Breton G, Para A, Kay SA (2009) A functional genomics approach reveals CHE as a component of the Arabidopsis circadian clock. *Science* 323:1481–1485
10. Jones MA, Covington MF, DiTacchio L, Vollmers C, Panda S et al (2010) Jumonji domain protein JMJD5 functions in both the plant and human circadian systems. *Proc Natl Acad Sci U S A* 107:21623–21628
11. Más P, Kim WY, Somers DE, Kay SA (2003) Targeted degradation of TOC1 by ZTL modulates circadian function in Arabidopsis thaliana. *Nature* 426:567–570
12. Kim WY, Fujiwara S, Suh SS, Kim J, Kim Y et al (2007) ZEITLUPE is a circadian photoreceptor stabilized by GIGANTEA in blue light. *Nature* 449:356–360
13. Baudry A, Ito S, Song YH, Strait AA, Kiba T et al (2010) F-Box proteins FKF1 and LKP2 act in concert with ZEITLUPE to control Arabidopsis clock progression. *Plant Cell* 22:606–622
14. Imaizumi T, Tran HG, Swartz TE, Briggs WR, Kay SA et al (2003) FKF1 is essential for photoperiodic-specific light signalling in Arabidopsis. *Nature* 426:302–306
15. Schultz TE, Kiyosue T, Yanovsky M, Wada M, Kay SA et al (2001) A role for LKP2 in the

- circadian clock of Arabidopsis. *Plant Cell* 13:2659–2670
16. Johansson M, McWatters HG, Bakó L, Takata N, Gyula P et al (2011) Partners in time. EARLY BIRD associates with ZEITLUPE and regulates the speed of the Arabidopsis clock. *Plant Physiol* 155:2108–2122
 17. Mizoguchi T, Wright L, Fujiwara S, Cremer F, Lee K et al (2005) Distinct roles of GIGANTEA in promoting flowering and regulating circadian rhythms in Arabidopsis. *Plant Cell* 17:2255–2270
 18. Gould PD, Locke JC, Larue C, Southern MM, Davis SJ et al (2006) The molecular basis of temperature compensation in the Arabidopsis circadian clock. *Plant Cell* 18:1177–1187
 19. Locke JC, Kozma-Bognar L, Gould PD, Feher B, Kevei E et al (2006) Experimental validation of a predicted feedback loop in the multi-oscillator clock of Arabidopsis thaliana. *Mol Syst Biol* 2:59
 20. Cao SQ, Ye M, Jiang ST (2005) Involvement of GIGANTEA gene in the regulation of the cold stress response in Arabidopsis. *Plant Cell Rep* 24:683–690
 21. Kim W-Y, Ali Z, Park HJ, Park SJ, Cha J-Y et al (2013) Release of SOS2 kinase from sequestration with GIGANTEA determines salt tolerance in Arabidopsis. *Nat Commun* 4:1352
 22. Farré EM, Harmer SL, Harmon FG, Yanovsky MJ, Kay SA et al (2005) Overlapping and distinct roles of PRR7 and PRR9 in the Arabidopsis circadian clock. *Curr Biol* 15:47–54
 23. Eriksson ME, Hanano S, Southern MM, Hall A, Millar AJ et al (2003) Response regulator homologues have complementary, light-dependent functions in the Arabidopsis circadian clock. *Planta* 218:159–162
 24. Nakamichi N, Kita M, Ito S, Yamashino T, Mizuno T et al (2005) PSEUDO-RESPONSE REGULATORS, PRR9, PRR7 and PRR5, together play essential roles close to the circadian clock of Arabidopsis thaliana. *Plant Cell Physiol* 46:686–698
 25. Kiba T, Henriques R, Sakakibara H, Chua NH (2007) Targeted degradation of PSEUDO-RESPONSE REGULATOR5 by an SCFZTL complex regulates clock function and photomorphogenesis in Arabidopsis thaliana. *Plant Cell* 19:2516–2530
 26. Wang L, Fujiwara S, Somers DE (2010) PRR5 regulates phosphorylation, nuclear import and subnuclear localization of TOC1 in the Arabidopsis circadian clock. *EMBO J* 29:1903–1915
 27. Para A, Farré EM, Imaizumi T, Pruneda-Paz JL, Harmon FG et al (2007) PRR3 is a vascular regulator of TOC1 stability in the Arabidopsis circadian clock. *Plant Cell* 19:3462–3473
 28. Troncoso-Ponce MA, Mas P (2012) Newly described components and regulatory mechanisms of circadian clock function in Arabidopsis thaliana. *Mol Plant* 5:545–553
 29. Nakamichi N (2011) Molecular mechanisms underlying the Arabidopsis circadian clock. *Plant Cell Physiol* 52:1709–1718
 30. Brunner AM, Busov VB, Strauss SH (2004) Poplar genome sequence: functional genomics in an ecologically dominant plant species. *Trends Plant Sci* 9:49–56
 31. Jansson S, Douglas CJ (2007) Populus. A model system for plant biology. *Annu Rev Plant Biol* 58:435–458
 32. Filichkin SA, Breton G, Priest HD, Dharmawardhana P, Jaiswal P et al (2011) Global profiling of rice and poplar transcriptomes highlights key conserved circadian-controlled pathways and cis-regulatory modules. *PLoS One* 6:e16907
 33. Ouyang Y, Andersson C, Kondo T, Golden S, Johnson C et al (1998) Resonating circadian clocks enhance fitness in cyanobacteria. *Proc Natl Acad Sci U S A* 95:8660–8664
 34. Dodd AN, Salathia N, Hall A, Kevei E, Tóth R et al (2005) Plant circadian clocks increase photosynthesis, growth, survival, and competitive advantage. *Science* 309:630–633
 35. Yerushalmi S, Green RM (2009) Evidence for the adaptive significance of circadian rhythms. *Ecol Lett* 12:970–981
 36. Graf A, Schlereth A, Stitt M, Smith AM (2010) Circadian control of carbohydrate availability for growth in Arabidopsis plants at night. *Proc Natl Acad Sci U S A* 107:9458–9463
 37. Green RM, Tingay S, Wang ZY, Tobin EM (2002) Circadian rhythms confer a higher level of fitness to Arabidopsis plants. *Plant Physiol* 129:576–584
 38. Kozarewa I, Ibáñez C, Johansson M, Ögren E, Mozley D et al (2010) Alteration of PHYA expression change circadian rhythms and timing of bud set in Populus. *Plant Mol Biol* 73:143–156
 39. Ibáñez C, Kozarewa I, Johansson M, Ögren E, Rohde A et al (2010) Circadian clock components regulate entry and affect exit of seasonal dormancy as well as winter

- hardiness in *Populus* trees. *Plant Physiol* 153:1823–1833
40. Böhlenius H, Huang T, Charbonnel-Campaa L, Brunner AM, Jansson S et al (2006) CO/FT regulatory module controls timing of flowering and seasonal growth cessation in trees. *Science* 312:1040–1043
 41. Hsu C-Y, Adams JP, Kim H, No K, Ma C et al (2011) FLOWERING LOCUS T duplication coordinates reproductive and vegetative growth in perennial poplar. *Proc Natl Acad Sci U S A* 108:10756–10761
 42. Singh RK, Bhalerao RP, Eriksson ME (2020) Growing in time: exploring the molecular mechanisms of tree growth. *Tree Physiol* 41(4):657–678. <https://doi.org/10.1093/treephys/tpaa065>
 43. Karlberg A, Bakó L, Bhalerao RP (2011) Short day-mediated cessation of growth requires the downregulation of AINTEGUMENTAL-LIKE1 transcription factor in hybrid aspen. *PLoS Genet* 7:e1002361
 44. Takata N, Saito S, Saito CT, Nanjo T, Shinohara K et al (2008) Molecular phylogeny and expression of poplar circadian clock genes, LHY1 and LHY2. *New Phytol* 181:808–819
 45. Wang ZY, Kenigsbuch D, Sun L, Harel E, Ong MS et al (1997) A Myb-related transcription factor is involved in the phytochrome regulation of an *Arabidopsis* Lhcb gene. *Plant Cell* 9:491–507
 46. Higo K, Ugawa Y, Iwamoto M, Korenaga T (1999) Plant *cis*-acting regulatory DNA elements (PLACE) database: 1999. *Nucleic Acids Res* 27:297–300
 47. Ma X-F, Hall D, St Onge KRS, Jansson S, Ingvarsson PK et al (2010) Genetic differentiation, clinal variation and phenotypic associations with growth cessation across the *Populus tremula* photoperiodic pathway. *Genetics* 186:1033–1044
 48. Hall D, Ma X-F, Ingvarsson PK (2011) Adaptive evolution of the *Populus tremula* photoperiod pathway. *Mol Ecol* 20:1463–1474
 49. Takata N, Saito S, Satio CT, Uemura M (2010) Phylogenetic footprint of the plant clock system in angiosperms. evolutionary processes of pseudo-response regulators. *BMC Evol Biol* 10:126
 50. Ibáñez C (2006) Caracterización y expresión de genes implicados en la dormancia invernal del castaño (*Castanea Sativa Mill*). Universidad Politécnica de Madrid
 51. Mockler TC, Michael TP, Priest HD, Shen R, Sullivan CM et al (2007) The DIURNAL project. DIURNAL and circadian expression profiling, model-based pattern matching, and promoter analysis. *Cold Spring Harb Symp Quant Biol* 72:353–363
 52. Sjödin A, Street NR, Sandberg G, Gustafsson P, Jansson S et al (2009) The *Populus* Genome Integrative Explorer (PopGenIE): a new resource for exploring the *Populus* genome. *New Phytol* 182:1013–1025
 53. Perry TO (1971) Dormancy of trees in winter. *Science* 171:29–36
 54. Olsen J, Junntila O, Nilsen J, Eriksson ME, Martinussen I et al (1997) Ectopic expression of oat phytochrome A in hybrid aspen changes critical daylength for growth and prevents cold acclimatization. *Plant J* 12:1339–1350
 55. Welling A, Moritz T, Palva ET, Junntila O (2002) Independent activation of cold acclimation by low temperature and short photoperiod in hybrid aspen. *Plant Physiol* 129:1633–1641
 56. Fankhauser C, Staiger D (2002) Photoreceptors in *Arabidopsis thaliana*: light perception, signal transduction and entrainment of the endogenous clock. *Planta* 216:1–16
 57. Howe GT, Bucciaglia PA, Hackett WP, Furnier GR, Cordonnier-Pratt MM et al (1998) Evidence that the phytochrome gene family in black cottonwood has one PHYA locus and two PHYB loci but lacks members of the PHYC/F and PHYE subfamilies. *Mol Biol Evol* 15:160–175
 58. Tuskan GA, Difazio S, Jansson S, Bohlmann J, Grigoriev I et al (2006) The genome of black cottonwood, *Populus trichocarpa* (Torr & Gray). *Science* 313:1596–1604
 59. Mathews S (2010) Evolutionary studies illuminate the structural-functional model of plant phytochromes. *Plant Cell* 22:4–16
 60. Hsu C-Y, Liu Y, Luthe DS, Yuceer C (2006) Poplar FT2 shortens the juvenile phase and promotes seasonal flowering. *Plant Cell* 18:1846–1861
 61. Bünning E (1967) *The physiological clock*, 2nd edn. Springer-Verlag, New York
 62. Christensen S, Silverthorne J (2001) Origins of phytochrome-modulated Lhcb mRNA expression in seed plants. *Plant Physiol* 126:1609–1618
 63. Solomon OL, Berger DK, Myburg AA (2010) Diurnal and circadian patterns of gene expression in the developing xylem of *Eucalyptus* trees. *S Afr J Bot* 76:425–439
 64. Karlgren A, Gyllenstrand N, Källman T, Lagercrantz U, Hazen SP et al (2013) Conserved function of core clock proteins in the gymnosperm Norway spruce (*Picea abies* L. Karst). *PLoS One* 8:e60110

65. Sreekantan L, Mathiason K, Grimplet J, Schlauch K, Dickerson JA et al (2010) Differential floral development and gene expression in grapevines during long and short photoperiods suggests a role for floral genes in dormancy transitioning. *Plant Mol Biol* 73:191–205
66. Deluc LG, Grimplet J, Wheatley MD, Tillett RL, Quilici DR et al (2007) Transcriptomic and metabolite analyses of Cabernet Sauvignon grape berry development. *BMC Genomics* 8:429
67. Zdepski A, Wang W, Priest HD, Ali F, Alam M et al (2008) Conserved daily transcriptional programs in *Carica papaya*. *Trop Plant Biol* 1:236–245
68. Ramos A, Perez-Solis E, Ibáñez C, Casado R, Collada C et al (2005) Winter disruption of the circadian clock in chestnut. *Proc Natl Acad Sci U S A* 102:7037–7042
69. Ibáñez C, Ramos A, Acebo P, Contreras A, Casado R et al (2008) Overall alteration of circadian clock gene expression in the chestnut cold response. *PLoS One* 3:9
70. Bieniawska Z, Espinoza C, Schlereth A, Sulpice R, Hinch DK et al (2008) Disruption of the Arabidopsis circadian clock is responsible for extensive variation in the cold-responsive transcriptome. *Plant Physiol* 147:263–279
71. Nakamichi N, Kusano M, Fukushima A, Kita M, Ito S et al (2009) Transcript profiling of an Arabidopsis PSEUDO RESPONSE REGULATOR arrhythmic triple mutant reveals a role for the circadian clock in cold stress response. *Plant Cell Physiol* 50:447–462
72. Dong MA, Farré EM, Thomashow MF (2011) CIRCADIAN CLOCK-ASSOCIATED 1 and LATE ELONGATED HYPOCOTYL regulate expression of the C-REPEAT BINDING FACTOR (CBF) pathway in Arabidopsis. *Proc Natl Acad Sci U S A* 108:7241–7246
73. Horvath DP, Chao WS, Anderson JV (2002) Molecular analysis of signals controlling dormancy and growth in underground adventitious buds of leafy spurge. *Plant Physiol* 128:1439–1446
74. Horvath DP, Chao WS, Suttle JC, Thimmapuram J, Anderson JV et al (2008) Transcriptome analysis identifies novel responses and potential regulatory genes involved in seasonal dormancy transitions of leafy spurge (*Euphorbia esula* L.). *BMC Genomics* 9:536
75. Dogramaci M, Horvath DP, Chao WS, Foley ME, Christoffers MJ et al (2010) Low temperatures impact dormancy status, flowering competence, and transcript profiles in crown buds of leafy spurge. *Plant Mol Biol* 73:207–226
76. Foley ME, Anderson JV, Chao WS, Dogramaci M, Horvath DP et al (2010) Initial changes in the transcriptome of *Euphorbia esula* seeds induced to germinate with a combination of constant and diurnal alternating temperatures. *Plant Mol Biol* 73:131–142
77. Cooke JE, Eriksson ME, Junntila O (2012) The dynamic nature of bud dormancy in trees. *Environmental control and molecular mechanisms. Plant Cell Environ* 35:1707–1728
78. Olsen JE (2010) Light and temperature sensing and signaling in induction of bud dormancy in woody plants. *Plant Mol Biol* 73:37–47
79. Hall D, Luquez V, Garcia VM, St Onge KR, Jansson S et al (2007) Adaptive population differentiation in phenology across a latitudinal gradient in European Aspen (*Populus tremula*, L.). A comparison of neutral markers, candidate genes and phenotypic traits. *Evolution* 61:2849–2860
80. Storey KB, Tanino K (2012) Temperature adaptation in a changing climate. CABI, Wallingford
81. Mölmann JA, Junntila O JO, Olsen JE (2006) Effects of red, far-red and blue light in maintaining growth in latitudinal populations of Norway spruce (*Picea abies*). *Plant Cell Environ* 29:166–172
82. Luquez V, Hall D, Albrechtsen BR, Karlsson J, Ingvarsson P et al (2008) Natural phenological variation in aspen (*Populus tremula*): the SwAsp collection. *Tree Genet Genom* 4:279–292
83. Rohde A, Bastien C, Boerjan W (2011) Temperature signals contribute to the timing of photoperiodic growth cessation and bud set in poplar. *Tree Physiol* 31:472–482
84. Frewen BE, Chen THH, Howe GT, Davis J, Rohde A et al (2000) Quantitative trait loci and candidate gene mapping of bud set and bud flush in *Populus*. *Genetics* 154:837–845
85. Qamaruddin M, Ekberg I, Dormling I, Norell L, Clapham D, Eriksson G (1995) Early effects of long nights on budset, bud dormancy and abscisic acid content in two populations of *Picea abies*. *For Genet* 2:207–216

86. Rohde A, Bhalerao RP (2007) Plant dormancy in the perennial context. *Trends Plant Sci* 12:217–223
87. Espinosa-Ruiz A, Saxena S, Schmidt J, Mellerowicz E, Miskolczi P et al (2004) Differential stage-specific regulation of cyclin-dependent kinases during cambial dormancy in hybrid aspen. *Plant J* 38:603–615
88. Junttila O (1976) Apical growth cessation and shoot Ttp abscission in *Salix*. *Physiol Plant* 38:278–286
89. Heide OM, Prestrud AK (2005) Low temperature, but not photoperiod, controls growth cessation and dormancy induction and release in apple and pear. *Tree Physiol* 25:109–114
90. Wisniewski M, Norelli J, Bassett C, Artlip T, Macarisin D et al (2011) Ectopic expression of a novel peach (*Prunus persica*) CBF transcription factor in apple (*Malus × domestica*) results in short-day induced dormancy and increased cold hardiness. *Planta* 233:971–983
91. Olsen JE, Junttila O, Moritz T (1997) Long-day induced bud break in *Salix pentandra* is associated with transiently elevated levels of GA1 and gradual increase in indole-3-acetic acid. *Plant Cell Physiol* 38:536–540
92. Hoffman DE (2011) Changes in the transcriptome and metabolome during the initiation of growth cessation in hybrid aspens. Doctoral thesis, p 43
93. Ruonala R, Rinne PLH, Baghour M, Moritz T, Tuominen H et al (2006) Transitions in the functioning of the shoot apical meristem in birch (*Betula pendula*) involve ethylene. *Plant J* 46:628–640
94. Li C, Junttila O, Ernstsen A, Heino P, Palva ET et al (2003) Photoperiodic control of growth, cold acclimation and dormancy development in silver birch (*Betula pendula*) ecotypes. *Physiol Plant* 117:206–212
95. Karlberg A, Englund M, Petterle A, Molnar G, Sjödin A et al (2010) Analysis of global changes in gene expression during activity-dormancy cycle in hybrid aspen apex. *Plant Biotechnol* 27:1–16
96. Rikin A, Chalutz E, Anderson JD (1984) Rhythmicity in ethylene production in cotton seedlings. *Plant Physiol* 75:493–495
97. Kathiresan A, Reid DM, Chinnappa CC (1996) Light- and temperature-entrained circadian regulation of activity and mRNA accumulation of 1-aminocyclopropane-1-carboxylic acid oxidase in *Stellaria longipes*. *Planta* 199:329–335
98. Kathiresan A, Nagarathna KC, Moloney M, Reid D, Chinnappa CC et al (1998) Differential regulation of 1-aminocyclopropane-1-carboxylate synthase gene family and its role in phenotypic plasticity in *Stellaria longipes*. *Plant Mol Biol* 36:265–274
99. Ruttink T, Arend M, Morreel K, Storme V, Rombauts S et al (2007) A molecular timetable for apical bud formation and dormancy induction in poplar. *Plant Cell* 19:2370–2390
100. Seung D, Risopatron JPM, Jones BJ, Marc J (2012) Circadian clock-dependent gating in ABA signalling networks. *Protoplasma* 249:445–457
101. Nomoto Y, Kubozono S, Yamashino T, Nakamichi N, Mizuno T et al (2012) Circadian clock- and PIF4-controlled plant growth: a coincidence mechanism directly integrates a hormone signaling network into the photoperiodic control of plant architectures in *Arabidopsis thaliana*. *Plant Cell Physiol* 53:1950–1964
102. Ellison CT, Vandenbussche F, van der Straeten D, Harmer SL (2011) XAP5 CIRCADIAN TIMEKEEPER regulates ethylene responses in aerial tissues of *Arabidopsis*. *Plant Physiol* 155:988–999
103. Arana MV, La Marin-de Rosa N, Maloof JN, Blazquez MA, Alabadi D et al (2011) Circadian oscillation of gibberellin signaling in *Arabidopsis*. *Proc Natl Acad Sci U S A* 108:9292–9297
104. Howe GT, Davis J, Jeknić Z, Chen THH, Frewen B et al (1999) Physiological and genetic approaches to studying endodormancy-related traits in *Populus*. *HortScience* 34:1174–1184
105. Santamaría ME, Rodríguez R, Cañal MJ, Toorop PE (2011) Transcriptome analysis of chestnut (*Castanea sativa*) tree buds suggests a putative role for epigenetic control of bud dormancy. *Ann Bot* 108:485–498
106. Sogaard G, Johnsen O, Nilsen J, Junttila O (2008) Climatic control of bud burst in young seedlings of nine provenances of Norway spruce. *Tree Physiol* 28:311–320
107. Granhus A, Floistad IS, Sogaard G (2009) Bud burst timing in *Picea abies* seedlings as affected by temperature during dormancy induction and mild spells during chilling. *Tree Physiol* 29:497–503
108. Trainin T, Bar-Ya'akov I, Holland D (2013) ParSOC1, a MADS-box gene closely related to *Arabidopsis* AGL20/SOC1, is expressed in apricot leaves in a diurnal manner and is linked with chilling requirements for dormancy break. *Tree Genet Genom* 9:753–766
109. Derory J, Léger P, Garcia V, Schaeffer J, Hauser M-T et al (2006) Transcriptome analysis of

- bud burst in sessile oak (*Quercus petraea*). *New Phytol* 170:723–738
110. Halaly T, Pang X, Batikoff T, Crane O, Keren A et al (2008) Similar mechanisms might be triggered by alternative external stimuli that induce dormancy release in grape buds. *Planta* 228:79–88
 111. Hedley PE, Russell JR, Jorgensen L, Gordon S, Morris JA et al (2010) Candidate genes associated with bud dormancy release in blackcurrant (*Ribes nigrum* L.). *BMC Plant Biol* 10:202
 112. Vergara R, Rubio S, Perez FJ (2012) Hypoxia and hydrogen cyanamide induce bud-break and up-regulate hypoxic responsive genes (HRG) and VvFT in grapevine-buds. *Plant Mol Biol* 79:171–178
 113. O'Neill JS, van Ooijen G, Dixon LE, Troein C, Corellou F et al (2011) Circadian rhythms persist without transcription in a eukaryote. *Nature* 469:554–558
 114. Edgar RS, Green EW, Zhao Y, van Ooijen G, Olmedo M et al (2012) Peroxiredoxins are conserved markers of circadian rhythms. *Nature* 485:459–464
 115. Soolanayakanahally RY, Guy RD, Silim SN, Song M (2013) Timing of photoperiodic competency causes phenological mismatch in balsam poplar (*Populus balsamifera* L.). *Plant Cell Environ* 36:116–127
 116. Fitter AH, Fitter RSR (2002) Rapid changes in flowering time in British plants. *Science* 296:1689–1691
 117. Olson MS, Levens N, Soolanayakanahally RY, Guy RD, Schroeder WR et al (2013) The adaptive potential of *Populus balsamifera* L. to phenology requirements in a warmer global climate. *Mol Ecol* 22:1214–1230
 118. Terecskei K, Tóth R, Gyula P, Kevei E, Bindics J et al (2013) The circadian clock-associated small GTPase LIGHT INSENSITIVE PERIOD1 suppresses light-controlled endoreplication and affects tolerance to salt stress in *Arabidopsis*. *Plant Physiol* 161:278–290



Correction to: Period Estimation and Rhythm Detection in Timeseries Data Using BioDare2, the Free, Online, Community Resource

Tomasz Zieliński , Johnny Hay , and Andrew J. Millar 

Correction to:

Chapter 2 in: Dorothee Staiger et al. (eds.), *Plant Circadian Networks: Methods and Protocols*, Methods in Molecular Biology, vol. 2398, https://doi.org/10.1007/978-1-0716-1912-4_2

The original version of the chapter “Period Estimation and Rhythm Detection in Timeseries Data Using BioDare2, the Free, Online, Community Resource” was previously published non-open access. This has now been changed to open access under the terms of the Creative Commons Attribution 4.0 International License (<https://creativecommons.org/licenses/by/4.0/>), and the copyright holder updated to “The Author(s)”. For further details, see license information in the chapter. The chapter and the book have been updated with the change.

The updated online version of this chapter can be found at https://doi.org/10.1007/978-1-0716-1912-4_2

Dorothee Staiger et al. (eds.), *Plant Circadian Networks: Methods and Protocols*, Methods in Molecular Biology, vol. 2398, https://doi.org/10.1007/978-1-0716-1912-4_19, © The Author(s) 2022

INDEX

A

- Agrobacterium*
A. tumefaciens 9, 59
 Amplitude 7, 10, 16,
 21–24, 28–30, 34, 42, 57, 58, 70, 90, 91, 127,
 131, 142, 233
 Antibody 123, 125, 135, 138, 139,
 143, 146, 147, 189–191, 193, 194, 199–201
Arabidopsis thaliana 47–54, 58, 89,
 190, 193, 206, 207, 228

B

- Bifurcation diagram 78
 BioDare 96
 BioDare2 15–31, 40, 42, 52, 61
 Biological Rhythms Analysis Software System
 (BRASS) 3, 7, 11, 40, 69, 94
 Bioluminescence 7, 66, 68, 69, 71, 206, 212
 Bud
 burst 216–218, 221, 233–236
 set 216, 217, 219, 224, 231–236

C

- CCD camera 9, 49, 50, 52, 59,
 69–71, 210–212
 cDNA
 synthesis 152, 158, 171
 Chlorophyll
 fluorescence v, 33–45, 57
 Chromatin
 ChIP-Seq 135, 136
 chromatin immunoprecipitation
 (ChIP) 135, 136, 146
 modification 136
 Circadian 1–12, 15, 16,
 22, 24, 28–30, 33–45, 47–54, 57, 58, 61, 62, 65,
 66, 69, 70, 75–82, 89–96, 99–101, 121, 136,
 151, 152, 173, 174, 176, 180, 190, 205–212,
 216, 228–236
 Circadian clock associated 1 (CCA1) 2, 5, 7,
 9, 10, 12, 63, 66, 89, 90, 100, 136, 147, 211,
 228–230, 232, 233

- Clock 1–3, 6–9, 24, 27, 29, 47–54,
 57, 58, 65, 66, 75, 77, 78, 80, 89–96, 99–101,
 121, 136, 151, 173, 174, 180, 189, 190, 205,
 216, 217, 219, 228–236
 Cold acclimation 231
 CONSTANS 229
 Critical day length (CDL) 216, 219,
 220, 224, 231, 233
 Cross-linking
 formaldehyde 140

D

- Daylength 169, 170
 Differential equation
 ordinary differential equation (ODE) 75–87
 DIURNAL 9, 108, 121, 168,
 205, 211, 233, 235
 Dormancy 216, 220, 222, 225,
 231, 233–236

E

- Entrainment
 parametric 2
 non-parametric 2
 Epitope 139, 190
 Evening element 136

F

- Fast Fourier transform nonlinear least squares
 (FFT-NLLS) 7, 21, 22, 24, 34,
 40, 42, 70
 Feedback loop 57, 89, 136, 190, 228
 Flowering
 FLOWERING LOCUS T 229, 232
 Fluorescence 33–45, 50, 57, 66, 184, 206
 Fluorescent protein 47
 Freeze test 220
 Fructans 107–117

G

- G-box 148
 Gene targeting 139, 207, 230

GIGANTEA (GI)..... 52, 63, 90, 136,
 228, 230, 232, 233
 GREEN FLUORESCENT PROTEIN
 (GFP) 190, 197

H

Histone
 methylation 136
 modifications 136
 Homologous recombination 209
 Hybridization 158, 190, 206, 209,
 210, 221, 224, 231, 232, 234

I

Immunoblot 202
 Immunoprecipitation (IP) 123–125, 135,
 137–139, 143, 147, 190–192, 196–200, 202
 Input 1, 16, 18, 21, 22, 24,
 30, 31, 42, 47, 57, 128, 129, 139, 142–146,
 163–166, 190, 193, 194, 196, 199, 202, 232
 Internode 218, 222, 224
 Intron
 retention 178

J

JTK_Cycle 24
 Junction tracks 54, 105, 152, 178, 183

L

LATE ELONGATED HYPOCOTYL
 (LHY)..... 9, 77, 80, 82, 89, 90,
 136, 139, 147, 228–230, 233
 Light emitting diode (LED) 3, 34, 49,
 50, 53, 59, 71, 211, 212
 Limit-cycle oscillation 11
 Luciferase
 complementation 206, 211
 firefly (photinus pyralis) 47, 53, 66, 205–212
 Renilla luciferase (RLuc)..... 206
 Luciferin 5, 9, 51, 53, 61, 63, 68, 69, 71
 Luminescence 3, 7, 51, 53, 59, 61–63, 71, 94

M

Mass spectrometry (MS)..... 3, 8, 48,
 50, 51, 58, 60, 93, 101, 122, 189, 191, 200, 202,
 210, 212
 Microarray 174
 Micronutrient 176, 177
 MicroRNA (miRNA)..... 58
 Minimal medium 39, 53, 102
 Modelling 77, 80, 82
 Morning element 4, 99, 136, 229

N

Nuclei 122, 123, 125–132, 138, 142

O

Ordinary differential equation (ODE) 75–87
 Output 21, 22, 49, 53, 57, 58, 66,
 76, 79–82, 89, 121, 163–167, 190, 232

P

PCR
 quantitative PCR 145, 147
 Perennial 215, 216, 228–236
 Period 1, 7, 8, 10, 11, 16, 21–26,
 28–31, 34, 36, 40, 42, 44, 52, 58, 62, 63, 69,
 78–82, 90, 91, 94, 95, 105, 123, 147, 173, 182,
 216, 220, 225, 229, 232, 233, 235, 236
 Phase 1–12, 16, 21, 23, 24, 28–30,
 57, 58, 80–82, 90, 91, 94, 102, 156, 173, 174,
 219, 229, 230, 232, 233
 Post-transcriptional 174
 Protein immunoprecipitation 121–132, 135–149
 Protein-protein interaction 58, 122
 Protoplast 58, 66, 210

Q

Quantitative trait locus (QTL)
 mapping 89–96

R

Reactive oxygen species (ROS) 108
 Read quality assessment 163
 Real time PCR 135, 182
 Relative amplitude error (RAE) 7, 10, 24,
 42, 62, 69, 70, 90, 94
 Reporter construct 58
 Reverse transcription
 RT-PCR 178, 184
 Rhythm 1–11, 15–31, 33–45,
 47, 48, 51, 57, 58, 61–63, 65–71, 75, 78, 90, 91,
 94, 136, 152, 205, 206, 210, 228, 232, 233

RNA

RNA immunoprecipitation 137
 RNA-protein interaction 58, 122,
 189, 190, 200, 205–212
 RNA-seq 181
 RNA-Seq read tracks 152

S

Season
 seasonal regulation 229, 231–232, 234–236
 Simulation 79, 81
 Soybean hairy roots 65–71

Splicing
 alternatives 174, 178
 Sugars 58, 107–117

T

Tandem affinity purification
 TAP-tagging 189, 200
 Time-series 16, 18, 20, 24, 26, 27,
 30, 31, 52, 54, 70, 222
 TIMING OF CAB EXPRESSION 1 (TOC1) 9,
 63, 66, 77, 80, 82, 90, 100, 136, 147, 228–231,
 233, 234

TopCount 27, 67, 69, 71, 93,
 206, 207, 210–212
 Transcriptional 9, 57, 58, 89, 100,
 121, 136, 174, 228
 Transcriptome 152, 172, 174,
 177, 205, 229
 Transformation 9, 58, 61, 63, 66, 168

W

Western blot 122, 129–131,
 196, 199, 200, 202